TRANSLATIONAL APPROACHES TO UNDERSTANDING THE ROLE OF CYTOCHROME P450-DERIVED EPOXYEICOSATRIENOIC ACIDS IN CORONARY ARTERY DISEASE

Akinyemi Oni-Orisan

A dissertation submitted to the faculty at the University of North Carolina at Chapel Hill in partial fulfillment of the requirements for the degree of Doctor of Philosophy in the Division of Pharmacotherapy and Experimental Therapeutics in the UNC Eshelman School of Pharmacy (Pharmaceutical Sciences).

Chapel Hill
2015

Approved by:

Craig R. Lee

Tim Wiltshire

Brian C. Jensen

Jo E. Rodgers

John M. Seubert

Darryl C. Zeldin

ABSTRACT

Akinyemi Oni-Orisan: Translational Approaches to Understanding the Role of Cytochrome P450-Derived Epoxyeicosatrienoic Acids in Coronary Artery Disease
(Under the direction of Craig R. Lee)

Cardiovascular disease (CVD) remains the leading cause of morbidity and mortality in the United States (US). Most notably, coronary artery disease (CAD) including its clinical complications (acute myocardial infarction [AMI] and heart failure) is the primary source of this public health burden. This burden highlights the need for new therapies that target biological pathways integral to the pathophysiology of CAD and its consequences. However, a more thorough understanding of the mechanisms underlying the pathophysiology is necessary to facilitate the development of new therapeutic strategies.

Epoxyeicosatrienoic acids (EETs) are cytochrome P450 (CYP)-derived metabolites of arachidonic acid that are hydrolyzed by soluble epoxide hydrolase (sEH) into the less biologically active dihydroxyeicosatrienoic acids (DHETs). EETs yield potent cardiovascular protective effects in preclinical models of atherosclerosis, ischemia reperfusion (IR) injury, and post-AMI ventricular remodeling, suggesting that increasing EET levels may be a viable therapeutic strategy for CAD, AMI, and post-AMI maladaptive ventricular remodeling. Key questions, however, remain to be addressed prior to translation of therapeutic EET-promoting strategies into successful clinical trials.

The overall aim of this dissertation is to advance our understanding of the role of the EET metabolic pathway across the full spectrum of CAD and post-AMI consequences as a means to

determine the biological and therapeutic importance of EETs in the progression of this disease cascade. We used both pre-clinical and human studies to complete the specific aims of this work. We found that obstructive CAD is significantly and independently associated with lower circulating EET levels. In addition, we observed that a functionally relevant polymorphism linked with enhanced EET hydrolysis was potentially associated with mortality in a population of AMI patients. Moreover, we showed that mice with cardiomyocyte-specific overexpression of human sEH exhibited enhanced IR-induced myocardial collagen deposition. Overall, we demonstrated that the EET metabolic pathway may play a role in the pathophysiology of CAD and its associated complications including the development of coronary atherosclerosis, post-AMI early ventricular remodeling, and post-AMI mortality. These findings set the stage for future studies that investigate the therapeutic utility of modulating EETs in CAD patients.

ACKNOWLEDGMENTS

I would like to start off by thanking my major adviser Dr. Craig Lee for working tirelessly to hone my research skills and providing me with numerous opportunities to grow over the past five years. I am grateful for my committee chair Dr. Tim Wiltshire and the other members of my team including Dr. Brian Jensen, Dr. Jo Ellen Rodgers, Dr. John Seubert, and Dr. Darryl Zeldin for sharing their wisdom, challenging me, offering constructive feedback on this project, and for their overwhelming support of my career aspirations.

I would like to thank the current members of the Craig Lee lab including Kim Vendrov, Michael Wells, Erin Christensen, and Bobbie Nguyen for their hard work and dedication. I would like to thank past members of the lab including Dr. Robert Schuck, Dr. Katie Theken, Dr. Weibin Zha, and Dr. Yangmei Deng for teaching me a great deal of labotratory techniques. It was also a privilege working with the drug development fellows Dr. Melissa Polasek, Dr. John Andrew Lee, Dr. Robert Wittorf, Dr. Brian Simmons, and Dr. Savannah Steele.

I would also like to thank our collaborators at the National Institute of Environmental Health Sciences (NIEHS) including Dr. Artiom Gruzdev and Dr. Matthew Edin as well as Dr. George Stouffer from the UNC School of Medicine for their contribution to the projects. I would like to thank Dr. Mauricio Rojas, Ashley Ezzell, and Kirk Mcnaughton for all of their wonderful service. I would like to thank members of the Bruce Hammock lab, the Joan Taylor lab, and personnel of the TRIUMPH cohort for their helpful advice and assistance.

I would like to thank the Division of Pharmacotherapy and Experimental Therapeutics including the excellent faculty, staff, and trainees for being the best source of help a student could ask for. I would also like to thank the Center for Pharmacogenomics and Individualized Therapy for playing a key role in shaping my interests as a researcher. Furthermore, the UNC Eshelman School of Pharmacy has provided a world-class research training environment with excellent facilities and resources to work with.

I would like to acknowledge the financial support of my training including an American Heart Association pre-doctoral fellowship, an American Foundation for Pharmaceutical Education pre-doctoral fellowship, a NIH research supplement to promote diversity in health-related research, and a Royster Society of Fellows interdisciplinary fellowship.

I would also like to especially thank my close friends and family who were critical to my training as a PhD student well before I decide to pursue a PhD. In particular, I want to thank Mom and Dad for giving me life, for reading to me as a toddler, for sheltering us from the neighborhood that we grew up in, for encouraging me to embrace education, and for giving me confidence through positive feedback. I would like to thank Dapo, Deola, Debola, and Cecily for their continued encouragement throughout this process and for motivating me through their own work ethic and incredible accomplishments. Lastly, I would like to thank Baby Lana for being my key source of inspiration over the past 6 months.

TABLE OF CONTENTS

LIST OF TABLES

LIST OF FIGURES

LIST OF ABBREVIATIONS

α-SMA	α-smooth muscle actin
14,15-EEZE	14,15-epoxyeicosa-5(Z)-enoic acid
A	atrial
AA	arachidonic acid
ACS	acute coronary syndrome
AET	aortic ejection time
AMI	acute myocardial infarction
ANCOVA	analysis of covariance
ANOVA	analysis of variance
ANF	atrial natriuretic factor
Bax	B‐cell lymphoma 2‐associated X protein
Bcl-2	B-cell lymphoma-2
BHT	butylated hydroxytoluene
BNP	b-type natriuretic peptide
CABG	coronary artery bypass graft
CAD	coronary artery disease
cAMP	cyclic AMP
cDNA	complementary DNA
COPD	chronic obstructive pulmonary disease
COX	cyclooxygenase
CRP	C-reactive protein
CV	cardiovascular

CVD	cardiovascular disease
CYP	cytochrome P450
DHA	docosahexaenoic acid
DHET	dihydroxyeicosatrienoic acids
DHOME	dihydroxyoctadecaenoic acid
DiHN	dihydroxynondecanoic acid
Dr	deceleration rate
Dt	deceleration time
E	early
ECG	electrocardiogram
ECM	extracellular matrix
EET	epoxyeicosatrienoic acid
EF	ejection fraction
EGR-1	early growth response-1
EPA	eicosapentaenoic acid
EpHep	epoxyheptadecanoid acid
EpOME	epoxyoctadecaenoic acid
FDR	false discovery rate
FFR	fractional flow reserve
FGF-2	fibroblast growth factor-2
FS	fractional shortening
HDL	high density lipoprotein
HF*p*EF	heart failure with preserved ejection fraction

HF*r*EF	heart failure with reduced ejection fraction
HR	hazard ratio
hs-CRP	high sensitivity C reactive protein
ICAM-1	intercellular adhesion molecule-1
IL	interleukin
IQR	interquartile range
IR	ischemia reperfusion
IVCT	isovolumic contraction time
IVSd	inter ventricular septum at diastole
IVRT	isovolumic relaxation time
IVSs	inter ventricular septum at systole
LAD	left anterior descending
LC-MS/MS	liquid chromatography-tandem mass spectrometry
LDL	low-density lipoprotein
LO	lipoxygenase
LOX	lysyl oxidase
LSD	least significant difference
LV	left ventricle
LVDP	left ventricular developed pressure
LVIDd	left ventricular internal diameter at diastole
LVIDs	left ventricular internal diameter at systole
LVPWd	left ventricular posterior wall at diastole
LVPWs	left ventricular posterior wall at systole

MAF	minor allele frequency
MHC	myosin heavy chain
MIP-2α	macrophage inflammatory protein-2α
MCP-1	monocyte chemoattractant protein-1
MMP	matrix metalloproteinases
MPI	myocardial performance index
MPO	myeloperoxidase
NF-κB	nuclear factor-kappaB
NSTEMI	non-ST-segment elevation myocardial infarction
PCI	percutaneous coronary intervention
PGE2-d4	prostaglandin E_2-d4
PI3K	phosphoinositide-3-kinase
PKA	cAMP-dependent protein kinase
PO	permanent occlusion
proBNP	pro-B-type natriuretic peptide
QEA	quantitative enrichment analysis
qPCR	quantitative real-time polymerase chain reaction
RAAS	renin–angiotensin–aldosterone system
sEH	soluble epoxide hydrolase
SEM	standard error of the mean
SNP	single nucleotide polymorphisms
STEMI	ST-segment elevation myocardial infarction
t-PA	tissue plasminogen activator

TGF-β	transforming growth factor-β
TIMP	tissue inhibitor of matrix metalloproteinase
US	United States
Vols	volume at systole
Vold	volume at diastole

CHAPTER 1 – INTRODUCTION

The full cascade of coronary artery disease and its public health impact

Health burden of coronary artery disease

Despite advances in evidence-based medical therapies, cardiovascular disease (CVD) as a whole remains the leading cause of mortality in the United States (US). CVD has been the leading cause of death for over a century (causing 800 thousand deaths in 2011) and its prevalence (at 86 million adults) is expected to continue to rise tremendously. Most notably, coronary artery disease (CAD), which includes acute myocardial infarction (AMI) and angina pectoris (chest pain), is the primary source of this public health burden causing almost half (375 thousand) of all CVD deaths in 2011 (1). Of those who have not already developed CAD at the early age of 40, about 25% will develop some manifestation of CAD within 6 years (2). AMI alone was responsible for 120 thousand deaths in 2011 and it is estimated that death from a coronary event occurs every 84 seconds in America. The survival rate of AMI has improved, largely due to advances in revascularization and secondary prevention therapies; however, the prevalence of heart failure, a key clinical outcome of CAD, is estimated to now be at almost 6 million (1). Approximately 25% of patients that experience a first AMI develop heart failure within 30 days (3). CAD and heart failure together are responsible for 116 billion dollars in direct and 99 billion dollars in indirect health care costs annually (1). The extensive health and economic burden associated with CAD highlights the need for new therapies that target

biological pathways integral to the pathogenesis and progression of CAD. However, a more thorough understanding of the mechanisms underlying the pathophysiology of CAD is necessary to facilitate the development of new therapeutic strategies that mitigate atherosclerosis, prevent AMI events, delay the progression of cardiac remodeling to heart failure, and ultimately improve public health outcomes.

Coronary atherosclerosis

Atherosclerosis is the progressive deposition of plaque along the walls of the arteries (Figure 1.1a). When this plaque buildup occurs in the coronary arteries in particular, this is termed CAD. Coronary atherosclerosis pathogenesis is a complex inflammatory process that develops over decades (4). Briefly, atherosclerosis begins when low-density lipoprotein (LDL) is retained in the arterial intima and oxidized causing the activation of endothelial cells. Activated endothelial cells then trigger an inflammatory response through the expression of cellular adhesion molecules, which promote the accumulation of monocytes and neutrophils into the plaque (5). Differentiated monocytes (macrophages) drive the pathogenesis of atherosclerosis by producing inflammatory cytokines and chemoattractants such as monocyte chemoattractant protein-1 (MCP-1). This leads to the further accumulation of leukocytes into the plaque (6). Macrophages accumulate lipids thereby transforming into isolated lipid-laden foam cells which eventually come together to form what is known as the 'fatty streak' (7, 8). The lesion continues to develop with the infiltration of smooth muscle cells and connective tissue. Development of the early lesion occurs over decades and is accelerated by the presence of conditions such as hypertension, hyperlipidemia, smoking, and diabetes mellitus, which are known as cardiovascular (CV) risk factors. When extracellular lipids and cholesterol esters become a major

component of the developing lesion, an atheroma develops (8). Symptoms of stable angina occur when the atheroma grows to the point that it causes chronic narrowing of the artery (stenosis) and blood flow reduction, thereby limiting supply of oxygen to the myocardium (ischemia). Symptoms are especially evident in the setting of increased oxygen demand such as exercise and emotional stress (9). Thus, for some individuals, this stage of atherosclerosis development is when stenosis can first be visualized by coronary angiography and when symptoms first manifest (8). The clinical definition of nonobstructive CAD is having one or more lesions that are not anatomically (<50% stenosis in the left main and <70% stenosis in all non-left main coronary arteries) or functionally (fractional flow reserve [FFR] that reduces blood flow mildly by ≥0.8) 'significant'. Revascularization by percutaneous coronary intervention (PCI) or coronary artery bypass graft (CABG) in nonobstructive CAD patients to improve symptoms/mortality has been found to cause more harm than benefit and is not recommended (10). The risk of developing stable angina pectoris increases as the degree of artery stenosis increases in size. When the lesion advances to the extent that stenosis is anatomically 'significant' (≥50% in the left main coronary artery or ≥70% in any of the other major epicardial coronary arteries), patients are said to have obstructive CAD. Patients may also have functionally obstructive CAD if the lesion reduces blood flow to less than 80% of its original pressure (FFR<0.8). Obstructive CAD patients are thought to have lesions that have advanced to the point that blood flow is 'significantly' obstructed and thus have a highest likelihood of suffering from anginal symptoms. Consequently, obstructive CAD patients meet the anatomical and functional criteria for coronary artery revascularization by PCI or CABG to improve symptoms (10).

Acute myocardial infarction

Atheromatous plaques are protected from the coronary artery lumen by a fibrous cap. A thin fibrous cap reduces the stability of the atherosclerotic lesion making it more prone to rupture. The thickness of the fibrous cap is correlated with the degree of stenosis where obstructive lesions have the thickest fibrous caps. Thus, although obstructive lesions are more likely to cause anginal symptoms, as described earlier, nonobstructive lesions are more prone to plaque rupture (4). Indeed, obstructive CAD patients have the highest risk of lesion disruption only because they usually also have the greatest amount of nonobstructive lesions, which are spread throughout the coronary vasculature (4, 11). That being said, it is becoming more appreciated that nonobstructive CAD patients are also at increased risk of experiencing plaque rupture of a nonobstructive lesion. As a patient's CAD status progresses from no CAD to nonobstructive CAD to obstructive CAD, the risk of rupture and resultant cardiovascular onsequences increases in a stepwise fashion (11).

When a ruptured atheromatous plaque is exposed to the lumen, it activates platelets and the coagulation cascade acutely producing an occlusive intracoronary thrombus (Figure 1.1b) (4). Often a formed thrombus does not affect blood flow or spontaneously resolves and the patient experiences no symptoms (8). When a thrombus causes profound myocardial ischemia, a key adverse event of CAD, this is known as an acute coronary syndrome (ACS) (4, 8). Consequences of ACS ranging from unstable angina to AMI (including non-ST-segment elevation myocardial infarction [NSTEMI] and ST-segment elevation myocardial infarction [STEMI]) depend on the degree, location, and duration of the occlusion (8). All ACS patients experience chest pain and electrocardiogram (ECG) changes consistent with ischemia (12). Unstable angina causes chest pain at rest, often characterized by occlusion by a labile thrombus that may only last 15 minutes on average. Infarcted tissue is not a result of unstable angina. A

prolonged period of ischemia from a coronary thrombus results in AMI (13). Myocardial cell necrosis is exclusive to AMI and typically occurs in myocardial tissue of the left ventricle (LV) (12). The presence of cardiac troponin in blood is an indicator of myocardial necrosis and the preferred diagnostic biomarker of AMI (14). STEMI patients have a total occlusion of the artery from an intracoronary thrombus (15). These patients require immediate PCI to restore blood flow, reduce infarct expansion, and prevent death (14). The majority of patients who die from sudden ischemic death (death from CAD within 6 hours of symptom onset) have evidence of intracoronary thrombus formation based on autopsy reports (16, 17). The development of ventricular arrhythmia is also a cause of sudden ischemic death (8, 16).

Consequences following acute myocardial infarction

The restoration of blood flow by revascularization, termed ischemia-reperfusion (IR), is imperative to prevent expansion of the myocardial infarct. Paradoxically, IR also triggers injury to the myocardium (18). Injury initially causes cardiomyocyte necrosis (uncontrolled cell death) and apoptosis (programmed cell death), each of which independently contribute to the resulting infarct (Figure 1.1c) (19). Changes in the myocardial expression of the anti-apoptotic B-cell lymphoma (Bcl-2) and the pro-apoptotic B‑cell lymphoma 2‑associated X protein (Bax) regulate activation of the caspase family which is primarily pro-apoptotic. An agent is considered to be 'cardioprotective' if it reduces IR-induced infarct size by preventing myocardial cell death (20). Necrosis but not apoptosis is recognized as the primary mediator of the acute inflammatory response (Figure 1.1c) (19).

Inflammatory-mediated induction of a class of chemoattractants called chemokines promotes leukocyte recruitment to the site of injury. Notably, MCP-1 and macrophage

inflammatory protein-2α (MIP-2α), which are chemotactic for monocytes and neutrophils, respectively, are induced by myocardial necrosis (21). Recruited leukocytes subsequently initiate the cytokine cascade including the synthesis of interleukin (IL)-6 in leukocytes and cardiomyocytes. Cytokines induce the myocardial expression of adhesion molecules such as intercellular adhesion molecule-1 (ICAM-1), which specifically aid in the recruitment of further neutrophils to the site of infarct and mediate neutrophil-derived cytotoxicity (22). In tandem, IL-1β inhibits the activation of fibrosis by preventing the expression of α-smooth muscle actin (α-SMA). It is also becoming recognized that fibroblasts are phenotypically pro-inflammatory during this stage (from stimulation by IL-1β) and producing cytokines/chemokines (23).

This marked inflammatory response is followed by maladaptive ventricular remodeling (22). In particular, transforming growth factor-β (TGF-β) and IL-10 are important mediators involved in the resolution of the inflamed myocardium. The resolution of inflammation is followed by rapid proliferation (mediated by fibroblast growth factor-2 [FGF-2]) and activation (largely mediated by TGF-β) of fibroblasts which soon become the predominant cell type in the heart (Figure 1.2). Activated myofibroblasts are distinguished from their quiescent precursors via the expression of TGF-β/Smad3 pathway-induced α-SMA. Following activation, fibroblasts infiltrate the infarct zone of the myocardium where they function to produce extracellular matrix (ECM) proteins that ultimately cause scar formation (23). Levels of the structural components of ECM including collagens, glycoproteins, proteoglycans, glycosaminoglycans, and matricellular proteins are increased post-AMI contributing to dynamic changes in the matrix. The ECM also includes proteases that are involved in the degradation of these structural components and are also altered post-AMI, contributing to further changes in the matrix. In addition to myofibroblasts which are the most abundant source of ECM proteins post-AMI, endothelial

cells, neutrophils, mast cells, lymphocytes, and macrophages are other major sources of ECM proteins. Collagens are considered the structural backbone of the ECM and are present at low levels in the normal, non-infarcted heart. Post-AMI, collagen expression increases in all regions of the heart, with the greatest magnitude of expression in the infarct zone (24). Only myofibroblasts synthesize collagen. Lysyl oxidase (LOX) mediates the maturation of scar tissue by cross-linking collagen fibrils. However, before the maturation of the fibrotic scar, ECM remodeling can occur as a consequence of mediators such as osteopontin, fibronectin, tissue inhibitor of matrix metalloproteinases (TIMPs), and matrix metalloproteinases (MMPs) that regulate ECM turnover (25). Only MMP can degrade collagen (26). Following scar tissue maturation, myofibroblasts halt production of further profibrotic mediators and become less abundant in the myocardium, potentially through apoptosis (23).

The development of fibrosis is often accompanied by activation of the fetal gene program, which results in the dysregulation of a set of genes associated with maladaptive ventricular remodeling. Increased b-type natriuretic peptide (BNP) expression and a "switch" from expression of the adult α-myosin heavy chain (MHC) to the fetal β-MHC are biomarkers of this process (27). BNP promotes compensatory vasodilator and natriuretic responses that indicate that myocardial strain (i.e. an abnormal structural change) is occurring (28). Fetal gene activation begins early and is thought to be promoted at least partially by initial mechanical stretch-induced activation of early growth response-1 (EGR-1) (29). It is evident that the induction of these mediators during the acute phase following IR activates responses that promote ventricular remodeling during the chronic stages. Together, myocardial fibrosis and cardiac structural changes from fetal gene activation ultimately lead to adverse consequences, notably the first signs/symptoms of heart failure (Figure 1.1c) (22).

Heart failure is a clinical syndrome that manifests in patients as dyspnea (shortness of breath) and/or fluid retention (edema). Symptoms of heart failure result primarily from structural or functional deficits from advanced ventricular remodeling that lead to a reduced ability in ventricular filling (diastolic dysfunction) or ejection of blood (systolic dysfunction). It is important to note that structural abnormalities in heart failure patients range from having no changes at all to having marked ventricular dilation. Likewise, functional impairment may or may not coexist with structural changes and range from having a normal ability to eject blood (commonly measured as ejection fraction [EF]) to having severely reduced EF. Thus there is no definitive test to diagnose heart failure. Both the evaluation of signs/symptoms and cardiac structure/function testing (most commonly via echocardiography) are necessary to diagnose heart failure. Heart failure patients who have reduced EF are categorized as having 'Heart failure with reduced ejection fraction' (HF*r*EF). One of the most common causes of HF*r*EF is AMI. The specific definition of HF*r*EF in terms of EF varies between <35%, <40%, and ≤40%. Heart failure patients who have preserved EF have structural and/or functional deficits that compromise ventriclular relaxation and are categorized as 'Heart failure with preserved ejection fraction' (HF*p*EF) (30).

In addition to promoting the development of heart failure, early ventricular remodeling responses also elevate the risk of a subsequent AMI and myocardial electrical conduction abnormalities that promote sudden cardiac death (31). Indeed, the degree of scar tissue formation and cardiac dysfunction are each predictors of the risk of cardiac events following AMI (32-34). Importantly, progression can occur quickly (35) and clinical trial data show that the development of heart failure in first-time AMI patients with no history of heart failure can occur within a week (36). Consequently, early treatment post-AMI has been found to reduce the occurrence of heart

failure (37, 38), likely due to attenuation of the early maladaptive ventricular remodeling response.

Moreover, established and emerging biomarkers of inflammation and ventricular remodeling processes have been found to have prognostic and therapeutic utility in patients (28). Circulating biomarkers of inflammation such as MCP-1, myeloperoxidase (MPO), IL-6, C-reactive protein (CRP) and ICAM-1 are independent predictors of poor prognosis following an AMI in humans (39-44). Biomarkers of myocardial remodeling including cardiac β- and α-MHC expression as well as circulating BNP levels are associated with the presence and severity of heart failure and AMI in humans (45, 46). Novel biomarkers of fibrosis such as circulating ST2 offer prognostic value in heart failure patients on top of traditional biomarkers and established risk factors (47). Consequently, these biomarkers of inflammation and myocardial remodeling are valuable phenotypic endpoints in pre-clinical and human studies, and inhibition of these responses has enormous potential to improve prognosis in AMI patients. It is clear that early and aggressive therapy well before the manifestation of symptomatic heart failure improves outcomes.

The need for novel therapeutic strategies and novel drug development approaches

It is evident that novel therapies which further delay the development of coronary atherosclerosis, prevent the expansion of IR-induced infarct ('cardioprotective' therapies), slow the progression of post-infarct early ventricular remodeling, or facilitate a combination of the above will reduce poor complications associated with CAD. These therapeutic strategies for the treatment of CAD and its complications have been in development for decades. However, the majority of these drug candidates have failed. For example, the cornerstone therapies for AMI

have consisted of antiplatelet agents, beta blockers, statins, and renin-angiotensin aldosterone system inhibitors post-AMI for decades (48-50), but drug candidates from novel therapeutic classes for AMI have not been successfully translated to standard practice guidelines (49). Furthermore, in the realm of cardioprotective therapies, no pharmacological therapies and only early reperfusion (as a strategy to reduce infarct size) has been successfully translated into clinical practice (10).

One explanation for poor success rates is flawed preclinical research. For example, preclinical models of post-AMI myocardial remodeling are critical tools to screen/develop novel therapeutic strategies (51). Induction of AMI in rodents *in vivo* is feasible and produces injury comparable to the more established large animal models of AMI. However, full characterization of the pathophysiology of the disease in post-AMI models is necessary to determine how predictive and translational the model is to humans. Surprisingly, the acute and chronic impact of some of the most commonly used AMI models have not been fully characterized in the literature and requires further investigation. A more thorough understanding of the pathophysiology of myocardial remodeling following AMI in mice will facilitate the design of experimental studies that elucidate the role of therapeutic pathways in the disease.

These failures also suggest that innovative approaches during late drug development (clinical trials) are needed to mitigate increasing attrition rates and more successfully translate novel therapies into clinical practice (18, 52, 53). Compared to the conventional 'one-size fits all' methodology to drug development, a precision medicine approach has the potential to increase the probability of success for promising therapeutic candidates (54). Although targeted therapies are routinely used in oncology, this strategy has not been readily adopted in CVD, but opportunities exist to implement precision medicine in heart disease (Appendix A) (55).

Biomarkers offer considerable promise to prospectively identify subsets of CAD patients at high risk of experiencing a cardiovascular event that exhibit dysfunction in a specific pathway (putative responders), consequently enabling novel therapies that target the pathway to maximize their therapeutic effect and improve outcomes.

The epoxyeicosatrienoic acid metabolic pathway and parallel pathways of eicosanoid metabolism

The epoxyeicosatrienoic acid metabolic pathway

Epoxyeicosatrienoic acids (EETs) are cytochrome P450 (CYP)-derived metabolites of arachidonic acid. Specifically, CYP epoxygenases from the CYP2C and CYP2J subfamilies metabolize arachidonic acid into four EET regioisomers (5,6-, 8,9-, 11,12- and 14,15-EET). EETs have a variery of biological functions, but are rapidly hydrolyzed by soluble epoxide hydrolase (sEH, *EPHX2*) into the less biologically active dihydroxyeicosatrienoic acids (DHETs) (56). The CYP epoxygenases known to metabolize arachdidonic acid in humans are CYP2J2, CYP2C8, and CYP2C9. These enzymes as well as sEH are expressed in the cardiovascular system including the myocardium and blood vessels (57-59).

Epoxyeicosatrienoic acid action in coronary artery disease and acute myocardial infarction

EETs are endogenous lipid mediators that elicit potent vasodilatory effects by hyperpolarizing vascular smooth muscle cells (60, 61), anti-inflammatory effects by attenuating nuclear factor-kappaB (NF-κB) signaling (62, 63), fibrinolytic effects by induction of tissue plasminogen activator (t-PA) expression (64), antimigratory effects on smooth muscle cells through the cAMP-dependent protein kinase (PKA) pathway (65), anti-apoptotic effects by promoting phosphoinositide-3-kinase (PI3K)/Akt signaling (66, 67), and pro-survival effects by preserving mitochondrial function (68). Concordant with these basic mechanistic effects, therapeutically promoting the effects of EETs yields potent cardiovascular protective effects in preclinical models of cardiovascular disease (69). For example, inhibition of sEH genetically or

pharmacologicallay increased plasma EET levels and prevented femoral artery neointima formation in a mouse model of vascular inflammation (70). In addition, pharmacological administration of a sEH inhibitor reduced lesion accelerated lesion formation in a mouse model of cardiovascular atherosclerosis (71). Moreover, *Ephx2*$^{-/-}$ mice had improved recovery of left ventricular developed pressure (LVDP) and reduced infarct size following IR. This was reversed by 14,15-epoxyeicosa-5(Z)-enoic acid (14,15-EEZE), a putative EET receptor antagonist, implicating EETs as the mediator of the effect (72). Furthermore, pharmacological sEH inhibition attenuated collagen deposition in a preclinical model of post-IR maladaptive ventricular remodeling. This effect was found to be independent of infarct size reduction (73). Taken together, these data suggest that increasing EET levels may be a viable therapeutic strategy for CAD, AMI, and post-AMI ventricular remodeling. However, the direct contribution of increased cardiomyocyte sEH expression to the pathogenesis and progression of maladaptive ventricular remodeling post-AMI *in vivo* has not been investigated.

Other pathways of eicosanoid metabolism

In addition to arachidonic acid, another ω-6 fatty acid (linoleic acid) and ω-3 fatty acids (docosahexaenoic acid [DHA] and eicosapentaenoic acid [EPA]) are metabolized by CYP epoxygenase enzymes into a variety of epoxy-derivatives (74). These epoxyeicosanoids (Figure 1.3) are also potent biological mediators in the cardiovascular system and may be subsequently metabolized into vicinal diols by epoxide hydrolases (75, 76). Moreover, these fatty acids are also metabolized by cyclooxygenase (COX), lipoxygenase (LO), and CYP hydroxylase enzymes to produce biologically active metabolites that play a functional role in CVD (Figure 1.4) (77-

79). The role of EETs in the initiation and progression of CAD relative to other eicosanoids remains unknown and requires further investigation.

CYP epoxygenases and soluble epoxide hydrolase in human CAD

Since pharmacological tools that directly and specifically manipulate sEH to modulate EET levels are currently not available for clinical use, investigators have relied on genetic observational studies to understand the role of the EET metabolic pathway in human CVD.

Multiple functionally relevant polymorphisms in genes responsible for EET biosynthesis (*CYP2C8, CYP2J2*) and EET hydrolysis (*EPHX2*) have been identified and found to alter enzyme expression or activity. At the population level, associations between genetic polymorphisms in the EET metabolic pathway and the risk of developing CAD have been reported in humans (80).

G-50T is a common functional polymorphism in *CYP2J2* within the promoter region that leads to decreased expression of the enzyme *in vitro* (81). It has been found to be associated with increased the risk of CAD development as well as the premature onset of AMI (before the age of 45) (82, 83). The *CYP2C8* p.Lys399Arg variant allele reduces CYP-derived EET biosynthesis *in vitro* (84). Subjects carrying *CYP2C8* Arg399 had a higher risk of incident CAD in Caucasian smokers and a higher risk of AMI in a Scandinavian cohort compared to wildtype individuals (85, 86).

The two most common non-synonymous single nucleotide polymorphisms (SNPs) in *EPHX2* have been found to decrease (p.Arg287Gln) or increase (p.Lys55Arg) the activity of sEH *in vitro* (87, 88). Specifically, the Arg287Gln polymorphism is thought to reduce the stability of the homodimer (87) which is necessary for hydrolase activity (89). The Lys55Arg polymorphism

is located in a domain that allows for increased stabilization of the dimer (90). Lys55Arg and Arg287Gln are not in linkage disequilibrium (91).

The allele frequencies for Arg287Gln are approximately 8% and 10% in African American and Caucasian populations respectively (80). Lys55Arg has been studied less extensively then Arg287Gln, but it is the most common functional SNP in the population (87, 91). The allele frequencies for Lys55Arg are approximately 22% and 7% in African Americans and Caucasians (80).

Associations between functional genetic polymorphisms in *EPHX2* and the risk of developing CVD have been reported in humans (91-96). The Arg287Gln variant has been linked to reduced plasma cholesterol and triglyceride concentrations in patients with familial hypercholesterolemia (97), reduced risk of coronary artery calcification in African-Americans (93, 94), increased ischemic stroke risk in white Europeans (98), carotid artery calcified plaque in Europeans (99), improved vascular dysfunction in African Americans (95), and increased risk of atrial fibrillation recurrence after catheter ablation (100). The Lys55Arg polymorphism is associated with higher sEH metabolic function *in vivo* and is linked to development of CAD in Caucasian patients (91), ischemic stroke in Swedish men (96), and vascular dysfunction in Caucasian volunteers (95).

Taken together, these data suggest that the EET metabolic pathway may be important in the pathogenesis of CAD in humans and that therapeutic interventions that promote the cardioprotective effects of EETs by modulation of sEH offer considerable promise as a novel therapeutic strategy to reduce sequelae following AMI; however, key questions remain to be addressed prior to translation of EET-promoting strategies into successful proof-of-concept

phase I and II clinical trials. Evaluation of functional variants in *EPHX2* and prognosis in AMI patients has not been completed.

In collaboration with Dr. John Spertus (Mid America Heart Institute) and Dr. Sharon Cresci (Washington University School of Medicine), the Craig Lee lab has previously investigated the association of *CYP2J2* -50G>T, *CYP2C8* Lys399Arg, *EPHX2* Lys55Arg, and *EPHX2* Arg287Gln genotype with 5-year survival in a 2-center cohort of CAD patients hospitalized for an ACS event (INvestigation oF Outcomes from acute coronary syndRoMes study [INFORM]). Consistent with our hypothesis that variants which result in lower EET biosynthesis or greater EET hydrolysis would have a deleterious effect on cardiovascular disease risk and survival, *EPHX2* Arg55 variant allele carriers had a significantly higher risk of death following an ACS compared to noncarriers (HR 1.50, 95% CI 1.02-2.22, P=0.042). In contrast to our hypothesis, *CYP2J2* -50G>T genotype was significantly associated with survival such that variant allele carriers had lower 5-year mortality compared to noncarriers (HR 0.51, 95% CI 0.26-0.99, P=0.049). Furthermore, no association was observed with *CYP2C8* Lys399Arg (HR 0.87, 95% CI 0.55-1.41, P=0.598) or *EPHX2* Arg287Gln (HR 0.88, 95% CI 0.55-1.41, P=0.597). A race-stratified analysis was conducted to account for the potential confounding effects of population stratification. Associations in Caucasians were consistent with the overall cohort, and persisted after adjusting for demographic and clinical covariates predictive of prognosis. The magnitude of the associations were comparable to established prognostic predictors (e.g., diabetes: HR 2.2, 95% CI 1.5-3.2, P<0.01). However, associations were not evaluated in African Americans, due to a small sample size (N=124) and suboptimal power (101). Validation of the association found with *EPHX2* Lys55Arg in an independent population remains necessary to substantiate these preliminary observations.

Systemic levels of cytochrome P450-derived EETs in humans

We recently reported that multiple clinical factors were associated with EET levels in patients with established CAD (102). Furthermore, it is well-established that inflammatory stimuli suppress CYP metabolism through a variety of mechanisms, including cytokine-mediated down-regulation of CYP expression (103). Moreover, hepatic and extra-hepatic CYP2C/2J expression and EET biosynthesis were suppressed in an endotoxin mouse model of acute inflammation (104). Taken together, these data suggest multiple factors (beyond germline genetic polymorphisms) regulate EET biosynthesis and hydrolysis and that quantifying EET levels may provide important insight into the role of these mediators in the pathogenesis and progression of CAD. However, due to the technical complexity of quantifying EETs, which are present at low concentrations in blood and tissue, these metabolites are not commonly quantified on traditional metabolomic or eicosanoid analytical platforms (105). As a consequence, major gaps in knowledge surrounding the biological and therapeutic importance of CYP-derived EETs in human CAD exist.

Translational approaches to understanding the role of EETs in CAD

Therapeutic interventions that promote the cardioprotective effects of EETs offer considerable promise as a novel therapeutic strategy to delay the pathogenesis/progression of CAD and reduce sequelae following AMI. Importantly, agents that promote the effects of EETs have not reached clinical trials for the indication of CAD or AMI, thus an opportunity exists to gain a more thorough understanding of the role of the EET metabolic pathway across the full course of CAD and post-AMI myocardial remodeling prior to translation of EET-promoting

strategies into successful proof-of-concept phase I and II clinical trials. In general addressing these aforementioned gaps would lay the foundation for the design of clinical trials that select the EET-promonting agent, dosing strategy, and patient population most likely to circumvent clinical failure (Appendix B discusses the key questions that remain to be addressed in greater detail) (69). Both preclinical and human investigations are necessary to address this gap in knowledge and improve the probability of translational success from a rapidly emerging body of evidence into a clinically applicable therapeutic strategy for CAD patients.

Perspective

Despite advances in its detection and management, CAD remains a major health burden in the US (1). Consequently, novel therapeutic strategies are needed to further improve outcomes. A more thorough understanding of the mechanisms underlying the pathogenesis of CAD, AMI, and its associated sequelae are necessary for the development of new therapeutic strategies that mitigate this devastating disease across its full spectrum and ultimately improve public health outcomes. Precision medicine is a promising therapeutic approach that may increase the probability of success for prospective therapeutic candidates. Thus, the discovery of biomarkers involved in the pathogenesis of CAD offers considerable promise to facilitate the development of novel therapeutics by identifying subsets of high-risk patients who would derive the greatest benefit from therapy. Increasing EET levels has emerged as a viable therapeutic strategy for CAD, AMI, and post-AMI ventricular remodeling in preclinical models; however, key questions remain to be addressed prior to translation of therapeutic EET-promoting strategies into successful proof-of-concept phase I and II clinical trials. We hypothesize that promoting the beneficial effects of EETs offers therapeutic potential in CAD patients and that subsets of the population predisposed to low EET levels will derive the greatest benefit from this therapeutic strategy.

Thus, the overall aim of this dissertation is to advance our understanding of the role of the EET metabolic pathway across the full spectrum of CAD and post-AMI consequences as a means to determine the biological and therapeutic importance of EETs in the progression of this disease cascade. We seek to accomplish this aim using an integrated combination of targeted metabolomics (Aim 1) and candidate gene (Aim 2) approaches in humans, as well as a genetic

manipulation (Aim 3) approach in mice. Aim 1 will provide some insight into the role of the EET metabolic pathway in the coronary vasculature; Aims 2 and 3 are focused more on the role of the pathway in myocardiocytes post-AMI.

Completion of this dissertation will (1) identify individuals across the full spectrum of CAD predisposed to a deficiency in the EET metabolic pathway and poor prognosis, who may derive the greatest benefit from EET promoting strategies using a precision medicince approach to drug development; (2) determine the role of sEH/*EPHX2* in the pathophysiology of post-AMI ventricular remodeling as a means to determine the therapeutic potential of promoting EETs following AMI; and (3) promote precision medicine and pharmacogenomics as a future avenue for cardiovascular drug development by laying the foundation for clinical trials that evaluate the therapeutic utility of a novel strategy.

Specific Aims

1) Elucidate the relationship between the extent (stenosis) of CAD and CYP-derived EET levels in patients referred for coronary angiography

Hypotheses:

a. Increasing CAD extent will be significantly and independently associated with lower circulating EET levels.

b. The association between increasing CAD extent and lower EET levels will correlate with both lower CYP-derived EET biosynthesis and higher sEH-derived EET hydrolysis.

c. The association between CAD extent and EET levels will be more pronounced than the association between CAD extent and eicosanoids from other metabolism pathways.

2) Determine the relationship between the *EPHX2* p.Lys55Arg polymorphism and survival in AMI patients

Hypothesis:

a. Carriers of the *EPHX2* Arg55 variant allele will exhibit higher risk of mortality following hospitalization for an AMI

3) Determine the contribution of cardiac sEH to maladaptive ventricular remodeling in mice post-AMI *in vivo*

Hypotheses:

a. The 30-minute left anterior descending (LAD) coronary artery ligation ischemia-reperfusion model of *in vivo* AMI in mice will induce ventricular remodeling including the induction of fibrosis, structural changes, and cardiac dysfunction.

b. Mice with transgenic overexpression of sEH in cardiomyocytes and enhanced cardiac EET hydrolysis will have worsened ventricular remodeling post-AMI including enhanced fibrosis, structural changes, and cardiac dysfunction.

Figures

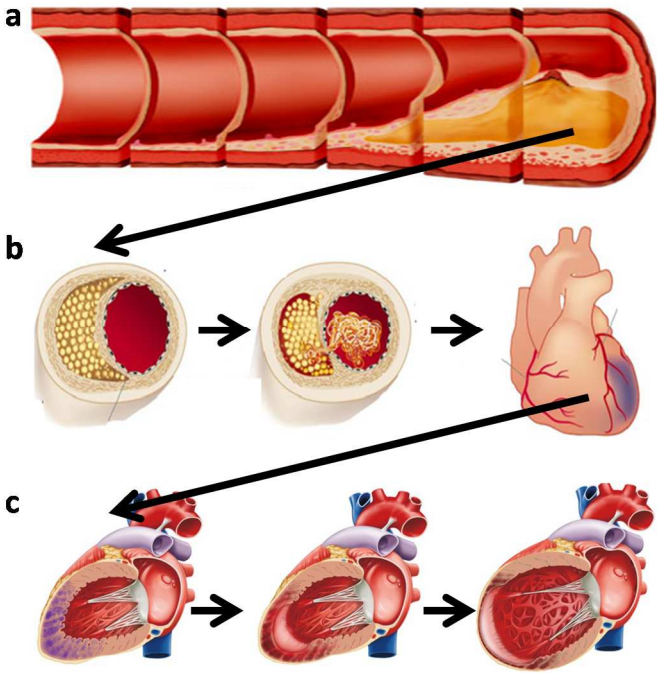

Figure 1.1 The full cascade of coronary artery disease (CAD) and its associated consequences

(a) Atherosclerosis, the progressive buildup of plaque along the walls of the arteries, initiates CAD and correlates with the risk of stable angina. (b) Atheromatous lesions with thin fibrous caps are more like to rupture and lead to acute myocardial infarction. (c) Infarcted tissue from an AMI activates an inflammatory response which promotes the development of maladaptive ventricular remodeling. Adapted/modified from Nature. 2002 Dec 19-26;420(6917):868-74 and J Am Heart Assoc. 2012 Oct;1(5):e004408.

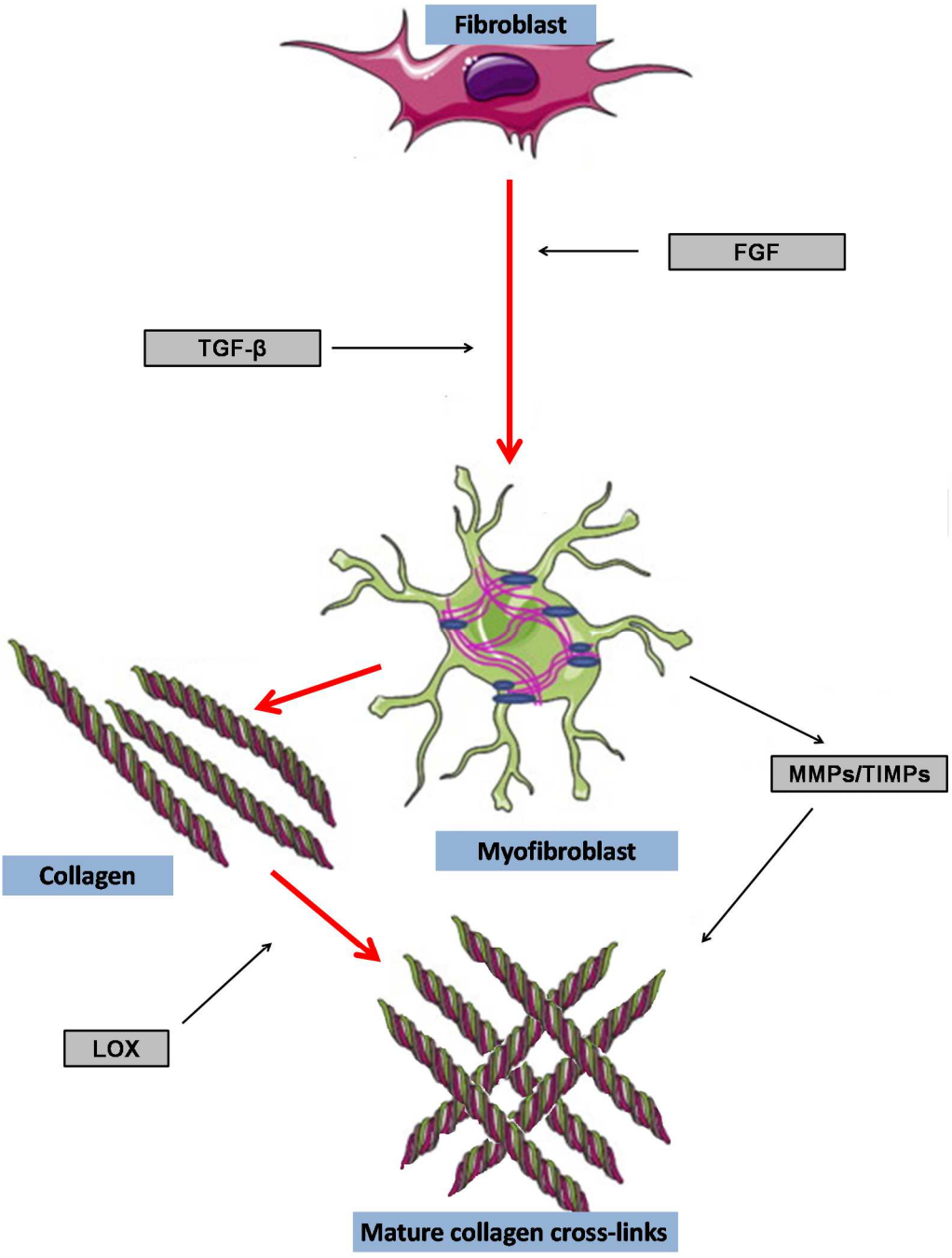

Figure 1.2 Myocardial fibrosis post-acute myocardial infarction (AMI)

Following AMI, fibroblast proliferation is mediated by fibroblast growth factor (FGF). Thereafter, transforming growth factor (TGF)-β mediates the transformation of fibroblasts to differentiated myofibroblasts. Profibrotic myofibroblasts synthesize collagen fibers, which are

ultimately cross-linked by lysyl oxidase (LOX) into mature scar tissue. Proteases (matrix metalloproteinases [MMPs] and tissue inhibitor of matrix metalloproteinases [TIMPs]) can alter the extent of collagen deposition before final maturation. Adapted/modified from J Mol Cell Cardiol. 2014 May;70C:74-82.

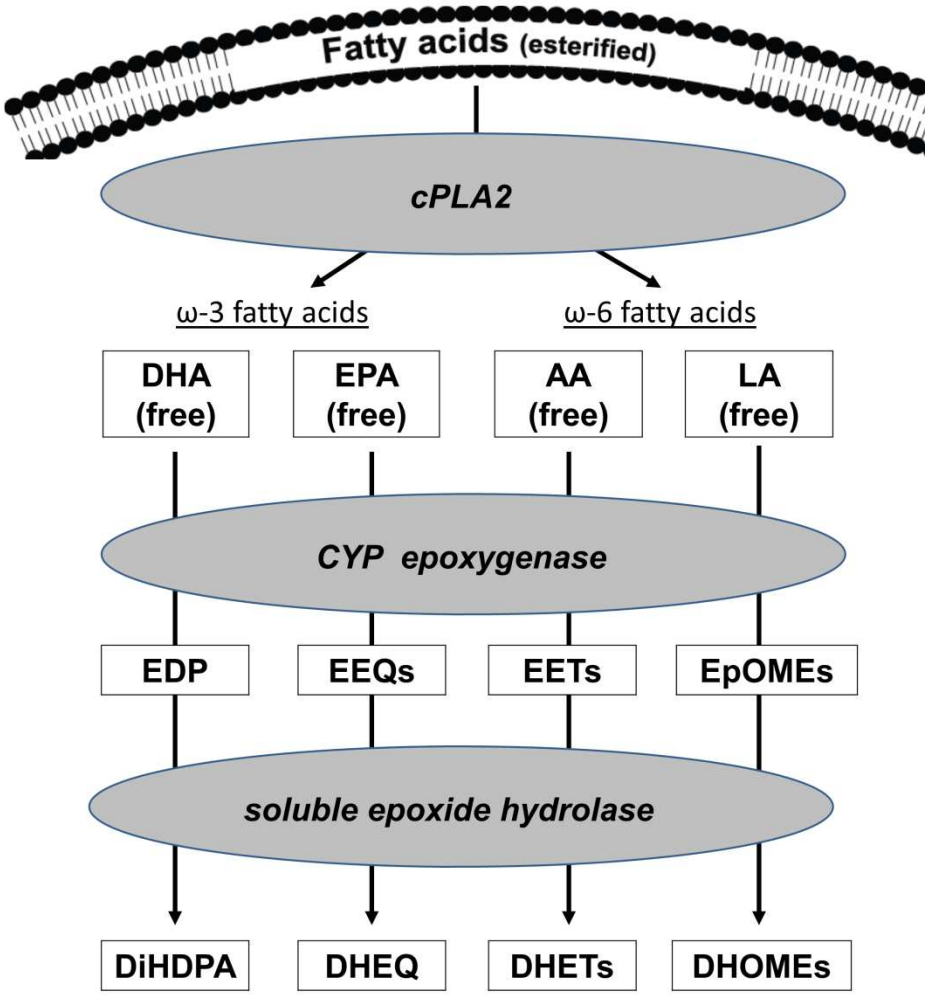

Figure 1.3 Cytochrome P450 (CYP)-derived epoxyeicosanoids.

Bioactive epoxyeicosanoids from arachidonic acid (AA), linoleic acid (LA), docosahexaenoic acid (DHA), and eicosapentaenoic acid (EPA) elicit various biological effects in the cardiovascular system and are extensively hydrolyzed by soluble epoxide hydrolase. DHEQ, dihydroxy-eicosatetraenoic acid; DHOME, dihydroxyoctadecaenoic acid; DiHDPA, dihydroxy-

docosapentaenoic acid; EDP, epoxydocosapentaenoic acid; EEQ, epoxyeicosatetraenoic acid; EpOME, epoxyoctadecaenoic acid. Adapted from J Mol Cell Cardiol. 2014 Sep;74:199-208.

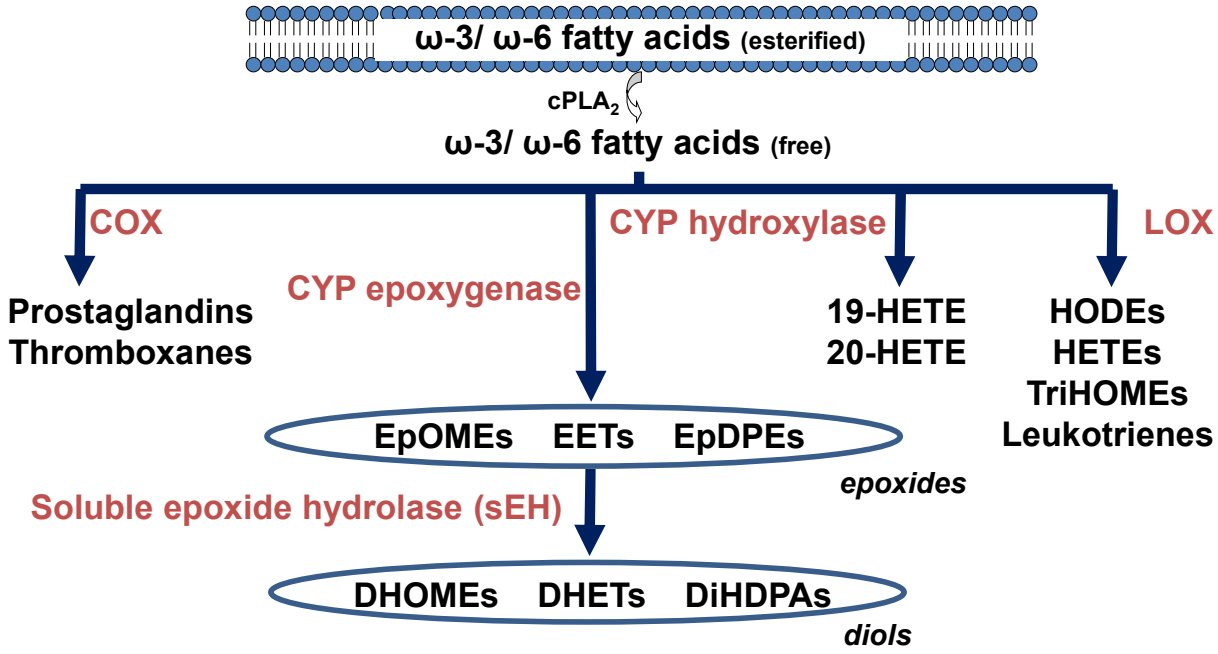

Figure 1.4 The eicosanoid metabolism pathway.

ω-3 and ω-6 fatty acids are metabolized by cyclooxygenase (COX), lipoxygenase (LO), and cytochrome P450 (CYP) enzymes to produce biologically active eicosanoids that play a functional role in cardiovascular disease (CVD). $cPLA_2$, cytosolic phospholipases A_2; DHET, dihydroxyeicosatrienoic acid; DHOME, dihydroxyoctadecaenoic acid; DiHDPA, dihydroxy-docosapentaenoic acid; EET, epoxyeicosatrienoic acid; EpDPE, epoxydocosapentaenoic acid; EpOME, epoxyoctadecaenoic acid; HETE, hydroxyeicosatetraenoic acid; HODE, hydroxyoctadecadienoic acids; TriHOME, trihydroxyoctadecenoic acid.

REFERENCES

(1) Mozaffarian, D. *et al.* Heart disease and stroke statistics--2015 update: a report from the American Heart Association. *Circulation* 131, e29-322 (2015).

(2) Rao Golla, M.S., Paul, T., Rao, S., Wiesen, C., Yeung, M. & Stouffer, G.A. Risk of developing coronary artery disease following a normal coronary angiogram in middle-aged adults. *J Invasive Cardiol* 26, 624-8 (2014).

(3) Velagaleti, R.S. *et al.* Long-term trends in the incidence of heart failure after myocardial infarction. *Circulation* 118, 2057-62 (2008).

(4) Libby, P. & Theroux, P. Pathophysiology of coronary artery disease. *Circulation* 111, 3481-8 (2005).

(5) Steinberg, D., Parthasarathy, S., Carew, T.E., Khoo, J.C. & Witztum, J.L. Beyond cholesterol. Modifications of low-density lipoprotein that increase its atherogenicity. *N Engl J Med* 320, 915-24 (1989).

(6) Becker, L.C. Yin and yang of MCP-1. *Circ Res* 96, 812-4 (2005).

(7) Ley, K., Miller, Y.I. & Hedrick, C.C. Monocyte and macrophage dynamics during atherogenesis. *Arterioscler Thromb Vasc Biol* 31, 1506-16 (2011).

(8) Gutstein, D.E. & Fuster, V. Pathophysiology and clinical significance of atherosclerotic plaque rupture. *Cardiovasc Res* 41, 323-33 (1999).

(9) Agarwal, M., Mehta, P.K. & Bairey Merz, C.N. Nonacute coronary syndrome anginal chest pain. *Med Clin North Am* 94, 201-16 (2010).

(10) Levine, G.N. *et al.* 2011 ACCF/AHA/SCAI guideline for percutaneous coronary intervention: a report of the American College of Cardiology Foundation/American Heart Association Task Force on Practice Guidelines and the Society for Cardiovascular Angiography and Interventions. *Catheter Cardiovasc Interv* 82, E266-355 (2013).

(11) Maddox, T.M. *et al.* Nonobstructive coronary artery disease and risk of myocardial infarction. *JAMA* 312, 1754-63 (2014).

(12) Achar, S.A., Kundu, S. & Norcross, W.A. Diagnosis of acute coronary syndrome. *Am Fam Physician* 72, 119-26 (2005).

(13) Fuster, V., Badimon, L., Badimon, J.J. & Chesebro, J.H. The pathogenesis of coronary artery disease and the acute coronary syndromes (1). *N Engl J Med* 326, 242-50 (1992).

(14) O'Gara, P.T. *et al.* 2013 ACCF/AHA guideline for the management of ST-elevation myocardial infarction: a report of the American College of Cardiology Foundation/American Heart Association Task Force on Practice Guidelines. *Circulation* 127, e362-425 (2013).

(15) Daga, L.C., Kaul, U. & Mansoor, A. Approach to STEMI and NSTEMI. *J Assoc Physicians India* 59 Suppl, 19-25 (2011).

(16) Davies, M.J. & Thomas, A. Thrombosis and acute coronary-artery lesions in sudden cardiac ischemic death. *N Engl J Med* 310, 1137-40 (1984).

(17) Burke, A.P., Farb, A., Malcom, G.T., Liang, Y.H., Smialek, J. & Virmani, R. Coronary risk factors and plaque morphology in men with coronary disease who died suddenly. *N Engl J Med* 336, 1276-82 (1997).

(18) Yellon, D.M. & Hausenloy, D.J. Myocardial reperfusion injury. *N Engl J Med* 357, 1121-35 (2007).

(19) Zhao, Z.Q. & Vinten-Johansen, J. Myocardial apoptosis and ischemic preconditioning. *Cardiovasc Res* 55, 438-55 (2002).

(20) West, M.B. *et al.* Cardiac myocyte-specific expression of inducible nitric oxide synthase protects against ischemia/reperfusion injury by preventing mitochondrial permeability transition. *Circulation* 118, 1970-8 (2008).

(21) Tarzami, S.T., Cheng, R., Miao, W., Kitsis, R.N. & Berman, J.W. Chemokine expression in myocardial ischemia: MIP-2 dependent MCP-1 expression protects cardiomyocytes from cell death. *J Mol Cell Cardiol* 34, 209-21 (2002).

(22) Frangogiannis, N.G. Regulation of the inflammatory response in cardiac repair. *Circ Res* 110, 159-73 (2012).

(23) Shinde, A.V. & Frangogiannis, N.G. Fibroblasts in myocardial infarction: a role in inflammation and repair. *J Mol Cell Cardiol* 70, 74-82 (2014).

(24) Rienks, M., Papageorgiou, A.P., Frangogiannis, N.G. & Heymans, S. Myocardial extracellular matrix: an ever-changing and diverse entity. *Circ Res* 114, 872-88 (2014).

(25) Turner, N.A. & Porter, K.E. Regulation of myocardial matrix metalloproteinase expression and activity by cardiac fibroblasts. *IUBMB Life* 64, 143-50 (2012).

(26) Sutton, M.G. & Sharpe, N. Left ventricular remodeling after myocardial infarction: pathophysiology and therapy. *Circulation* 101, 2981-8 (2000).

(27) Cox, E.J. & Marsh, S.A. A systematic review of fetal genes as biomarkers of cardiac hypertrophy in rodent models of diabetes. *PLoS One* 9, e92903 (2014).

(28) Iqbal, N. *et al.* Cardiac biomarkers: new tools for heart failure management. *Cardiovasc Diagn Ther* 2, 147-64 (2012).

(29) Gupta, M.P., Gupta, M., Zak, R. & Sukhatme, V.P. Egr-1, a serum-inducible zinc finger protein, regulates transcription of the rat cardiac alpha-myosin heavy chain gene. *J Biol Chem* 266, 12813-6 (1991).

(30) Yancy, C.W. *et al.* 2013 ACCF/AHA guideline for the management of heart failure: a report of the American College of Cardiology Foundation/American Heart Association Task Force on Practice Guidelines. *J Am Coll Cardiol* 62, e147-239 (2013).

(31) Gheorghiade, M. *et al.* Navigating the crossroads of coronary artery disease and heart failure. *Circulation* 114, 1202-13 (2006).

(32) Kwon, D.H. *et al.* Extent of left ventricular scar predicts outcomes in ischemic cardiomyopathy patients with significantly reduced systolic function: a delayed hyperenhancement cardiac magnetic resonance study. *JACC Cardiovasc Imaging* 2, 34-44 (2009).

(33) Dagres, N. & Hindricks, G. Risk stratification after myocardial infarction: is left ventricular ejection fraction enough to prevent sudden cardiac death? *Eur Heart J* 34, 1964-71 (2013).

(34) Rockey, D.C., Bell, P.D. & Hill, J.A. Fibrosis - A Common Pathway to Organ Injury and Failure. *N Engl J Med* 372, 1138-49 (2015).

(35) Pfeffer, M.A. & Braunwald, E. Ventricular remodeling after myocardial infarction. Experimental observations and clinical implications. *Circulation* 81, 1161-72 (1990).

(36) Pitt, B. *et al.* Eplerenone, a selective aldosterone blocker, in patients with left ventricular dysfunction after myocardial infarction. *N Engl J Med* 348, 1309-21 (2003).

(37) de Lemos, J.A. *et al.* Early intensive vs a delayed conservative simvastatin strategy in patients with acute coronary syndromes: phase Z of the A to Z trial. *JAMA* 292, 1307-16 (2004).

(38) Pizarro, G. *et al.* Long-term benefit of early pre-reperfusion metoprolol administration in patients with acute myocardial infarction: results from the METOCARD-CNIC trial (Effect of Metoprolol in Cardioprotection During an Acute Myocardial Infarction). *J Am Coll Cardiol* 63, 2356-62 (2014).

(39) Armstrong, E.J., Morrow, D.A. & Sabatine, M.S. Inflammatory biomarkers in acute coronary syndromes: part IV: matrix metalloproteinases and biomarkers of platelet activation. *Circulation* 113, e382-5 (2006).

(40) Armstrong, E.J., Morrow, D.A. & Sabatine, M.S. Inflammatory biomarkers in acute coronary syndromes: part III: biomarkers of oxidative stress and angiogenic growth factors. *Circulation* 113, e289-92 (2006).

(41) Armstrong, E.J., Morrow, D.A. & Sabatine, M.S. Inflammatory biomarkers in acute coronary syndromes: part II: acute-phase reactants and biomarkers of endothelial cell activation. *Circulation* 113, e152-5 (2006).

(42) Armstrong, E.J., Morrow, D.A. & Sabatine, M.S. Inflammatory biomarkers in acute coronary syndromes: part I: introduction and cytokines. *Circulation* 113, e72-5 (2006).

(43) Gonzalez-Quesada, C. & Frangogiannis, N.G. Monocyte chemoattractant protein-1/CCL2 as a biomarker in acute coronary syndromes. *Current atherosclerosis reports* 11, 131-8 (2009).

(44) de Lemos, J.A. *et al.* Serial measurement of monocyte chemoattractant protein-1 after acute coronary syndromes: results from the A to Z trial. *J Am Coll Cardiol* 50, 2117-24 (2007).

(45) Chan, D. & Ng, L.L. Biomarkers in acute myocardial infarction. *BMC Med* 8, 34 (2010).

(46) Nakao, K., Minobe, W., Roden, R., Bristow, M.R. & Leinwand, L.A. Myosin heavy chain gene expression in human heart failure. *J Clin Invest* 100, 2362-70 (1997).

(47) Bayes-Genis, A. *et al.* Head-to-head comparison of 2 myocardial fibrosis biomarkers for long-term heart failure risk stratification: ST2 versus galectin-3. *J Am Coll Cardiol* 63, 158-66 (2014).

(48) O'Gara, P.T. *et al.* 2013 ACCF/AHA guideline for the management of ST-elevation myocardial infarction: executive summary: a report of the American College of Cardiology Foundation/American Heart Association Task Force on Practice Guidelines. *Circulation* 127, 529-55 (2013).

(49) Amsterdam, E.A. *et al.* 2014 AHA/ACC guideline for the management of patients with non-ST-elevation acute coronary syndromes: executive summary: a report of the American College of Cardiology/American Heart Association Task Force on Practice Guidelines. *Circulation* 130, 2354-94 (2014).

(50) Dargie, H. Heart failure post-myocardial infarction: a review of the issues. *Heart* 91 Suppl 2, ii3-6; discussion ii31, ii43-8 (2005).

(51) Lefer, D.J. & Bolli, R. Development of an NIH consortium for preclinicAl AssESsment of CARdioprotective therapies (CAESAR): a paradigm shift in studies of infarct size limitation. *J Cardiovasc Pharmacol Ther* 16, 332-9 (2011).

(52) Mullard, A. GSK's darapladib failures dim hopes for anti-inflammatory heart drugs. *Nat Rev Drug Discov* 13, 481-2 (2014).

(53) Pammolli, F., Magazzini, L. & Riccaboni, M. The productivity crisis in pharmaceutical R&D. *Nat Rev Drug Discov* 10, 428-38 (2011).

(54) Pacanowski, M.A., Leptak, C. & Zineh, I. Next-generation medicines: past regulatory experience and considerations for the future. *Clin Pharmacol Ther* 95, 247-9 (2014).

(55) Oni-Orisan, A. & Lanfear, D.E. Pharmacogenomics in heart failure: where are we now and how can we reach clinical application? *Cardiol Rev* 22, 193-8 (2014).

(56) Zeldin, D.C. Epoxygenase pathways of arachidonic acid metabolism. *J Biol Chem* 276, 36059-62 (2001).

(57) Enayetallah, A.E., French, R.A., Thibodeau, M.S. & Grant, D.F. Distribution of soluble epoxide hydrolase and of cytochrome P450 2C8, 2C9, and 2J2 in human tissues. *J Histochem Cytochem* 52, 447-54 (2004).

(58) Delozier, T.C. *et al.* Detection of human CYP2C8, CYP2C9, and CYP2J2 in cardiovascular tissues. *Drug Metab Dispos* 35, 682-8 (2007).

(59) Wu, S., Moomaw, C.R., Tomer, K.B., Falck, J.R. & Zeldin, D.C. Molecular cloning and expression of CYP2J2, a human cytochrome P450 arachidonic acid epoxygenase highly expressed in heart. *J Biol Chem* 271, 3460-8 (1996).

(60) Campbell, W.B., Gebremedhin, D., Pratt, P.F. & Harder, D.R. Identification of epoxyeicosatrienoic acids as endothelium-derived hyperpolarizing factors. *Circ Res* 78, 415-23 (1996).

(61) Fisslthaler, B. *et al.* Cytochrome P450 2C is an EDHF synthase in coronary arteries. *Nature* 401, 493-7 (1999).

(62) Node, K. *et al.* Anti-inflammatory properties of cytochrome P450 epoxygenase-derived eicosanoids. *Science* 285, 1276-9 (1999).

(63) Deng, Y. *et al.* Endothelial CYP epoxygenase overexpression and soluble epoxide hydrolase disruption attenuate acute vascular inflammatory responses in mice. *FASEB J* 25, 703-13 (2011).

(64) Node, K. *et al.* Activation of Galpha s mediates induction of tissue-type plasminogen activator gene transcription by epoxyeicosatrienoic acids. *J Biol Chem* 276, 15983-9 (2001).

(65) Sun, J., Sui, X., Bradbury, J.A., Zeldin, D.C., Conte, M.S. & Liao, J.K. Inhibition of vascular smooth muscle cell migration by cytochrome p450 epoxygenase-derived eicosanoids. *Circ Res* 90, 1020-7 (2002).

(66) Dhanasekaran, A. *et al.* Multiple antiapoptotic targets of the PI3K/Akt survival pathway are activated by epoxyeicosatrienoic acids to protect cardiomyocytes from hypoxia/anoxia. *Am J Physiol Heart Circ Physiol* 294, H724-35 (2008).

(67) Yang, S. *et al.* Cytochrome P-450 epoxygenases protect endothelial cells from apoptosis induced by tumor necrosis factor-alpha via MAPK and PI3K/Akt signaling pathways. *Am J Physiol Heart Circ Physiol* 293, H142-51 (2007).

(68) Katragadda, D., Batchu, S.N., Cho, W.J., Chaudhary, K.R., Falck, J.R. & Seubert, J.M. Epoxyeicosatrienoic acids limit damage to mitochondrial function following stress in cardiac cells. *J Mol Cell Cardiol* 46, 867-75 (2009).

(69) Oni-Orisan, A., Alsaleh, N., Lee, C.R. & Seubert, J.M. Epoxyeicosatrienoic acids and cardioprotection: the road to translation. *J Mol Cell Cardiol* 74, 199-208 (2014).

(70) Revermann, M. *et al.* Soluble epoxide hydrolase deficiency attenuates neointima formation in the femoral cuff model of hyperlipidemic mice. *Arterioscler Thromb Vasc Biol* 30, 909-14 (2010).

(71) Ulu, A. *et al.* Soluble epoxide hydrolase inhibitors reduce the development of atherosclerosis in apolipoprotein e-knockout mouse model. *J Cardiovasc Pharmacol* 52, 314-23 (2008).

(72) Seubert, J.M. *et al.* Role of soluble epoxide hydrolase in postischemic recovery of heart contractile function. *Circ Res* 99, 442-50 (2006).

(73) Sirish, P. *et al.* Unique mechanistic insights into the beneficial effects of soluble epoxide hydrolase inhibitors in the prevention of cardiac fibrosis. *Proc Natl Acad Sci U S A* 110, 5618-23 (2013).

(74) Baum, S.J. *et al.* Fatty acids in cardiovascular health and disease: a comprehensive update. *J Clin Lipidol* 6, 216-34 (2012).

(75) Spector, A.A., Fang, X., Snyder, G.D. & Weintraub, N.L. Epoxyeicosatrienoic acids (EETs): metabolism and biochemical function. *Prog Lipid Res* 43, 55-90 (2004).

(76) Arnold, C. *et al.* Arachidonic acid-metabolizing cytochrome P450 enzymes are targets of {omega}-3 fatty acids. *J Biol Chem* 285, 32720-33 (2010).

(77) Gross, G.J., Falck, J.R., Gross, E.R., Isbell, M., Moore, J. & Nithipatikom, K. Cytochrome P450 and arachidonic acid metabolites: role in myocardial ischemia/reperfusion injury revisited. *Cardiovasc Res* 68, 18-25 (2005).

(78) Poeckel, D. & Funk, C.D. The 5-lipoxygenase/leukotriene pathway in preclinical models of cardiovascular disease. *Cardiovasc Res* 86, 243-53 (2010).

(79) Yuhki, K. *et al.* Roles of prostanoids in the pathogenesis of cardiovascular diseases: Novel insights from knockout mouse studies. *Pharmacol Ther* 129, 195-205 (2011).

(80) Theken, K.N. & Lee, C.R. Genetic variation in the cytochrome P450 epoxygenase pathway and cardiovascular disease risk. *Pharmacogenomics* 8, 1369-83 (2007).

(81) King, L.M. *et al.* Cloning of CYP2J2 gene and identification of functional polymorphisms. *Mol Pharmacol* 61, 840-52 (2002).

(82) Liu, P.Y. *et al.* Synergistic effect of cytochrome P450 epoxygenase CYP2J2*7 polymorphism with smoking on the onset of premature myocardial infarction. *Atherosclerosis* 195, 199-206 (2007).

(83) Spiecker, M. *et al.* Risk of coronary artery disease associated with polymorphism of the cytochrome P450 epoxygenase CYP2J2. *Circulation* 110, 2132-6 (2004).

(84) Dai, D. *et al.* Polymorphisms in human CYP2C8 decrease metabolism of the anticancer drug paclitaxel and arachidonic acid. *Pharmacogenetics* 11, 597-607 (2001).

(85) Lee, C.R., North, K.E., Bray, M.S., Couper, D.J., Heiss, G. & Zeldin, D.C. CYP2J2 and CYP2C8 polymorphisms and coronary heart disease risk: the Atherosclerosis Risk in Communities (ARIC) study. *Pharmacogenet Genomics* 17, 349-58 (2007).

(86) Yasar, U. *et al.* Allelic variants of cytochromes P450 2C modify the risk for acute myocardial infarction. *Pharmacogenetics* 13, 715-20 (2003).

(87) Przybyla-Zawislak, B.D. *et al.* Polymorphisms in human soluble epoxide hydrolase. *Mol Pharmacol* 64, 482-90 (2003).

(88) Koerner, I.P. *et al.* Polymorphisms in the human soluble epoxide hydrolase gene EPHX2 linked to neuronal survival after ischemic injury. *J Neurosci* 27, 4642-9 (2007).

(89) Nelson, J.W., Subrahmanyan, R.M., Summers, S.A., Xiao, X. & Alkayed, N.J. Soluble epoxide hydrolase dimerization is required for hydrolase activity. *The Journal of biological chemistry* 288, 7697-703 (2013).

(90) Argiriadi, M.A., Morisseau, C., Hammock, B.D. & Christianson, D.W. Detoxification of environmental mutagens and carcinogens: structure, mechanism, and evolution of liver epoxide hydrolase. *Proceedings of the National Academy of Sciences of the United States of America* 96, 10637-42 (1999).

(91) Lee, C.R. *et al.* Genetic variation in soluble epoxide hydrolase (EPHX2) and risk of coronary heart disease: The Atherosclerosis Risk in Communities (ARIC) study. *Hum Mol Genet* 15, 1640-9 (2006).

(92) Fornage, M. *et al.* The soluble epoxide hydrolase gene harbors sequence variation associated with susceptibility to and protection from incident ischemic stroke. *Hum Mol Genet* 14, 2829-37 (2005).

(93) Fornage, M., Boerwinkle, E., Doris, P.A., Jacobs, D., Liu, K. & Wong, N.D. Polymorphism of the soluble epoxide hydrolase is associated with coronary artery calcification in African-American subjects: The Coronary Artery Risk Development in Young Adults (CARDIA) study. *Circulation* 109, 335-9 (2004).

(94) Wei, Q. *et al.* Sequence variation in the soluble epoxide hydrolase gene and subclinical coronary atherosclerosis: interaction with cigarette smoking. *Atherosclerosis* 190, 26-34 (2007).

(95) Lee, C.R. *et al.* Genetic variation in soluble epoxide hydrolase (EPHX2) is associated with forearm vasodilator responses in humans. *Hypertension* 57, 116-22 (2011).

(96) Fava, C. *et al.* Homozygosity for the EPHX2 K55R polymorphism increases the long-term risk of ischemic stroke in men: a study in Swedes. *Pharmacogenet Genomics* 20, 94-103 (2010).

(97) Sato, K. *et al.* Soluble epoxide hydrolase variant (Glu287Arg) modifies plasma total cholesterol and triglyceride phenotype in familial hypercholesterolemia: intrafamilial association study in an eight-generation hyperlipidemic kindred. *Journal of human genetics* 49, 29-34 (2004).

(98) Gschwendtner, A. *et al.* Genetic Variation in Soluble Epoxide Hydrolase (EPHX2) Is Associated With an Increased Risk of Ischemic Stroke in White Europeans. *Stroke* 39, 1593-6 (2008).

(99) Burdon, K.P. *et al.* Genetic analysis of the soluble epoxide hydrolase gene, EPHX2, in subclinical cardiovascular disease in the Diabetes Heart Study. *Diabetes & vascular disease research : official journal of the International Society of Diabetes and Vascular Disease* 5, 128-34 (2008).

(100) Wutzler, A. *et al.* Variations in the human soluble epoxide hydrolase gene and recurrence of atrial fibrillation after catheter ablation. *Int J Cardiol* 168, 3647-51 (2013).

(101) Theken, K.N. Cytochrome P450-derived eicosanoids, inflammation, and atherosclerotic cardiovascular disease. *PhD Dissertation* Chapter 6, (2011).

(102) Theken, K.N. *et al.* Evaluation of cytochrome P450-derived eicosanoids in humans with stable atherosclerotic cardiovascular disease. *Atherosclerosis* 222, 530-6 (2012).

(103) Morgan, E.T. Regulation of cytochrome p450 by inflammatory mediators: why and how? *Drug Metab Dispos* 29, 207-12 (2001).

(104) Theken, K.N., Deng, Y., Kannon, M.A., Miller, T.M., Poloyac, S.M. & Lee, C.R. Activation of the acute inflammatory response alters cytochrome P450 expression and eicosanoid metabolism. *Drug Metab Dispos* 39, 22-9 (2011).

(105) Kofeler, H.C., Fauland, A., Rechberger, G.N. & Trotzmuller, M. Mass spectrometry based lipidomics: an overview of technological platforms. *Metabolites* 2, 19-38 (2012).

CHAPTER 2 - CYTOCHROME P450-DERIVED EPOXYEICOSATRIENOIC ACID BIOMARKERS ARE ASSOCIATED WITH THE EXTENT OF CORONARY ARTERY DISEASE IN HUMANS: A TARGETED METABOLOMICS STUDY

Introduction

Despite significant advances in its treatment, CAD remains the leading cause of morbidity and mortality worldwide (1). Consequently, novel therapeutic strategies are needed to further improve outcomes. The discovery of biomarkers involved in the pathogenesis of CAD offers considerable promise to facilitate the development of novel therapeutics by identifying subsets of high-risk patients who would derive the greatest benefit from therapy (2, 3).

In addition to their well-established role as xenobiotic metabolizing enzymes, CYP also metabolize fatty acids to bioactive lipids that regulate numerous cellular and physiologic processes relevant to the pathogenesis of CAD (4). Most notably, CYP epoxygenases from the CYP2C and CYP2J subfamilies metabolize arachidonic acid (AA) into four epoxyeicosatrienoic acid regioisomers (5,6-, 8,9-, 11,12- and 14,15-EET) (5). The EETs elicit potent vasodilatory, anti-inflammatory and cellular protective effects in the cardiovascular system, but are rapidly hydrolyzed by sEH into less biologically active DHETs (6, 7).

An accumulating body of preclinical evidence has demonstrated that promoting the effects of EETs yield potent cardiovascular protective effects in multiple preclinical models (8) including models of vascular inflammation (9), atherosclerosis (10), and myocardial ischemia-reperfusion injury (11). In epidemiologic studies, associations between functional

polymorphisms in genes responsible for EET biosynthesis (*CYP2C8*, *CYP2J2*) and EET hydrolysis (*EPHX2*) and the development of CAD have been reported (12-14). Taken together, these data suggest that modulation of CYP-derived EET levels may be a viable therapeutic strategy for CAD.

We recently reported that multiple clinical factors were associated with low EET levels in patients with established CAD (15), suggesting that quantifying EET metabolite levels may provide insight into factors associated with inter-individual variation in EET biosynthesis and EET hydrolysis (beyond germline genetic polymorphisms). Unfortunately, due to the technical complexity of quantifying EETs, which are present at low concentrations in blood and tissue, these metabolites are not commonly quantified on traditional metabolomic or eicosanoid analytical platforms (16). As a consequence, major gaps in knowledge surrounding the biological and therapeutic importance of CYP-derived EETs in human CAD exist. Thus, a more thorough understanding of the relationship between inter-individual variation in EET levels and extent of CAD in humans is needed to facilitate the translation of these promising therapies into rationally designed clinical trials.

The primary objective of the current study was two-fold: (1) to elucidate the relationship between CYP-derived EET levels and the extent of CAD in patients referred for coronary angiography, and (2) to evaluate the strength of this association relative to eicosanoids derived from the parallel COX, LO, and CYP4A/4F hydroxylase metabolic pathways. In order to accomplish these objectives, a panel of 28 CYP-, COX-, and LO-derived lipid metabolites was quantified in 162 patients with suspected or worsening obstructive CAD using a targeted metabolomics approach.

Materials and Methods

Study population

A cohort of individuals 18-80 years of age referred for coronary angiography to detect new or worsening CAD were identified in the cardiac catheterization laboratories at the University of North Carolina-Chapel Hill between September 2012 and February 2014. Exclusion criteria included severe concurrent illness (such as active pneumonia and acute decompensated heart failure), systemic inflammatory disease, malignancy with active treatment, hematologic disorders affecting platelet function, prior heart transplantation, hematocrit <30%, STEMI, end-stage liver disease, end-stage renal disease on dialysis, and corticosteroid use. Eligible participants provided written informed consent. The study protocol was approved by the UNC Biomedical Institutional Review Board and was completed in accordance with the Declaration of Helsinki.

Classification of CAD extent

Obstructive CAD was defined according to anatomical or physiological 'criteria for revascularization' in recent clinical practice guidelines (17). Briefly, the anatomic criteria for revascularization (PCI or CABG) are the presence of ≥50% stenosis in the left main coronary artery or ≥70% stenosis in one or more of the non-left main coronary arteries. The classification of nonobstructive CAD included those without obstructive CAD that had mild stenosis (10-69% in one or more non-left main coronary arteries and/or 10-49% stenosis in the left main coronary artery), whereas the classification of no apparent CAD included those with no angiographic evidence of CAD (<10% stenosis in all coronary arteries). Coronary stenting impacts the

inflammatory state in the index lesion. Indeed, in-stent restenosis is an inflammatory response to stent placement which can reocclude the artery and drug-eluting stents reduce the risk of restenosis due to their immunosuppressive properties (18). Thus, in order to reflect the extent of CAD at the time of blood sampling unrelated to prior revascularization, only unprotected lesions (lesions not bypassed by collateral vessels, CABG, or stents) in native coronary arteries were considered for classification.

Quantification of eicosanoid metabolite concentrations

Whole blood was drawn in the catheterization lab from the indwelling arterial sheath that had been placed as part of the coronary angiography procedure. Plasma was immediately separated by centrifugation and stored at -80°C for future biomarker analysis. Plasma eicosanoid metabolite concentrations were quantified by targeted liquid chromatography-tandem mass spectrometry (LC-MS/MS) as previously described, with minor modifications (19, 20). Brielfy, plasma (0.25 mL) was diluted in 0.1% acetic acid/5% methanol solution (0.25 mL) containing 0.009 mM butylated hydroxytoluene (BHT), spiked with internal standards (3 ng each of prostaglandin E_2-d4 [PGE2-d4; Cayman Chemical, Ann Arbor, MI], 10,11-dihydroxynondecanoic acid [DiHN] and 10,11- epoxyheptadecanoid acid [EpHep; kindly provided by Dr. Bruce Hammock, University of California-Davis (21)]), and processed by liquid-liquid extraction (0.1% acetic acid/5% methanol and ethyl acetate) to isolate lipids. Extracts in ethyl acetate were then dried by centrifugation under vacuum, covered in argon, and stored at -80°C for future processing. Dried extracts were reconstituted in 80% methanol (containing 10mg/ml BHT) for elution through phospholipid removal columns (Phree, Phenomenex, Torrance, CA), as directed by the manufacturer, for enhanced purification of the

extracts. Extracts were then dried a second time by centrifugation under vacuum and stored at -80°C for future analysis. At the time of analysis, extracts were reconstituted in 50 µL of 30% ethanol and a panel of 34 eicosanoid metabolites (Table 2.2) was quantified by targeted LC-MS/MS as previously described (19, 20). Data was acquired and concentrations were quantified with Analyst software, version 1.5 (Applied Biosystems) using analyte and internal standard peaks for each sample. Extraction efficiency for each sample was determined based on the recovery of the internal standards. Concentration values falling below the lower limit of quantitation were imputed as a concentration equal to half of the lowest standard. Analytes with more than 50% of the values below or above the lower or upper limit of quantitation, respectively, were not included in the analysis (Table 2.2) (19). Among the 28 metabolites that met these criteria, 24 of 28 (86%) had <10% values out of the quantitation range.

Longitudinal evaluation of cardiovascular events

The incidence of cardiovascular events over time was abstracted from the electronic medical record from the time of the index angiography through August 2014. Those who did not present to a hospital or clinic in the UNC health care system (for routine follow-up or emergent care) after the index coronary angiography visit were considered to be lost to follow-up, and were excluded from the analysis. The prespecified primary endpoint was the time to the first occurrence of death due to a cardiovascular cause, hospitalization for a non-fatal ACS event (unstable angina, NSTEMI, STEMI), or hospitalization for a coronary revascularization procedure (PCI or CABG). Clinician reported outcomes were verified from the electronic medical records by two individuals.

Statistical analysis

Data are presented as mean ± standard deviation, median (interquartile range), or count (%) unless otherwise indicated. Study population characteristics were compared across CAD extent using one-way ANOVA, chi-squared test, or Fisher's exact test as appropriate. All analyses were performed using SAS 9.3 (SAS Institute, Cary, NC) unless otherwise indicated.

Metabolite levels and epoxide:diol ratios were not normally distributed and thus log-transformed prior to statistical analysis. Pearson correlations were conducted to determine the correlation between individual metabolites. Established biomarkers of metabolic function within the EET metabolic pathway were used as previously described (19, 22). Briefly, the concentrations of EET regioisomers (14,15-EET; 11,12-EET; and 8,9-EET) and DHET regioisomers (14,15-DHET; 11,12-DHET; 8,9-DHET; and 5,6-DHET) were summed to evaluate total plasma concentrations of EETs and DHETs, respectively.

The primary (sum EETs, sum EETs+DHETs, and 14:15-EET:DHET ratio) and secondary biomarkers of EET biosynthesis and hydrolysis (Table 2.3) were compared across CAD extent by ANOVA. Post-hoc pairwise comparisons were conducted using Fisher's LSD test. A secondary analysis was conducted using a model that adjusts for demographic factors (age, race, sex), clinical factors (diabetes, peripheral artery disease, and prior MI), and medication use (beta blocker, angiotensin-converting enzyme inhibitor) that were independently associated with CAD extent ($P<0.15$) in a multivariable model.

To determine the magnitude of the association between EET levels and CAD extent relative to other demographic and clinical factors, multiple regression analysis was performed. Potential covariates included demographic factors (age, gender, race), indices of CAD extent (index revascularization, index ACS, prior revascularization, presence of collaterals, maximum

coronary artery stenosis), cardiovascular risk factors (obesity, hypertension, diabetes, cigarette smoking, hyperlipidemia, peripheral artery disease, prior acute myocardial infarction, prior transient ischemia attack/stroke), comorbidities (lung disease, heart failure), body mass index, and chronic medication use pre-angiography (angiotensin-converting enzyme inhibitor, angiotensin receptor blockers, aspirin, beta blockers, statins, calcium channel blockers, $P2Y_{12}$ inhibitors, metformin, nitrates, non-statin lipid modifiers, fish oil, proton pump inhibitors). Only covariates with $P<0.15$ in univariate analysis were carried forward into a stepwise multivariate analysis. Collinear variables were removed and covariates with $P<0.15$ were included in the final model.

All metabolomic analyses (global student t-test and FDR analyses, quantitative enrichment analysis [QEA], and Pearson correlations) were performed with Metaboanalyst 3.0 (23). For these analyses where indicated, biomarker comparisons between those with obstructive CAD (N=72) and other patients (N=90) were conducted. Global student t-test analyses were conducted on each of the 28 metabolites in the full panel. Metabolites with $P<0.05$ and FDR $q<0.05$ were considered significantly different across obstructive CAD status. Metabolites were then assigned to 9 distinct eicosanoid metabolic pathways according to their parent substrate and biosynthesis enzyme. QEA was conducted to determine the relative impact of obstructive CAD on the 9 eicosanoid metabolic pathways. P-values (Holm's corrected) were generated from estimated Q-statistics, and pathways were considered significantly enriched when $P<0.05$ and corresponding FDR $q<0.05$.

Longitudinal analyses were conducted in the cohort of patients with reliable follow-up data (N=121). The relationship between baseline CAD extent and time to occurrence of the primary endpoint was assessed with Cox proportional hazards regression. Due to the low number

of events in those with no apparent (0 events) or nonobstructive (4 events) CAD, we proceeded to explore the association between baseline EET levels (tertiles) and risk of future cardiovascular events exclusively within the obstructive CAD patients that had reliable follow-up data (N=63). Likewise, due to the low number of events, the longitudinal analyses were unadjusted and considered exploratory in nature. Kaplan-Meier curves were generated using GraphPad Prism 6.0.

Results

Study population

The demographic and clinical characteristics of the study population are shown in Table 2.1. The extent of CAD was classified based on the results of the coronary angiography. Seventy-two (44%) patients were diagnosed with obstructive CAD (≥70% stenosis in ≥1 major coronary artery), whereas 51 (31%) patients were diagnosed with nonobstructive CAD (10-69% stenosis) and 39 (24%) patients exhibited no apparent CAD (<10% stenosis). Several indices of CAD burden were significantly more prevalent with increasing CAD extent including history of a prior revascularization procedure (P=0.009) and diagnosis of an ACS during the index visit (P<0.001). The prevalence of CAD risk factors and medication use were comparable to previously reported coronary angiography cohorts and reflected clinical practice guidelines (24, 25).

Quantification of eicosanoid metabolite biomarkers

Of the total eicosanoid panel, 28 of the 34 metabolites met the criteria for further analysis (Table 2.2). Plasma concentrations ranged from nM to μM. Plasma EET and DHET regioisomers were positively correlated with each other (Figure 2.1). To minimize redundancy, the sum of the 8,9-, 11,12- and 14,15-EET regioisomers (sum EETs) was calculated and used as a single biomarker (19). In addition, the sum of the EET and DHET regioisomers (sum EETs+DHETs) and the ratio of 14,15-EET to 14,15-DHET (14,15-EET:14,15-DHET ratio) were calculated and used as the primary biomarkers of CYP epoxygenase and sEH metabolic function, respectively (22).

Association of EET metabolic pathway biomarkers and CAD extent

Sum EET levels (the sum of 8,9-, 11,12- and 14,15-EET regioisomers) were inversely associated with CAD extent, such that EET levels in obstructive CAD patients were significantly lower than EET levels in patients with either no apparent CAD or nonobstructive CAD (Figure 2.2a, Table 2.3). After adjusting for covariates (demographic factors, clinical factors, and medication use), the difference between no CAD and obstructive CAD remained significant whereas the difference between nonobstructive CAD and obstructive CAD was not statistically significant (P=0.069). A significant difference in EET levels was not observed between patients with no apparent CAD and nonobstructive CAD. Consistent results were observed with the individual 8,9-, 11,12- and 14,15-EET regioisomers and the DHET metabolites (Table 2.3). Furthermore, higher maximum coronary artery stenosis (the percent narrowing of the most obstructed coronary artery and another indicator of CAD extent) was significantly associated with lower sum EETs (Pearson's r=-0.26, P=0.001).

A similar inverse relationship was observed between CAD extent and sum EETs+DHETs (Figure 2.2b, Table 2.3). In contrast, 14,15-EET:DHET ratio (a biomarker of sEH metabolic function) was not significantly associated with CAD extent (Figure 2.2c, Table 2.3). Similarly, no association was observed between CAD extent and either the sum EET:DHET ratio (Table 2.3) or the 12,13-epoxyoctadecaenoic acid to dihydroxyoctadecaenoic acid (EpOME:DHOME) ratio biomarkers of sEH metabolic function (P=0.992).

In a multivariate analysis, the strongest predictor of EET levels was CAD extent; there was an inverse association (Table 2.4). A similar relationship existed with sum EETs+DHETs (r^2=0.08, P<0.001). The presence of collaterals, compensatory anastomotic connections between the distal portion of an occluded coronary artery and a different coronary artery without an

intervening capillary bed (26), was also associated with lower EET levels. Female sex was associated with significantly higher EET levels. Moreover, use of certain medications was associated with higher (statins, calcium channel blockers) and lower (beta blockers, angiotensin-converting enzyme inhibitors) EET levels (Table 2.4).

Identification of altered eicosanoid pathways across obstructive CAD status

Among all of the individual eicosanoid metabolites quantified, 11 were significantly altered across obstructive CAD status (Figure 2.3a and 2.3b; Table 2.5). The three EET (8,9-, 11,12-, and 14,15-EET) and four DHET (5,6-, 8,9-, 11,12-, and 14,15-DHET) regioisomers were among the 11 analytes associated with CAD extent. In order to determine the most enriched eicosanoid metabolic pathways across obstructive CAD status, we subsequently grouped the metabolites into pathways based on their parent substrate and biosynthesis enzyme. Metabolites within the same pathway tended to be positively correlated with each other (Figure 2.1). QEA revealed that only the AA-derived CYP epoxide and AA-derived sEH diol pathways were significantly associated with the presence of obstructive CAD (Figure 2.3c; Table 2.6).

Risk of Future Cardiovascular Events

Participants were prospectively followed to determine the relationship between CAD extent and risk of subsequent cardiovascular events. Follow-up data was available in 121 (75%) of the enrolled participants, and the median length of follow-up was 1.0 years. Cardiovascular death, a non-fatal ACS event or a coronary revascularization procedure occurred in 21 participants (0, 10, and 11 events, respectively). CAD extent at baseline was significantly

associated with incidence of a cardiovascular event, with 17 of the 21 events occurring in those with obstructive CAD (Figure 2.4a), similar to previous studies (25).

Although the presence of obstructive CAD is associated with lower EET levels, considerable inter-individual variability in EET levels existed within the obstructive CAD group (median [IQR]: 639 [286] pg/mL). Consequently, we explored the relationship between baseline EET levels and risk of a future cardiovascular event exclusively within the subset of patients with obstructive CAD. A stepwise inverse relationship between EET levels and cardiovascular event incidence appeared to exist, such that the highest number of events was observed in those in the lowest EET level tertile (Figure 2.4b); however, this relationship was not statistically significant.

Discussion

This is the first study that reports a relationship between circulating EET metabolite levels and the extent of CAD in humans. In a well characterized CAD population, we observed that the presence of obstructive CAD is significantly and independently associated with lower circulating EET levels. Furthermore, the association between obstructive CAD and lower EET levels (a) correlates with lower CYP epoxygenase metabolic function, but not higher sEH metabolic function, and (b) is significantly more pronounced than other eicosanoid metabolism pathways. Collectively, these findings demonstrate that patients with obstructive CAD are predisposed to low EET metabolite levels secondary to suppressed EET biosynthesis, and suggest that novel strategies that promote the effects of EETs may have therapeutic promise in patients with obstructive CAD.

It has become increasingly clear that CYPs metabolize AA into bioactive eicosanoids with potent cellular and physiologic effects in the cardiovascular system (27). Most notably, CYP epoxygenase-derived EETs elicit protective effects in preclinical models (6, 7), including vasodilation by hyperpolarizing vascular smooth muscle cells (28, 29), anti-inflammation by attenuating NF-κB signaling (30, 31), and anti-apoptosis by promoting PI3K/Akt signaling (32, 33). Consequently, promoting the effects of EETs, most notably by inhibiting sEH and increasing endogenous EET levels, has emerged as a cardiovascular protective therapeutic strategy with potential clinical utility (34). Due to the technical complexity of measuring EETs, which are not quantified on traditional metabolomic or eicosanoid panels (16), major gaps in knowledge surrounding the biological and therapeutic importance of this pathway in human cardiovascular disease remain (8). Importantly, characterizing the relationship between EET

metabolite levels and CAD extent in humans is central to a better understanding of the functional role of this pathway in the initiation and progression of CAD. Through application of a highly sensitive and specific targeted LC-MS/MS assay that simultaneously quantifies CYP-, COX-, and LO-derived lipid metabolites in human plasma, the current study identified a significant inverse relationship between EET levels and angiographic extent of CAD. Moreover, pathway analyses revealed that these differences were significantly more pronounced than metabolites derived from COX, LO and CYP hydroxylase pathways. Taken together, these findings suggest that CYP-derived EETs may play an important role in the pathogenesis and progression of CAD in humans.

In the current study, CAD extent was also associated with lower sum EETs+DHETs, but surprisingly not EET:DHET ratios. These data suggest that the inverse association between EET levels and CAD extent was mediated by suppression of CYP epoxygenase metabolic function (EET biosynthesis), and not an increase in sEH metabolic function (EET hydrolysis). Accordingly, it is well-established that inflammatory stimuli suppress CYP-mediated xenobiotic metabolism through a variety of mechanisms, including cytokine-mediated transcriptional downregulation of CYP expression (35); fittingly, inflammatory stimuli also drive the development and progression of CAD (36). We recently demonstrated that hepatic CYP epoxygenase expression, hepatic CYP epoxygenase metabolic function, and plasma EET levels are suppressed in an atherogenic diet mouse model of inflammatory non-alcoholic fatty liver disease (37). In contrast, no changes in sEH expression or EET hydrolysis were observed. Although most studies have investigated the impact of inflammation on hepatic CYP expression and function, cytokines have also been reported to downregulate CYP epoxygenase expression in endothelial cells of the vasculature (38). Moreover, hepatic, renal, pulmonary and myocardial

Cyp2c/2j expression and EET biosynthesis were suppressed in an endotoxin mouse model of acute inflammation (39). Altogether, these findings suggest that suppression of CYP-mediated EET biosynthesis may be a key pathological consequence of the inflammation-mediated development and progression of CAD. Future studies are necessary to elucidate the mechanisms underlying the association between lower EET levels and advanced CAD in humans.

A few additional studies have quantified plasma EET levels in patients at risk for or with established cardiovascular disease. Ramirez et al. found that presence of the metabolic syndrome was associated with lower circulating EET levels (40). Furthermore, Minuz et al. reported that patients with renovascular disease had lower circulating EETs compared to both healthy volunteer and essential hypertension controls (41). In contrast, we previously reported that patients with established stable CAD (≥50% coronary artery stenosis or a prior revascularization procedure) had significantly higher plasma EET levels compared to a population of healthy volunteer controls at low risk for CAD (15). This observed increase in EET levels was driven by suppressed sEH metabolic function, such that the median 14,15-EET:DHET ratio was significantly higher in patients with established CAD compared to controls (0.37 versus 0.18, respectively). In the present study, no differences in sEH metabolic function were observed across CAD extent, and the median 14,15-EET:DHET ratio observed in those with no apparent (0.35), nonobstructive (0.33) and obstructive (0.34) CAD was comparable to the CAD population of the prior study. It is important to note that the controls in the previous study were healthy volunteers that had no risk factors for cardiovascular disease or chronic medication use. Consequently, multiple potential confounding factors may have driven the observed suppression of sEH metabolic function in CAD cases in the previous study. The present study, however, employed a cross-sectional design within a population of patients referred for coronary

angiography; thus, the reference population with no apparent angiographic evidence of CAD had similar CAD risk factors and medication use compared to those with non-obstructive and obstructive CAD. Importantly, the inverse association between EET levels and CAD extent was independent of clinical factors and medication use in an adjusted model. Future prospective studies will be needed to delineate the direct effects of risk factor control and medications on EET biosynthesis and hydrolysis over time in patients at risk for or with established CAD.

The relationship between metabolite biomarkers of the EET metabolic pathway and prognosis in patients with established CAD has not been studied to date. Consequently, in a secondary analysis, we explored the relationship between inter-individual variation in EET metabolite levels and risk of a future adverse cardiovascular event in patients with obstructive CAD at baseline. We observed a stepwise relationship across the EET tertiles where the highest event incidence occurred in those with the lowest EET levels at baseline. Although this relationship was not statistically significant and should be observed with caution due to the small number of events, these findings are biologically plausible considering the anti-inflammatory and protective effects of EETs in numerous preclinical models of cardiovascular disease. Furthermore, these data are consistent with a previously reported inverse association between circulating EET and MCP-1 concentrations (a pro-inflammatory chemokine predictive of poor prognosis in CAD (42)), in which patients with stable CAD in the lowest and middle EET tertiles had significantly higher MCP-1 levels compared to those in the highest EET tertile (22). These preliminary observations underscore the need to rigorously evaluate the relationship between EET metabolite levels and the risk of cardiovascular events in a larger population.

Although the current study is the largest to date evaluating the relationship between CYP-derived eicosanoid metabolites and CAD in humans, our analysis has limitations that must be

acknowledged. The cross-sectional design precludes us from establishing causality between increasing CAD extent and lower EET levels because there is no data on which event occurred first. Furthermore, coronary angiography is an inexact method to quantify the burden and extent of CAD. Our analysis also included multiple statistical comparisons. To account for the possibility of false-positive findings, a false discovery rate (FDR) was calculated for each comparison. The association between obstructive CAD and lower EET and DHET levels had a FDR of 5% or less, which enhances confidence in our results. Lastly, this was a single-center study and our results may not be generalizable to other CAD populations. Validation of the observed relationships in an independent cohort will ultimately be necessary.

Recent failures in CAD drug development suggest that innovative approaches are needed to mitigate increasing attrition rates and more successfully translate novel therapies into clinical practice (43-45). Compared to the conventional 'one-size fits all' methodology to drug development, a precision medicine approach has the potential to increase the probability of success for promising therapeutic candidates (46). Although targeted therapies are routinely used in oncology, this strategy has not been readily adopted in CAD. Biomarkers offer considerable promise to prospectively identify subsets of CAD patients at high risk of experiencing a cardiovascular event that exhibit dysfunction in a specific pathway (putative responders), thereby enabling novel therapies that target the pathway to maximize their therapeutic effect and improve outcomes. Our findings collectively demonstrate that obstructive CAD is significantly and independently associated with lower circulating EET levels secondary to suppressed EET biosynthesis. These results offer important insight into the potential functional role of CYP-derived EETs in the pathogenesis and progression of CAD in humans, and suggest that promoting the effects of EETs may have therapeutic utility in CAD patients predisposed to low

EET levels. Importantly, agents that promote the effects of EETs are in development for a variety of therapeutic indications (47-49). In parallel, technology for the high-throughput quantification of CYP-derived eicosanoids in the clinical setting is advancing (50). Consequently, our results set the foundation for future clinical research in this area, including the rational design of prospective, biomarker-guided interventional studies in targeted subsets of the CAD population (low EET levels) with enriched potential to derive clinical benefit from emerging EET-promoting therapies.

Figures

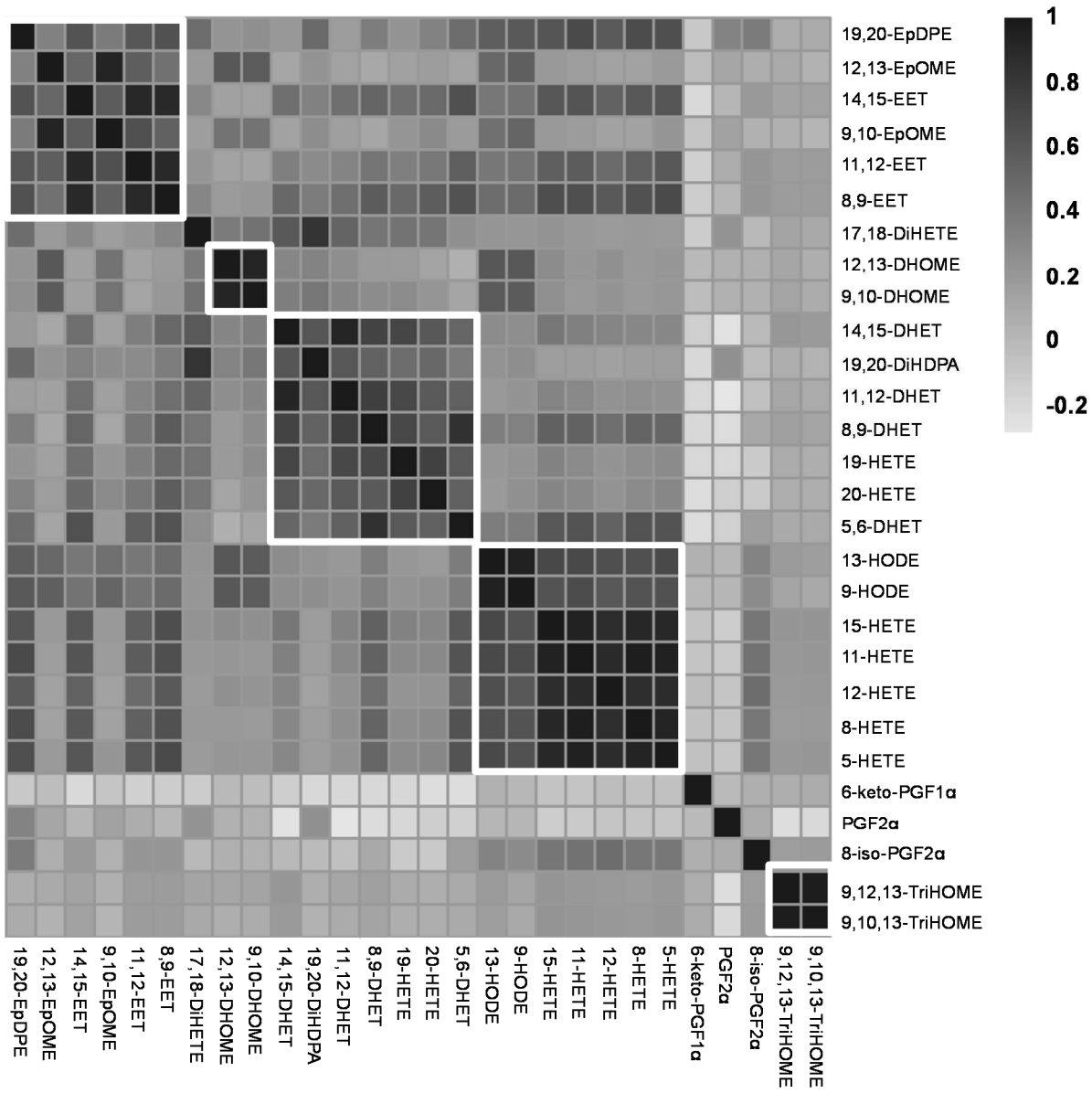

Figure 2.1. Correlation matrix of eicosaniods. Scale above indicates Pearson correlation coefficients on log-transformed data. Dark and light indicate positive and negative correlations, respectively. All 28 quantafiable metabolites are listed. Analyses revealed that eicosanoids

within the same pathway (by class and substrate) tend to be positively correlated (white borders indicate strongest clusters). DHET, dihydroxyeicosatrienoic acid; DHOME, dihydroxyoctadecaenoic acid; DiHDPA, dihydroxy-docosapentaenoic acid; DiHETE, dihydroxytetraenoic acid; EET, epoxyeicosatrienoic acid; EpDPE, epoxydocosapentaenoic acid; EpOME, epoxyoctadecaenoic acid; HETE, hydroxyeicosatetraenoic acid; HODE, hydroxyoctadecadienoic acids; PGF1α, prostaglandin F1alpha; PGF2α, prostaglandin F2alpha; TriHOME, trihydroxyoctadecenoic acid

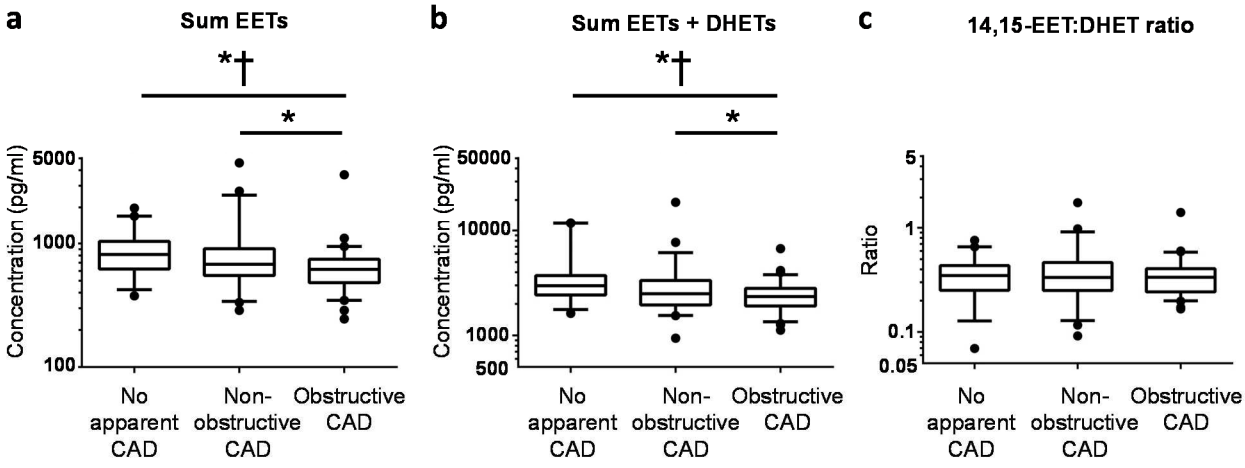

Figure 2.2 Plasma biomarkers of cytochrome P450 (CYP)-mediated epoxyeicosatrienoic acids (EETs) biosynthesis and hydrolysis across coronary artery disease (CAD) extent. (a) Sum EETs were inversely associated with CAD extent across no apparent CAD (N=39), nonobstructive CAD (N=51), and obstructive CAD (N=72) patients (ANOVA: unadjusted P=0.003, adjusted P=0.004). (b) A significant inverse association was also observed with sum EETs+DHETs (ANOVA: unadjusted P=0.001, adjusted P=0.001). (c) In contrast, the 14,15-EET:DHET ratio was not associated with CAD extent (ANOVA: unadjusted P=0.693, adjusted P=0.859). Untransformed data are presented as median (line), interquartile range (box), and 95% confidence intervals (whiskers) on a log scale. *P<0.05 in unadjusted pairwise comparisons. †P<0.05 in adjusted pairwise comparisons. DHET, dihydroxyeicosatrienoic acid

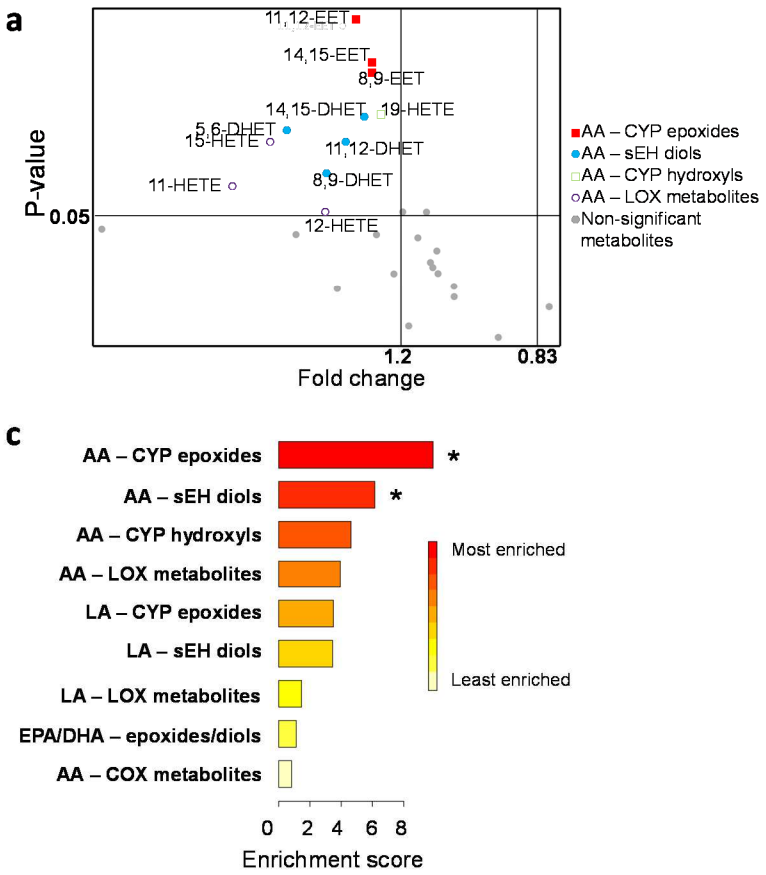

Figure 2.3 Enrichment of eicosanoid pathways across obstructive coronary artery disease (CAD) status. Twenty-eight eicosanoid metabolites were assigned to 9 distinct eicosanoid metabolic pathways according to their parent substrate (arachidonic acid [AA], linoleic acid [LA], eicosapentaenoic acid [EPA]/docosahexaenoic acid [DHA] fatty acids) and biosynthesis enzyme (cytochrome P450 [CYP], lipoxygenase [LO], cyclooxygenase [COX], soluble epoxide hydrolase [sEH]), and compared between obstructive CAD patients (N=72) and all other patients (N=90). The EPA and DHA derived metabolites (all derived from CYP or sEH biosynthesis) were combined into one pathway due to the low number of metabolites in that group. (a) A volcano plot shows how each of the 28 individual metabolites within pathways differs between obstructive CAD patients and all other patients. Metabolites in the upper left box (fold

change>1.2 and P<0.05) were considered to be significantly altered. P-value decreases as Y-axis value increases. (b) A list (rank ordered by p-value with accompanying false discovery rate [FDR] and fold change) of the top metabolites that significantly differed by obstructive CAD status is provided. (c) Quantitative enrichment analysis (QEA) revealed that AA-derived epoxides (P=0.01; FDR q=0.01) and AA-derived diols (P=0.049; FDR q=0.03) were enriched across obstructive CAD status relative to parallel pathways. *QEA P<0.05 (Holm's corrected) and FDR q<0.05. DHET, dihydroxyeicosatrienoic acid; EET, epoxyeicosatrienoic acid; FC, fold change; HETE, hydroxyeicosatetraenoic acid

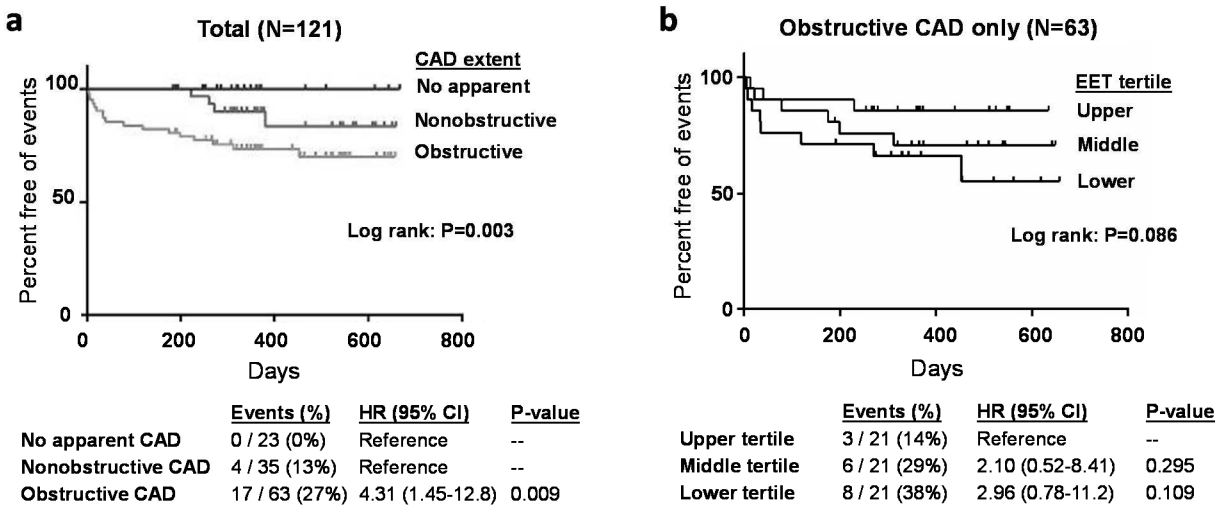

	Events (%)	HR (95% CI)	P-value
No apparent CAD	0 / 23 (0%)	Reference	--
Nonobstructive CAD	4 / 35 (13%)	Reference	--
Obstructive CAD	17 / 63 (27%)	4.31 (1.45-12.8)	0.009

	Events (%)	HR (95% CI)	P-value
Upper tertile	3 / 21 (14%)	Reference	--
Middle tertile	6 / 21 (29%)	2.10 (0.52-8.41)	0.295
Lower tertile	8 / 21 (38%)	2.96 (0.78-11.2)	0.109

Figure 2.4 Coronary artery disease (CAD) extent, epoxyeicosatrienoic acid (EETs), and risk of subsequent cardiovascular events. Kaplan-Meier curves were generated for incidence of the primary endpoint (time to the occurrence of death from cardiovascular causes, acute coronary syndrome event, or coronary revascularization procedure) according to (a) CAD extent at baseline in all patients with reliable follow-up data (N=121) and (b) EET levels at baseline (tertiles) exclusively within the subset of patients with obstructive CAD (N=63). The log rank P-value (unadjusted) for each Kaplan-Meier curve is provided. Below the curves, the number and frequency of events within each CAD extent and EET tertile group, along with the unadjusted hazard ratio (HR), 95% confidence interval (CI) and P-value, is provided. Due to the lack of events in those with no apparent CAD at baseline, the no apparent CAD and nonobstructive CAD groups were combined and served as a single referent group.

Tables

Table 2.1 Characteristics of the total study population and across the angiographic extent of coronary artery disease (CAD)

Characteristic	Total (N=162)	No apparent CAD (N=39)	Nonobstructive CAD (N=51)	Obstructive CAD (N=72)	P
Demographics					
Age (years)	61.8 ± 10.3	58.2 ± 10.4	62.1 ± 9.9	63.6 ± 10.2	0.028
Female	70 (43.2%)	18 (46.2%)	22 (43.1%)	30 (41.7%)	0.901
African American	34 (21.0%)	10 (25.6%)	11 (21.6%)	13 (18.1%)	0.640
Past medical history					
Current/recent (<1 year) smoker	46 (28.4%)	11 (28.2%)	15 (29.4%)	20 (27.8%)	0.980
Obese (body mass index ≥30 kg/m^2)	79 (48.8%)	25 (64.1%)	19 (37.3%)	35 (48.6%)	0.041
History of hypertension	130 (80.3%)	28 (71.2%)	41 (80.4%)	61 (84.7%)	0.263
History of diabetes	51 (31.5%)	9 (23.1%)	14 (27.5%)	28 (38.9%)	0.174
History of hyperlipidemia	111 (68.5%)	23 (59.0%)	34 (66.7%)	54 (75.0%)	0.209
History of peripheral artery disease	20 (12.4%)	2 (5.1%)	5 (9.8%)	13 (18.1%)	0.130
Prior myocardial infarction	24 (14.8%)	1 (2.6%)	6 (11.8%)	17 (23.6%)	0.006
Prior revascularization	56 (34.6%)	6 (15.4%)	18 (35.3%)	32 (44.4%)	0.009
Medication use					
ACE inhibitor use	73 (45.1%)	14 (35.9%)	18 (35.3%)	41 (56.9%)	0.025
ARB use	33 (20.4%)	10 (25.6%)	13 (25.5%)	10 (13.9%)	0.187
Aspirin use	122 (75.3%)	29 (74.4%)	37 (72.6%)	56 (77.8%)	0.793
Beta blocker use	99 (61.1%)	16 (41.0%)	32 (62.8%)	51 (70.8%)	0.009
Statin use	123 (75.9%)	27 (69.2%)	39 (76.5%)	57 (79.2%)	0.502
Calcium channel blocker use	46 (28.4%)	13 (33.3%)	14 (27.5%)	19 (26.4%)	0.729
Cardiac catheterization laboratory					
ACS on presentation	29 (17.9%)	3 (7.7%)	3 (5.9%)	23 (31.9%)	<0.001
Presence of collateral	20 (12.4%)	5 (12.8%)	4 (7.8%)	11 (15.3%)	<0.001
Stenosis in most severe vessel (%)	50 (80)	0 (0)	40 (25)	90 (15)	<0.001

ACE, angiotensin-converting enzyme; ACS, acute coronary syndrome; ARB, angiotensin receptor blocker. Data presented as mean ± standard deviation, median (interquartile range), or count (%).

One-way ANOVA across CAD extent was performed for continuous variables and Chi-square test or Fisher's exact test was performed for categorical variables as appropriate.

Table 2.2 List of all eicosanoid metabolites

Pathway	Analyte	Plasma Concentration (pg/mL)
AA – CYP epoxides	14,15-EET	299 (139)
	11,12-EET	163 (86)
	8,9-EET	197 (94)
	5,6-EET*	<LLOQ
AA – sEH diols	14,15-DHET	937 (433)
	11,12-DHET	594 (322)
	8,9-DHET	244 (150)
	5,6-DHET	253 (160)
AA – CYP hydroxyls	20-HETE	1,188 (762)
	19-HETE	646 (348)
AA – LO metabolites	15-HETE	937 (503)
	12-HETE	63 (42)
	11-HETE	5,706 (3,600)
	9,12,13-TriHOME	688 (798)
	9,10,13-TriHOME	9,150 (12,200)
	8-HETE	12,628 (6,656)
	5-HETE	2,243 (1,759)
AA – COX metabolites	8-iso-PGF2α	29 (12)
	6-keto-PGF1α	51 (21)
	PGB2*	<LLOQ
	PGD2*	<LLOQ
	PGE2*	<LLOQ
	PGF2α	238 (712)
	TXB2*	<LLOQ
LA – LO metabolites	13-HODE	21,356 (11,200)
	9-HODE	15,222 (9,844)
LA – CYP epoxides	12,13-EpOME	1,714 (1,000)
	9,10-EpOME	4,200 (2,867)
LA – sEH diols	12,13-DHOME	2,809 (1,881)
	9,10-DHOME	1,742 (1,274)
EPA/DHA – CYP/sEH metabolites	19,20-DiHDPA	1,193 (706)
	17,18-DiHETE	2,794 (1,937)
	19,20-EpDPE	1,659 (1,019)
	17,18-EpETE*	<LLOQ

AA, arachidonic acid; COX, cyclooxygenase; CYP, cytochrome P450; DHA, docosahexaenoic acid; DHET, dihydroxyeicosatrienoic acid; DHOME, dihydroxyoctadecaenoic acid; DiHDPA, dihydroxy-docosapentaenoic acid; DiHETE, dihydroxytetraenoic acid; EET, epoxyeicosatrienoic acid; EPA; eicosapentaenoic acid; EpDPE, epoxydocosapentaenoic acid; EpETE, epoxyeicosatetraenoic acid; EpOME, epoxyoctadecaenoic acid; HETE, hydroxyeicosatetraenoic acid; HODE, hydroxyoctadecadienoic acids; LA, linoleic acid; LO, lipoxygenase; PGB2, prostaglandin B2; PGD2, prostaglandin D2; PGE2, prostaglandin E2; PGF1α, prostaglandin F1alpha; PGF2α, prostaglandin F2alpha; sEH, soluble epoxide hydrolase; TriHOME, trihydroxyoctadecenoic acid; TXB2, thromboxane B2.

Data presented as median (interquartile range).

*Analyte plasma levels were below lower limit of quantification (LLOQ) and could not be accurately quantified

Table 2.3 Comparison of plasma cytochrome P450 (CYP) epoxygenase-derived and soluble epoxide hydrolase (sEH)-derived arachidonic acid metabolite biomarkers across coronary artery disease (CAD) extent

Analyte	No apparent CAD (N=39)	Nonobstructive CAD (N=51)	Obstructive CAD (N=72)	P [a]
AA – CYP epoxides (pg/mL)				
14,15-EET	368 (170)	295 (170)	286 (117)*†	0.006
11,12-EET	192 (89)	171 (99)	152 (85)*†	0.003
8,9-EET	235 (125)	205 (112)	189 (87)*†	0.007
Sum EETs [b]	815 (417)	678 (356)	618 (258)*†	0.003
AA – sEH diols (pg/mL)				
14,15-DHET	1,007 (568)	971 (449)	845 (442)*	0.006
11,12-DHET	657 (393)	633 (367)*	563 (257)*	0.005
8,9-DHET	300 (193)	229 (206)	217 (110)*	0.039
5,6-DHET	290 (145)	244 (198)	229 (122)*	0.028
Sum DHETs	2,324 (1305)	2,084 (1605)	1,956 (875)*	0.004
CYP epoxygenase function (pg/mL)				
Sum EETs + DHETs	3,321 (1,441)	2,737 (1,670)	2,593 (997)*†	0.001
sEH function (ratio)				
14,15-EET:14,15-DHET	0.35 (0.18)	0.33 (0.22)	0.34 (0.16)	0.693
11,12-EET: 11,12-DHET	0.28 (0.19)	0.29 (0.19)	0.27 (0.16)	0.413
8,9-EET: 8,9-DHET	0.80 (0.44)	0.81 (0.51)	0.78 (0.31)	0.880
Sum EETs: DHETs [b]	0.37 (0.22)	0.38 (0.22)	0.36 (0.18)	0.649

DHET, dihydroxyeicosatrienoic acid; EET, epoxyeicosatrienoic acid. Data presented as median (interquartile range)

[a]One-way ANOVA was performed on log-transformed data

[b]Plasma concentrations of the 5,6-EET regioisomer were below the limit of quantification and not included in the calculation

*P<0.05 versus no apparent CAD (Fisher's LSD). †P<0.05 versus nonobstructive CAD (Fisher's LSD)

Table 2.4 Multivariate relationships between clinical factors and plasma epoxyeicosatrienoic acids (N=162)

	Parameter Estimate	SE	Partial R^2	P [a]
CAD extent	-0.047	0.017	0.067	0.001
Female	0.106	0.028	0.049	0.003
Presence of collaterals	-0.100	0.041	0.032	0.016
Statin use	0.096	0.033	0.024	0.037
Beta blocker use	-0.081	0.029	0.036	0.009
Calcium channel blocker use	0.063	0.030	0.022	0.039
ACE inhibitor use	-0.050	0.028	0.016	0.077
Full model			0.244	<0.001

ACE, angiotensin-converting enzyme; CAD, coronary artery disease; SE standard error
[a]Factors with P<0.15 in the univariate analysis were included in the multivariate analysis.

Table 2.5 Comparison of plasma eicosanoid metabolites across obstructive coronary artery disease (CAD) status

Analyte (pg/mL)	No obstructive CAD (n=90)	Obstructive CAD (n=72)	P [a]	FDR q
AA – CYP epoxides				
14,15-EET	312 (164)	286 (117)	0.002	0.021
11,12-EET	181 (99)	152 (85)	<0.001	0.019
8,9-EET	211 (100)	189 (87)	0.002	0.021
AA – sEH diols				
14,15-DHET	981 (490)	845 (442)	0.006	0.031
11,12-DHET	642 (367)	563 (257)	0.009	0.034
8,9-DHET	252 (194)	217 (110)	0.019	0.059
5,6-DHET	268 (177)	229 (122)	0.008	0.034
AA – CYP hydroxyls				
19-HETE	694 (408)	588 (267)	0.006	0.031
20-HETE	1,270 (827)	1,087 (664)	0.076	0.134
AA – LO metabolites				
15-HETE	1,021 (620)	847 (382)	0.010	0.036
11-HETE	6,361 (3,944)	5,361 (3,222)	0.024	0.066
12-HETE	70 (42)	53 (38)	0.047	0.101
8-HETE	13,028 (8,100)	12,094 (5,639)	0.068	0.134
5-HETE	2,426 (1,707)	2,068 (1,478)	0.076	0.134
9,12,13-TriHOME	718 (742)	668 (829)	0.240	0.292
9,10,13-TriHOME	9,478 (742)	8,406 (13,552)	0.304	0.340
LA – CYP epoxides				
12,13-EpOME	1,786 (918)	1,652 (1,127)	0.083	0.135
9,10-EpOME	4,350 (2,562)	3,817 (2,921) *	0.046	0.101
LA – sEH diols				
12,13-DHOME	2,911 (1,916)	2,466 (1,929)	0.109	0.170
9,10-DHOME	1,961 (1,162)	1,432 (1,158) *	0.046	0.101
LA – LO metabolites				
13-HODE	21,839 (10,222)	19,661 (12,561)	0.141	0.208
9-HODE	15,489 (8,711)	14,728 (10,611)	0.180	0.230
EPA/DHA – epoxides/diols				
19,20-EpDPE	1,666 (1,477)	1,641 (888)	0.253	0.295
19,20-DiHDPA	1,206 (741)	1,188 (596)	0.581	0.603
17,18-DHET	2,806 (2,184)	2,671 (1,740)	0.181	0.230
AA – COX metabolites				
8-iso-PGF2α	29 (11)	28 (12)	0.157	0.220
6-keto-PGF1α	51 (20)	50 (21)	0.748	0.748
PGF2α	229 (539)	326 (788)	0.379	0.409

See Table 2.2 for abbreviations.

Data presented as median (interquartile range)

[a]Student's t-test was performed on log-transformed data followed by FDR calculations for multiple testing

Table 2.6 Quantitative enrichment analysis (QEA) results on eicosanoid metabolic pathways

	Metabolites (N)	Actual Q	Expected Q	P [a]	FDR q
AA – CYP epoxides	**3**	**6.14**	**0.62**	**0.010**	**0.010**
AA – sEH diols	**4**	**3.82**	**0.62**	**0.050**	**0.028**
AA – CYP hydroxyls	2	2.87	0.62	0.163	0.070
AA – LO metabolites	5	2.45	0.62	0.247	0.090
LA – CYP epoxides	2	2.17	0.62	0.290	0.090
LA – sEH diols	2	2.14	0.62	0.290	0.090
LA – LO metabolites	4	0.91	0.62	0.663	0.284
EPA/DHA – epoxides/diols	3	0.70	0.62	0.663	0.341
AA – COX metabolites	3	0.51	0.62	0.663	0.374

AA, arachidonic acid; COX, cyclooxygenase; CYP, cytochrome P450; DHA, docosahexaenoic acid; EPA; eicosapentaenoic acid; FDR, false discovery rate; LA, linoleic acid; LO, lipoxygenase; sEH, soluble epoxide hydrolase

[a]Global test was performed on log-transformed data and p-values (Holm's corrected) were generated from estimated Q-statistics

REFERENCES

(1) Mozaffarian, D. *et al.* Heart disease and stroke statistics-2015 update: a report from the American Heart Association. *Circulation* 131, e29-e322 (2015).

(2) Ganesh, S.K. *et al.* Genetics and genomics for the prevention and treatment of cardiovascular disease: update: a scientific statement from the American Heart Association. *Circulation* 128, 2813-51 (2013).

(3) Waldman, S.A. & Terzic, A. Molecular insights provide the critical path to disease mitigation. *Clin Pharmacol Ther* 95, 3-7 (2014).

(4) Bernhardt, R. Cytochromes P450 as versatile biocatalysts. *J Biotechnol* 124, 128-45 (2006).

(5) Zeldin, D.C. Epoxygenase pathways of arachidonic acid metabolism. *J Biol Chem* 276, 36059-62 (2001).

(6) Deng, Y., Theken, K.N. & Lee, C.R. Cytochrome P450 epoxygenases, soluble epoxide hydrolase, and the regulation of cardiovascular inflammation. *J Mol Cell Cardiol* 48, 331-41 (2010).

(7) Imig, J.D. Epoxides and soluble epoxide hydrolase in cardiovascular physiology. *Physiol Rev* 92, 101-30 (2012).

(8) Oni-Orisan, A., Alsaleh, N., Lee, C.R. & Seubert, J.M. Epoxyeicosatrienoic acids and cardioprotection: the road to translation. *J Mol Cell Cardiol* 74, 199-208 (2014).

(9) Revermann, M. *et al.* Soluble epoxide hydrolase deficiency attenuates neointima formation in the femoral cuff model of hyperlipidemic mice. *Arterioscler Thromb Vasc Biol* 30, 909-14 (2010).

(10) Ulu, A. *et al.* Soluble epoxide hydrolase inhibitors reduce the development of atherosclerosis in apolipoprotein e-knockout mouse model. *J Cardiovasc Pharmacol* 52, 314-23 (2008).

(11) Seubert, J.M. *et al.* Role of soluble epoxide hydrolase in postischemic recovery of heart contractile function. *Circ Res* 99, 442-50 (2006).

(12) Spiecker, M. *et al.* Risk of coronary artery disease associated with polymorphism of the cytochrome P450 epoxygenase CYP2J2. *Circulation* 110, 2132-6 (2004).

(13) Lee, C.R., North, K.E., Bray, M.S., Couper, D.J., Heiss, G. & Zeldin, D.C. CYP2J2 and CYP2C8 polymorphisms and coronary heart disease risk: the Atherosclerosis Risk in Communities (ARIC) study. *Pharmacogenet Genomics* 17, 349-58 (2007).

(14) Lee, C.R. *et al.* Genetic variation in soluble epoxide hydrolase (EPHX2) and risk of coronary heart disease: The Atherosclerosis Risk in Communities (ARIC) study. *Hum Mol Genet* 15, 1640-9 (2006).

(15) Theken, K.N. *et al.* Evaluation of cytochrome P450-derived eicosanoids in humans with stable atherosclerotic cardiovascular disease. *Atherosclerosis* 222, 530-6 (2012).

(16) Kofeler, H.C., Fauland, A., Rechberger, G.N. & Trotzmuller, M. Mass spectrometry based lipidomics: an overview of technological platforms. *Metabolites* 2, 19-38 (2012).

(17) Levine, G.N. *et al.* 2011 ACCF/AHA/SCAI guideline for percutaneous coronary intervention: a report of the American College of Cardiology Foundation/American Heart Association Task Force on Practice Guidelines and the Society for Cardiovascular Angiography and Interventions. *Catheter Cardiovasc Interv* 82, E266-355 (2013).

(18) Hansson, G.K. & Libby, P. The immune response in atherosclerosis: a double-edged sword. *Nat Rev Immunol* 6, 508-19 (2006).

(19) Zha, W. *et al.* Functional characterization of cytochrome P450-derived epoxyeicosatrienoic acids in adipogenesis and obesity. *J Lipid Res* 55, 2124-36 (2014).

(20) Edin, M.L. *et al.* Endothelial expression of human cytochrome P450 epoxygenase CYP2C8 increases susceptibility to ischemia-reperfusion injury in isolated mouse heart. *FASEB J* 25, 3436-47 (2011).

(21) Newman, J.W., Watanabe, T. & Hammock, B.D. The simultaneous quantification of cytochrome P450 dependent linoleate and arachidonate metabolites in urine by HPLC-MS/MS. *J Lipid Res* 43, 1563-78 (2002).

(22) Schuck, R.N. *et al.* Cytochrome P450-derived eicosanoids and vascular dysfunction in coronary artery disease patients. *Atherosclerosis* 227, 442-8 (2013).

(23) Xia, J., Mandal, R., Sinelnikov, I.V., Broadhurst, D. & Wishart, D.S. MetaboAnalyst 2.0--a comprehensive server for metabolomic data analysis. *Nucleic Acids Res* 40, W127-33 (2012).

(24) Fihn, S.D. *et al.* 2012 ACCF/AHA/ACP/AATS/PCNA/SCAI/STS guideline for the diagnosis and management of patients with stable ischemic heart disease: executive summary: a report of the American College of Cardiology Foundation/American Heart Association task force on practice guidelines, and the American College of Physicians, American Association for Thoracic Surgery, Preventive Cardiovascular Nurses Association, Society for Cardiovascular Angiography and Interventions, and Society of Thoracic Surgeons. *Circulation* 126, 3097-137 (2012).

(25) Maddox, T.M. *et al.* Nonobstructive coronary artery disease and risk of myocardial infarction. *JAMA* 312, 1754-63 (2014).

(26) Koerselman, J., van der Graaf, Y., de Jaegere, P.P. & Grobbee, D.E. Coronary collaterals: an important and underexposed aspect of coronary artery disease. *Circulation* 107, 2507-11 (2003).

(27) Roman, R.J. P-450 metabolites of arachidonic acid in the control of cardiovascular function. *Physiol Rev* 82, 131-85 (2002).

(28) Campbell, W.B., Gebremedhin, D., Pratt, P.F. & Harder, D.R. Identification of epoxyeicosatrienoic acids as endothelium-derived hyperpolarizing factors. *Circ Res* 78, 415-23 (1996).

(29) Fisslthaler, B. *et al.* Cytochrome P450 2C is an EDHF synthase in coronary arteries. *Nature* 401, 493-7 (1999).

(30) Node, K. *et al.* Anti-inflammatory properties of cytochrome P450 epoxygenase-derived eicosanoids. *Science* 285, 1276-9 (1999).

(31) Deng, Y. *et al.* Endothelial CYP epoxygenase overexpression and soluble epoxide hydrolase disruption attenuate acute vascular inflammatory responses in mice. *FASEB J* 25, 703-13 (2011).

(32) Dhanasekaran, A. *et al.* Multiple antiapoptotic targets of the PI3K/Akt survival pathway are activated by epoxyeicosatrienoic acids to protect cardiomyocytes from hypoxia/anoxia. *Am J Physiol Heart Circ Physiol* 294, H724-35 (2008).

(33) Yang, S. *et al.* Cytochrome P-450 epoxygenases protect endothelial cells from apoptosis induced by tumor necrosis factor-alpha via MAPK and PI3K/Akt signaling pathways. *Am J Physiol Heart Circ Physiol* 293, H142-51 (2007).

(34) Imig, J.D. & Hammock, B.D. Soluble epoxide hydrolase as a therapeutic target for cardiovascular diseases. *Nature Reviews Drug Discovery* 8, 794-805 (2009).

(35) Morgan, E.T. Regulation of cytochrome p450 by inflammatory mediators: why and how? *Drug Metab Dispos* 29, 207-12 (2001).

(36) Hansson, G.K. Inflammation, atherosclerosis, and coronary artery disease. *N Engl J Med* 352, 1685-95 (2005).

(37) Schuck, R.N. *et al.* The cytochrome P450 epoxygenase pathway regulates the hepatic inflammatory response in fatty liver disease. *PLoS One* 9, e110162 (2014).

(38) Kessler, P., Popp, R., Busse, R. & Schini-Kerth, V.B. Proinflammatory mediators chronically downregulate the formation of the endothelium-derived hyperpolarizing factor in arteries via a nitric oxide/cyclic GMP-dependent mechanism. *Circulation* 99, 1878-84 (1999).

(39) Theken, K.N., Deng, Y., Kannon, M.A., Miller, T.M., Poloyac, S.M. & Lee, C.R. Activation of the acute inflammatory response alters cytochrome P450 expression and eicosanoid metabolism. *Drug Metab Dispos* 39, 22-9 (2011).

(40) Ramirez, C.E. *et al.* Arg287Gln variant of EPHX2 and epoxyeicosatrienoic acids are associated with insulin sensitivity in humans. *Prostaglandins Other Lipid Mediat* 113-115, 38-44 (2014).

(41) Minuz, P. *et al.* Altered release of cytochrome p450 metabolites of arachidonic acid in renovascular disease. *Hypertension* 51, 1379-85 (2008).

(42) de Lemos, J.A. *et al.* Serial measurement of monocyte chemoattractant protein-1 after acute coronary syndromes: results from the A to Z trial. *J Am Coll Cardiol* 50, 2117-24 (2007).

(43) Yellon, D.M. & Hausenloy, D.J. Myocardial reperfusion injury. *N Engl J Med* 357, 1121-35 (2007).

(44) Mullard, A. GSK's darapladib failures dim hopes for anti-inflammatory heart drugs. *Nat Rev Drug Discov* 13, 481-2 (2014).

(45) Pammolli, F., Magazzini, L. & Riccaboni, M. The productivity crisis in pharmaceutical R&D. *Nat Rev Drug Discov* 10, 428-38 (2011).

(46) Pacanowski, M.A., Leptak, C. & Zineh, I. Next-generation medicines: past regulatory experience and considerations for the future. *Clin Pharmacol Ther* 95, 247-9 (2014).

(47) Shen, H.C. & Hammock, B.D. Discovery of inhibitors of soluble epoxide hydrolase: a target with multiple potential therapeutic indications. *J Med Chem* 55, 1789-808 (2012).

(48) Falck, J.R. *et al.* 14,15-Epoxyeicosa-5,8,11-trienoic Acid (14,15-EET) surrogates: carboxylate modifications. *J Med Chem* 57, 6965-72 (2014).

(49) Podolin, P.L. *et al.* In vitro and in vivo characterization of a novel soluble epoxide hydrolase inhibitor. *Prostaglandins Other Lipid Mediat* 104-105, 25-31 (2013).

(50) Zhu, P., Peck, B., Licea-Perez, H., Callahan, J.F. & Booth-Genthe, C. Development of a semi-automated LC/MS/MS method for the simultaneous quantitation of 14,15-epoxyeicosatrienoic acid, 14,15-dihydroxyeicosatrienoic acid, leukotoxin and leukotoxin diol in human plasma as biomarkers of soluble epoxide hydrolase activity in vivo. *J Chromatogr B Analyt Technol Biomed Life Sci* 879, 2487-93 (2011).

CHAPTER 3 - THE RELATIONSHIP BETWEEN *EPHX2* P.LYS55ARG POLYMORPHISM AND SURVIVAL IN PATIENTS FOLLOWING AN ACUTE MYOCARDIAL INFARCTION

Introduction

Cardiovascular disease (CVD) has been the leading cause of mortality in the US for over a century. Most notably, acute myocardial infarction (AMI) events, complications of CVD, are a primary source of the mortality associated with this illness (1). Identification and characterization of the key pathways underlying the pathophysiology of post-AMI complications will facilitate the development of novel therapeutic strategies that reduce the risk of adverse outcomes following AMI.

Arachidonic acid is metabolized by CYP epoxygenase enzymes to form bioactive EETs (2). CYP2J and CYP2C epoxygenases are the primary sources of all four EET regioisomers (5,6-, 8,9-, 11,12-, and 14,15-EETs) (3). EETs are lipophilic compounds containing highly-reactive epoxide functional groups. The predominant fate of EETs is through rapid metabolism by soluble epoxide hydrolase (sEH) into diol functional group-containing dihydroxyeicosatrienoic acids (DHETs), which generally have less biological activity than their epoxide-containing counterpart (4, 5).

EPHX2 codes for human sEH (6), is located on chromosomal region 8p21-p12 (6), contains 19 exons, and has a coding sequence that spans 555 amino acids (7). Furthermore, *EPHX2* has considerable genetic heterogeneity (8). Many of these SNPs are non-synonymous

and alter sEH hydrolysis activity *in vitro* (8). *EPHX2* is also expressed in a multitude of cell types and tissues; importantly, it is highly expressed in the cardiovascular system incluing the myocardium and blood vessels (9).

The two most common non-synonymous SNPs in *EPHX2* have been found to decrease (p.Arg287Gln) or increase (p.Lys55Arg) the activity of sEH *in vitro.* (8, 10) Specifically, the Arg287Gln polymorphism is located at an area of the enzyme responsible for dimerization; its presence is thought to reduce the stability of the homodimer (8) which is necessary for hydrolase activity (11). The Lys55Arg polymorphism is similarly not located near the catalytic site responsible for hydrolase activity (8), but is located in a domain that allows for increased stabilization of the dimer (12). Lys55Arg and Arg287Gln are not in linkage disequilibrium (13).

The allele frequencies for Arg287Gln are approximately 8% and 10% in African American and Caucasian populations respectively (14). Lys55Arg has been studied less extensively then Arg287Gln, but is the most common functional SNP in the population (15, 16). The allele frequencies for Lys55Arg are approximately 22% and 7% in African Americans and Caucasians. (14)

Due to their cardioprotective effects in preclinical models, EETs are a promising therapeutic target for AMI. Accumulating preclinical evidence from *in vitro*, *ex vivo*, and *in vivo* models of AMI demonstrates that EETs directly protect the myocardium following ischemia via a variety of mechanisms (5, 17, 18). Thus, genetic variation in sEH activity may have important clinical implications.

Since pharmacological tools that directly and specifically manipulate sEH to modulate EET levels are currently not available for clinical use, investigators have relied on genetic observational studies to understand the role of the EET metabolic pathway in human CVD.

Associations between functional genetic polymorphisms in *EPHX2* and the risk of developing CVD have been reported in humans (13, 19-23). The Arg287Gln variant has been linked to reduced plasma cholesterol and triglyceride concentrations in patients with familial hypercholesterolemia (24), reduced risk of coronary artery calcification in African-Americans (20, 21), increased ischemic stroke risk in white Europeans (25), carotid artery calcified plaque in Europeans (26), improved vascular dysfunction in African Americans (27), and increased risk of atrial fibrillation recurrence after catheter ablation (28). The Lys55Arg polymorphism is associated with higher sEH metabolic function *in vivo* and is linked to development of CAD in Caucasian patients (13), ischemic stroke in Swedish men (23), and vascular dysfunction in Caucasian volunteers (22).

Taken together with the preclinical evidence, these data suggest that the EET metabolic pathway may be important in the pathogenesis of CAD in humans and that therapeutic interventions that promote the cardioprotective effects of EETs by modulation of sEH offer considerable promise as a novel therapeutic strategy to reduce sequelae following AMI; however, key questions remain to be addressed prior to translation of EET-promoting strategies into successful proof-of-concept phase I and II clinical trials. Evaluation of functional variants in *EPHX2* and prognosis in AMI patients has not been completed.

In collaboration with Dr. John Spertus (Mid America Heart Institute) and Dr. Sharon Cresci (Washington University School of Medicine), the Craig Lee lab has previously investigated the association of both *EPHX2* Lys55Arg and *EPHX2* Arg287Gln genotype with 5-year survival in a 2-center cohort of CAD patients hospitalized for an ACS event including unstable angina or AMI (INFORM). Compared to noncarriers, *EPHX2* Arg55 variant allele carriers had a significantly higher risk of death (22.4% vs. 15.3%; HR 1.50, 95% CI 1.02-2.22,

P=0.042), however, no association was observed with *EPHX2* Arg287Gln (15.2% vs 17.4%; HR 0.88, 95% CI 0.55-1.41, P=0.597). A race-stratified analysis was conducted to account for the potential confounding effects of population stratification. Associations in Caucasians were consistent with the overall cohort, and persisted after adjusting for demographic and clinical covariates predictive of prognosis. The magnitude of the associations were comparable to established prognostic predictors (e.g., diabetes: HR 2.2, 95% CI 1.5-3.2, P<0.01). However, associations were not evaluated in African Americans, due to a small sample size (N=124) and suboptimal power (29).

The association between *EPHX2* Lys55Arg genotype and survival provide support for our hypothesis that CAD patients predisposed to greater EET hydrolysis exhibit poorer prognosis post-ACS. However, evaluation of this association specifically in the AMI subpopulation remains necessary to determine whether CAD patients predisposed to greater EET hydrolysis also exhibit poorer prognosis post-AMI. Furthermore, replication in a larger independent population of AMI patients would provide further confirmation to the initial results and facilitate race-stratified analyses in African Americans. Finally, elucidation of the underlying mechanisms responsible for this association is necessary. Consequently, the objective of the present study was to determine the relationship between *EPHX2* p.Lys55Arg polymorphism and survival in patients recently admitted for an AMI.

Materials and methods

Study participants

INFORM is a prospective, observational study of consecutive ACS patients at 2 US hospitals (Kansas City, KS) from March 2001 to October 2002 (30, 31). Only Caucasian and African American subjects were included for analyses. Of these subjects, genetic information was available in 667 ACS patients including 273 unstable angina patients, 204 NSTEMI patients, and 190 STEMI patients. Analyses in the present study were done on the 394 Caucasian and African American subjects presenting with an AMI.

Translational Research Investigating Underlying Disparities in Acute Myocardial Infarction Patients' Health Status (TRIUMPH) is a prospective, observational study of 4,340 consecutive AMI adult patients across 24 US hospitals from April 2005 to December 2008, as described (32-34). DNA was available in 2,979 participants. Analyses in the present study were conducted on Caucasians and African Americans (n=2712) with genetic information.

Diagnosis of AMI was based on standard definitions as described earlier above (Chapter 1: Acute myocardial infarction) and in the literature (35, 36). Briefly, patients who had an elevated troponin value in the setting of symptoms or ECG changes during the index hospitalization were diagnosed as having an AMI. All participating institutions obtained approval from their respective ethics committees and all participants signed an informed consent during the initial screening period, as reported previously (32, 37).

Genotyping

The *EPHX2* p.Lys55Arg polymorphism (rs41507953) was genotyped in the TRIUMPH

Applied Genomics Core facility using the PSQ 96 HS Pyrosequencer automated genotyping system (Biotage AB, Uppsala, Sweden) (38).

Measurement of circulating biomarkers

Plasma troponin T, high sensitivity C reactive protein (hs-CRP), and pro-B-type natriuretic peptide (proBNP) were measured in a subset of TRIUMPH subjects at baseline, 1 month, and 6 months following index hospitalization (32). For follow-up visits at 1 month and 6 months, blood was collected by trained medical personnel via an in-home visit or with a kit that was mailed to the subject and sent back to the lab for processing for subjects who agreed to provide follow-up samples. Data on 24% of subjects for all 3 blood collection periods were available. Analysis of blood for biomarker levels were done at the Clinical Reference Laboratory (Lenexa, KS).

CV outcomes

In the current analysis, all-cause mortality was captured as the primary endpoint by query of the Social Security Death Masterfile or the Center for Disease Control National Death Index. Mortality is reported at 3-month, 6-month, 9-month, 1-year, 2 year, 3-year, 4-year, and 5-year time intervals in INFORM. For TRIUMPH, mortality is reported at 1 month and every 6 months thereafter (i.e., 7-month, 13-month, etc.) up to 55-month interval.

Statistical analysis

For baseline characteristics, continuous variables were compared using Student's T-test and categorical variables were compared using chi-square or Fisher's exact test if >20% of

expected cell frequencies were >5. *EPHX2* Lys55Arg did not deviate from Hardy-Weinberg equilibrium in INFORM or TRIUMPH within Caucasian and African American populations, thus further statistical analyses were carried forward in these subsets. Genotype-survival associations were evaluated in each cohort using (a) a Cox proportional hazards model (unadjusted and adjusted) and (b) the log-rank test to compare Kaplan-Meier survival curves across genotypes. In TRIUMPH, two adjustment models were used. Model 1 corrected for age sex and race. Model 2 corrected for pre-specified baseline covariates known to predict adverse outcomes in AMI patients including age, race, sex, AMI type (STEMI or NSTEMI), diabetes, and AMI treatment strategy (medical management or PCI/CABG) (29). In INFORM, only unadjusted analyses were conducted since adjusted models had been previously used in the full ACS cohort (Chapter 1: The epoxyeicosatrienoic acid metabolic pathway and parallel pathways of eicosanoid metabolism) (29). Analyses were completed assuming either an additive mode of inheritance or a dominant mode of inheritance. Genotype-survival race-stratified analyses were also conducted. For biomarker analysis, continuous variables were compared in a dominant mode of inheritance using Student's t-test. Biomarker analyses were repeated with an additive mode of inheritance with the non-parametric Kruskal-Wallis test to lessen the impact of skew that occurs with smaller number in each cell. Analyses were performed using SAS 9.2 (SAS Institute, Cary, NC). $P<0.05$ was considered to be statistically significant. Power calculations were conducted using Quanto (39). Mortality estimates to derive power were based on 4.5-year mortality (36% of patients had 4.5-year mortablity data available) as a conservative estimate since 5-year mortality data was not available.

Results

INFORM baseline characteristics in ACS population

In the full ACS population, 79% of participants were Caucasian and 36% were female. The 5-year mortality rate in the full population was 17%. Patient characteristics by genotype are shown in Table 3.1. No significant differences in baseline characteristics were observed by genotype other than African American race which was more prevalent in the Arg55 Carrier group warranting race-stratified analyses. The MAF was 11.7% in Caucasians and 21.7% in African Americans, consistent with previous literature (14). Of the total INFORM ACS population with *EPHX2* Lys55Arg data available (n=667), 394 participants were AMI patients. Of these, 88% were Caucasian and the total 5-year mortality rate was 17%.

EPHX2 Lys55Arg genotype and mortality in the AMI population from INFORM

EPHX2 Lys55Arg genotype was significantly associated with survival following an AMI in the total INFORM study population where variant carriers had a significantly higher risk of death (Figure 3.1a). This association persisted in the Caucasian subset (Figure 3.1b).

TRIUMPH baseline characteristics

Of the 2712 participants with genetic information, the average age was 59, 76% were Caucasian, 32% were female, 44% were suffering from a STEMI, and 76% underwent coronary artery vascularization during the index hospitalization (Table 3.2). Patient characteristics by race are shown in Table 3.2. There were significant differences in baseline demographics (age and sex), ACS classification type, past medical history (smoking, hypertension, diabetes,

hyperlipidemia, heart failure, MI), cholesterol (high density lipoprotein [HDL], triglycerides), treatment strategy, and beta blocker use between Caucasians and African Americans, warranting race-stratified genetic analyses. The MAF was 11.2% in Caucasians and 22.4% in African Americans, consistent with prior reports (14). Patient characteristics by genotype for the total population, Caucasians, and African Americans are shown in Tables 3.3-3.5. In the total population, variant allele carriers were less likely to be admitted for a STEMI and more likely to be using beta blocker medication. Within the Caucasian subset, there were no significant differences in baseline characteristics. In African Americans, variant carriers had higher LDL, higher cholesterol levels, higher beta-blocker use, and lower aspirin use.

EPHX2 Lys55Arg genotype and mortality in TRIUMPH

Follow-up data were not available in the full population as shown (Table 3.6). Complete follow-up data at 3 years was available in 75% of the population. The observed 3-year mortality rate was 12.1% overall (327 deaths), 10.1% in Caucasiancs (206 deaths), and 18.3% in African Americans (121 deaths).

EPHX2 Lys55Arg genotype was not significantly associated with survival following an AMI in the total TRIUMPH study population (Log-rank P=0.144; Figure 3.2a). Based on mortality estimates generated from the subset of participants with full 3-year mortality data, genotype was not significantly associated with 3-year mortality (All Subjects: HR 1.19 95% CI 0.94-1.51, P=0.156; Figure 3.2a). Furthermore, there was no association between genotype and survival in race-stratified analyses (Caucasians: log-rank P=0.742; Figure 3.2b-c; African Americans: log-rank P=0.269; Figure 3.2b-c). Genotype was not significantly associated with 3-year mortality (Caucasians: HR 0.96 95% CI 0.68-1.36, P=0.831; African Americans: HR 0.84

95% CI 0.61-1.17, P=0.303; Figure 3.2b-c). The association remained non-significant after adjusting for demographic and clinical covariates (Table 3.7).

Using an additive mode of inheritance (unadjusted analyses) in the combined Caucasian and African American population, Arg/Arg subjects (n=75) had a HR of 1.62-fold greater risk of projected 3-year mortality relative to Lys/Lys patients following AMI, however this did not meet the threshold of significance (95% 0.88-2.96, P=0.194). No significant differences across genotype were observed using an additive mode of inheritance in unadjusted analyses for projected 3-year mortality data (Caucasians: P=0.675; African Americans: P=0.758; Figure 3.3, Table 3.8).

EPHX2 Lys55Arg genotype and cardiac biomarkers in TRIUMPH

To provide mechanistic insight into the genotype-prognosis association, Troponin T (myocardial injury), hs-CRP (inflammation), and proBNP (myocardial stretch) were measured in a subset of subjects. There was no significant difference between troponin T levels in Arg55 variant carriers compared to wildtype individuals at baseline (P=0.656), 1 month (P=0.057), and 6 months (P=0.215) following AMI (Table 3.9). Similarly no differences in hs-CRP were observed at baseline, 1 month, and 6 months (P=0.899, P=0.059, P=0.931, respectively). No differences were observed in proBNP between Lys/Lys and Arg55 carriers. Using the additive mode of inheritance, genotype was not associated with Troponin T at baseline (P=0.563) or 6 months (P=0.225). However, Troponin T levels were significantly associated with genotype at 1 month across Lys/Lys (0.02 ± 0.02 mg/dL), Lys/Arg (0.02 ± 0.03), and Arg/Arg patients (0.25 ± 0.96 mg/dL). No differences were observed in hs-CRP and proBNP levels across genotype using the additive mode of inheritance at baseline, 1 month, and 6 months following AMI.

Discussion

Our group has previously observed an association between *EPHX2* p.Lys55Arg genotype with 5-year survival in a cohort of ACS patients (INFORM) (29), where *EPHX2* Arg55 variant allele carriers had a significantly higher risk of death. The objective of the present study was to determine the relationship between *EPHX2* Lys55Arg polymorphism and survival in patients recently admitted for an AMI. Using the AMI subpopulation of INFORM as well as a larger cohort of AMI patients (TRIUMPH), we determined that *EPHX2* Lys55Arg was significantly associated with mortality in AMI patients from INFORM, but that this association was not validated in the larger population of AMI patients from TRIUMPH.

Although TRIUMPH has a larger sample size compared to INFORM and thus should have more power to detect differences, it is important to reiterate that full mortality data was not available for analysis in this cohort. Whereas INFORM data had 5-year mortality data in all patients available for analysis, no patients in TRIUMPH had 5-year mortality data available and only 36% had full 4.5 year data. Thus, power to validate a genotype-survival association in TRIUMPH was limited. Based on the available mortality data at 3 years, we had 74% power to detect an association assuming a hazard ratio (HR) of 1.4 in a dominant model. With full 4.5-year mortality, we anticipate 80% power (Table 3.10). Additionally, it is qualitatively evident in the results of the INFORM AMI patients that survival curves don't begin to separate until 3 years post-AMI. Thus, although speculative in nature, it is plausible that a similar pattern could occur in TRIUMPH with complete mortality data. A final analysis when full 5-year mortality data are available is necessary to rule out the possibility that lack of sufficient power prevented the positive INFORM results from being replicated in TRIUMPH. Full 4-year mortality data will be available in summer 2015 and 5-year data is anticipated to be available within a year thereafter.

Biologically, separation of survival curves at 3 years indicates that the EET metabolic pathway may play an important role in the chronic period after AMI (rather than the acute period), further justifying the need for longer term mortality follow-up in TRIUMPH.

Considering the well-established cardioprotective/anti-inflammatory effects of EETs in preclinical studies (4) and to gain more insight into a potential association between genotype and survival, we explored the impact of *EPHX2* Lys55Arg on established plasma biomarkers of myocardial injury, inflammation, and remodeling in TRIUMPH subjects at baseline, 1 month, and 6 months following AMI. In the overall population, we determined that for the majority of biomarkers and time points, genotype was not associated with levels. However, we observed that *EPHX2* Lys55Arg genotype was associated with plasma troponin T at 1 month using an additive mode of inheritance (P=0.038), where mean levels in Arg/Arg patients were 12.5-fold higher than levels in Lys/Lys and Lys/Arg. Using a dominant mode of inheritance, mean plasma troponin T levels in Arg55 carriers were 2-fold greater than mean levels in noncarriers (P=0.057). These associations are in the direction hypothesized since we would predict that enhanced sEH-derived hydrolysis would have a deleterious effect and suggest that Arg/Arg subjects may have evidence of increased myocardial infarct size following AMI compared to Lys/Lys and Lys/Arg participants. It is important to note, however, that clinical guidelines recommend measuring troponin levels within hours of symptom onset for AMI diagnosis and potentially once on day 3 or 4 after symptom onset for post-AMI prognosis. Furthermore, the rise and falling pattern of troponin levels is similarly important for prognosis following AMI as the levels themselves (40). Thus the clinical relevance of an association between genotype and a single 1-month troponin level is unknown. Nevertheless, troponin levels have been found to predict survival in CVD patients not suffering from an AMI (41). Overall, results of this

exploratory analysis must be interpreted with caution due to small numbers in the Arg/Arg group (n=19) from loss to follow-up in biomarker sample collection (Kruskal-Wallis non-parametric analyses were conducted to alleviate the effects of skewed biomarker data which are inflated with small data). Additionally, these results underscore the need for follow-up TRIUMPH analysis with full 5-year mortality data to determine if the relationship between genotype and troponin T following AMI contributes to an association between genotype and survival.

As mentioned, insufficient power may be the reason why there was a lack of genotype-survival association. However, if current findings in the TRIUMPH cohort hold when full mortality data are available, this would be discordant with several previous studies that have shown that *EPHX2* Lys55Arg polymorphism is associated with the risk of cardiovascular disease (13, 22, 23). Nevertheless, several key studies reported a lack of association between Lys55Arg and the incidence of CVD. There was no relationship between *EPHX2* Lys55Arg genotype and restenosis in a population of CAD patients following PCI (42). *EPHX2* Arg287Gln, but not Lys55Arg was found to be associated with the incidence of atrial fibrillation following catheter ablation (28). Likewise, *EPHX2* Arg287Gln, but not Lys55Arg was associated with the occurrence of ischemic stroke in Caucasians with multiple risk factors for CVD (43). Interestingly, although *in vitro* transfection of the Arg287Gln polymorphism into cell lines has been found to reduce cell death compared to non-transfected cells in both cardiomyocytes (44) and neuronal cells (10) undergoing ischemic injury, transfection with Lys55Arg in the same respective models did not cause any significant change in the rate of cell death. Although our lab previously did not find an association between *EPHX2* Arg287Gln and mortality following ACS in the full INFORM cohort, further analysis investigating the association between *EPHX2* Arg287Gln and survival following AMI is needed to better understand the role of *EPHX2*

genetic variation in prognosis following CVD.

The aforementioned lack of consistent findings across studies suggests that the relationship between genetic markers and CVD is highly complex and may involve other factors. Indeed, associations between CAD and *EPHX2* variation are more pronounced in cigarette smokers (13, 21). We recently reported that multiple clinical factors were associated with low EET levels in patients with established CAD (45), suggesting that quantifying EET metabolite levels may provide insight into factors associated with inter-individual variation in EET biosynthesis and EET hydrolysis (beyond genetic polymorphisms). The quantification of EET levels in humans would provide further insight into this association; circulating levels of EETs was not obtained sample from the TRIUMPH or INFORM cohort. Prior evidence, however, functionally links *EPHX2* Lys55Arg genotype to sEH activity and suggests that eicosanoids are altered by this polymorphism in humans (8, 13). Furthermore, we reported that EET levels were associated with the extent of CAD in the largest observational human study to date that quantifies EET levels in humans with CVD (Chapter 2: Figure 1). We also showed in exploratory analyses that baseline EETs may predict the risk of CV events in obstructive CAD patients (Chapter 2: Figure 3). Investigation of the relationship between baseline EET levels and survival in a large cohort of AMI patients would provide further insight into a genotype-prognosis association (or lack thereof) with *EPHX2* Lys55Arg genotype following AMI.

There are some limitations to this study. First, mortality rates were determined using the full sample size as the denominator (for all analyses including the power calculations), thus they underestimate the actual mortality rate. However, using sample size based on the proportion of patients with full mortality data available as the denominator grossly overestimates the sample size (i.e., 40% mortality rate at 4.5 years in total population), because this approach assumes

incorrectly that patients who did not survive would have had full follow-up data 5 years had they not died during this time interval. In the absence of full mortality data, future interim analyses should include a projected/estimated mortality calculation for a more accurate estimation of the mortality rate. Second, even with full mortality data available, power calculations reveal that we are underpowered to detect associations in the African American subset (Table 3.10). However, it is well established that African Americans are poorly represented in clinical trials despite having a greater risk of CVD. TRIUMPH is one of the largest registries to provide detailed information on clinical, genetic, and metabolic characteristics in a racially-diverse population. Indeed, one of the goals of TRIUMPH was to investigate racial disparities in post-AMI outcomes. Consequently, 16 of the 24 recruitment sites were located in large urban centers to enable enrollment of a racially diverse population (32). When full mortality data are available, the relatively large sample size of African Americans in TRIUMPH provides more power to detect associations in this subpopulation, which was one of the limitations of the INFORM cohort. Low MAF and small numbers in TRIUMPH preclude analysis in populations who are not African American or Caucasian. The association between variants in *EPHX2* and CVD in Asian and Hispanic population has not been investigated and is a potential future direction. Third, smaller effect sizes than anticipated (HR<1.5) would limit power to detect significant associations even in Caucasians when full mortality data are available. Nevertheless, 80% power exists to detect an HR of 1.4 in the overall population when full mortality data are available. Furthermore, HR (95% CI) was 2.33 (1.43-3.79) and 2.42 (1.40-4.19) in INFORM total population and Caucasian cohorts, respectively. This indicates that assuming a HR of 1.4 or 1.5 (along with using 4.5-year mortality rates) to estimate power is conservatively low for the incoming 5-year mortality data. Moreover, effect sizes may be larger in the presence of an

environmental exposure such as current cigarette smoker or other clinically distinct high-risk subset such as hs-CRP >2 g/dL (46). Our group and others have shown that associations between *EPHX2* and CAD risk are most pronounced in cigarette smokers (47). Evaluation of such interactions is an important area of further investigation.

In conclusion, we observed that *EPHX2* Lys55Arg was associated with 5-year mortality following AMI, but we were not able to replicate this in an independent cohort of AMI patients. Future analysis with full 5-year mortality data is needed as a follow-up to this interim analysis to validate the association with adequate power.

Figures

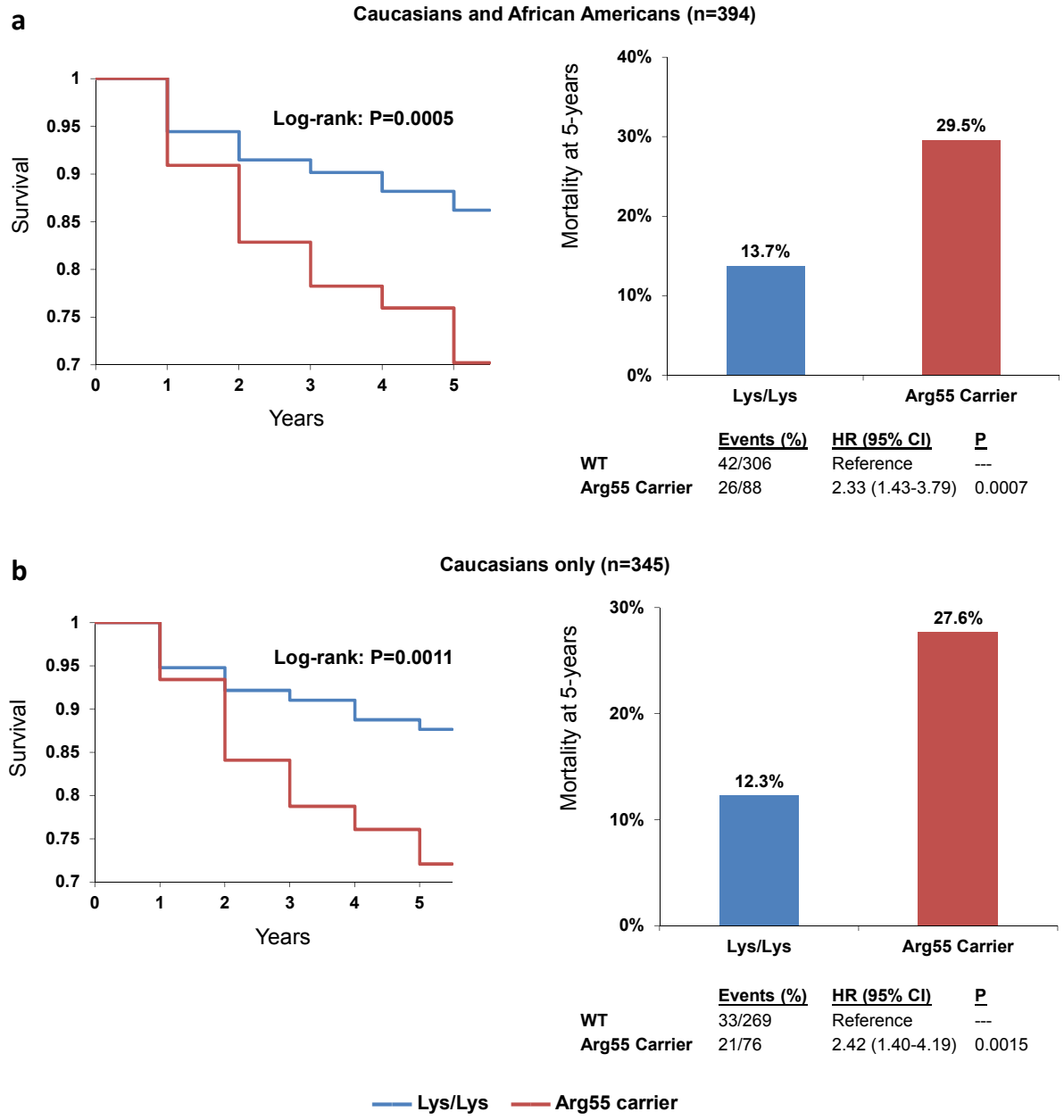

Figure 3.1 Mortality in acute myocardial infarction (AMI) patients from the INFORM cohort by genotype using a dominant mode of inheritance. A comparison of Kaplan-Meier curves and a comparison of 5-year mortality rates between noncarriers and *EPHX2* Lys55Arg

carriers in (a) Caucasian + African American (n=394) and (b) Caucasian (n=345) subjects. Log-rank P-values and hazard ratio (HR) for each population are unadjusted.

a Caucasians and African Americans (n=2712)

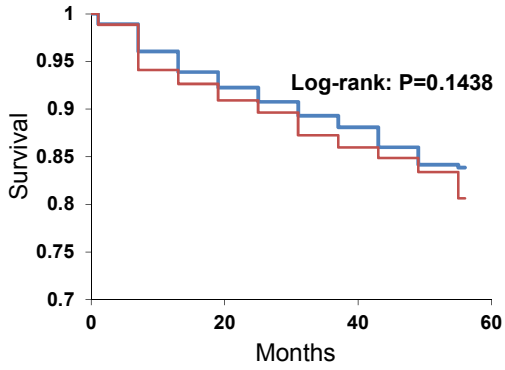

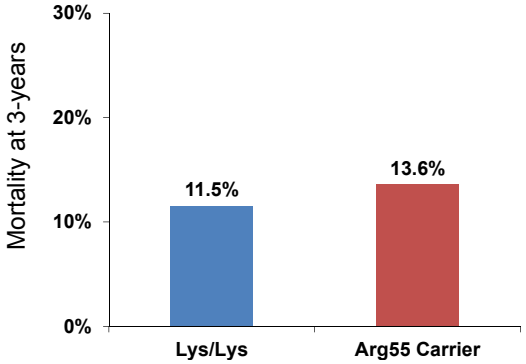

	Events (%)	HR (95% CI)	P
WT	233/2020	Reference	---
Arg55 Carrier	94/692	1.19 (0.94-1.51)	0.1561

b Caucasians only (n=2049)

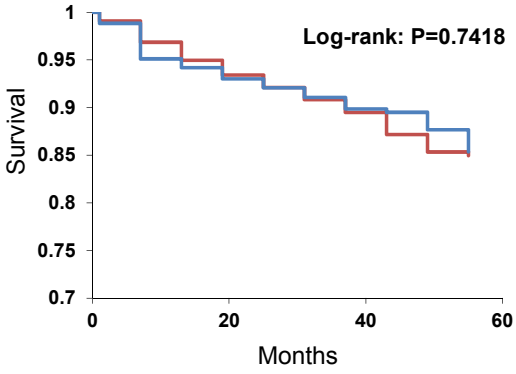

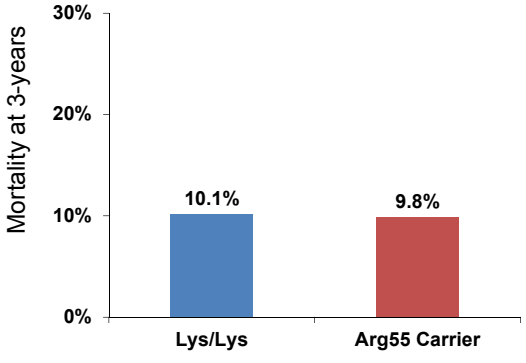

	Events (%)	HR (95% CI)	P
WT	164/1620	Reference	---
Arg55 Carrier	42/429	0.96 (0.68-1.36)	0.8309

c African Americans only (n=663)

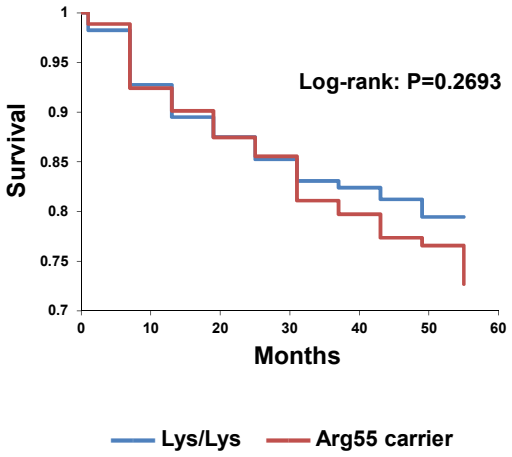

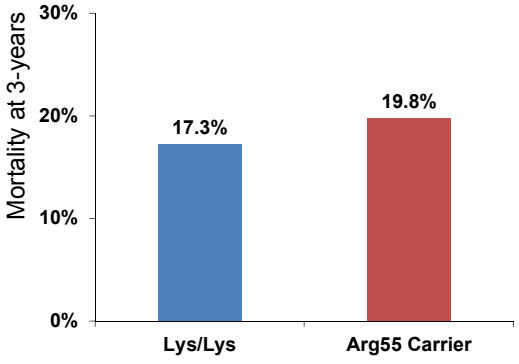

	Events (%)	HR (95% CI)	P
WT	69/400	Reference	---
Arg55 Carrier	52/263	1.14 (0.61-1.17)	0.3033

Figure 3.2 Mortality in acute myocardial infarction (AMI) patients from the TRIUMPH cohort by genotype using a dominant mode of inheritance. A comparison of Kaplan-Meier curves and a comparison of observed 3-year mortality rates between noncarriers and *EPHX2* Lys55Arg carriers in (a) Caucasian + African American (n=2712) , (b) Caucasian (n=2049), and (c) African American (n=663) subjects. Log-rank P-values and hazard ratio (HR) for each population are unadjusted.

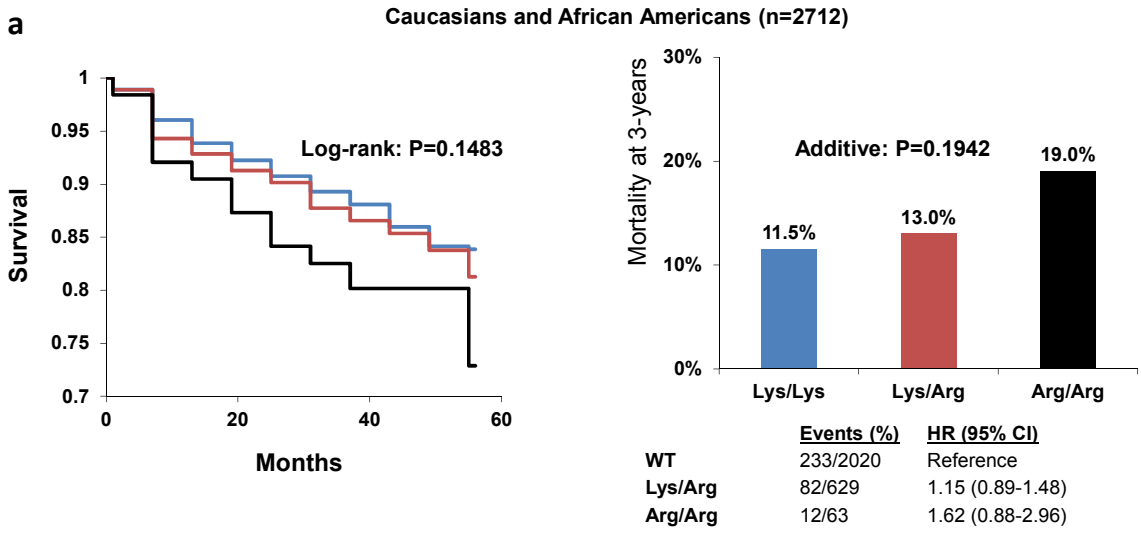

	Events (%)	HR (95% CI)
WT	233/2020	Reference
Lys/Arg	82/629	1.15 (0.89-1.48)
Arg/Arg	12/63	1.62 (0.88-2.96)

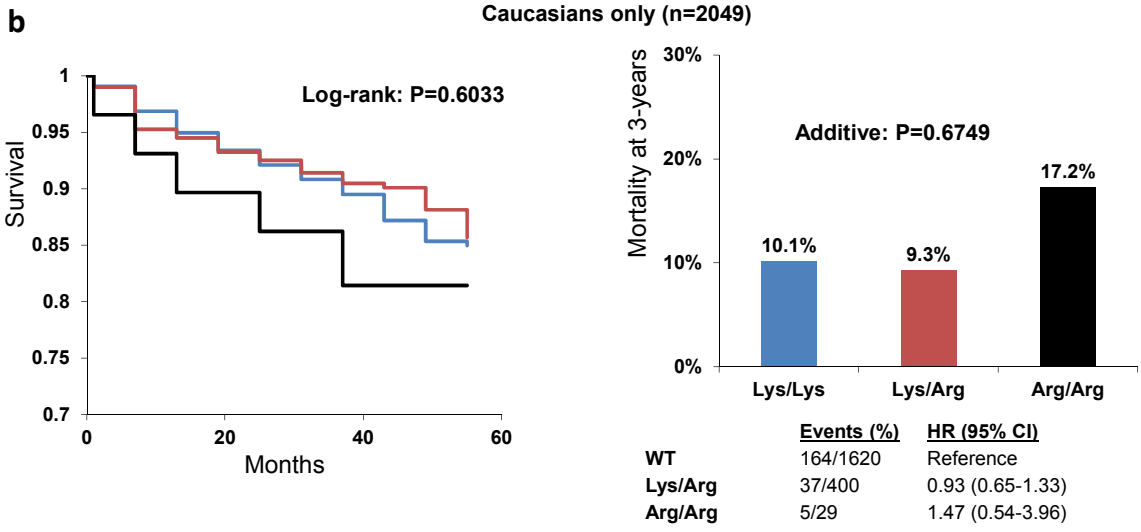

	Events (%)	HR (95% CI)
WT	164/1620	Reference
Lys/Arg	37/400	0.93 (0.65-1.33)
Arg/Arg	5/29	1.47 (0.54-3.96)

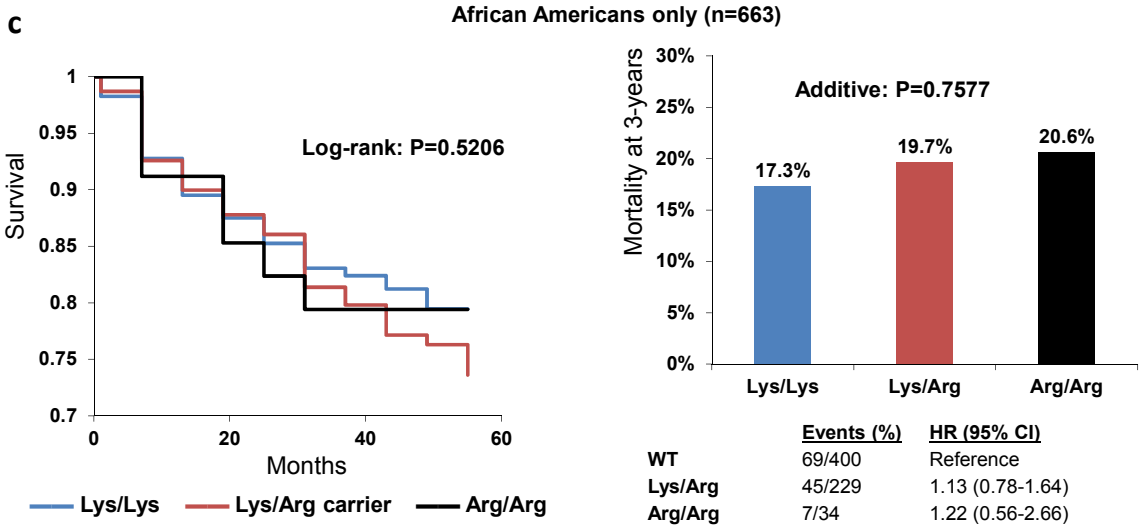

	Events (%)	HR (95% CI)
WT	69/400	Reference
Lys/Arg	45/229	1.13 (0.78-1.64)
Arg/Arg	7/34	1.22 (0.56-2.66)

Figure 3.3 Mortality in acute myocardial infarction (AMI) patients from the TRIUMPH cohort by genotype using an additive mode of inheritance. A comparison of Kaplan-Meier curves and a comparison of projected 3-year mortality rates between noncarriers and *EPHX2* Lys55Arg carriers in (a) Caucasian + African American (n=2712) , (b) Caucasian (n=2049), and (c) African American (n=663) subjects. Log-rank P-values and hazard ratio (HR) for each population are unadjusted.

Tables

Table 3.1 Characteristics of the acute coronary syndrome (ACS) study population from the INFORM cohort by genotype

Characteristic	Lys/Lys (n=502)	Arg55 Carrier (n=165)	P
Age (years)	60.4 ± 12.4	60.8 ± 12.8	0.69
Female	177 (35.3%)	64 (38.8%)	0.413
African-American race	76 (15.1%)	46 (27.9%)	<0.001
ACS Classification Type			0.064
ST elevation MI/LBBB	154 (30.7%)	36 (21.8%)	
Non ST elevation MI	152 (30.3%)	52 (31.5%)	
Unstable angina	196 (39.0%)	77 (46.7%)	
Past medical history			
History of hypertension	324 (64.5%)	113 (68.5%)	0.355
History of diabetes	136 (27.1%)	51 (30.9%)	0.344
History of hyperlipidemia	295 (58.8%)	109 (66.1%)	0.096
Current heart failure	38 (7.6%)	14 (8.5%)	0.704
Prior MI	159 (31.7%)	58 (35.2%)	0.408
Smoking Status			0.869
Current	183 (36.5%)	57 (34.5%)	
Former	178 (35.5%)	62 (37.6%)	
Never	140 (27.9%)	46 (27.9%)	
BMI (kg/m2) *	29.6 ± 6.3	30.2 ± 6.7	0.282
Total cholesterol (mg/dL) #	178.4 ± 39.6 [65]	181.6 ± 49.1 [14]	0.436
LDL (mg/dL) #	103.5 ± 34.5 [91]	102.3 ± 44.2 [24]	0.757
HDL (mg/dL) #	41.6 ± 14.7 [71]	43.6 ± 17.9 [17]	0.183
Triglycerides (mg/dL) #	176.4 ± 117.8 [70]	181.2 ± 144.9 [17]	0.698
Treatment Strategy			0.252
Medical Management	182 (36.3%)	68 (41.2%)	
PCI	299 (59.6%)	87 (52.7%)	
CABG	21 (4.2%)	10 (6.1%)	
Discharge Medications			
Beta-blocker	412 (82.2%)	124 (75.6%)	0.063
Statin	382 (76.1%)	121 (73.3%)	0.475
Aspirin	463 (92.4%)	157 (95.7%)	0.142

BMI, body mass index; CABG, coronary artery bypass graft; HDL, high density lipoprotein; LBBB, left bundle branch block; LDL, low density lipoprotein; MAF, minor allele frequency; MI, myocardial infarction; PCI, percutaneous coronary intervention. Data presented as mean ± standard deviation or count (%). Number of participants with missing values is in brackets

Student's t-test was performed for continuous variables and chi-squared test or Fisher's exact test was performed for categorical variables as appropriate.

* Measured at admission # Measured at discharge

Table 3.2 Characteristics of the TRIUMPH cohort overall and by race

Characteristic	Total (n=2712)	Caucasian (n=2049)	African American (n=663)	P
Age (years)	59.2 ± 12.2	59.8 ± 12.1	57.4 ± 12.2	<0.001
Sex				<0.001
Male	1855 (68.4%)	1483 (72.4%)	372 (56.1%)	
Female	857 (31.6%)	566 (27.6%)	291 (43.9%)	
AMI Classification Type				<0.001
ST elevation MI	1186 (43.7%)	985 (48.1%)	201 (30.3%)	
Non ST elevation MI	1526 (56.3%)	1064 (51.9%)	462 (60.7%)	
Past medical history				
Current smoker	1062 (39.5%) [21]	760 (37.3%) [14]	302 (46.0%) [7]	<0.001
Obese (BMI ≥30 kg/m^2)	1105 (42.6%) [118]	844 (42.1%) [42]	261 (44.5%) [76]	0.299
History of hypertension	1775 (65.4%)	1256 (61.3%)	519 (78.3%)	<0.001
History of diabetes	795 (29.3%)	532 (26.0%)	263 (39.7%)	<0.001
History of hyperlipidemia	1326 (48.9%)	1037 (50.6%)	289 (43.6%)	0.002
Current heart failure	217 (8.0%)	112 (5.5%)	105 (15.8%)	<0.001
Prior myocardial infarction	532 (19.6%)	379 (18.5%)	153 (23.1%)	0.010
Total cholesterol (mg/dL) *	156.1 ± 38.0 [592]	155.3 ± 37.3 [479]	158.6 ± 39.7 [113]	0.076
LDL (mg/dL) *	95.5 ± 31.9 [592]	95.3 ± 31.1 [479]	96.1 ± 33.8 [113]	0.583
HDL (mg/dL) *	40.0 ± 10.6 [592]	38.7 ± 9.8 [479]	43.6 ± 12.0 [113]	<0.001
Triglycerides (mg/dL) *	154.0 ± 102.7 [592]	162.0 ± 108.1 [479]	131.3 ± 81.2 [113]	<0.001
Treatment Strategy				
PCI/CABG during index visit	2056 (75.8%)	1665 (81.3%)	391 (59.0%)	<0.001
Discharge Medications				
Beta-blocker	2459 (90.7%)	1878 (91.7%)	581 (87.6%)	0.002
Statin	2398 (88.4%)	1824 (89.0%)	574 (86.6%)	0.087
Aspirin	2579 (95.1%)	1958 (95.6%)	621 (93.7%)	0.050
EPHX2 Lys55Arg MAF	13.9%	11.2%	22.4%	

BMI, body mass index; CABG, coronary artery bypass graft; HDL, high density lipoprotein; LDL, low density lipoprotein; MAF, minor allele frequency; MI, myocardial infarction; PCI, percutaneous coronary intervention. Data presented as mean ± standard deviation or count (%). Number of participants with missing values is in brackets

Student's t-test was performed for continuous variables and chi-squared test or Fisher's exact test was performed for categorical variables as appropriate.

* Measured at admission

Table 3.3 Characteristics of the TRIUMPH cohort overall and by genotype using a dominant mode of inheritance

Characteristic	Total (n=2712)	Lys/Lys (n=2020)	Arg55 Carrier (n=692)	P
Age (years)	59.2 ± 12.2	59.2 ± 12.2	59.1 ± 12.2	0.879
Sex				0.488
Male	1855 (68.4%)	1389 (68.8%)	466 (67.3%)	
Female	857 (31.6%)	631 (31.2%)	226 (32.7%)	
AMI Classification Type				0.005
ST elevation MI	1186 (43.7%)	915 (45.3%)	271 (39.2%)	
Non ST elevation MI	1526 (56.3%)	1105 (54.7%)	421 (60.8%)	
Past medical history				
Current smoker	1062 (39.5%) [21]	803 (40.0%) [10]	259 (38.0%) [11]	0.376
Obese (BMI ≥30 kg/m^2)	1105 (42.6%) [118]	822 (42.4%) [82]	283 (43.1%) [36]	0.745
History of hypertension	1775 (65.4%)	1306 (64.7%)	469 (67.8%)	0.136
History of diabetes	795 (29.3%)	576 (28.5%)	219 (31.6%)	0.118
History of hyperlipidemia	1326 (48.9%)	980 (48.5%)	346 (50.0%)	0.500
Current heart failure	217 (8.0%)	152 (7.5%)	65 (9.4%)	0.118
Prior myocardial infarction	532 (19.6%)	395 (19.6%)	137 (19.8%)	0.889
Total cholesterol (mg/dL) *	156.1 ± 38.0 [592]	155.9 ± 37.3 [451]	156.7 ± 39.8 [141]	0.671
LDL (mg/dL) *	95.5 ± 31.9 [592]	95.4 ± 31.3 [451]	95.8 ± 33.5 [141]	0.817
HDL (mg/dL) *	40.0 ± 10.6 [592]	39.7 ± 10.2 [451]	40.6 ± 11.6 [141]	0.096
Triglycerides (mg/dL) *	154.0 ± 102.7 [592]	156.2 ± 107.4 [451]	147.6 ± 87.4 [141]	0.088
Treatment Strategy				
PCI/CABG during index visit	2056 (75.8%)	1547 (76.6%)	509 (73.6%)	0.108
Discharge Medications				
Beta-blocker	2459 (90.7%)	1814 (89.8%)	645 (93.2%)	0.008
Statin	2398 (88.4%)	1782 (88.2%)	616 (89.0%)	0.571
Aspirin	2579 (95.1%)	1918 (95.0%)	661 (95.5%)	0.549

BMI, body mass index; CABG, coronary artery bypass graft; HDL, high density lipoprotein; LDL, low density lipoprotein; MI, myocardial infarction; PCI, percutaneous coronary intervention. Data presented as mean ± standard deviation or count (%). Number of participants with missing values is in brackets

Student's t-test was performed for continuous variables and chi-squared test or Fisher's exact test was performed for categorical variables as appropriate.

* Measured at admission

Table 3.4 Characteristics of the TRIUMPH cohort overall and by genotype using a dominant mode of inheritance in Caucasian patients only

Characteristic	Total (n=2049)	Lys/Lys (n=1620)	Arg55 Carrier (n=429)	P
Age (years)	59.8 ± 12.1	59.8 ± 12.0	59.2 ± 12.2	0.989
Sex				0.248
Male	1483 (72.4%)	1163 (71.8%)	320 (74.6%)	
Female	566 (27.6%)	457 (28.2%)	109 (25.4%)	
AMI Classification Type				0.498
ST elevation MI	985 (48.1%)	785 (48.5%)	200 (46.6%)	
Non ST elevation MI	1064 (51.9%)	835 (51.5%)	229 (53.4%)	
Past medical history				
Current smoker	760 (37.3%) [14]	610 (37.8%) [8]	150 (35.5%) [6]	0.368
Obese (BMI ≥30 kg/m^2)	844 (42.1%) [42]	664 (41.9%) [34]	180 (42.8%) [8]	0.743
History of hypertension	1256 (61.3%)	990 (61.1%)	266 (62.0%)	0.735
History of diabetes	532 (26.0%)	414 (25.6%)	118 (27.5%)	0.413
History of hyperlipidemia	1037 (50.6%)	809 (49.9%)	228 (53.1%)	0.237
Current heart failure	112 (5.5%)	88 (5.4%)	24 (5.6%)	0.895
Prior myocardial infarction	379 (18.5%)	297 (18.3%)	82 (19.1%)	0.711
Total cholesterol (mg/dL) *	155.3 ± 37.3 [479]	156.0 ± 37.7 [382]	152.5 ± 35.9 [97]	0.124
LDL (mg/dL) *	95.3 ± 31.1 [479]	95.9 ± 31.3 [382]	93.0 ± 30.5 [97]	0.140
HDL (mg/dL) *	38.7 ± 9.8 [479]	38.7 ± 9.6 [382]	38.6 ± 10.4 [97]	0.808
Triglycerides (mg/dL) *	162.0 ± 108.1 [479]	163.1 ± 110.8 [382]	157.5 ± 97.3 [97]	0.400
Treatment Strategy				
PCI/CABG during index visit	1665 (81.3%)	1320 (81.5%)	345 (80.4%)	0.616
Discharge Medications				
Beta-blocker	1878 (91.7%)	1476 (91.1%)	402 (93.7%)	0.084
Statin	1824 (89.0%)	1437 (88.7%)	387 (90.2%)	0.375
Aspirin	1958 (95.6%)	416 (97.0%)	1542 (95.2%)	0.111

BMI, body mass index; CABG, coronary artery bypass graft; HDL, high density lipoprotein; LDL, low density lipoprotein; MI, myocardial infarction; PCI, percutaneous coronary intervention. Data presented as mean ± standard deviation or count (%). Number of participants with missing values is in brackets

Student's t-test was performed for continuous variables and chi-squared test or Fisher's exact test was performed for categorical variables as appropriate.

* Measured at admission

Table 3.5 Characteristics of the TRIUMPH cohort overall and by genotype using a dominant mode of inheritance in African American patients only

Characteristic	Total (n=663)	Lys/Lys (n=400)	Arg55 Carrier (n=263)	P
Age (years)	57.4 ± 12.2	56.9 ± 12.0	58.0 ± 12.4	0.238
Sex				0.802
Male	372 (56.1%)	226 (56.5%)	146 (55.5%)	
Female	291 (43.9%)	174 (43.5%)	117 (44.5%)	
AMI Classification Type				0.131
ST elevation MI	201 (30.3%)	130 (32.5%)	71 (27.0%)	
Non ST elevation MI	462 (69.7%)	270 (67.5%)	192 (73.0%)	
Past medical history				
Current smoker	302 (46.0%) [7]	193 (48.5%) [5]	109 (42.2%) [2]	0.117
Obese (BMI ≥30 kg/m^2)	261 (44.5%) [76]	158 (44.9%) [48]	103 (43.8%) [28]	0.801
History of hypertension	519 (78.3%)	316 (79.0%)	203 (77.2%)	0.580
History of diabetes	263 (39.7%)	162 (40.5%)	101 (38.4%)	0.589
History of hyperlipidemia	289 (43.6%)	171 (42.8%)	118 (44.9%)	0.591
Current heart failure	105 (15.8%)	64 (16.0%)	41 (15.6%)	0.887
Prior myocardial infarction	153 (23.1%)	98 (24.5%)	55 (20.9%)	0.283
Total cholesterol (mg/dL) *	158.6 ± 39.7 [113]	155.6 ± 36.1 [69]	163.2 ± 44.3 [44]	0.028
LDL (mg/dL) *	96.1 ± 33.8 [113]	93.6 ± 31.2 [69]	99.9 ± 37.1 [44]	0.033
HDL (mg/dL) *	43.6 ± 12.0 [113]	43.7 ± 12.7 [69]	43.5 ± 11.5 [44]	0.878
Triglycerides (mg/dL) *	131.3 ± 81.2 [113]	130.4 ± 89.2 [69]	132.5 ± 67.4 [44]	0.772
Treatment Strategy				
PCI/CABG during index visit	391 (59.0%)	227 (56.8%)	164 (62.4%)	0.151
Discharge Medications				
Beta-blocker	581 (87.6%)	338 (84.5%)	243 (92.4%)	0.003
Statin	574 (86.6%)	345 (86.3%)	229 (87.1%)	0.761
Aspirin	515 (77.7%)	329 (82.3%)	186 (70.7%)	<0.001

BMI, body mass index; CABG, coronary artery bypass graft; HDL, high density lipoprotein; LDL, low density lipoprotein; MI, myocardial infarction; PCI, percutaneous coronary intervention. Data presented as mean ± standard deviation or count (%). Number of participants with missing values is in brackets

Student's t-test was performed for continuous variables and chi-squared test or Fisher's exact test was performed for categorical variables as appropriate.

* Measured at admission

Table 3.6 Mortality follow-up status in TRIUMPH

Interval	Evaluable *	Mortality rate (deaths) †
2-year	2654 (98%)	9.6% (259 deaths)
3-year	2024 (75%)	12.1% (327 deaths)
4-year	1298 (48%)	14.1% (382 deaths)
4.5-year	981 (36%)	14.4% (391 deaths)
5-year	0 (0%)	N/A

* Total population with evaluable mortality data (%)
† Overall mortality rate based on data available

Table 3.7 Hazard ratios between *EPHX2* Lys55Arg and 3-year mortality using a dominant mode of inheritance

	HR (95% CI)	P
All subjects		
Arg55 carrier vs Lys/Lys		
Unadjusted	1.19 (0.94-1.51)	0.156
Model 1	1.02 (0.80-1.30)	0.889
Model 2	1.00 (0.78-1.28)	0.999
Caucasians		
Arg55 carrier vs Lys/Lys		
Unadjusted	0.96 (0.68-1.36)	0.831
Model 1	0.98 (0.69-1.38)	0.889
Model 2	0.90 (0.64-1.27)	0.564
African Americans		
Arg55 carrier vs Lys/Lys		
Unadjusted	1.14 (0.80-1.64)	0.473
Model 1	1.08 (0.75-1.55)	0.688
Model 2	1.11 (0.77-1.59)	0.591

Model 1: adjusted for age, sex, and race (age and sex in race-stratified analyses)

Model 2: adjusted for age, sex, race, AMI type (STEMI, NSTEMI), diabetes, treatment strategy (medical management, PCI, CABG)

CI=confidence interval, HR=hazard ratio

Table 3.8 Hazard ratios between *EPHX2* Lys55Arg and 3-year mortality using an additive mode of inheritance

	Unadjusted) HR (95% CI)	P	Model 1 HR (95% CI)	P	Model 2 HR (95% CI)	P
All subjects						
		0.194		0.954		0.840
Lys/Lys	Reference		Reference		Reference	
Lys/Arg	1.15 (0.89-1.48)		1.01 (0.78-1.30)		0.98 (0.76-1.27)	
Arg/Arg	1.62 (0.88-2.96)		1.10 (0.60-2.03)		1.19 (0.64-2.19)	
Caucasians						
		0.675		0.812		0.484
Lys/Lys	Reference		Reference		Reference	
Lys/Arg	0.93 (0.65-1.33)		0.95 (0.66-1.36)		0.87 (0.61-1.24)	
Arg/Arg	1.47 (0.54-3.96)		1.33 (0.49-3.57)		1.54 (0.57-4.16)	
African Americans						
		0.758		0.921		0.865
Lys/Lys	Reference		Reference		Reference	
Lys/Arg	1.13 (0.78-1.64)		1.08 (0.74-1.57)		1.11 (0.76-1.61)	
Arg/Arg	1.22 (0.56-2.66)		1.06 (0.48-2.31)		1.10 (0.50-2.42)	

Model 1: adjusted for age, sex, and race (age and sex in race stratified-analyses)

Model 2: adjusted for age, sex, race, AMI type (STEMI, NSTEMI), diabetes, treatment strategy (medical management, PCI, CABG)
CI=confidence interval, HR=hazard ratio

Table 3.9 Relationship between *EPHX2* Lys55Arg and biomarkers of myocardial injury, inflammation, and ventricular remodeling

Dominant	Overall	Lys/Lys	Arg55 carrier	P
Baseline				
Troponin T (mg/L)	1.57 ± 2.14 [684]	1.55 ± 2.11 [516]	1.60 ± 2.23 [168]	0.656
hs-CRP (mg/L)	3.64 ± 4.79 [558]	3.63 ± 4.80 [424]	3.66 ± 4.76 [134]	0.899
proBNP (g/L)	2.94 ± 8.13 [568]	2.82 ± 7.95 [434]	3.25 ± 8.64 [134]	0.284
1 month				
Troponin T (mg/L)	0.02 ± 0.14 [1796]	0.02 ± 0.02 [1341]	0.04 ± 0.28 [455]	0.057
hs-CRP (mg/L)	0.55 ± 1.16 [1789]	0.50 ± 0.88 [1339]	0.67 ± 1.73 [450]	0.059
proBNP (g/L)	1.67 ± 9.93 [1789]	1.78 ± 11.36 [1337]	1.36 ± 3.44 [452]	0.568
6 months				
Troponin T (mg/L)	0.02 ± 0.03 [2070]	0.01 ± 0.03 [1537]	0.02 ± 0.04 [533]	0.215
hs-CRP (mg/L)	0.39 ± 0.63 [2062]	0.39 ± 0.63 [1530]	0.38 ± 0.66 [532]	0.931
proBNP (g/L)	1.00 ± 5.15 [2061]	1.09 ± 5.61 [1530]	0.71 ± 3.42 [531]	0.413
Additive	Lys/Lys	Lys/Arg	Arg/Arg	P
Baseline				
Troponin T (mg/L)	1.55 ± 2.11 [516]	1.63 ± 2.31 [151]	1.31 ± 1.14 [17]	0.997
hs-CRP (mg/L)	3.63 ± 4.80 [424]	3.60 ± 4.64 [120]	4.29 ± 5.85 [14]	0.878
proBNP (g/L)	2.82 ± 7.95 [434]	3.25 ± 8.82 [120]	3.27 ± 6.65 [14]	0.655
1 month				
Troponin T (mg/L)	0.02 ± 0.02 [1341]	0.02 ± 0.03 [411]	0.25 ± 0.96 [44]	0.038
hs-CRP (mg/L)	0.50 ± 0.88 [1339]	0.66 ± 1.78 [407]	0.78 ± 1.02 [43]	0.523
proBNP (g/L)	1.78 ± 11.36 [1337]	1.20 ± 2.98 [408]	3.14 ± 6.72 [44]	0.403
6 months				
Troponin T (mg/L)	0.01 ± 0.03 [1537]	0.02 ± 0.04 [485]	0.03 ± 0.06 [48]	0.780
hs-CRP (mg/L)	0.39 ± 0.63 [1530]	0.39 ± 0.68 [484]	0.26 ± 0.31 [48]	0.295
proBNP (g/L)	1.09 ± 5.61 [1530]	0.74 ± 3.6 [483]	0.37 ± 0.34 [48]	0.690

proBNP, pro-B-type natriuretic peptide; hs-CRP, high sensitivity C reactive protein. Data presented as mean ± standard deviation. Number of participants with missing values is in brackets

One-way ANOVA was performed for dominant mode of inheritance data and Kruskal-Wallis test was performed for additive mode of inheritance data

Table 3.10 Power calculations

Population	**Power**			
	Current analysis		Projected full analysis	
	HR=1.4	HR=1.5	HR=1.4	HR=1.5
Total population	74%	88%	80%	92%
Caucasians only	50%	66%	57%	74%
African Americans only	38%	51%	41%	55%

Power calculations to detect a hazard of 1.4 or 1.5 between EPHX2 Lys55Arg genotype (dominant model) and mortality based on the current 3-year mortality data available and if full 4.5 year mortality data was available
Power calculations of the current analysis were based on the 3-year mortality rates in the current report (total population: 12.1%, Caucasians: 10.1%, and African Americans: 18.3%)
Power calculations of the projected full analysis were based on the 4.5-year mortality rates in the current report (total population: 14.4%, Caucasians: 12.5%, and African Americans: 20.4%) and assuming that all patients had full mortality data at 4.5 years

REFERENCES

(1) Mozaffarian, D. *et al.* Heart disease and stroke statistics--2015 update: a report from the American Heart Association. *Circulation* 131, e29-322 (2015).

(2) Capdevila, J.H., Falck, J.R. & Estabrook, R.W. Cytochrome P450 and the arachidonate cascade. *FASEB J* 6, 731-6 (1992).

(3) Spector, A.A., Fang, X., Snyder, G.D. & Weintraub, N.L. Epoxyeicosatrienoic acids (EETs): metabolism and biochemical function. *Prog Lipid Res* 43, 55-90 (2004).

(4) Deng, Y., Theken, K.N. & Lee, C.R. Cytochrome P450 epoxygenases, soluble epoxide hydrolase, and the regulation of cardiovascular inflammation. *J Mol Cell Cardiol* 48, 331-41 (2010).

(5) Seubert, J.M., Zeldin, D.C., Nithipatikom, K. & Gross, G.J. Role of epoxyeicosatrienoic acids in protecting the myocardium following ischemia/reperfusion injury. *Prostaglandins Other Lipid Mediat* 82, 50-9 (2007).

(6) Larsson, C., White, I., Johansson, C., Stark, A. & Meijer, J. Localization of the human soluble epoxide hydrolase gene (EPHX2) to chromosomal region 8p21-p12. *Hum Genet* 95, 356-8 (1995).

(7) Sandberg, M. & Meijer, J. Structural characterization of the human soluble epoxide hydrolase gene (EPHX2). *Biochemical and biophysical research communications* 221, 333-9 (1996).

(8) Przybyla-Zawislak, B.D. *et al.* Polymorphisms in human soluble epoxide hydrolase. *Mol Pharmacol* 64, 482-90 (2003).

(9) Enayetallah, A.E., French, R.A., Thibodeau, M.S. & Grant, D.F. Distribution of soluble epoxide hydrolase and of cytochrome P450 2C8, 2C9, and 2J2 in human tissues. *J Histochem Cytochem* 52, 447-54 (2004).

(10) Koerner, I.P. *et al.* Polymorphisms in the human soluble epoxide hydrolase gene EPHX2 linked to neuronal survival after ischemic injury. *J Neurosci* 27, 4642-9 (2007).

(11) Nelson, J.W., Subrahmanyan, R.M., Summers, S.A., Xiao, X. & Alkayed, N.J. Soluble epoxide hydrolase dimerization is required for hydrolase activity. *The Journal of biological chemistry* 288, 7697-703 (2013).

(12) Argiriadi, M.A., Morisseau, C., Hammock, B.D. & Christianson, D.W. Detoxification of environmental mutagens and carcinogens: structure, mechanism, and evolution of liver epoxide hydrolase. *Proceedings of the National Academy of Sciences of the United States of America* 96, 10637-42 (1999).

(13) Lee, C.R. *et al.* Genetic variation in soluble epoxide hydrolase (EPHX2) and risk of coronary heart disease: The Atherosclerosis Risk in Communities (ARIC) study. *Hum Mol Genet* 15, 1640-9 (2006).

(14) Theken, K.N. & Lee, C.R. Genetic variation in the cytochrome P450 epoxygenase pathway and cardiovascular disease risk. *Pharmacogenomics* 8, 1369-83 (2007).

(15) Lee, C.R. *et al.* Genetic variation in soluble epoxide hydrolase (EPHX2) and risk of coronary heart disease: the atherosclerosis risk in communities (ARIC) study. *Human molecular genetics* 15, 1640-9 (2006).

(16) Przybyla-Zawislak, B.D. *et al.* Polymorphisms in Human Soluble Epoxide Hydrolase. *Mol Pharmacol* 64, 482-90 (2003).

(17) Nithipatikom, K. & Gross, G.J. Review article: epoxyeicosatrienoic acids: novel mediators of cardioprotection. *J Cardiovasc Pharmacol Ther* 15, 112-9 (2010).

(18) Imig, J.D. Epoxides and soluble epoxide hydrolase in cardiovascular physiology. *Physiol Rev* 92, 101-30 (2012).

(19) Fornage, M. *et al.* The soluble epoxide hydrolase gene harbors sequence variation associated with susceptibility to and protection from incident ischemic stroke. *Hum Mol Genet* 14, 2829-37 (2005).

(20) Fornage, M., Boerwinkle, E., Doris, P.A., Jacobs, D., Liu, K. & Wong, N.D. Polymorphism of the soluble epoxide hydrolase is associated with coronary artery calcification in African-American subjects: The Coronary Artery Risk Development in Young Adults (CARDIA) study. *Circulation* 109, 335-9 (2004).

(21) Wei, Q. *et al.* Sequence variation in the soluble epoxide hydrolase gene and subclinical coronary atherosclerosis: interaction with cigarette smoking. *Atherosclerosis* 190, 26-34 (2007).

(22) Lee, C.R. *et al.* Genetic variation in soluble epoxide hydrolase (EPHX2) is associated with forearm vasodilator responses in humans. *Hypertension* 57, 116-22 (2011).

(23) Fava, C. *et al.* Homozygosity for the EPHX2 K55R polymorphism increases the long-term risk of ischemic stroke in men: a study in Swedes. *Pharmacogenet Genomics* 20, 94-103 (2010).

(24) Sato, K. *et al.* Soluble epoxide hydrolase variant (Glu287Arg) modifies plasma total cholesterol and triglyceride phenotype in familial hypercholesterolemia: intrafamilial association study in an eight-generation hyperlipidemic kindred. *Journal of human genetics* 49, 29-34 (2004).

(25) Gschwendtner, A. *et al.* Genetic Variation in Soluble Epoxide Hydrolase (EPHX2) Is Associated With an Increased Risk of Ischemic Stroke in White Europeans. *Stroke* 39, 1593-6 (2008).

(26) Burdon, K.P. *et al.* Genetic analysis of the soluble epoxide hydrolase gene, EPHX2, in subclinical cardiovascular disease in the Diabetes Heart Study. *Diabetes & vascular disease research : official journal of the International Society of Diabetes and Vascular Disease* 5, 128-34 (2008).

(27) Lee, C.R. *et al.* Genetic variation in soluble epoxide hydrolase (EPHX2) is associated with forearm vasodilator responses in humans. *Hypertension* 57, 116-22 (2011).

(28) Wutzler, A. *et al.* Variations in the human soluble epoxide hydrolase gene and recurrence of atrial fibrillation after catheter ablation. *Int J Cardiol* 168, 3647-51 (2013).

(29) Theken, K.N. Cytochrome P450-derived eicosanoids, inflammation, and atherosclerotic cardiovascular disease. *PhD Dissertation* Chapter 6, (2011).

(30) Lanfear, D.E., Jones, P.G., Marsh, S., Cresci, S., McLeod, H.L. & Spertus, J.A. Beta2-adrenergic receptor genotype and survival among patients receiving beta-blocker therapy after an acute coronary syndrome. *JAMA* 294, 1526-33 (2005).

(31) Zineh, I. *et al.* Epithelial neutrophil-activating peptide (ENA-78), acute coronary syndrome prognosis, and modulatory effect of statins. *PLoS One* 3, e3117 (2008).

(32) Arnold, S.V. *et al.* Translational Research Investigating Underlying Disparities in Acute Myocardial Infarction Patients' Health Status (TRIUMPH): design and rationale of a prospective multicenter registry. *Circ Cardiovasc Qual Outcomes* 4, 467-76 (2011).

(33) Salisbury, A.C. *et al.* Incidence, correlates, and outcomes of acute, hospital-acquired anemia in patients with acute myocardial infarction. *Circ Cardiovasc Qual Outcomes* 3, 337-46 (2010).

(34) Smolderen, K.G. *et al.* Health care insurance, financial concerns in accessing care, and delays to hospital presentation in acute myocardial infarction. *JAMA* 303, 1392-400 (2010).

(35) Thygesen, K. *et al.* Universal definition of myocardial infarction. *Circulation* 116, 2634-53 (2007).

(36) Alpert, J.S., Thygesen, K., Antman, E. & Bassand, J.P. Myocardial infarction redefined--a consensus document of The Joint European Society of Cardiology/American College of Cardiology Committee for the redefinition of myocardial infarction. *J Am Coll Cardiol* 36, 959-69 (2000).

(37) Spertus, J., Safley, D., Garg, M., Jones, P. & Peterson, E.D. The influence of race on health status outcomes one year after an acute coronary syndrome. *J Am Coll Cardiol* 46, 1838-44 (2005).

(38) Marsh, S., King, C.R., Garsa, A.A. & McLeod, H.L. Pyrosequencing of clinically relevant polymorphisms. *Methods Mol Biol* 311, 97-114 (2005).

(39) Gauderman, W.J. Candidate gene association analysis for a quantitative trait, using parent-offspring trios. *Genet Epidemiol* 25, 327-38 (2003).

(40) Amsterdam, E.A. *et al.* 2014 AHA/ACC guideline for the management of patients with non-ST-elevation acute coronary syndromes: executive summary: a report of the American College of Cardiology/American Heart Association Task Force on Practice Guidelines. *Circulation* 130, 2354-94 (2014).

(41) Stanton, E.B. *et al.* Cardiac troponin I, a possible predictor of survival in patients with stable congestive heart failure. *Can J Cardiol* 21, 39-43 (2005).

(42) Kullmann, S. *et al.* Variation in the human soluble epoxide hydrolase gene and risk of restenosis after percutaneous coronary intervention. *BMC Cardiovasc Disord* 9, 48 (2009).

(43) Gschwendtner, A. *et al.* Genetic variation in soluble epoxide hydrolase (EPHX2) is associated with an increased risk of ischemic stroke in white Europeans. *Stroke* 39, 1593-6 (2008).

(44) Merkel, M.J. *et al.* Inhibition of soluble epoxide hydrolase preserves cardiomyocytes: role of STAT3 signaling. *Am J Physiol Heart Circ Physiol* 298, H679-H87 (2010).

(45) Theken, K.N. *et al.* Evaluation of cytochrome P450-derived eicosanoids in humans with stable atherosclerotic cardiovascular disease. *Atherosclerosis* 222, 530-6 (2012).

(46) Ridker, P.M. *et al.* Rosuvastatin to prevent vascular events in men and women with elevated C-reactive protein. *N Engl J Med* 359, 2195-207 (2008).

(47) Theken, K.N. *et al.* Evaluation of cytochrome P450-derived eicosanoids in humans with stable atherosclerotic cardiovascular disease. *Atherosclerosis* 222, 530-6 (2012).

CHAPTER 4 - CHARACTERIZATION OF MALADAPTIVE VENTRICULAR REMODELING IN AN *IN VIVO* MOUSE MODEL OF MYOCARDIAL ISCHEMIA REPERFUSION INJURY

Introduction

A key consequence of CAD is heart failure, which afflicts almost 6 million Americans and is predicted to increase by an additional 46% by 2030. Patients who survive an AMI are at especially increased risk of developing heart failure. Consistent with the overall heart failure incidence, the incidence of post-AMI heart failure has also increased in recent decades (1). This devastating disease is a major reason why CVD as a whole remains the leading cause of morbidity and mortality worldwide (2).

Heart failure is a clinical syndrome that manifests in patients as dyspnea (shortness of breath) and/or fluid retention (edema). Symptoms of heart failure result primarily from structural or functional deficits that lead to a reduced ability in ventricular filling (diastolic dysfunction) or ejection of blood (systolic dysfunction). It is important to reiterate that structural abnormalities in heart failure patients range from having no changes at all to having marked ventricular dilation. Likewise, functional impairment may or may not coexist with structural changes and range from having HF*p*EF to having HF*r*EF (Chapter 1: Introduction).

Post-AMI heart failure is preceded by myocardial cell death, inflammation, and maladaptive ventricular remodeling which are integral to its pathogenesis and progression. The initial injury caused by prolonged ischemia and subsequent reperfusion ultimately leads to

cardiomyocyte necrosis (uncontrolled cell death) and apoptosis (programmed cell death), each of which independently contribute to the resulting infarct (3). Troponin is a cardiac enzyme that is highly specific to myocardial damage and is released primarily by necrosed cardiomyocytes (4). Changes in the myocardial expression of the anti-apoptotic Bcl-2 and the pro-apoptotic Bax regulate activation of the caspase family, which is primarily pro-apoptotic.

Necrosis but not apoptosis is recognized as the primary mediator of the acute inflammatory response (3). Inflammatory-mediated induction of a class of chemoattractants called chemokines promotes leukocyte recruitment to the site of injury. Notably, MCP-1 and MIP-2α, which are chemotactic for monocytes and neutrophils, respectively, are induced by myocardial necrosis (5). Recruited leukocytes subsequently initiate the cytokine cascade including the synthesis of IL-6 in leukocytes and cardiomyocytes. Cytokines induce the myocardial expression of adhesion molecules such as ICAM-1, which specifically aid in the recruitment of further neutrophils to the site of infarct and mediate neutrophil-derived cytotoxicity. This marked inflammatory response is followed by maladaptive ventricular remodeling.

Mediators involved in the resolution of the inflamed myocardium initiate a maladaptive ventricular remodeling response including scar tissue formation, structural changes to cardiomyocytes, and cardiac dysfunction (6). Fibrosis is initiated following the early inflammatory phase of AMI when circulating and resident fibroblasts infiltrate the myocardium in the infarct zone (Figure 1.2). In tandem, these fibroblasts undergo rapid proliferation (mediated by FGF-2) followed by activation into myofibroblasts (a process largely mediated by transforming growth factor TGF-β). Subsequently, activated myofibroblasts, distinguished from their quiescent precursors via the expression of TGF-β/Smad3 pathway-induced α-smooth

muscle actin SMA, function to produce extracellular matrix ECM proteins that ultimately cause scar formation (7). The ECM proteins including the structural proteins collagens, glycoproteins, proteoglycans, glycosaminoglycans, and matricellular proteins are induced post-AMI contributing to dynamic changes in ECM structure. The ECM proteins also include proteases that are involved in the degradation of these structural components, further contributing to dynamic changes post-AMI. In addition to myofibroblasts which are the most abundant source of ECM proteins post-AMI, endothelial cells, neutrophils, mast cells, lymphocytes, and macrophages are other major sources of ECM proteins. Collagens are considered the structural backbones of the ECM and are present at low levels in the normal, non-infarcted heart. Post-AMI, collagen expression increases in all regions of the heart, with the greatest magnitude of expression in the infarct zone (8). Only myofibroblasts synthesize collagen. LOX mediates the maturation of scar tissue by cross-linking collagen fibrils. Following this process, myofibroblasts halt production of further profibrotic mediators and become less abundant in the myocardium, potentially through apoptosis (7).

The development of fibrosis is often accompanied by activation of the fetal gene program, which results in the dysregulation of a set of genes associated with maladaptive ventricular remodeling. Increased BNP expression and a "switch" from expression of the adult α-myosin heavy chain MHC to the fetal β-MHC are biomarkers of this process (9). BNP promotes compensatory vasodilator and natriuretic responses that indicate that myocardial strain (i.e. an abnormal structural change) is occurring (10). Fetal gene activation begins early and is thought to be promoted at least partially by initial mechanical stretch-induced activation of EGR-1 (11). It is evident that the induction of these mediators during the acute phase following IR activates responses that promote ventricular remodeling during the early chronic and late chronic stages.

Established and emerging biomarkers of these ventricular remodeling processes have been found to have prognostic and therapeutic utility in patients (10).

The extracellular matrix governs not only the structure of the heart, but also the connections between heart muscle bundles that regulate the ability of the heart to contract (12). Thus fibrosis development can cause abnormalities in cardiac function. In addition to the aforementioned molecular changes, the neurohormonal system including the renin–angiotensin–aldosterone system (RAAS) and the sympathetic nervous system is activated. These systems cause vasoconstriction and increased cardiac output in order to compensate further for the loss of cardiomyocytes from the IR injury (12). When overcompensation occurs, these processes in tandem with advanced structural changes including severe wall thinning progresses to systolic and/or diastolic dysfunction ultimately leading to the first signs and symptoms of heart failure (6). Importantly, progression can occur quickly (13) and clinical trial data shows that the development of heart failure in AMI patients with no previous history of AMI or heart failure can occur within a week (14). Indeed, early treatment post-AMI has been found to reduce the occurrence of heart failure (15, 16), likely due to attenuation of the early maladaptive ventricular remodeling response. It is clear that early and aggressive therapy well before the manifestation of symptomatic heart failure improves outcomes.

For decades, the cornerstone therapies for AMI have consisted of antiplatelet agents, beta blockers, statins, and renin-angiotensin aldosterone system inhibitors post-AMI (17-19). Considering the aforementioned projections of heart failure, novel therapeutic strategies are necessary to attenuate this rising burden. Preclinical models of post-AMI myocardial remodeling are critical tools to screen/develop novel therapeutic strategies (20).

Induction of AMI in rodents *in vivo* is feasible and produces injury comparable to the more established large animal models of AMI. Mice in particular are more amenable to genetic manipulation compared to other rodents, enabling the evaluation of key biological pathways that mediate AMI evoked maladaptive cardiac remodeling and the development of heart failure and discovery of new therapeutic targets (21, 22). The LAD coronary artery is the artery most commonly manipulated in these models compared to other regions of the coronary anatomy (23). Clinically, it also usually supplies the largest amount of blood to the myocardium among the three major non-left main epicardial branches (24). Surgical ligation is the most common technique to evoke myocardial IR (25). Multiple mouse models of LAD coronary artery ligation each offer specific advantages depending on the objective of the experiment. Permanent occlusion (PO) of the LAD induces a great degree of damage which improves the ability to measure the impact of protective interventions. The *in vivo* model of myocardial IR is a more clinically relevant approach to understanding the pathophysiology of AMI; unlike PO, AMI patient undergo reperfusion procedures through coronary artery revascularization. Furthermore, it allows for the study of maladaptive ventricular remodeling without causing the overt dilated cardiomyopathy phenotype that permanent ligation causes (23). Thus, mouse myocardial IR can be considered a model of early ventricular remodeling before the onset of symptomatic heart failure. Moreover, since experimental transient myocardial ischemia produces injury of less magnitude than permanent ischemia, this approach may be better suited for experimental interventions hypothesized to enhance myocardial injury and/or remodeling. Surprisingly, the acute and chronic impact of this model on parameters of ventricular remodeling has not been fully characterized in the literature and requires further investigation. A more thorough understanding of the pathophysiology of myocardial remodeling following IR in mice will

facilitate the design of experimental studies that elucidate the role of therapeutic pathways in the disease. As an initial means to design a future mouse study characterizing the role of the EET metabolic pathway in post-IR ventricular remodeling, the objective of the present study was to systematically characterize a time course of the molecular, structural, functional, and histological alterations that occur in the mouse myocardium *in vivo* at time points widely considered to be acute (<1 week) and chronic (1-3 weeks) following IR (26, 27).

Materials and Methods

Mice

All mice used to complete these experiments were adult, male, and wild-type on a C57BL/6 background. Mice were acquired from Taconic Laboratories (Hudson, NY), from Charles River Laboratories (Wilmington, MA), or the NIEHS/NIH (Research Triangle Park, NC). Mice derived from the NIEHS/NIH were kindly provided by Dr. Darryl Zeldin. Mice were 2-5 months of age at the time of ligation. All mice had free access to food and water, and were housed in controlled conditions for temperature and humidity using a 12-h light/dark cycle. All experiments were completed in accordance with the US National Institutes of Health (NIH) Guide for the Care and Use of Laboratory Animals and were approved by the Institutional Animal Care and Use Committee at the University of North Carolina at Chapel Hill and the National Institute of Environmental Health Sciences.

Myocardial IR injury model

The LAD coronary artery ligation model was utilized to evaluate the impact of myocardial IR on myocardial injury, inflammatory responses, myocardial fibrosis, and cardiac function. Surgeries were conducted by the UNC McAllister Heart Institute Mouse Cardiovascular Models Core laboratory under the direction of Dr. Mauricio Rojas.

Briefly, the mice were anesthetized with pentobarbital (45 mg/kg). Under direct visualization of the trachea, an endotracheal tube was inserted and connected to a Harvard rodent volume-cycle ventilator. The chest cavity was opened by a 0.5 cm incision of the left third intercostal space, the pericardial sac was opened, and the LAD artery was visualized. Ligation

was performed with an 8-0 silk suture passed with a tapered needle underneath the LAD artery about 1 mm lower than the tip of the left auricle. The artery was compressed by tightening the ligature, producing myocardial blanching and electrocardiographic S-T segment elevation (indicative of ischemia). After occlusion of the desired time (30 minutes), blood flow was restored by removing the ligature to produce an IR response similar to that produced in humans undergoing a revascularization procedure. Lidocaine (6 mg/kg) was administered as needed to prevent lethal ventricular arrhythmias and atropine (0.04-0.1 mg/kg) was administered as necessary to combat bradycardia. The chest wall was then closed with a prolene or silk suture. Sham surgery mice (control) underwent an identical procedure except there was no tightening of ligature and therefore no IR. A subset of mice also underwent an identical procedure except the ligature was not removed to determine the impact of permanent LAD occlusion. Post-operatively, each mouse was kept on rodent warming pads until they regained consciousness, after which they are housed in their respective cages and observed until they have recovered to normal activity. Mice were euthanized by CO_2 or isoflurane inhalation at short-term (2 hours, 24 hours) or long term (2 weeks) time points following IR. Blood was collected through the inferior vena cava, and plasma was separated by centrifugation, aliquoted and stored at -80°C. Whole hearts were extracted, blotted dry, and, weighed. Hearts that were reserved for histological analysis were fixed in 4% paraformaldehyde (24-48 hours). A subset of hearts was flash frozen in liquid nitrogen and stored at -80°C for subsequent molecular phenotyping after being dissected into LV, right ventricle, and atria upon extraction.

Quantitative real-time PCR

RNA was isolated from frozen LV and right ventricle tissue using the RNeasy Mini Kit (Qiagen, Valencia, CA) and reverse transcribed to complementary (cDNA) using the High Capacity cDNA Reverse Transcription Kit (Applied Biosystems, Foster City, CA, USA). Quantitative real-time PCR (qPCR) analysis was performed in triplicate using the 7300 Real-Time PCR system (Applied Biosystems), as described (28). Expression of myocardial α-MHC (*Myh6*), β-MHC (*Myh7*), Bax *(Bax)*, Bcl-2 *(Bcl2)*, BNP (*Nppb*), EGR-1 *(Egr1)*, ICAM-1 *(Icam1),* IL-6 *(Il6),* LOX *(Lox),* MCP-1 *(Mcp1)*, MIP-2α *(Cxcl2),* and TGF-β (*Tgfb*) mRNA levels were quantified using Taqman Assays on Demand (Applied Biosystems). Data was normalized to *Gapdh* (endogenous reference) and expressed relative to a designated experimental control group using the $2^{-\Delta\Delta Ct}$ method (29). Only mouse hearts from experiments (sham and IR procedure) evaluating the impact of IR underwent analysis form gene expression at acute time points. Mouse hearts from experiments evaluating the impact of PO were not analyzed for gene expression at acute time points.

Myocardial necrosis

Twenty-four hour plasma cardiac troponin levels were measured by ELISA (Life Diagnostics, West Chester, PA), according to the manufacturer instructions, as a biomarker of cardiomyocyte necrosis and an early index of infarct size (30).

Cardiac structure and function

Echocardiography on conscious mice was performed over the course of 2 weeks (baseline, 24 hours, 72 hours, 1 week, 2 weeks) following IR using a Vevo 2100 Imaging System

(VisualSonics, Toronto, ON). M-mode images were traced to measure direct parameters of cardiac structure at diastole and systole of the cardiac cycle during all 5 of the aforementioned time points. Direct parameters of structure from M-mode images included ventricle wall thickness and chamber size. Wall thickness parameters were inter ventricular septum at systole (IVSs), inter ventricular septum at diastole (IVSd), left ventricular posterior wall at systole (LVPWs), and left ventricular posterior wall at diastole (LVPWd). Chamber size parameters were left ventricular internal diameter at systole (LVIDs) and left ventricular internal diameter at diastole (LVIDd). The calculated parameters of structure (LV Mass) and systolic function (fractional shortening [FS], EF) were derived from the direct parameters of structure as well as from LV volume at systole (Vols) and LV volume at diastole (Vold) as follows:

$$EF\ (\%) = 100 * ((LV\ Vold - LV\ Vols) / LV\ Vold)$$

$$LV\ Vold\ (\mu L) = ((7.0 / (2.4 + LVIDd)) * LVIDd^3)$$

$$LV\ Vols\ (\mu L) = ((7.0 / (2.4 + LVIDs)) * LVIDs^3)$$

$$FS\ (\%) = 100 * ((LVIDd - LVIDs) / LVIDd)$$

$$LV\ Mass\ (corrected)\ (mg) = 0.8424 * ((LVIDd + LVPWd + IVSd)^3 - LVIDd^3)$$

Pulsed wave Doppler on mitral valve images were traced to measure direct parameters of diastolic function and systolic function at baseline and 2 weeks following IR. Direct parameters of diastolic function from Doppler images included early (E)-peak velocity, atrial (A)-peak velocity, isovolumic relaxation time (IVRT), deceleration rate (Dr), and deceleration time (Dt). Direct parameters of systolic function included isovolumic contraction time (IVCT) and aortic ejection time (AET). Each calculated parameter of diastolic dysfunction (E/A ratio) and global function (myocardial performance index [MPI]) was derived from direct parameters of diastolic dysfunction and systolic function as follows:

E/A ratio = E-peak velocity / A-peak velocity

MPI (ratio) = (IVRT + IVCT) / AET

At each time point for each mouse, all direct echocardiography parameters were averaged across a series of ≥3 sets of ≥3 consecutive beats. Heart weight/tibial length ratio at 2 weeks was measured as a secondary parameter of non-echocardiography cardiac structure.

Histology

Fixed hearts were embedded in paraffin, and cut into 5μm transverse sections to measure evidence of fibrosis. Specifically, serial interrupted sectioning was performed to the hearts. Starting from the apex, the most inferior distance where sections were collected occurred where both the left and right ventricle could be visualized. A series of sections (4-6) were collected at this distance. The next series of sections were collected at a distance 200 microns superior to the previous distance. This was repeated for several distances to cover a large portion of the heart where injury was anticipated to occur. For hearts of mice undergoing IR, sections from 8 distances (spanning 1800 microns from the most inferior distance) were collected per sample (note: only 4 distances were collected from an IR experiment described later where sections were stained with both Masson's Trichrome and Picrosirius Red stain). Sections from 5 distances (spanning 1000 microns) were collected per sample for hearts of mice undergoing permanent ischemia. For each sample, a slide contained a section from each distance where sections were collected. The result was that each slide contained serial sections with each section representing a specific distance from the apex of the heart. Our group believed that this technique was advantageous over the traditional approach of analyzing an isolated section from each sample. Furthermore, each heart sample had multiple slides which allowed for multiple stains to be done

at each specific distance from the heart's apex. Embedding and processing of samples were completed in the Cell Services & Histology Core within the UNC Center for Gastrointestinal Biology and Disease. Sectioning and staining by was done in the Histology Research Core within the Department of Cell Biology and Physiology under the direction of Kirk McNaughton.

Sections were stained with Picrosirius Red (collagen) or Masson's Trichrome (connective tissue including collagen and proteoglycans) for image analysis.

All images were digitally scanned with the ScanScope CS System (Aperio Technologies, Vista, CA). From the digital scans, one 1x zoom image was taken per section of each sample, which allowed for the coverage of the entire heart cross-section. The area of fibrosis was measured with NIH ImageJ (31). Specifically, two sets of color thresholding minimums and maximums for red, green, and blue colors were generated to capture the area of the stain and the area of the total ventricle cross-section. These thresholding ranges were generated from three randomly-selected representative images. The same ranges for stain and total cross-section were applied to all sections used in the study without regards to treatment groups to minimize observer bias. The surface area of staining was normalized to the surface area of total myocardial tissue for each section. The resulting % stained value averaged over the total amount of serial sections used for each sample (sections from 4-8 distances) generated a single value per mouse that reflected the average staining throughout the infarcted region. All quantification was averaged over multiple sections per heart sample using NIH ImageJ.

Statistical analysis

Data are expressed as mean± standard error of the mean (SEM) unless stated otherwise. All analyses were conducted on log-transformed data. Gene expression and troponin data were

compared across experimental groups with Student's t-test at every given time point. For M-mode-derived echocardiography analysis in mice from IR experiments, data from 3 different experiments that used different time points were merged together for graphical purposes but were analyzed as 3 separate data sets statistically to compare parameters between experimental groups. Echocardiography data at 1 and 3 days were each analyzed with ANCOVA with baseline as a covariate followed by Fisher's LSD *post hoc* tests (if overall ANCOVA was significant). Echocardiography data at 7 and 14 days were from the same experiment and analyzed together using repeated measures ANOVA with baseline as a covariate followed by Fisher's LSD *post hoc* tests (if overall repeated measures ANOVA was significant). For Pulse Wave Doppler-derived echocardiography analysis, data were compared across experimental groups using ANCOVA at 2 weeks with baseline as a covariate followed by Fisher's LSD *post hoc* tests (if overall ANCOVA was significant). For M-mode-derived echocardiography analysis in mice from PO experiments, data at 7 and 14 days were from the same experiment and analyzed together across experimental groups together using repeated measures ANOVA with baseline values as a covariate followed by Fisher's LSD *post hoc* tests (if overall ANCOVA was significant). For histology data analyzed across two experimental groups, comparisons were performed with Student's t-test at 2 weeks. For histology data comparing staining methods, linear regression analysis was conducted and Pearson's correlation coefficient was calculated. $P<0.05$ was considered to be statistically significant. Statistical analyses were performed using SAS 9.2 (SAS Institute, Cary, NC).

Results

Acute biomarkers of myocardial injury, inflammation, and remodeling following ischemia reperfusion

Myocardial ischemia for 30 minutes significantly increased biomarkers of cardiomyocyte necrosis and apoptosis compared to sham treatment. In particular, IR increased plasma troponin levels after 2 and 24 hours of reperfusion (Figure 4.1a) and myocardial Bax:Bcl-2 ratio mRNA levels at 24 hours of reperfusion compared to sham-treated mice (Figure 4.1b). Similarly, IR increased myocardial inflammatory gene expression compared to sham-treated mice at 2 hours, 24 hours, or 2 and 24 hours of reperfusion (Figure 4.2). LV *Il6* expression was significantly increased by IR at 2 and 24 hours following IR (Figure 4.2a). Right ventricle *Il6* expression was significantly increased in IR-treated mice at 24 hours following IR (Figure 4.2b). Importantly, the magnitude of induction in the right ventricle was less pronounced than in the LV. Expression of subsequent markers is only reported in the LV. LV *Mcp1* expression was significantly greater in IR-treated hearts compared to sham at 2 hours following IR (Figure 4.2c), demonstrating IR-induced upregulation of monocyte expression. Expression of *Cxcl2* in the LV was significantly increased by IR at 2 and 24 hours following IR (Figure 4.2d). Expression of *Icam1* in the LV was greater in IR-treated hearts compared to sham-treated hearts at 2 hours following IR (Figure 4.2e).

IR also increased the myocardial mRNA levels of a majority of the markers associated with ventricular remodeling at acute time points following initial injury (Figure 4.3). IR induction of *Egr1* expression was significantly pronounced 2 hours following IR (Figure 4.3a). Expression of LV *Tgfb* was not significantly increased by IR injury at 2 hours (P=0.68) or 24

hours (P=0.25) of reperfusion (Figure 4.3b). However, *Lox* expression was significantly increased at 2 and 24 hours of reperfusion in IR-treated mice compared to sham-treated mice (Figure 4.3c). Expression of LV *Myh7:Myh6* was significantly increased by IR at 24 hours following IR injury (Figure 4.3d). LV atrial natriuretic factor (ANF) expression was not significantly induced by IR at 2 hours (P=0.91) or 24 hours (P=0.22) of reperfusion (Figure 4.3e). In contrast, BNP gene expression in the LV was significantly greater in IR-treated mouse hearts compared to sham-treated hearts at 2 hours following IR (Figure 4.3f). BNP expression was not statistically significant at 24 hours following IR (P=0.14).

Systolic function

IR did not significantly alter EF over time compared to sham treatment (Analysis A [1 day] P=0.070, Analysis B [3 days] P=0.202, Analysis C [7 and 14 days] P=0.460; Figure 4.4a). Likewise, IR did not significantly alter FS over time compared to sham treatment (Analysis A [1 day] P=0.113, Analysis B [3 days] P=0.172, Analysis C [7 and 14 days] P=0.539; Figure 4.4b). EF and FS were lower in IR-treated mice compared to sham-treated mice at 2 weeks; however, the difference was not statistically significant and should be interpreted with caution (EF: overall repeated measures ANOVA P=0.460, Fisher's post-hoc P=0.048; FS: overall repeated measures ANOVA P=0.539, Fisher's post-hoc P=0.054).

Similar results were seen with Pulse Wave Doppler image-derived parameters of systolic function Table 4.1). IVCT was not impacted by IR-treatment compared to sham treatment at 2 weeks (P=0.41). AET was not affected by IR compared to sham (P=0.14).

Diastolic function

Diastolic dysfunction indicated by a reduction in E/A ratio, was unchanged between sham and IR at 2 weeks following IR (P=0.678; Figure 4.5a). Likewise, IVRT was not affected by IR treatment compared to sham treatment at 2 weeks of reperfusion (P=0.951; Figure 4.5b). This was confirmed in all other parameters of diastolic dysfunction (P>0.05 for all parameters, Analyses A-C Table 4.1).

Cardiac structure

Mean echocardiography-derived parameters of cardiac structure over 2 weeks for sham and IR mice are summarized in Table 4.2. IR did not significantly alter any of these indices over time compared to sham treatment (P>0.05 for all parameters in Analyses A-C). Likewise, there was no difference in heart weight/tibial length between IR and sham (5.82 ± 0.35 versus 6.18 ± 0.24 mg/mm, respectively, P=0.486).

Myocardial fibrosis

Given the early induction of LOX in myocardial tissue acutely following IR, heart sections were stained for evidence of collagen deposition. Histological stains of collagen were examined using two different staining approaches. Collagen deposition as measured by Picrosirius Red was significantly correlated with connective tissue deposition from Masson's trichrome staining (Figure 4.6) at 2 weeks following IR. Following the confirmation of a correlation between the stains, further analysis was conducted with Picrosirius Red stained slides only since thresholding was more time-efficient thresholding compared to Masson's Trichrome (2-color stain vs 3-color stain). An independent experiment was conducted to determine the

impact of IR on collagen deposition. Although sham-treated hearts did show evidence of collagen at 2 weeks, induction of collagen was significantly increased in the IR-treated mice (Figure 4.7a-b) with a mean % collagen deposition of 3.43 ± 0.64%.

Impact of permanent occlusion

A subset of mice were subjected to permanent LAD ligation surgery (2 weeks of ischemia) for comparison with the above results in IR-treated mice as a means to further characterize the impact of IR on ventricular remodeling. PO did not significantly alter LVIDs (Figure 4.8a) or EF (Figure 4.8b). In particular, at 1 and 2 weeks following PO, LVIDs was non-significantly increased by 1.93-fold and 2.07-fold induction, respectively, by PO compared to sham. EF in PO-treated mice was 0.62-fold and 0.59-fold the value of sham-treated mice at 1 and 2 weeks, respectively. Similar results were observed with other parameters of cardiac structure that showed a lack of effect (LVIDd: Repeated measures ANOVA P=0.096) and function (FS: Repeated measures ANOVA P=0.510). In contrast, PO enhanced fibrosis extensively with a mean % connective tissue deposition of 29.07 ± 4.93% (Figure 4.8c-d). Myocardial structural changes (including ventricular wall thinning) were qualitatively evident in the majority of heart from mice that underwent permanent ischemia (Figure 4.8c), but not appreciable following IR (Figure 4.7b).

Discussion

Preclinical models of post-AMI myocardial remodeling are critical tools that aid in the discovery and development of novel therapeutic strategies (20), but they can only facilitate translation of novel strategies if they truly mimic the pathophysiology of AMI in humans. There are few reports in the literature fully dedicated to the characterization of pathological responses in mice following myocardial IR. Consequently, using molecular, echocardiography, and histological approaches, we determined that a 30-minute mouse model of myocardial ischemia followed by reperfusion caused time-dependent responses associated with ventricular remodeling. In particular, IR induced myocardial cell death and inflammation acutely following ischemia and generated substantial fibrosis at an early chronic time point, but did not cause significant changes in myocardial structure or function.

The acute myocardial cell death and inflammatory response in the current study peaked at 2 hours and dropped by 24 hours, though the drop was not to the level of sham-treated mice; this demonstrates the transient but marked acute response that occurs in the myocardium following IR. These effects were most pronounced in the left ventricule. Importantly, they were also present in the right ventricle (to a lesser degree), despite the fact that the LAD does not supply the right ventricle. These acute myocardial necrotic and inflammatory responses mirror what has been shown by others. It has been previously shown that IR in mice causes acute increases in troponin levels that are low in sham-operated mice (32). An investigation of the time course of myocardial inflammatory gene expression showed that IR induced IL-6 expression markedly at 3 hours of reperfusion. This increase in cytokine expression had largely dissipated after 24 hours of reperfusion, but levels remained significantly elevated compared to sham (33).

Fibrosis is a key component of ventricular remodeling and biomarkers of fibrosis are independent predictors of poor prognosis in patients with ventricular remodeling on top of established risk factors (34, 35). In the current study, myocardial fibrosis formation was the most altered phenotype during the early chronic phase following IR. IR promoted the deposition of collagen into the myocardial tissue. This finding was supported by the foreboding induction of myocardial LOX gene expression, a key mediator of collagen maturation, during the acute phase following IR. The induction of left ventricular TGF-β expression by IR was not statistically significant; however, evidence exists that this important fibrosis mediator may reach its peak at 72 hours following IR in C57BL/6 mice (36). Furthermore, a greater than 2-fold change at 24 hours suggests that this lack of a statistically significant difference was due, at least partially, to low power (n=3, coefficient of variation at 24 hours in IR-treated mice=52.11%). Moreover, *Gapdh* may not be the most stable housekeeping gene in the AMI model and may have increased variability within experimental groups (37). Thus further exploration including validation with a larger n, follow-up with myocardial protein expression analysis, the inclusion of an additional 'subacute' time point (3 days following IR), and confirmation with a second housekeeping gene is necessary to address limitations with the evaluation of mRNA expression data in this study.

In contrast to induction of myocardial fibrosis, IR did not produce significant changes in cardiac structure demonstrating that there was no evidence of ventricular wall thinning or hypertrophy. Furthermore, IR did not produce significant changes in either systolic or diastolic function during the acute (24 hours), subacute (3 days) and early chronic (7, 14 days) time points. This discrepancy between the induction of myocardial fibrosis and structural/functional changes was unexpected. One possible explanation for this finding is that changes in cardiac function actually occurred, but echocardiography was not sensitive enough to pick up these

changes. The use of alternate tools that may be more sensitive in detecting cardiac function changes (i.e., catheter-based invasive analyses (38)) would provide more insight as to whether technical difficulties contributed to the lack of association between fibrosis and cardiac dysfunction. Another plausible explanation for these findings is that perhaps the fibrosis changes truly did not correlate with cardiac function. Indeed, these findings agree with clinical data showing that fibrosis does not correlate with ejection fraction. In heart failure participants from the Cardiovascular Health Study, circulating BNP levels, but not markers of collagen deposition discriminated heart failure patients with preserved ejection fraction from those with reduced ejection fraction even after adjustment for covariates (39). This is further corroborated in another clinical study in which no association was found between a marker of collagen deposition and either structural or functional cardiac dysfunction (40). In line with this explanation, it is possible that enhanced fibrosis compensated for and thus masked any worsening of IR-induced systolic dysfunction by replacing dead myocardial cells and preserving the structural integrity of the ventricle. This is supported by our data which shows an early increase in expression of fetal gene activation mediators, demonstrating that mediators of cardiac dysfunction had been, at least transiently, activated. Furthermore, we do not differentiate between adaptive and maladaptive fibrosis which would provide insight as to if the increased fibrosis compensated for changes in dysfunction. However, few studies investigating fibrosis address this issue because techniques that delineate protective and harmful fibrosis have not been developed (41). This is an important future area of investigation because novel therapies that attenuate adaptive fibrosis would be deleterious. New approaches are needed to better discriminate between adaptive and maladaptive fibrosis as well as the relationship between these processes and cardiac function/structure in this mouse model of AMI.

Any subtle differences in systolic function that *did* occur were observed at the earliest (24 hours) and latest (2 weeks) measured time points following IR. This biphasic pattern of dysfunction likely derives from two independent sources of tissue damage with the initial hit being related to infarct size and the second drop occurring in latter stages when fleeting attempts to recover from the acute injury causes overcompensating, maladaptive ventricular remodeling. Considering the lack of a statistical significance in cardiac dysfunction at these two time points, these data must be interpreted with major caution. However, this postulation is supported by clinical evidence that recovery of initial systolic dysfunction is a common clinical occurrence (42). Furthermore, evidence exists in C57BL/6 mice that the most pronounced drop in EF may occur at about 7 weeks of reperfusion following IR (43), shining light on the possibility of a triphasic pattern of systolic dysfunction in this strain of mice. Moreover, structural changes related to dilated cardiomyopathy (increased end diastolic volume and reduced ventricular wall thickness) have been found to peak after 7 weeks of reperfusion following IR (43). A future investigation evaluating the impact of 30-minute myocardial IR in mice on cardiac structure and function at prolonged reperfusion time points is warranted (late chronic phase: >7 weeks post-IR).

Thus, the *in vivo* mouse model of 30-minute ischemia followed by 2 weeks of reperfusion is best suited for investigating the impact of intervention on inflammatory and fibrotic responses independent of cardiac structure or function. On the other hand, we found that an *in vivo* mouse model of permanent LAD coronary artery ligation for 2 weeks caused gross histological evidence of ventricular dilation, myocardial wall thinning, and myocardial fibrosis. This agrees with previous data showing structural changes as early as 1 week following surgery (23). Furthermore, an acute inflammatory response is blunted in the permanent ischemia model (23,

33), which precludes the investigation of acute inflammatory response with that model. PO did not significantly alter systolic and diastolic function at 2 weeks of ischemia. Considering the large absolute decline in EF (0.59 fold at 2 weeks) and increase in LVIDs (2.07-fold at 2 weeks) which are indicative of reduced systolic function and dilated cardiomyopathy, respectively, as well as the aforementioned PO-induced histological alterations of ventricular remodeling, statistical power may have played a role, at least partially, in the non-significant findings (coefficient of variation in EF at 2 weeks in IR-treated mice=61.40%). Although conscious echocardiography measurements offer the advantage of deriving physiological parameters, they also may increase variability due to varying levels of excitement and sympathetic activation from being manipulated (25); this may potentially reduce power. This hypothesis needs confirmation in future studies with a larger sample size or with echocardiography using anesthetized mice.

There are limitations in this study. The reproducibility of the extent of injury varies since placement of the ligature influences the size of the infarct. Sources of this problem include the small size of the mouse heart and variation in coronary branching pattern even among inbred mice, but technology to improve the consistency of mouse infarcts within experiments are improving (32). Moreover, results may not translate to humans for a variety of reasons. Firstly, this model of IR does not entirely replicate revascularization following an AMI in humans because our mice do not have underlying atherosclerotic cardiovascular disease at the time of surgery. Efforts have begun to utilize mice with comorbid conditions in models of AMI (44). Secondly, suture ligation does not mimic the etiology of AMI, which most commonly involves the disruption and occlusion of an atheromatous plaque in the coronary artery. Preclinical models of thrombosis-induced AMI are in the infancy phases in large animals and rodents and are not yet routinely used as established methods (45, 46). Thirdly, results are only from C57BL/6 mice,

though myocardial IR injury in mice varies by strain (43, 47). The Collaborative Cross is a large panel of novel inbred mouse strains that simulate genetic diversity in humans (48). Application of this tool to AMI is a potential avenue for further investigation that could increase the generalizability of results. Altogether, scarce data exist in the literature that utilize IR models more closely resembling AMI in clinical practice, thus these are issues that have not been adequately addressed by the scientific community and warrant further investigation.

In conclusion, the present study demonstrates that myocardial IR injury induces myocardial cell death, inflammation, and collagen deposition. As a whole, these results provide a better understanding of the pathology that occurs after AMI and facilitate the design and interpretation of future studies that investigate the role of pathways as novel therapeutic targets in mouse models of AMI. For our research group, these findings lay the foundation for the evaluation of the contribution of cardiomyocyte sEH to maladaptive ventricular remodeling in mice post-AMI *in vivo*.

Figures

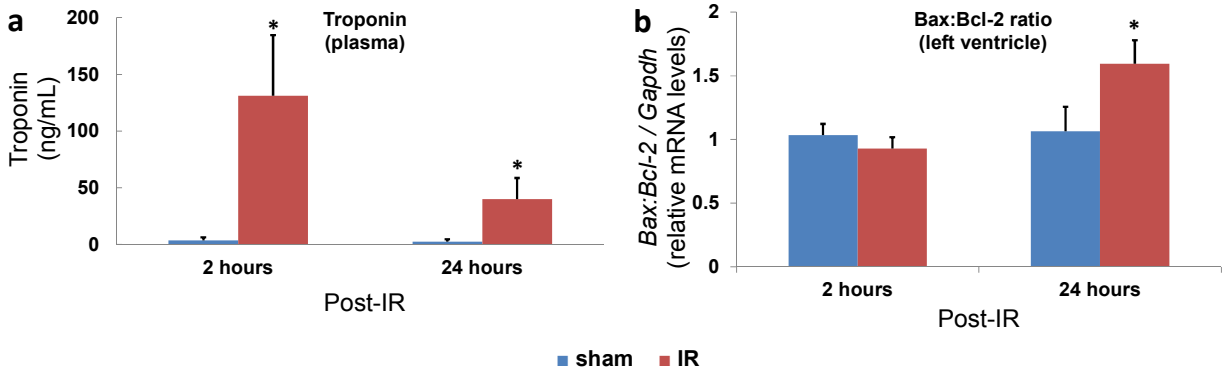

Figure 4.1 Impact of myocardial ischemia reperfusion (IR) on myocardial cell death. Time course of myocardial IR-induced (a) necrosis and (b) apoptosis. Reference group for relative mRNA levels: sham levels at 24 hours. Sham: n = 3-5 per group. IR: n = 4-8 per group. * $P <$ 0.05 for sham vs IR at each time point. Bax, bcl-2-like protein 4; Bcl-2, B-cell lymphoma 2.

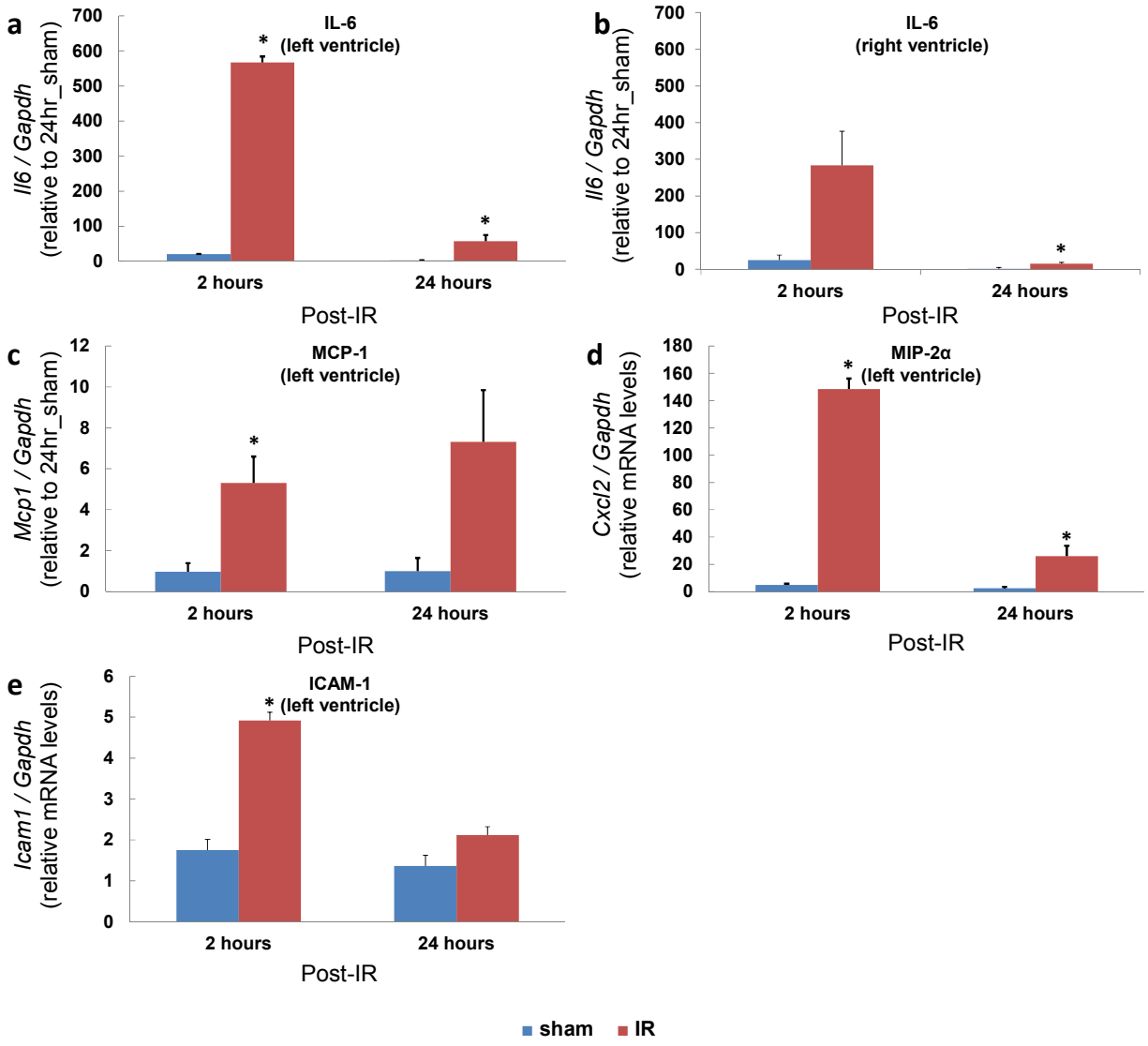

Figure 4.2 Impact of myocardial ischemia reperfusion (IR) on acute inflammatory responses. Time course of myocardial IR-induced (a-b) cytokine, (c-d) chemokine, and (e) cellular adhesion molecule expression in the left ventricle (LV) or right ventricle. Reference group for relative mRNA levels: sham levels at 24 hours. Sham: n = 3 per group. IR: n = 4-5 per group. * $P < 0.05$ for sham vs IR at each time point. ICAM-1, intercellular adhesion molecule 1; IL-6, interleukin 6; MCP-1, monocyte chemoattractant protein-1; MIP-2α, macrophage inflammatory protein 2-alpha.

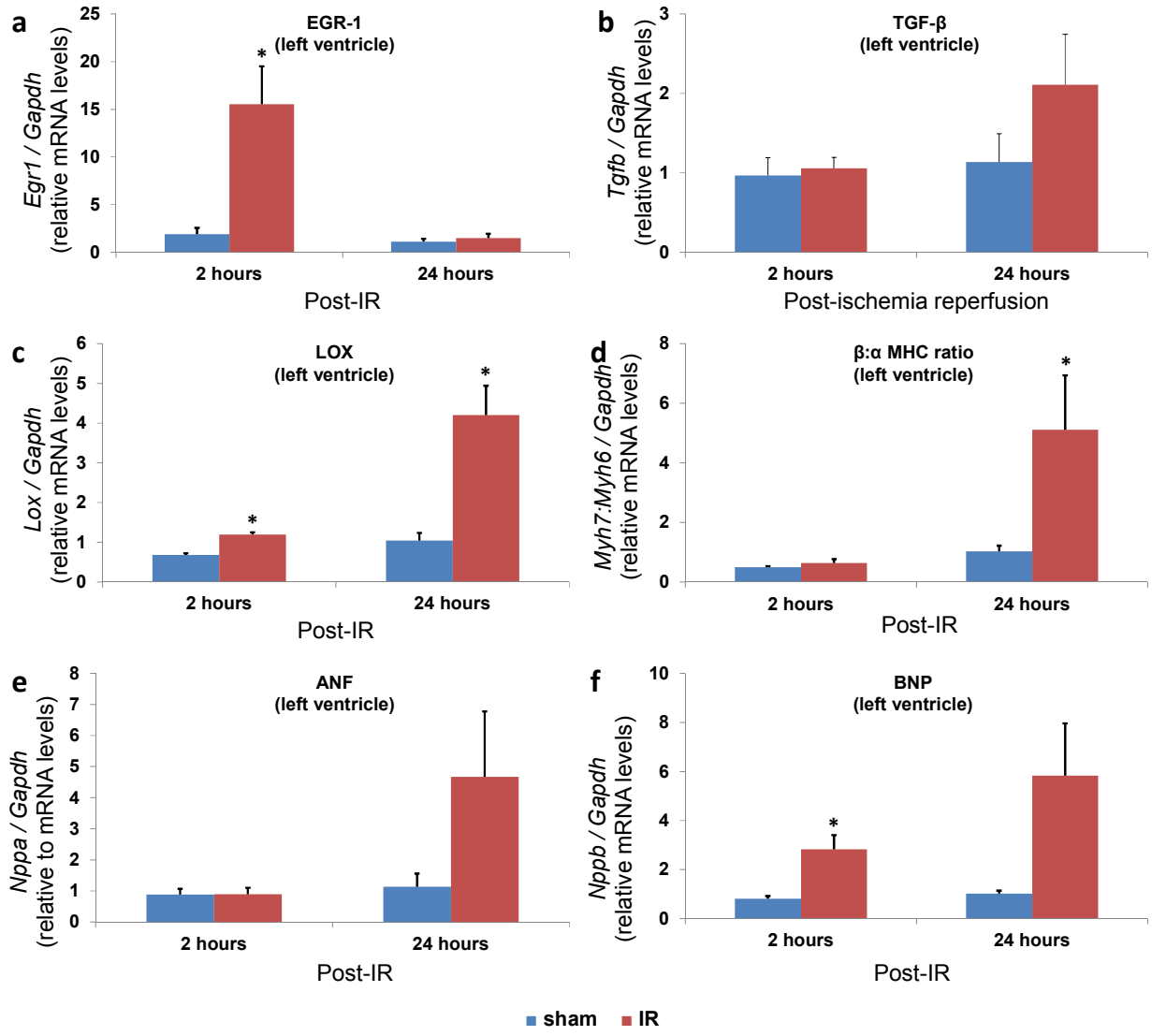

Figure 4.3 Impact of myocardial ischemia reperfusion (IR) on early maladaptive ventricular remodeling. Time course of myocardial IR-induced (a) early response, (b-c) fibrosis, and (d-f) fetal gene activation expression. Reference group for relative mRNA levels: sham levels at 24 hours. Sham: n = 3 per group. IR: n = 3-5 per group. * $P < 0.05$ for sham vs IR at each time point. ANF, atrial natriuretic factor; BNP, brain natriuretic peptide; EGR-1, early growth response protein 1; LOX, lysyl oxidase; MHC, myosin heavy chain; TGF-β, transforming growth factor beta

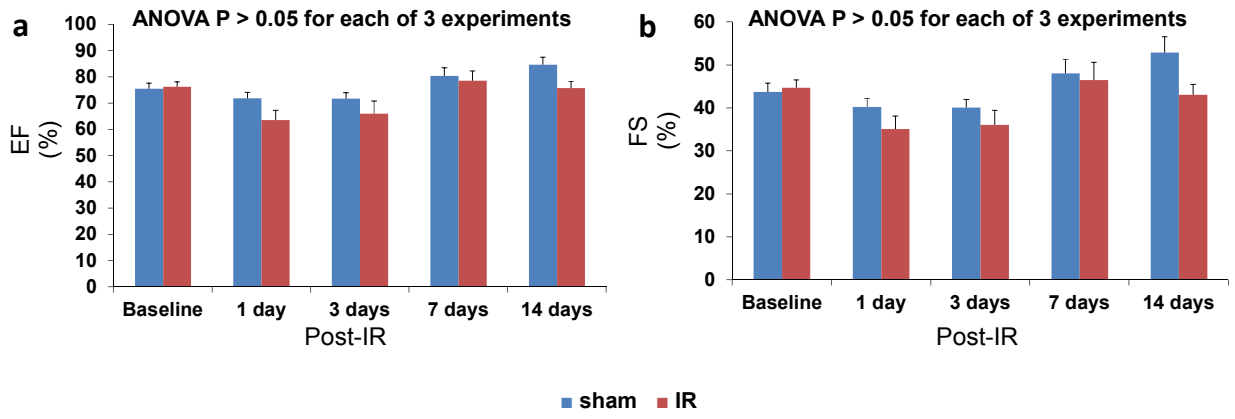

Figure 4.4 Impact of myocardial ischemia reperfusion (IR) on systolic function. Time course of myocardial IR-induced changes on (a) ejection fraction (EF) and (b) fractional shortening (FS). Combined mean±SEM from 3 experiments are displayed. Experiment 1 measured parameters at baseline, 7 days, and 14 days: N = 6-7 per group. Experiment 2 measured parameters at baseline, 1 day, and 3 days: N = 2-7 per group. Experiment 3 measured parameters at baseline and 1 day: N = 7-12 per group. Total: n = 2-26 per time-group (n=2 in sham group at 3 days only). Due to sample size differences and experiment differences for each time point, analyses were conduct as 3 individual data sets. Analysis A involved '1 day' data corrected for baseline using ANCOVA. Analysis B involved '3 days' data corrected for baseline using ANCOVA. Analysis C involved '7 days' and '14 days' data corrected for baseline using repeated measures ANOVA.

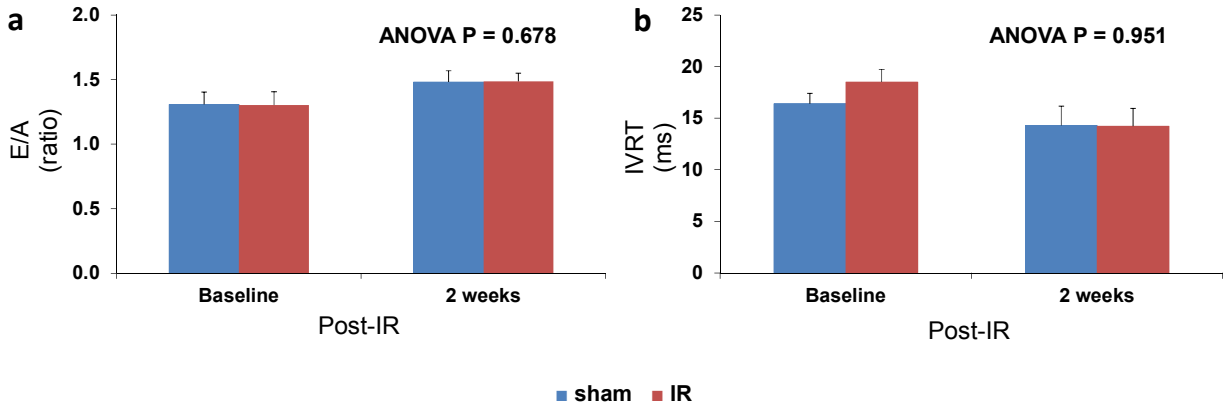

Figure 4.5 Impact of myocardial ischemia reperfusion (IR) on diastolic function.

Myocardial IR-induced changes on (a) E-peak velocity / A-peak velocity (E/A) ratio and (b) isovolumic relaxation time (IVRT) at 2 weeks following IR. n = 7-9 per group. $P > 0.05$ for sham vs IR at 2 weeks corrected for baseline

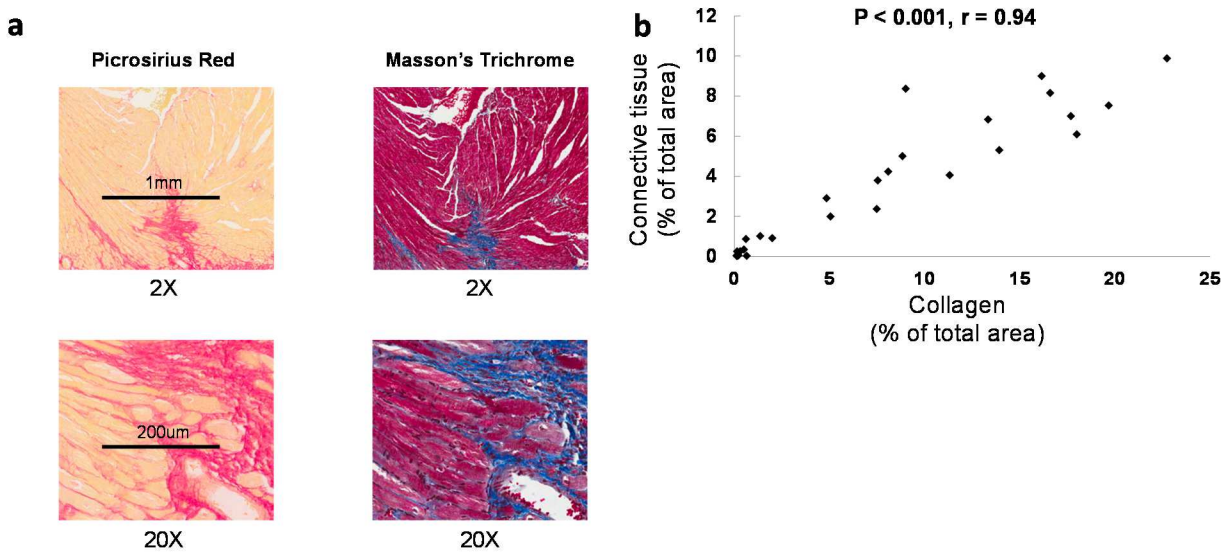

Figure 4.6 Correlation between staining methods of fibrosis. (a) Representative images and (b) correlation of Picrosirius Red- and Masson's Trichrome-blue stained heart sections (averaged from 4 distances of the heart) at 2 weeks following ischemia reperfusion (IR). n = 27.

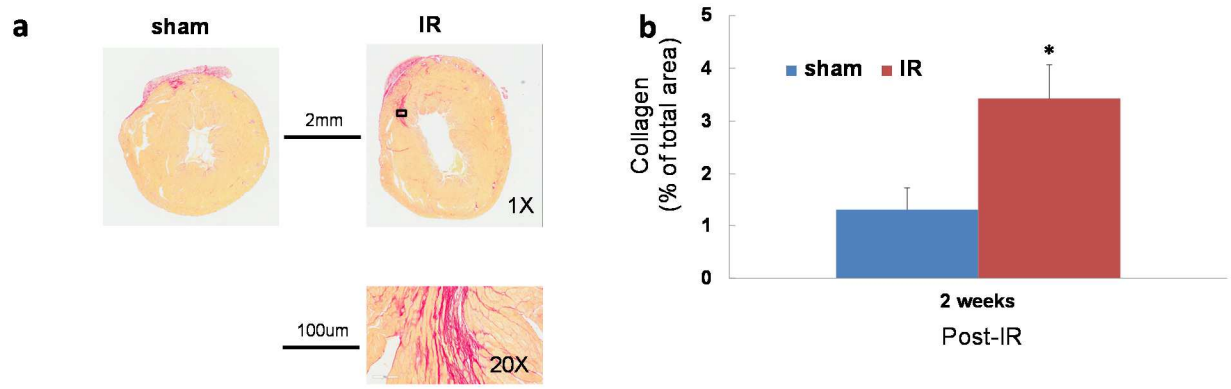

Figure 4.7 Impact of myocardial ischemia reperfusion (IR) on fibrosis. (a) Representative 1X images between groups as well as a zoomed 20X image detailing pattern the of collagen deposition in an IR-treated mouse and (b) quantification of collagen deposition from Picrosirius Red-stained heart sections (averaged from 8 distances of the heart) at 2 weeks following IR. Each set of images has a different scale. Sham: n = 6. IR: n = 8. * $P < 0.05$

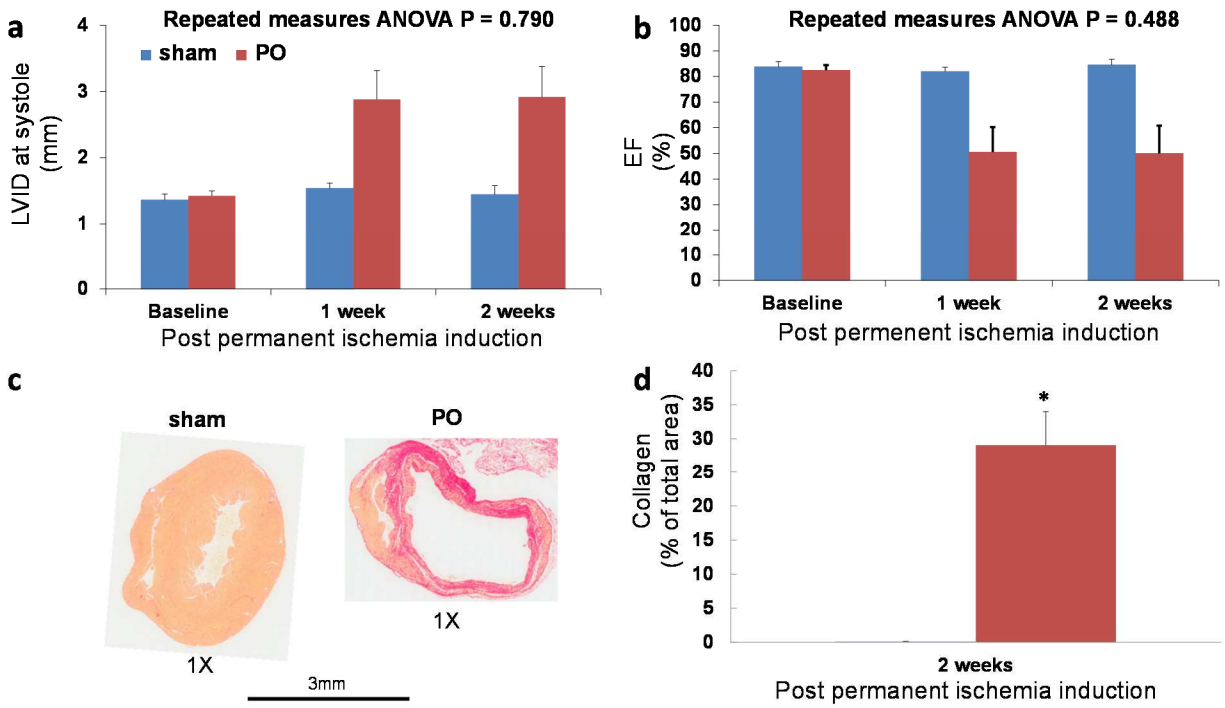

Figure 4.8 Impact of myocardial permanent occlusion (PO) on maladaptive ventricular remodeling. Impact of permanent ischemia on (a) left ventricular internal diameter (LVID) and (b) ejection fraction (EF) as well as (c) representative images and (d) quantification of collagen deposition from Picrosirius Red-stained heart sections (averaged from 5 distances of the heart) at 2 weeks of PO. Sham: n = 5. IR: n = 8. * $P < 0.05$.

Tables

Table 4.1 Impact of myocardial ischemia reperfusion (IR) on mitral pulse Doppler parameters of cardiac dysfunction

Parameters	Baseline	2 weeks	P
Isovolumic contraction time (IVCT), ms			
sham	11.0 ± 0.9	16.1 ± 2.0	0.421
IR	12.2 ± 1.0	13.3 ± 1.5	
Aortic ejection time (AET), ms			
sham	29.8 ± 2.0	34.1 ± 1.2	0.326
IR	28.4 ± 1.8	36.7 ± 1.6	
Early-peak velocity (E), mm/s			
sham	441.4 ± 39.8	579.9 ± 49.9	0.859
IR	457.4 ± 36.5	585.5 ± 64.0	
Atrial-peak velocity (A), mm/s			
sham	341.7 ± 33.2	402.3 ± 44.6	0.961
IR	356.8 ± 25.1	397.7 ± 45.5	
E/A, ratio			
sham	441.4 ± 39.8	579.9 ± 49.9	0.902
IR	457.4 ± 36.5	585.5 ± 64.0	
Deceleration (Dt), ms			
sham	24.2 ± 2.8	21.9 ± 2.1	0.575
IR	27.7 ± 2.9	21.5 ± 2.4	
Deceleration (Dr), mm/s^2			
sham	-19.2 ± 2.1	-27.6 ± 3.8	0.906
IR	-18.9 ± 3.2	-28.2 ± 5.3	
Isovolumic relaxation time (IVRT), ms			
sham	16.4 ± 1.0	14.3 ± 1.9	0.877
IR	18.5 ± 1.2	14.2 ± 1.7	
Myocardial performance index (MPI), ratio			
sham	1.0 ± 0.1	0.9 ± 0.1	0.481
IR	1.1 ± 0.1	0.8 ± 0.1	

Comparisons at 2 weeks between sham and IR were corrected for baseline levels. N = 7-9 per group. * $P < 0.05$ for sham vs. IR

Table 4.2 Impact of myocardial ischemia reperfusion (IR) on cardiac structure over time

Parameters	Baseline	1 day	3 days	7 days	14 days
LVIDs (mm)					
sham	1.74 ± 0.10	1.94 ± 0.08	2.08 ± 0.17	1.39 ± 0.11	1.20 ± 0.15
IR	1.73 ± 0.09	2.07 ± 0.13	2.09 ± 0.05	1.44 ± 0.19	1.53 ± 0.07
LVIDd (mm)					
sham	3.06 ± 0.08	3.24 ± 0.10	3.48 ± 0.02	2.67 ± 0.15	2.49 ± 0.17
IR	3.09 ± 0.09	3.14 ± 0.10	3.25 ± 0.11	2.63 ± 0.22	2.71 ± 0.12
IVSs (mm)					
sham	1.72 ± 0.05	1.68 ± 0.05	1.69 ± 0.16	1.86 ± 0.08	1.88 ± 0.05
IR	1.65 ± 0.03	1.48 ± 0.07	1.49 ± 0.08	1.82 ± 0.07	1.86 ± 0.07
IVSd (mm)					
sham	1.19 ± 0.03	1.14 ± 0.04	1.08 ± 0.03	1.33 ± 0.04	1.33 ± 0.04
IR	1.13 ± 0.03	1.09 ± 0.04	1.10 ± 0.07	1.36 ± 0.08	1.33 ± 0.07
LVPWs (mm)					
sham	1.64 ± 0.07	1.57 ± 0.05	1.49 ± 0.11	1.71 ± 0.11	1.83 ± 0.13
IR	1.71 ± 0.04	1.51 ± 0.08	1.48 ± 0.03	1.69 ± 0.13	1.66 ± 0.05
LVPWd (mm)					
sham	1.09 ± 0.05	1.13 ± 0.05	1.03 ± 0.00	1.21 ± 0.07	1.38 ± 0.16
IR	1.07 ± 0.03	1.03 ± 0.04	0.98 ± 0.05	1.25 ± 0.17	1.27 ± 0.06
Echocardiography-derived LV mass corrected (mg)					
sham	104.48 ± 4.89	113.33 ± 5.77	111.97 ± 3.85	104.21 ± 8.57	104.01 ± 4.28
IR	99.57 ± 3.17	97.23 ± 4.32	99.93 ± 10.36	104.53 ± 6.10	109.82 ± 7.17

Combined mean±SEM from 3 experiments are displayed.

Experiment 1 measured parameters at baseline, 7 days, and 14 days: N = 6-7 per group. Experiment 2 measured parameters at baseline, 1 day, and 3 days: N = 2-7 per group. Experiment 3 measured parameters at baseline and 1 day: N = 7-12 per group. Total: n = 2-26 per time-group (n=2 in sham group at 3 days only). Due to sample size differences and experiment differences for each time point, analyses were conducted as 3 individual data sets. Analysis A involved '1 day' data corrected for baseline using ANCOVA. Analysis B involved '3 days' data corrected for baseline using ANCOVA. Analysis C involved '7 days' and '14 days' data corrected for baseline using repeated measures ANOVA. * $P < 0.05$.

IVSd, interventricular septum at diastole; IVSs, interventricular septum at systole; LV, left ventricle; LVIDd, left ventricular internal diameter at diastole; LVIDs, left ventricular internal diameter at systole; LVPWd, left ventricular posterior wall at diastole; LVPWs, left ventricular posterior wall at systole

REFERENCES

(1) Velagaleti, R.S. *et al.* Long-term trends in the incidence of heart failure after myocardial infarction. *Circulation* 118, 2057-62 (2008).

(2) Mozaffarian, D. *et al.* Heart disease and stroke statistics-2015 update: a report from the american heart association. *Circulation* 131, e29-e322 (2015).

(3) Zhao, Z.Q. & Vinten-Johansen, J. Myocardial apoptosis and ischemic preconditioning. *Cardiovasc Res* 55, 438-55 (2002).

(4) White, H.D. Pathobiology of troponin elevations: do elevations occur with myocardial ischemia as well as necrosis? *J Am Coll Cardiol* 57, 2406-8 (2011).

(5) Tarzami, S.T., Cheng, R., Miao, W., Kitsis, R.N. & Berman, J.W. Chemokine expression in myocardial ischemia: MIP-2 dependent MCP-1 expression protects cardiomyocytes from cell death. *J Mol Cell Cardiol* 34, 209-21 (2002).

(6) Frangogiannis, N.G. Regulation of the inflammatory response in cardiac repair. *Circ Res* 110, 159-73 (2012).

(7) Shinde, A.V. & Frangogiannis, N.G. Fibroblasts in myocardial infarction: a role in inflammation and repair. *J Mol Cell Cardiol* 70, 74-82 (2014).

(8) Rienks, M., Papageorgiou, A.P., Frangogiannis, N.G. & Heymans, S. Myocardial extracellular matrix: an ever-changing and diverse entity. *Circ Res* 114, 872-88 (2014).

(9) Cox, E.J. & Marsh, S.A. A systematic review of fetal genes as biomarkers of cardiac hypertrophy in rodent models of diabetes. *PLoS One* 9, e92903 (2014).

(10) Iqbal, N. *et al.* Cardiac biomarkers: new tools for heart failure management. *Cardiovasc Diagn Ther* 2, 147-64 (2012).

(11) Gupta, M.P., Gupta, M., Zak, R. & Sukhatme, V.P. Egr-1, a serum-inducible zinc finger protein, regulates transcription of the rat cardiac alpha-myosin heavy chain gene. *J Biol Chem* 266, 12813-6 (1991).

(12) Armstrong, P.W. Left ventricular dysfunction: causes, natural history, and hopes for reversal. *Heart* 84 Suppl 1, i15-7:discussion i50 (2000).

(13) Pfeffer, M.A. & Braunwald, E. Ventricular remodeling after myocardial infarction. Experimental observations and clinical implications. *Circulation* 81, 1161-72 (1990).

(14) Pitt, B. *et al.* Eplerenone, a selective aldosterone blocker, in patients with left ventricular dysfunction after myocardial infarction. *N Engl J Med* 348, 1309-21 (2003).

(15) de Lemos, J.A. *et al.* Early intensive vs a delayed conservative simvastatin strategy in patients with acute coronary syndromes: phase Z of the A to Z trial. *JAMA* 292, 1307-16 (2004).

(16) Pizarro, G. *et al.* Long-term benefit of early pre-reperfusion metoprolol administration in patients with acute myocardial infarction: results from the METOCARD-CNIC trial (Effect of Metoprolol in Cardioprotection During an Acute Myocardial Infarction). *J Am Coll Cardiol* 63, 2356-62 (2014).

(17) O'Gara, P.T. *et al.* 2013 ACCF/AHA guideline for the management of ST-elevation myocardial infarction: executive summary: a report of the American College of Cardiology Foundation/American Heart Association Task Force on Practice Guidelines. *Circulation* 127, 529-55 (2013).

(18) Amsterdam, E.A. *et al.* 2014 AHA/ACC guideline for the management of patients with non-ST-elevation acute coronary syndromes: executive summary: a report of the American College of Cardiology/American Heart Association Task Force on Practice Guidelines. *Circulation* 130, 2354-94 (2014).

(19) Dargie, H. Heart failure post-myocardial infarction: a review of the issues. *Heart* 91 Suppl 2, ii3-6; discussion ii31, ii43-8 (2005).

(20) Lefer, D.J. & Bolli, R. Development of an NIH consortium for preclinicAl AssESsment of CARdioprotective therapies (CAESAR): a paradigm shift in studies of infarct size limitation. *J Cardiovasc Pharmacol Ther* 16, 332-9 (2011).

(21) Michael, L.H. *et al.* Myocardial ischemia and reperfusion: a murine model. *Am J Physiol* 269, H2147-54 (1995).

(22) Travis, J. Scoring a technical knockout in mice. *Science* 256, 1392-4 (1992).

(23) Vandervelde, S., van Amerongen, M.J., Tio, R.A., Petersen, A.H., van Luyn, M.J. & Harmsen, M.C. Increased inflammatory response and neovascularization in reperfused vs. non-reperfused murine myocardial infarction. *Cardiovasc Pathol* 15, 83-90 (2006).

(24) Mahmarian, J.J., Pratt, C.M., Boyce, T.M. & Verani, M.S. The variable extent of jeopardized myocardium in patients with single vessel coronary artery disease: quantification by thallium-201 single photon emission computed tomography. *J Am Coll Cardiol* 17, 355-62 (1991).

(25) Gao, S., Ho, D., Vatner, D.E. & Vatner, S.F. Echocardiography in Mice. *Curr Protoc Mouse Biol* 1, 71-83 (2011).

(26) Kanamori, H. *et al.* The role of autophagy emerging in postinfarction cardiac remodelling. *Cardiovasc Res* 91, 330-9 (2011).

(27) Aguor, E.N. *et al.* Quantitative T 2* assessment of acute and chronic myocardial ischemia/reperfusion injury in mice. *MAGMA* 25, 369-79 (2012).

(28) Theken, K.N., Deng, Y.M., Kannon, M.A., Miller, T.M., Poloyac, S.M. & Lee, C.R. Activation of the Acute Inflammatory Response Alters Cytochrome P450 Expression and Eicosanoid Metabolism. *Drug Metabolism and Disposition* 39, 22-9 (2011).

(29) Livak, K.J. & Schmittgen, T.D. Analysis of relative gene expression data using real-time quantitative PCR and the 2(-Delta Delta C(T)) Method. *Methods* 25, 402-8 (2001).

(30) Tanaka, H. *et al.* Serum levels of cardiac troponin I and troponin T in estimating myocardial infarct size soon after reperfusion. *Coron Artery Dis* 8, 433-9 (1997).

(31) Rangan, G.K. & Tesch, G.H. Quantification of renal pathology by image analysis. *Nephrology (Carlton)* 12, 553-8 (2007).

(32) Xu, Z., Alloush, J., Beck, E. & Weisleder, N. A murine model of myocardial ischemia-reperfusion injury through ligation of the left anterior descending artery. *J Vis Exp*, (2014).

(33) Nossuli, T.O. *et al.* A chronic mouse model of myocardial ischemia-reperfusion: essential in cytokine studies. *Am J Physiol Heart Circ Physiol* 278, H1049-55 (2000).

(34) Bayes-Genis, A. *et al.* Head-to-head comparison of 2 myocardial fibrosis biomarkers for long-term heart failure risk stratification: ST2 versus galectin-3. *J Am Coll Cardiol* 63, 158-66 (2014).

(35) Mann, D.L. Mechanisms and models in heart failure: A combinatorial approach. *Circulation* 100, 999-1008 (1999).

(36) Christia, P. *et al.* Systematic characterization of myocardial inflammation, repair, and remodeling in a mouse model of reperfused myocardial infarction. *J Histochem Cytochem* 61, 555-70 (2013).

(37) Everaert, B.R., Boulet, G.A., Timmermans, J.P. & Vrints, C.J. Importance of suitable reference gene selection for quantitative real-time PCR: special reference to mouse myocardial infarction studies. *PLoS One* 6, e23793 (2011).

(38) James, J.F., Hewett, T.E. & Robbins, J. Cardiac physiology in transgenic mice. *Circ Res* 82, 407-15 (1998).

(39) Barasch, E. *et al.* Association between elevated fibrosis markers and heart failure in the elderly: the cardiovascular health study. *Circ Heart Fail* 2, 303-10 (2009).

(40) Wang, T.J. *et al.* Clinical and echocardiographic correlates of plasma procollagen type III amino-terminal peptide levels in the community. *Am Heart J* 154, 291-7 (2007).

(41) Burchfield, J.S., Xie, M. & Hill, J.A. Pathological ventricular remodeling: mechanisms: part 1 of 2. *Circulation* 128, 388-400 (2013).

(42) Sheiban, I. *et al.* Time course and determinants of left ventricular function recovery after primary angioplasty in patients with acute myocardial infarction. *J Am Coll Cardiol* 38, 464-71 (2001).

(43) Smiley, D. *et al.* Increased fibrosis and progression to heart failure in MRL mice following ischemia/reperfusion injury. *Cardiovasc Pathol* 23, 327-34 (2014).

(44) Ferdinandy, P., Schulz, R. & Baxter, G.F. Interaction of cardiovascular risk factors with myocardial ischemia/reperfusion injury, preconditioning, and postconditioning. *Pharmacol Rev* 59, 418-58 (2007).

(45) Miya, Y., Kanda, T., Tamura, J., Sumino, H. & Kurabayashi, M. A new murine model of coronary artery thrombosis and role of interleukin-8 in the development of coronary thrombosis. *Res Commun Mol Pathol Pharmacol* 108, 108-15 (2000).

(46) Dogne, J.M. *et al.* Characterization of an original model of myocardial infarction provoked by coronary artery thrombosis induced by ferric chloride in pig. *Thromb Res* 116, 431-42 (2005).

(47) Barnabei, M.S., Palpant, N.J. & Metzger, J.M. Influence of genetic background on ex vivo and in vivo cardiac function in several commonly used inbred mouse strains. *Physiol Genomics* 42A, 103-13 (2010).

(48) Churchill, G.A. *et al.* The Collaborative Cross, a community resource for the genetic analysis of complex traits. *Nat Genet* 36, 1133-7 (2004).

CHAPTER 5 - THE CONTRIBUTION OF CARDIOMYOCYTE SOLUBLE EPOXIDE HYDROLASE TO ACUTE MYOCARDIAL INFARCTION-INDUCED MALADAPTIVE VENTRICULAR REMODELING IN MICE

Introduction

Following the acute recovery phases of an AMI, the infarcted and inflamed myocardium promotes maladaptive ventricular remodeling, a chronic and progressive pathological process that manifests as scar tissue formation (fibrosis) and LV dysfunction within the first few weeks to months after the index event (1, 2). Progression of these maladaptive processes, and the presence of LV fibrosis and dysfunction, markedly increases the risk of worsening systolic and/or diastolic function and the development of clinical heart failure, ventricular arrhythmias and sudden cardiac death, and overall mortality (3-5). Thus, this chronic maladaptive remodeling process is a key driver of worsened prognosis following AMI. The identification of key pathways that regulate remodeling following AMI offers enormous potential to facilitate the development of novel therapeutic strategies that prevent the development of heart failure and its associated morbidity and mortality.

CYP epoxygenases from the CYP2J and CYP2C subfamilies catalyze the metabolism of arachidonic acid into EETs, which have become increasingly recognized to possess potent anti-inflammatory, vasodilatory, fibrinolytic, anti-apoptotic, pro-angiogenic, and smooth muscle cell anti-migratory effects in the cardiovascular system (6). The life of circulating EETs, however, is ephemeral as they are quickly hydrolyzed into the less potent DHETs by sEH.

Early chronic preclinical models of IR-induced ventricular remodeling (3-4 weeks of reperfusion following 45 minutes of ischemia) have recently been utilized to determine the role of EETs in maladaptive remodeling following AMI (7, 8). These data have shown that increasing EETs via pharmacological sEH inhibition attenuates myocardial fibrosis and systolic function.

Although inhibition of sEH to promote the effects of EETs has been proposed as a novel cardioprotective therapeutic strategy following AMI (6, 9), more rigorous investigation is warranted to further define the contribution of sEH and EETs to the pathogenesis and progression of ventricular remodeling. In particular, the direct contribution of increased myocardial sEH expression to the pathogenesis and progression of maladaptive ventricular remodeling post-AMI in vivo has not been studied to date. Consequently, we investigated the role of myocardial sEH in maladaptive ventricular remodeling post-IR *in vivo* using a transgenic mouse model with cardiomyocyte-specific overexpression of human sEH driven by the α-myosin heavy chain promoter (α-MHC-*EPHX2* mice).

Materials and Methods

Mice

All experiments were completed in adult male mice on a C57BL/6N background. Transgenic mice that overexpress human *EPHX2* in cardiomyocytes under control of the murine α-MHC promoter (α-MHC-*EPHX2*) were developed on a C57BL/6N background (Xenogen, now Taconic, Germantown, NY) by the laboratory of Dr. Darryl Zeldin (NIEHS/NIH; unpublished), similar to past studies, and kindly provided for these experiments. Briefly, the human sEH cDNA (NM001979.5) was amplified with primers (Fwd: 5′-TAAGCTTGGCTGCAGACCCGCCGCCATGACG-3′, Rev: 5′-TAGCGGCCGCTCTACATCTTTGAGACCACC-3′) and subcloned downstream of the murine α-MHC promoter and upstream of the human growth hormone (hGH) polyadenylation signal (kindly provided by Dr. Jeffrey Robbins, University of Cincinnati) (Figure 5.1a), as described previously (10). Linearized constructs were agarose gel-purified, microinjected into pronuclei of single cell C57BL/6 mouse embryos, and implanted into pseudopregnant mice. Hemizygous founder pups were identified by PCR genotyping of genomic DNA.

All mice used in these experiments were ages 2-6 months. Heterozygous transgenic mice from only one founder mouse line [C57BL/6-Tg(Myh6-EPHX2)12Dcz] were used in the study to minimize inter-line variability in the magnitude of sEH overexpression. A subset of the control mice were age/sex-matched wildtype littermates from Tr12, however additional wildtype C57BL/6N mice were purchased from Charles River Laboratories (Wilmington, MA, USA) and used as controls.

The α-MHC promoter is expressed almost exclusively in cardiomyocytes (11). Characterization of α-MHC-*EPHX2* mice were performed by Artiom Gruzdev and colleagues (NIEHS/NIH).

All procedures and experiments were conducted in accordance with the *US National Institutes of Health (NIH) Guide for the Care and Use of Laboratory Animals* and were approved by the Institutional Animal Care and Use Committee at the University of North Carolina at Chapel Hill and the National Institute of Environmental Health Sciences.

Myocardial IR injury model

The LAD coronary artery ligation IR model was utilized to evaluate the impact of cardiomyocyte-specific sEH overexpression on ventricular remodeling as described previously (Chapter 4). Briefly, the chest cavity was opened to visualize the LAD artery and the artery was compressed by tightening a ligature, producing myocardial blanching and electrocardiographic S-T segment elevation. After occlusion of the LAD for the desired time (30 minutes; ischemia), blood flow was restored by removing the ligature (reperfusion). The chest wall was then closed with a prolene or silk suture. Sham surgery mice (control) underwent an identical procedure except there was no tightening of ligature.

At 24 hours following surgery, blood was collected by modified tail-clip technique which may reduce stress to mice compared to the use of a restraint device (12). Plasma was then separated by centrifugation and stored at -80^{0}C for future troponin quantification.

Mice were euthanized at 2 weeks following IR. Blood was collected through the inferior vena cava and plasma was separated by centrifugation, aliquoted, and stored at -80^{0}C. Whole

hearts were extracted, blotted dry, and, weighed before being fixed for future histological analysis.

A portion of wildtype mice were euthanized at 2 hours or 24 hours following IR. In these mice, whole hearts were flash frozen in liquid nitrogen and stored at -80°C for subsequent molecular phenotyping after being dissected into LV, right ventricle, and atria upon extraction.

Quantitative real-time PCR

To determine the impact of myocardial IR on *Ephx2* expression in wildtype mice, qPCR was performed on LV tissue from the hearts that were stored at -80°C. Briefly, RNA was isolated from mouse LV tissue (Qiagen) and reverse transcribed to cDNA (Applied Biosystems). Analysis was performed in triplicate using the 7300 Real-Time PCR system (Applied Biosystems), as described (13). Expression of myocardial mouse sEH mRNA levels was quantified using Taqman Assays on Demand (Applied Biosystems). Data was normalized to *Gapdh* (endogenous reference) and expressed relative to a designated experimental control group using the $2^{-\Delta\Delta Ct}$ method (14).

Myocardial necrosis

Twenty-four hour plasma cardiac troponin I levels were measured by ELISA (Life Diagnostics, West Chester, PA), according to the manufacturer instruction, as a biomarker of cardiomyocyte necrosis and an early index of infarct size (15).

Cardiac structure and function

Echocardiography on conscious mice was performed at baseline and following IR using a Vevo 2100 Imaging System (VisualSonics, Toronto, ON) as previously described (Chapter 4). Briefly, M-mode images were traced to measure direct parameters of cardiac structure at baseline and 24 hours. The calculated parameters of structure (LV Mass) and systolic function (FS and EF) were derived from the direct parameters of structure as well as from LV Vold and LV Vold. Pulsed wave Doppler images were traced to measure parameters of systolic, diastolic, and global function at baseline and 2 weeks. Heart weight-to-tibia length ratio at 2 weeks was measured as a parameter of cardiac size.

Histology

Fixed hearts were embedded in paraffin, and cut into 5μm transverse sections to measure evidence of fibrosis. Specifically, serial interrupted sectioning was performed to the hearts. Starting from the apex, the most inferior distance where sections were collected occurred where both the left and right ventricle could be visualized. A series of sections (4-6) were collected at this distance. The next series of sections were collected at a distance 200 microns superior to the previous distance. This was repeated for several distances to cover a large portion of the heart where injury was anticipated to occur. For hearts of mice undergoing IR, sections from 8 distances (spanning 1800 microns from the most inferior distance) were collected per sample.

For collagen, sections were stained with Picrosirius Red, as described (16). For activated myofibroblasts, after being baked at 37^0C overnight and 60^0C for 1.5 hours, slides were deparaffinized, rehydrated, and blocked for endogenous peroxidase in 3% hydrogen peroxide for 10 minutes. Sections were then blocked with Rodent Block M (DAKO, Carpinteria, CA) for

non-specific binding according to the manufacturer's protocol. Slides were incubated with mouse monoclonal anti-alpha smooth muscle actin (α-SMA) primary antibody (DAKO, Carpinteria, CA), diluted 1:400 for two hours at room temperature, followed by Mouse-on-Mouse HRP Polymer (Thermo Fisher Scientific, Waltham, MA) for 15 minutes at room temperature. Immunoreactivity was visualized by DAB chromogen (Thermo Fisher Scientific).

For quantification of Picrosirius red stain-derived collagen deposition, digitally scanned images of the entire heart section were used to generate staining data using NIH ImageJ thresholding technology, as previously described (Chapter 4: Methods, Histology). For anti-α-SMA stained slides, slides were digitally scanned using ScanScope CS System (Aperio). From the digital scans, one 10x zoom image was taken per section of each sample capturing about 1/10 of the total cross-section. The region that had the most intense anti-α-SMA stain was chosen as long there was evidence of collagen deposition based on Picrosirius red stained section from the same heart distance. Thresholding ranges were set by averaging the ranges of all samples in a representative section for each batch. Imaging and threshold setting was done by an investigator blinded to treatment groups. The surface area of staining was normalized to the surface area of total myocardial tissue for each section. The resulting % stained value averaged over 8 serial sections for each mouse heart generated a single value per mouse that reflected the average staining throughout the infarcted region.

Data were pooled from two independent experiments. In order to control for interexperiment variability in the absolute % stain values, values were normalized to the IR (wildtype) group within each experiment prior to analysis; thus, the % stain data are presented relative to the IR (wildtype) group.

Statistical analysis

Data are expressed as mean±SEM unless stated otherwise. Gene expression, troponin, and histology data were log-transformed and compared across experimental groups using one-way ANOVA followed by Fisher's LSD *post hoc* tests (if overall ANOVA was significant). Echocardiography data were log-transformed and compared across experimental groups using ANCOVA with baseline values set as the covariate followed by Fisher's LSD *post hoc* tests (if overall ANCOVA was significant). Statistical analyses were performed using SAS 9.2 (SAS Institute, Cary, NC). $P<0.05$ was considered to be statistically significant.

Results

Initial characterization of a transgenic mouse model with cardiomyocyte-specific overexpression of human sEH driven by the α-myosin heavy chain promoter

The design of the α-MHC-*EPHX2* construct is shown in Figure 5.1a. RNA isolation from hearts was done with the RNAeasy Mini kit (Qiagen, Valencia, CA) followed by conversion of RNA to cDNA with High Capacity cDNA Archive kit (Applied Biosystems, Foster City, CA). Native mouse *Ephx2* mRNA levels detected by qPCR were not significantly different between α-MHC-*EPHX2* and wildtype mouse hearts (Figure 5.1b), however total mouse (*Ephx2*) + human (*EPHX2*) sEH mRNA levels were significantly higher in α-MHC-*EPHX2* mouse hearts (Figure 5.1c). Western blotting confirmed the expression of human sEH in whole heart homogenates (Figure 5.1d) isolated from α-MHC-*EPHX2* but not in wildtype mice. Immunohistochemical staining showed that human isoform was abundantly expressed in cardiomyocytes, but not kidney or liver tissue of α-MHC-*EPHX2* mice (Figure 5.1e). The heart, kidney, and tissue of wildtype mice showed no detection of human sEH isoform (Figure 5.1e).

Levels of the 14,15-EET:DHET ratio were significantly lower in α-MHC-*EPHX2* mice compared to wildtype mice (Figure 5.1f), suggesting that sEH metabolic function was significantly higher in transgenic mice compared to wildtype mice. An *ex vivo* sEH activity assay confirmed that α-MHC-*EPHX2* mouse hearts had markedly increased 14,15-EET hydrolysis activity compared to wildtype (Figure 5.1g).

Myocardial expression of soluble epoxide hydrolase

Relative murine *Ephx2* mRNA levels were not significantly different between IR-treated and sham-treated mice in LV tissue at 2 and 24 hours following surgery (Figure 5.2).

Circulating biomarker of myocardial cell death

Plasma troponin levels in IR-treated wildtype mice were greater than levels in sham-treated mice, since levels in sham treated mice were undetectable. There was no significant difference (P=0.10) in troponin levels between α-MHC-*EPHX2* mice and wildtype mice undergoing IR (Figure 5.3).

Echocardiograph indices of cardiac function and structure

For M-mode image-derived parameters of systolic function, there were no significant differences in FS (Figure 5.4a) or EF (Figure 5.4b) across sham-treated wildtype, IR-treated wildtype, and IR-treated α-MHC-*EPHX2* mice at 1 day following IR.

For Pulsed Wave Doppler image-derived parameters of systolic function, AET and IVCT were not significantly different across sham-treated wildtype, IR-treated wildtype, and IR-treated α-MHC-*EPHX2* mice at 2 weeks following IR (Table 5.1).

For Pulsed Wave Doppler image-derived parameters of diastolic and global function, there were no significant differences in E/A ratio (Figure 5.5a) across sham-treated wildtype, IR-treated wildtype, and IR-treated α-MHC-*EPHX2* mice at 2 weeks following IR. Likewise, there were no significant differences for the individual E-peak velocity and A-peak velocity components of the E/A ratio (Table 5.2). IVRT was not significantly different across groups (Figure 5.5b). Furthermore, deceleration rate and time of mitral valve blood flow during ventricle

relaxation were not significantly different across treatment groups at 2 weeks following IR (Table 5.2). Finally MPI, an index of global function derived from IVCT and IVRT was also not different across groups.

For cardiac structure, there were no significant differences in ventricle wall thickness (IVS, LVPW) at systole or diastole across sham-treated wildtype, IR-treated wildtype, and IR-treated α-MHC-*EPHX2* mice (Table 5.3) at day 1 (adjusted for baseline), demonstrating no evidence of either hypertrophy or myocardial wall thinning in any of the experimental groups. Echocardiography-derived LV mass (Table 5.3) at day 1 as well as heart weight/ tibial length at 2 weeks (6.18 ± 0.24, 5.82 ± 0.35, 6.57 ± 0.60 mg/mm; P = 0.49) were also not different between sham-treated wildtype, IR-treated wildtype, and IR-treated α-MHC-*EPHX2* mice, respectively. Finally, no differences were detected in ventricle diameter (LVIDs or LVIDd) across groups (Table 5.3). Collectively these echocardiography results demonstrate that there was no evidence of differences in systolic function, diastolic function, and cardiac structure across experimental groups.

Myocardial fibrosis

There was a significant difference in collagen deposition staining across sham-treated wildtype, IR-treated wildtype, and IR-treated α-MHC-*EPHX2* mice ($P<0.01$; Figure 5.6a) at 2 weeks of reperfusion. Pairwise comparisons revealed significantly increased collagen deposition in IR-treated wildtype mice compared to sham-treated wildtype mice ($P<0.01$). Likewise, collagen deposition in IR-treated α-MHC-*EPHX2* was significantly increased compared to IR-treated wildtype mice ($P=0.02$). Finally, collagen was significantly higher in IR-treated α-MHC-*EPHX2* mice compared to sham-treated wildtype mice ($P<0.01$).

The extent of staining for activated myofibroblasts was also significantly different across sham-treated wildtype, IR-treated wildtype, and IR-treated α-MHC-*EPHX2* mice ($P<0.01$; Figure 5.6b). In post-hoc analyses however, the extent of α-SMA staining in wildtype mouse hearts was not significantly increased compared to sham-treated wildtype mice ($P=0.09$). Similarly, staining in IR-treated α-MHC-*EPHX2* mouse hearts was not significantly increased compared to IR-treated wildtype mice ($P=0.08$). Although these comparisons were not significant, the direction of the effect is consistent with out hypothesis that IR-injury induces myofibroblast activity, which is further enhanced in IR-treated α-MHC-*EPHX2* mice. Furthermore, α-SMA staining was significantly correlated with collagen staining ($P<0.01$, $r=0.66$). Hearts from IR-treated α-MHC-*EPHX2* mice had increased staining compared to sham-treated wildtype mouse hearts ($P<0.01$).

Discussion

This is the first study to evaluate the direct contribution of cardiomyocyte-sEH expression to maladaptive ventricular remodeling following AMI *in vivo*. We demonstrated that transgenic mice with overexpression of human sEH in cardiomyocytes exhibited enhanced myocardial collagen deposition compared to wildtype controls following AMI, but did not exhibit altered cardiac function or structure. These data indicate increased myocardial sEH activity is a key mediator of collagen deposition during early chronic ventricular remodeling following IR, and suggest that strategies which reduce myocardial sEH activity may have therapeutic utility to prevent or delay the long term consequences (heart failure, sudden cardiac death) that are promoted by fibrosis.

The role of sEH in the development and progression of cardiovascular disease has been studied in a variety of preclinical models (17). The expression of sEH is significantly elevated in two rat models of angiotensin II-induced hypertension including in the aortic intima (18), the hypertrophic heart (19), and renal cortical tissue (20). Importantly, both *in vitro* and *in vivo* studies revealed that these effects were driven by angiotensin II (18). As an initial step in determining the role of sEH in maladaptive ventricular remodeling following AMI, we investigated whether myocardial *Ephx2* expression is induced by myocardial IR. We found that IR did not impact myocardial *Ephx2* expression acutely following injury. This suggests that acute induction of myocardial sEH is not a pathological response to IR *in vivo*. That being said, we measured sEH expression before, but not during the development of maladaptive ventricular remodeling. Future studies investigating the impact of IR on *Ephx2* expression at subacute and

early chronic points are warranted to fully characterize the impact of IR-induced ventricular remodeling on changes in myocardial sEH expression and function.

Although IR did not acutely alter *Ephx2* expression, interindividual variation in myocardial sEH expression was previously reported to exist within a group of patients with CAD. In particular, *EPHX2* expression in the heart biopsies of CAD patients was lower if the patient had reduced EF (21). Given the aforementioned evidence demonstrating the cardioprotective effects of sEH inhibition putatively mediated by EETs in preclinical models of maladaptive ventricular remodeling, these findings allude to the possible presence of a compensatory downregulation of myocardial sEH expression in the presence of HF*r*EF. However the direct effects of increasing myocardial sEH expression on IR-evoked maladaptive ventricular remodeling have not been studied. Consequently, using α-MHC-*EPHX2* transgenic mice, we investigated the impact of cardiomyocyte-specific overexpression of human sEH on structural (ventricle chamber dilatation and wall thinning), functional (systolic dysfunction, diastolic dysfunction), and fibrotic (collagen deposition, myofibroblasts activation) changes following IR to determine the direct functional contribution of cardiomyocyte sEH to IR-evoked maladaptive ventricular remodeling. Our data collectively demonstrated that overexpression of cardiomyocyte sEH resulted in enhanced collagen deposition, but did not impact cardiac dysfunction or maladaptive structural changes.

Previous preclinical studies have investigated the role of sEH in post-IR ventricular remodeling. Li et al. showed in a mouse model of 45 minutes of LAD occlusion followed by 3 weeks of reperfusion, that administration of a sEH inhibitor reduced collagen deposition (8), consistent with the current findings in which increasing myocardial sEH activity increased myocardial fibrosis. However, unlike the current results, sEH modulation also impacted cardiac

function and structure following AMI. In particular, sEH inhibition improved FS as well as LVID at diastole (8). The different models of AMI may be the cause for the discrepant findings between studies. A longer period of ischemia and reperfusion in the Li et al. study may have enhanced the remodeling response and thereby enabled the demonstration of an effect from the experimental intervention. Indeed, we show that myocardial IR in a model of AMI with a shorter ischemia time (30 minutes) and a shorter reperfusion time (2 weeks) did not result in worsened cardiac structure (ventricle chamber dilation, wall thinning) (Chapter 4: Results). This may have precluded our ability to determine the impact of sEH overexpression on cardiac structure following IR. Likewise, our model did not cause significant cardiac dysfunction (Chapter 4: Results) thus limiting our ability to determine the impact of cardiomyocyte sEH on cardiac function. An investigation of the impact of cardiomyocyte sEH overexpression in an AMI model that produces greater levels of maladaptive remodeling such as a permanent ischemia model or an IR model of late maladaptive chronic remodeling (by increasing the length of post-AMI reperfusion follow-up) would provide further insight into the role of cardiomyocyte sEH on maladaptive ventricular remodeling following AMI.

The fibrotic response following AMI is known to increase myocardial stiffness, precede the impairment of cardiac function, and ultimately lead to the development of heart failure progression (22). Thus, it is plausible to postulate that α-MHC-*EPHX2* mice have greater systolic and diastolic dysfunction in the later chronic stages following IR, compared to wildtype mice, at least partially due to enhanced myocardial collagen deposition during early chronic ventricular remodeling. However, as mentioned above, this hypothesis has not been investigated and needs to be tested. Circulating biomarkers of fibrosis predictive of poor prognosis following AMI correlate strongly with cardiac function (23). Furthermore, much remains unknown concerning

the precise mechanisms linking fibrosis to cardiac dysfunction following AMI (24). Addressing this gap in knowledge would provide clarity on the relevance of an experimental effect that alters fibrosis but not cardiac function following AMI. This would be of greatest importance if it is ultimately found that cardiomyocyte sEH overexpression does not impact cardiac function in the late chronic phase following IR.

Accumulating evidence, across multiple laboratories and species, has demonstrated that EETs abrogate a variety of acute pathophysiological responses following myocardial IR, including the reduction of left ventricular infarct size (25). Thus, it is unknown whether the observed enhancement of cardiac fibrosis in the presence of cardiomyocyte sEH overexpression was independent of infarct size following IR. This is of clinical significance, because an EET-promoting agent indicated to reduce IR injury would most likely be administered to patients during or after, and not prior to, the ischemic phase of an AMI. Overexpression of sEH in our transgenic mice did not significantly increase troponin levels, which suggests that the significantly enhanced myocardial fibrosis observed in these mice may be independent, at least in part, of infarct size *in vivo*. The impact of sEH overexpression on post-IR infarct size is also being investigated currently in an *ex vivo* model of AMI. Three recent studies have provided further insight into this important issue, by demonstrating the impact of sEH inhibition on post-AMI phenotypes. In one study, a sEH inhibitor was administered immediately following permanent LAD occlusion in rats; pharmacologic suppression of sEH attenuated LV ejection fraction (systolic function) independent of collagen deposition reduction in the infarct zone following 5 weeks of occlusion (26). A second study by a separate group utilized a chronic model of overt heart failure in rats (permanent LAD ligation for 50 days), but administered a sEH inhibitor at distinct time points after the initial phase of infarct healing: 8 days (42-day sEH

inhibitor treatment) or 47 days (3-day inhibitor treatment) following LAD occlusion. It was discovered that both regimens improved LV ejection fraction at 50 days; however, only long term treatment elicited an improvement in LV end-diastolic pressure (diastolic function) (27). A third study in mice utilizing a model of IR injury demonstrated that sEH inhibition administered a week following AMI was still able to attenuate chronic collagen deposition measured three weeks later (7). Collectively, these studies demonstrate that sEH inhibition improves maladaptive ventricular remodeling independent of the aforementioned acute reductions in infarct size elicited by EETs. Administration of a sEH inhibitor to α-MHC-*EPHX2* mice following the acute phase of IR would provide further insight on whether the enhanced fibrosis was independent of infarct size, and is an important future direction for this line of investigation.

It is also important to note that the aforementioned effects in previous studies were not reported to be related to blood pressure reduction, suggesting that direct EET action on the heart is a likely mechanism of cardioprotection. However, in addition to cardiomyocytes, the heart is also composed of fibroblasts, endothelial cells, and vascular smooth muscle cells (28). Although the transgene was only expressed in cardiomyocytes, it is unknown which cell types are most important to the observed enhancement of cardiac fibrosis in the transgenic mice. Cardiac fibroblasts certainly accelerate fibrosis via secretion of growth factors and cytokines (28). Furthermore, fibroblasts are the only cell type that synthesize collagen and are the most abundant source of ECM proteins. However, endothelial cells, neutrophils, mast cells, lymphocytes, and macrophages are other major sources of ECM proteins (28). Studies have shown that pharmacologic inhibition of sEH directly blocks the proliferation, differentiation, migration, and secretion capacity of fibroblasts (7, 26). Additionally, substantial evidence indicates that EETs, through inhibition of NF-κB activation, attenuate inflammation in endothelial cells and

monocytes (29) and mitigate macrophage/neutrophil infiltration in the vasculature (30); however, these effects have not been extensively studied in the coronary vasculature following myocardial ischemic injury. Kompa et al. demonstrated that sEH inhibition impedes the infiltration of macrophages in the peri-infarct region of the myocardium in rats following permanent LAD ligation. Intriguingly, sEH inhibition did not reduce macrophage infiltration in the infarct region of the myocardium (26). Overall, further studies are necessary to determine the relative functional role of myocardial cell-type in EET-mediated cardioprotection. Studies in individual cell types isolated from the hearts of the transgenic mice following AMI would elucidate which cells are most important in the observed enhancement of fibrosis in these mice.

Even within a specific cell-type of the heart, there are multiple mediators which promote fibrosis along the full cascade of its development, as described (Chapter 4: Introduction). Briefly, circulating and resident fibroblasts infiltrate the myocardium in the infarct zone and undergo rapid proliferation (mediated by FGF-2) followed by activation into myofibroblasts (largely mediated by TGF-β). Subsequently, activated myofibroblasts function to produce ECM proteins that ultimately cause scar formation (31). LOX mediates the maturation of scar tissue by cross-linking collagen fibrils. However, before the maturation of the fibrotic scar and after collagen fibers are synthesized further, ECM remodeling can occur as a consequence of mediators such as osteopontin, fibronectin, TIMPs, and MMPs that regulate ECM turnover (32). Notably, only MMP can degrade collagen (2). In renal tissue, *Ephx2* disruption reduced the extent of TGF-β signaling, fibronectin, activated myofibroblasts, and collagen deposition (33), suggesting that sEH may play a role in fibrosis development along the full spectrum of its pathogenesis. It is unknown if the observed changes in myocardial collagen deposition reported in the current study are a result of increased collagen synthesis upstream of ECM remodeling, impaired collagen

proteolytic degradation during the latter phases, or both. We observed that hearts of IR-treated α-MHC-*EPHX2* mice had increased collagen deposition compared to hearts of IR-treated wildtype mice ($P<0.01$), but did not observe a significant difference in activated myofibroblasts between these two groups at 14 days following IR ($P=0.08$). This suggests that the enhanced collagen deposition may be, at least in part, a consequence of reduced ECM degradation in α-MHC-*EPHX2* mouse hearts. Of note, the levels of activated myofibroblasts, TGF-β, and osteopontin in the mouse heart may peak at 3 days following IR (34). Future studies which investigate the role of cardiomyocyte sEH on the time course of the aforementioned mediators in the infarcted heart following IR would elucidate the mechanism by which sEH overexpression caused increased collagen deposition. For example, in characterizing the IR model used in this study, we measured early myocardial expression of mediators important in fibrosis such as LOX and TGF-β in wildtype mice (Chapter 4: Results). These markers should also be measured in future studies with the transgenic mice.

There are some limitations to our transgenic mouse model. First, the model exhibits supraphysiological levels of sEH expression in cardiomyocytes. However this was a proof of concept study to determine the impact of extreme increases in sEH expression on chronic phenotypes following AMI. Furthermore, pharmacological inducers of sEH to elucidate the effect of enhanced sEH-derived EET hydrolysis are not available, thus genetic modification remains the only method to increase sEH-derived hydrolysis of EETs. Moreover, this genetic tool offers the advantage of allowing the determination of the role of cardiomyocyte-specific sEH in remodeling. Future work investigating the impact of knocking in *EPHX2* Lys55Arg and *EPHX2* Arg287Gln in mice would increase our understanding of the role of common human polymorphisms on myocardial remodeling following AMI. A second limitation is that only one

founder mouse line was used across all experiments, thus we cannot rule out whether the transgene itself or the location where the transgene is inserted is driving the phenotype. However, using one mouse line allowed us to control for variation in the expression level of the transgene and thereby enhance reproducibility of the phenotype. Furthermore, Gruzdev et al. demonstrated in an *ex vivo* model of IR that two other founder lines showed nearly identical phenotypes (unpublished), highly suggesting that insertional mutagenesis by the transgene is unlikely to play a role in the observed ventricular remodeling.

In summary, mice with cardiomyocyte-specific overexpression of human sEH exhibited enhanced IR-induced myocardial collagen deposition *in vivo*. This suggests that lower cardiac EETs may promote fibrosis post-AMI; however, future studies are needed to elucidate the molecular mechanisms including the direct implication of EETs in these effects.

Figures

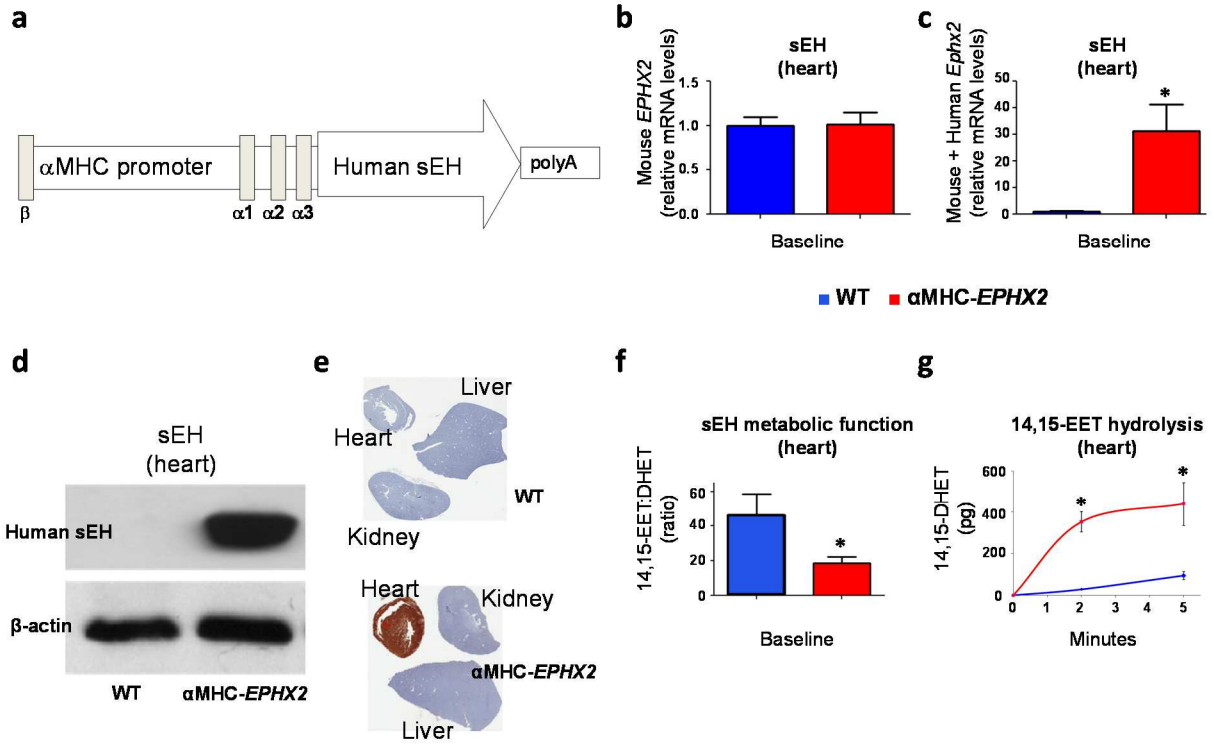

Figure 5.1 Characterization of cardiomyocyte-specific soluble epoxide hydrolase (sEH) overexpressing transgenic mice. (a) Schematic of the transgenic construct which contains the α-myosin heavy chain (α-MHC) promoter, human sEH isoform coding sequence, and polyA sequences. Bar graphs show baseline (b) native murine *Ephx2* and (c) total sEH (native *Ephx2* + transgenic *EPHX2*) expression in the whole heart. (d) A representative immunoblot of human sEH protein levels in the whole heart and β-actin loading control. (e) Representative immunohistochemistry staining for human sEH in the heart, kidney, and liver of α-MHC-*EPHX2* mice and wildtype (WT) control. (f) Baseline levels of 14,15-EET:DHET ratio in the whole heart. (g) Levels of 14,15-DHET (pg) as a measure of myocardial sEH function in an assay

where exogenous 14,15-EET was added to isolated protein in the heart tissue of α-MHC-*EPHX2* mice and WT controls. N = 3-5 per group. * $P < 0.05$. Figures adapted from Gruzdev et al. (unpublished). All characterization of transgenic mice was conducted by the Darryl Zeldin lab.

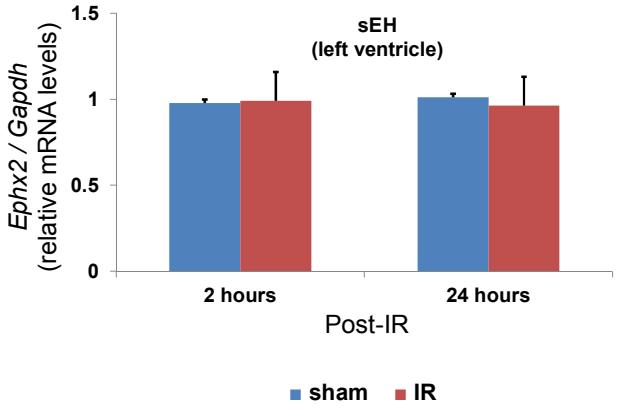

Figure 5.2 Impact of myocardial ischemia reperfusion (IR) on soluble epoxide (sEH) expression. Bar graph shows the time course of myocardial IR-induced *Ephx2* expression in the left ventricle (LV) of wildtype mice. Reference group for relative mRNA levels: sham levels at 24 hours. Sham: n = 3 per group. IR: n = 5 per group. * $P < 0.05$ for sham vs IR at each time point.

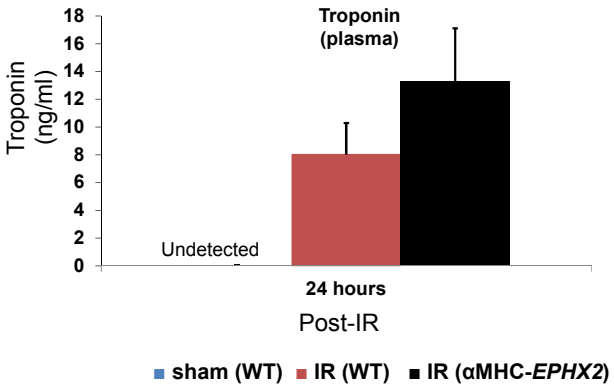

Figure 5.3 Impact of cardiomyocyte sEH overexpression on myocardial necrosis. Plasma troponin levels at 24 hours following ischemia reperfusion (IR) in sham-treated wildtype (WT), IR-treated WT, and IR-treated α-myosin heavy chain- (α-MHC)-*EPHX2* mice. IR: n = 17-19 per group. Sham: n = 8. * $P < 0.05$ for IR-treated WT versus IR-treated α-MHC-*EPHX2*.

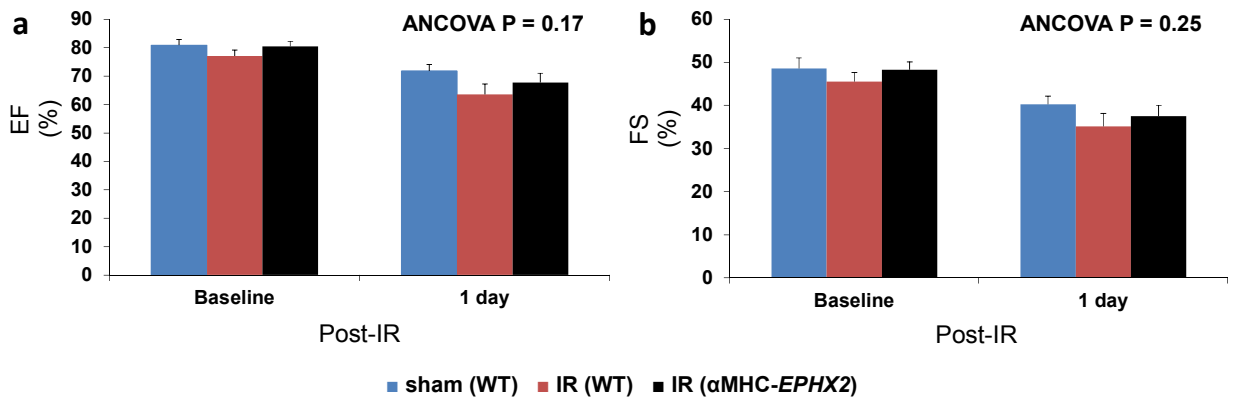

Figure 5.4 Impact of cardiomyocyte soluble epoxide hydrolase (sEH) overexpression on M-mode image-derived parameters of systolic function. Bar graphs show (a) ejection fraction (EF) and (b) fractional shortening (FS) at 1 day following ischemia reperfusion (IR) in sham-treated wildtype (WT), IR-treated WT, and IR-treated α-myosin heavy chain- (α-MHC)-*EPHX2* mice. Comparisons across groups were conducted at 1 day using ANCOVA with baseline as the covariate. IR: n = 17-19 per group. Sham: n = 9.

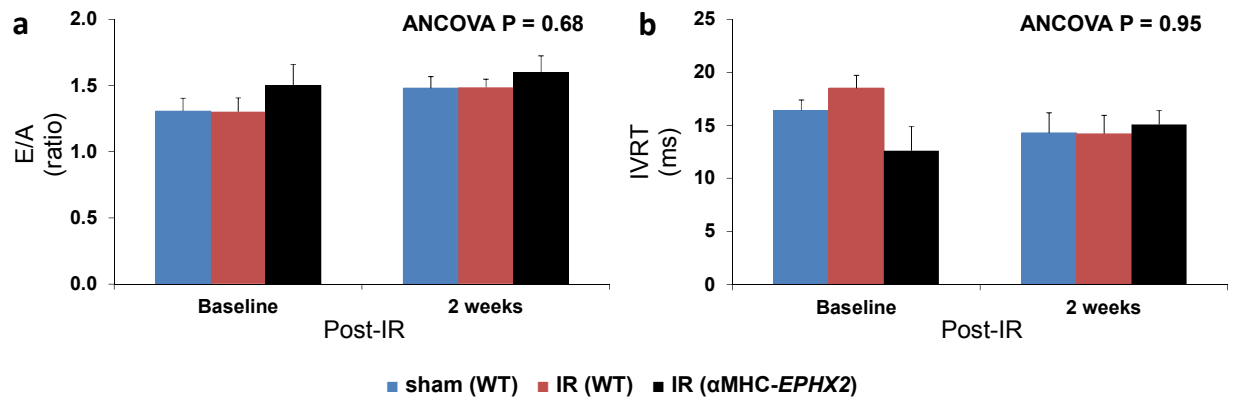

Figure 5.5 Impact of cardiomyocyte soluble epoxide hydrolase (sEH) overexpression on diastolic function. Bar graphs show (a) E-wave to A-wave (E/A) ratio and (b) isovolumic relaxation time (IVRT) at 2 weeks following ischemia reperfusion (IR) in sham-treated wildtype (WT), IR-treated WT, and IR-treated α-myosin heavy chain- (α-MHC)-*EPHX2* mice. Comparisons across groups were conducted at 2 weeks using ANCOVA with baseline as the covariate. n = 7-9 per group.

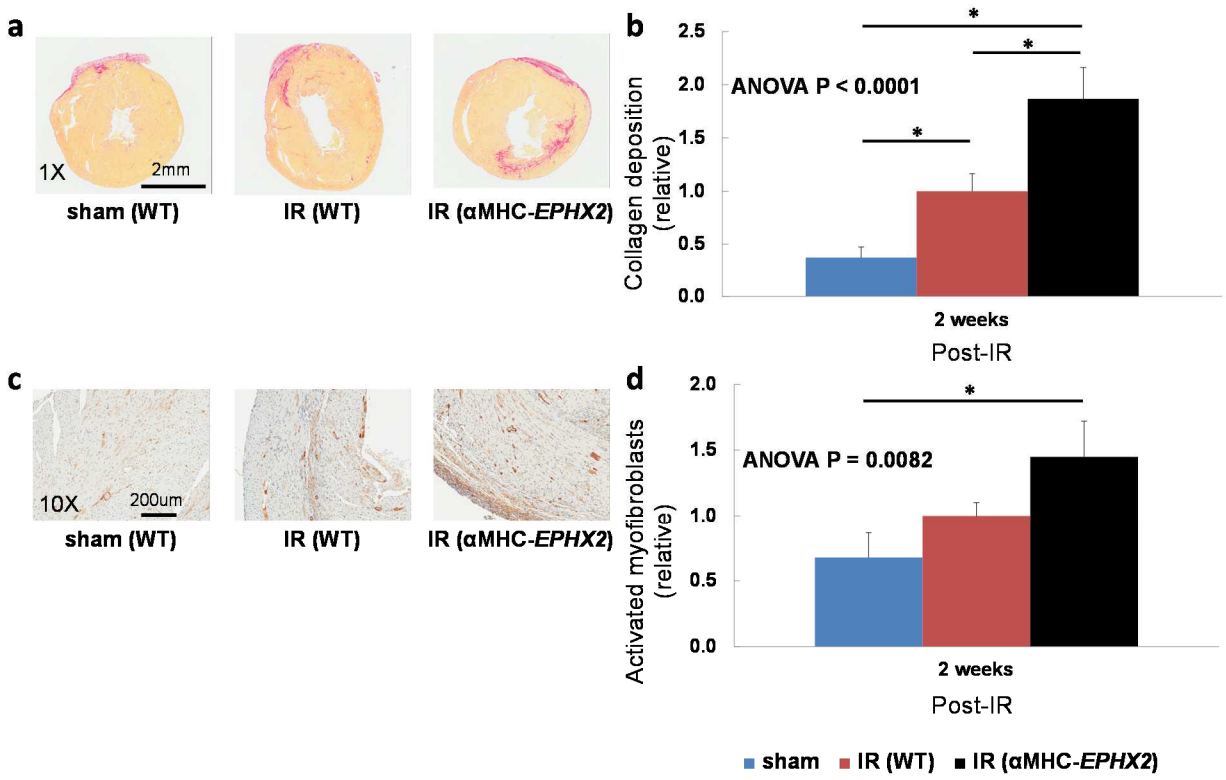

Figure 5.6 Impact of cardiomyocyte soluble epoxide hydrolase (sEH) overexpression on fibrosis. (a) Representative 1X images and (b) quantification of Picrosirius Red-stained collagen deposition as well as (c) representative 10X images and (d) quantification of anti-α-smooth muscle actin- (α-SMA)-stained myofibroblast activation at 2 weeks following ischemia reperfusion (IR) in sham-treated wildtype (WT), IR-treated WT, and IR-treated α-myosin heavy chain- (α-MHC)-*EPHX2* mice. Staining was completed on 8 serial-interrupted heart sections, quantified in each sectin, and then averaged across the 8 sections in each mouse. Data are expressed relative to the IR-treated WT group. Each set of representative images has a different scale. Sham: n = 6. IR: n = 14-15 per group. * $P < 0.05$ for Fisher's LSD *post hoc* test

Table 5.1 Impact of cardiomyocyte soluble epoxide hydrolase (sEH) overexpression on Pulsed Wave Doppler image-derived parameters of systolic function following ischemia-reperfusion (IR) injury.

Parameters	Baseline	2 weeks	P
Isovolumic contraction time (IVCT), ms			
sham (wildtype)	11.0 ± 0.9	16.1 ± 2.0	0.55
IR (wildtype)	12.2 ± 1.0	13.3 ± 1.5	
IR (α-MHC-*EPHX2*)	11.0 ± 2.7	14.0 ± 1.7	
Aortic ejection time (AET), ms			
sham (wildtype)	29.8 ± 2.0	34.1 ± 1.2	0.49
IR (wildtype)	28.4 ± 1.8	36.7 ± 1.6	
IR (α-MHC-*EPHX2*)	32.3 ± 2.0	33.8 ± 1.8	

Comparisons across groups were conducted at 2 weeks using ANCOVA with baseline as the covariate. n = 7-9 per group. * $P < 0.05$ (ANCOVA).
α-MHC, α-myosin heavy chain

Table 5.2 Impact of cardiomyocyte soluble epoxide hydrolase (sEH) overexpression on Pulsed Wave Doppler image-derived parameters of diastolic and global function following ischemia-reperfusion (IR) injury.

Parameters	Baseline	2 weeks	P
Early-peak velocity (E), mm/s			
sham (wildtype)	441.4 ± 39.8	579.9 ± 49.9	0.77
IR (wildtype)	457.4 ± 36.5	585.5 ± 64.0	
IR (α-MHC-*EPHX2*)	488.8 ± 50.8	528.5 ± 51.8	
Atrial-peak velocity (A), mm/s			
sham (wildtype)	341.7 ± 33.2	402.3 ± 44.6	0.46
IR (wildtype)	356.8 ± 25.1	397.7 ± 45.5	
IR (α-MHC-*EPHX2*)	353.6 ± 49.8	337.8 ± 33.0	
Deceleration (Dt), ms			
sham (wildtype)	24.2 ± 2.8	21.9 ± 2.1	0.61
IR (wildtype)	27.7 ± 2.9	21.5 ± 2.4	
IR (α-MHC-*EPHX2*)	21.8 ± 4.2	18.7 ± 1.8	
Deceleration (Dr), mm/s^2			
sham (wildtype)	-19.2 ± 2.1	-27.6 ± 3.8	0.96
IR (wildtype)	-18.9 ± 3.2	-28.2 ± 5.3	
IR (α-MHC-*EPHX2*)	-26.5 ± 5.0	-26.3 ± 2.3	
Myocardial performance index (MPI), ratio			
sham (wildtype)	1.0 ± 0.1	0.9 ± 0.1	0.54
IR (wildtype)	1.1 ± 0.1	0.8 ± 0.1	
IR (α-MHC-*EPHX2*)	0.8 ± 0.1	0.9 ± 0.1	

Comparisons across groups were conducted at 2 weeks using ANCOVA with baseline as the covariate. n = 7-9 per group. * $P < 0.05$ (ANCOVA).
α-MHC, α-myosin heavy chain

Table 5.3 Impact of cardiomyocyte soluble epoxide hydrolase (sEH) overexpression on cardiac structure following ischemia-reperfusion (IR) injury.

Parameters	Baseline	1 day	P
LVID, systolic (mm)			
sham (wildtype)	1.51 ± 0.10	1.94 ± 0.08	0.86
IR (wildtype)	1.69 ± 0.10	2.07 ± 0.13	
IR (α-MHC-*EPHX2*)	1.52 ± 0.08	1.94 ± 0.13	
LVID, diastolic (mm)			
sham (wildtype)	2.92 ± 0.10	3.24 ± 0.10	0.57
IR (wildtype)	3.05 ± 0.10	3.14 ± 0.10	
IR (α-MHC-*EPHX2*)	2.90 ± 0.07	3.07 ± 0.10	
IVS, systolic (mm)			
sham (wildtype)	1.85 ± 0.04	1.68 ± 0.05	0.12
IR (wildtype)	1.64 ± 0.04	1.48 ± 0.07	
IR (α-MHC-*EPHX2*)	1.79 ± 0.04	1.70 ± 0.08	
IVS, diastolic (mm)			
sham (wildtype)	1.24 ± 0.05	1.14 ± 0.04	0.06
IR (wildtype)	1.09 ± 0.03	1.09 ± 0.04	
IR (α-MHC-*EPHX2*)	1.18 ± 0.04	1.26 ± 0.06	
LVPW, systolic (mm)			
sham (wildtype)	1.78 ± 0.07	1.57 ± 0.05	0.75
IR (wildtype)	1.76 ± 0.04	1.51 ± 0.08	
IR (α-MHC-*EPHX2*)	1.81 ± 0.07	1.55 ± 0.07	
LVPW, diastolic (mm)			
sham (wildtype)	1.16 ± 0.04	1.13 ± 0.05	0.37
IR (wildtype)	1.08 ± 0.03	1.03 ± 0.04	
IR (α-MHC-*EPHX2*)	1.13 ± 0.04	1.09 ± 0.05	
Echocardiography-derived LV mass corrected (mg)			
sham (wildtype)	106.04 ± 4.68	113.33 ± 5.77	0.10
IR (wildtype)	95.86 ± 3.46	97.23 ± 4.32	
IR (α-MHC-*EPHX2*)	98.97 ± 4.24	111.15 ± 6.35	

Comparisons across groups were conducted at 1 day using ANCOVA with baseline as the covariate. IR: n = 17-19 per group. Sham: n = 8. * $P < 0.05$ (ANCOVA)

IVS, interventricular septum; LV, left ventricle; LVID, left ventricular internal diameter; LVPW, left ventricular posterior wall

REFERENCES

(1) van Nieuwenhoven, F.A. & Turner, N.A. The role of cardiac fibroblasts in the transition from inflammation to fibrosis following myocardial infarction. *Vascul Pharmacol* 58, 182-8 (2013).

(2) Sutton, M.G. & Sharpe, N. Left ventricular remodeling after myocardial infarction: pathophysiology and therapy. *Circulation* 101, 2981-8 (2000).

(3) Kober, L., Torp-Pedersen, C., Jorgensen, S., Eliasen, P. & Camm, A.J. Changes in absolute and relative importance in the prognostic value of left ventricular systolic function and congestive heart failure after acute myocardial infarction. TRACE Study Group. Trandolapril Cardiac Evaluation. *Am J Cardiol* 81, 1292-7 (1998).

(4) Carrabba, N., Parodi, G., Valenti, R., Migliorini, A., Bellandi, B. & Antoniucci, D. Prognostic value of reverse left ventricular remodeling after primary angioplasty for STEMI. *Atherosclerosis* 222, 123-8 (2012).

(5) Mehta, D., Curwin, J., Gomes, J.A. & Fuster, V. Sudden death in coronary artery disease: acute ischemia versus myocardial substrate. *Circulation* 96, 3215-23 (1997).

(6) Imig, J.D. & Hammock, B.D. Soluble epoxide hydrolase as a therapeutic target for cardiovascular diseases. *Nat Rev Drug Discov* 8, 794-805 (2009).

(7) Sirish, P. *et al.* Unique mechanistic insights into the beneficial effects of soluble epoxide hydrolase inhibitors in the prevention of cardiac fibrosis. *Proc Natl Acad Sci U S A* 110, 5618-23 (2013).

(8) Li, N. *et al.* Beneficial effects of soluble epoxide hydrolase inhibitors in myocardial infarction model: Insight gained using metabolomic approaches. *J Mol Cell Cardiol* 47, 835-45 (2009).

(9) Oni-Orisan, A., Alsaleh, N., Lee, C.R. & Seubert, J.M. Epoxyeicosatrienoic acids and cardioprotection: the road to translation. *J Mol Cell Cardiol* 74, 199-208 (2014).

(10) Seubert, J. *et al.* Enhanced postischemic functional recovery in CYP2J2 transgenic hearts involves mitochondrial ATP-sensitive K+ channels and p42/p44 MAPK pathway. *Circ Res* 95, 506-14 (2004).

(11) Gulick, J., Subramaniam, A., Neumann, J. & Robbins, J. Isolation and characterization of the mouse cardiac myosin heavy chain genes. *J Biol Chem* 266, 9180-5 (1991).

(12) Abatan, O.I., Welch, K.B. & Nemzek, J.A. Evaluation of saphenous venipuncture and modified tail-clip blood collection in mice. *J Am Assoc Lab Anim Sci* 47, 8-15 (2008).

(13) Theken, K.N., Deng, Y.M., Kannon, M.A., Miller, T.M., Poloyac, S.M. & Lee, C.R. Activation of the Acute Inflammatory Response Alters Cytochrome P450 Expression and Eicosanoid Metabolism. *Drug Metabolism and Disposition* 39, 22-9 (2011).

(14) Livak, K.J. & Schmittgen, T.D. Analysis of relative gene expression data using real-time quantitative PCR and the 2(-Delta Delta C(T)) Method. *Methods* 25, 402-8 (2001).

(15) Tanaka, H. *et al.* Serum levels of cardiac troponin I and troponin T in estimating myocardial infarct size soon after reperfusion. *Coron Artery Dis* 8, 433-9 (1997).

(16) Ding, S., Walton, K.L., Blue, R.E., McNaughton, K., Magness, S.T. & Lund, P.K. Mucosal healing and fibrosis after acute or chronic inflammation in wild type FVB-N mice and C57BL6 procollagen alpha1(I)-promoter-GFP reporter mice. *PLoS One* 7, e42568 (2012).

(17) Imig, J.D. Epoxides and soluble epoxide hydrolase in cardiovascular physiology. *Physiol Rev* 92, 101-30 (2012).

(18) Ai, D. *et al.* Angiotensin II up-regulates soluble epoxide hydrolase in vascular endothelium in vitro and in vivo. *Proc Natl Acad Sci U S A* 104, 9018-23 (2007).

(19) Ai, D. *et al.* Soluble epoxide hydrolase plays an essential role in angiotensin II-induced cardiac hypertrophy. *Proc Natl Acad Sci U S A* 106, 564-9 (2009).

(20) Imig, J.D., Zhao, X., Capdevila, J.H., Morisseau, C. & Hammock, B.D. Soluble epoxide hydrolase inhibition lowers arterial blood pressure in angiotensin II hypertension. *Hypertension* 39, 690-4 (2002).

(21) Monti, J. *et al.* Soluble epoxide hydrolase is a susceptibility factor for heart failure in a rat model of human disease. *Nat Genet* 40, 529-37 (2008).

(22) van den Borne, S.W., Diez, J., Blankesteijn, W.M., Verjans, J., Hofstra, L. & Narula, J. Myocardial remodeling after infarction: the role of myofibroblasts. *Nat Rev Cardiol* 7, 30-7 (2010).

(23) Wagner, D.R., Delagardelle, C., Ernens, I., Rouy, D., Vaillant, M. & Beissel, J. Matrix metalloproteinase-9 is a marker of heart failure after acute myocardial infarction. *J Card Fail* 12, 66-72 (2006).

(24) Fan, D., Takawale, A., Lee, J. & Kassiri, Z. Cardiac fibroblasts, fibrosis and extracellular matrix remodeling in heart disease. *Fibrogenesis Tissue Repair* 5, 15 (2012).

(25) Nithipatikom, K. & Gross, G.J. Review article: epoxyeicosatrienoic acids: novel mediators of cardioprotection. *J Cardiovasc Pharmacol Ther* 15, 112-9 (2010).

(26) Kompa, A.R. *et al.* Soluble epoxide hydrolase inhibition exerts beneficial anti-remodeling actions post-myocardial infarction. *Int J Cardiol* 167, 210-9 (2013).

(27) Merabet, N. *et al.* Soluble epoxide hydrolase inhibition improves myocardial perfusion and function in experimental heart failure. *J Mol Cell Cardiol* 52, 660-6 (2012).

(28) Souders, C.A., Bowers, S.L. & Baudino, T.A. Cardiac fibroblast: the renaissance cell. *Circ Res* 105, 1164-76 (2009).

(29) Deng, Y., Theken, K.N. & Lee, C.R. Cytochrome P450 epoxygenases, soluble epoxide hydrolase, and the regulation of cardiovascular inflammation. *J Mol Cell Cardiol* 48, 331-41 (2010).

(30) Deng, Y. *et al.* Endothelial CYP epoxygenase overexpression and soluble epoxide hydrolase disruption attenuate acute vascular inflammatory responses in mice. *FASEB J* 25, 703-13 (2011).

(31) Shinde, A.V. & Frangogiannis, N.G. Fibroblasts in myocardial infarction: a role in inflammation and repair. *J Mol Cell Cardiol* 70, 74-82 (2014).

(32) Turner, N.A. & Porter, K.E. Regulation of myocardial matrix metalloproteinase expression and activity by cardiac fibroblasts. *IUBMB Life* 64, 143-50 (2012).

(33) Kim, J., Imig, J.D., Yang, J., Hammock, B.D. & Padanilam, B.J. Inhibition of soluble epoxide hydrolase prevents renal interstitial fibrosis and inflammation. *Am J Physiol Renal Physiol* 307, F971-80 (2014).

(34) Christia, P. *et al.* Systematic characterization of myocardial inflammation, repair, and remodeling in a mouse model of reperfused myocardial infarction. *J Histochem Cytochem* 61, 555-70 (2013).

CHAPTER 6 - DISCUSSION AND PERSPECTIVE

Summary and Scope

Despite advances in evidence-based medical therapies, CVD has been the leading cause of death for over a century and its prevalence is expected to continue to rise tremendously. Most notably, CAD, which includes AMI and stable angina, is the primary source of this public health burden causing almost half of all CVD deaths. Heart failure, a key clinical outcome of CAD, is also a major source of the health burden (1). Recent failures in CAD drug development suggest that innovative approaches are needed to mitigate increasing attrition rates and more successfully translate novel therapies into clinical practice (2-4). Biomarkers offer considerable promise to prospectively identify subsets of CAD patients at high risk of experiencing a cardiovascular event that exhibit dysfunction in a specific pathway (putative responders), consequently enabling novel therapies that target the pathway to maximize their therapeutic effect and improve outcomes. A more thorough understanding of the mechanisms underlying the pathophysiology of CAD is necessary to facilitate the development of biomarkers and novel therapeutic strategies that ultimately prevent AMI events, delay the development of heart failure, and improve public health outcomes.

CAD is a complex disease involving the development of atherosclerosis along the walls of the coronary arteries as well as the formation of an intracoronary thrombus from a ruptured atheromatous plaque leading to an ACS (5). Myocardial cell death from an AMI promotes

maladaptive ventricular remodeling which leads to the development of heart failure (6). EETs yields potent cardiovascular protective effects in preclinical models of cardiovascular disease, which suggests that increasing EET levels may be a viable therapeutic strategy for CAD, AMI, post-AMI ventricular remodeling (7). Key questions, however, remain to be addressed prior to translation of therapeutic EET-promoting strategies into successful proof-of-concept phase I and II clinical trials (Appendix B). Thus, the overall aim of this dissertation was to advance our understanding of the role of the EET metabolic pathway across the full spectrum of CAD and post-AMI consequences as a means to determine the biological and therapeutic importance of EETs in the progression of this disease cascade. To accomplish this, we have taken a translational approach integrating both preclinical and clinical studies to evaluate the contribution of the EET metabolic pathway across the full spectrum of CAD. The major findings of this work include 1) the discovery that obstructive CAD is significantly and independently associated with lower circulating EET levels secondary to suppressed EET biosynthesis, 2) the preliminary, hypothesis-generating observation that *EPHX2* Lys55Arg may be associated with poor prognosis following AMI, and 3) a demonstration of the key contribution of cardiomyocyte-derived sEH to the development of fibrosis following AMI. Overall, these results demonstrate that the EET metabolic pathway may play a role in the pathophysiology of CAD and its associated complications including the development of coronary atherosclerosis, post-AMI early ventricular remodeling, and post-AMI mortality. Collectively, these data help to set the foundation for future clinical research in this area, including the rational design of prospective, biomarker-guided interventional studies in targeted subsets of the CAD population with enriched potential to derive clinical benefit from emerging EET-promoting therapies.

Key Findings

The clinical course of CAD is always initiated by the development of an atheroma in the lumen of the coronary artery and progresses from stable angina to AMI to heart failure to death (5). The overall aim of this dissertation was to advance our understanding of the role of the EET metabolic pathway across this full spectrum of CAD and post-AMI.

In Aim 1, we advanced our understanding of the role of the EET pathway in the earlier stages of this full CAD spectrum. Namely, we recruited a cohort of patients referred for coronary angiography; subjects were at varying stages of atherosclerotic-driven coronary artery stenosis where the majority of patients did not have a prior AMI (85%), were not suffering from an AMI at the index hospitalization (91%), and did not have a history of heart failure (87%). In order to elucidate the relationship between EET levels and the extent of CAD, we utilized a targeted metabolomics approach where we quantified a panel of eicosanoids in the participants. This is the largest study to date that quantifies EET levels in patients with or at risk for CVD.

We observed that the presence of atherosclerotic obstructive CAD was significantly associated with lower circulating EET levels. It is well established that patients with obstructive CAD are at the greatest risk of adverse CV outcomes compared to patients with less extensive CAD (8). These findings suggest that CYP-derived EETs may play an important role in the pathogenesis and progression of CAD in humans. Validation of the observed relationships in an independent cohort is necessary.

However, other eicosanoids derived from COX, LO, and CYP also play a role in cardiovascular disease (7, 9-11). Nevertheless, the association between EETs and CAD was significantly more pronounced than other eicosanoid metabolism pathways, further

demonstrating an important role for these lipid mediators in the pathophysiology of CAD. Although the panel of eicosanoids included 28 metabolites which were derived from various biosynthetic enzymes and fatty acid substrates, several other fatty acid metabolites including leukotrienes, resolvins, and protectins were not on the panel. Furthermore, it is unknown if changes in the levels the parent substrates themselves such as arachidonic acid impacted the relationship between EETs and CAD extent. The relative strength of the EET-CAD association compared to these other potent mediators is a future area of investigation.

CAD extent was also associated with lower sum EETs+DHETs (a biomarker of CYP epoxygenase-derived EET biosynthesis) as an inverse association, but not EET:DHET ratio (a biomarker of sEH-derived EET hydrolysis). These data suggest that the association between EET levels and CAD extent may be mediated by suppression of EET synthesis and not an increase in EET hydrolysis. Accordingly, it is well-established that inflammatory stimuli suppress CYP-mediated xenobiotic metabolism through a variety of mechanisms, including cytokine-mediated transcriptional downregulation of CYP expression (12); fittingly, inflammatory stimuli also drive the development and progression of CAD (13). These findings suggest that suppression of CYP-mediated EET biosynthesis may be a key pathological consequence of the inflammation-mediated development and progression of CAD. Future studies are necessary to elucidate the mechanisms underlying the association between lower EET levels and advanced CAD in humans.

In a secondary analysis of the coronary angiography patients, we explored the relationship between inter-individual variation in EET metabolite levels and risk of a future adverse cardiovascular event exclusively in patients with obstructive CAD at baseline. We observed a stepwise relationship across the EET tertiles where the highest event incidence

occurred in those with the lowest EET levels at baseline. Although this relationship was not statistically significant and should be observed with caution due to the small number of events, these findings are biologically plausible considering the anti-inflammatory and protective effects of EETs in numerous preclinical models of cardiovascular disease.

Altogether, these findings demonstrated that patients with obstructive CAD are predisposed to low EET metabolite levels secondary to suppressed EET biosynthesis, and suggest that novel strategies that promote the effects of EETs may have therapeutic promise in patients with obstructive CAD. Further investigation in needed to determine relationship between the EET metabolic pathway and prognosis in patients with established CAD. Indeed, nonobstructive lesions have thinner fibrous caps and are more vulnerable to rupture (5), thus a strong relationship between EETs and CAD extent may not equate to a correlation between EETs and adverse CV events.

Although sEH-derived EET hydrolysis was not associated with CAD extent suggesting that sEH may not play a role in CAD progression, preclinical and genetic observational studies have demonstrated a potential link between sEH and the complications of CAD such as AMI. In Aim 2, we advanced our understanding of the role of the EET metabolic pathway in prognosis following AMI (later in the clinical course of CAD compared to Aim 1). In particular, using a candidate gene approach, we determined the relationship between the *EPHX2* p.Lys55Arg polymorphism and survival two independent cohorts of AMI patients. INFORM is a 2-center cohort of ACS patients with full 5-year mortality data available and TRIUMPH is a 24-center, racially-diverse population of AMI patients. We observed that *EPHX2* Lys55Arg was associated with 5-year mortality following AMI in INFORM, but we were not able to replicate this finding in TRIUMPH. Notably, TRIUMPH only had full 2-year mortality data available. Thus, an

important issue in this study is the lack of statistical power that may have limited our ability to detect differences in TRIUMPH. A repeat analysis when full 5-year mortality data are available is necessary to rule out the possibility that lack of sufficient power prevented the INFORM results from being replicated in TRIUMPH. Futhermore, considering the impact of CYP-derived EET biosynthesis in the inititation and progression of coronary atherosclerosis in Aim 1, the association between SNPs in genes encoding for CYP epoxygenase and survival following AMI is necessary to fully understand the EET metabolic pathway in post-AMI mortality.

We investigated mortality in our candidate gene study, because it is an important endpoint following AMI; however, maladaptive ventricular remodeling is the key pathophysiological process that ultimately drives the progression to heart failure and death following AMI (14). Consistent with the overall aim of this translational project to better understand the role of the EET metabolic pathway in CAD and its associated complications, we used a genetic manipulation approach (Aim 3) to investigate the role of myocardial sEH in maladaptive ventricular remodeling post-IR *in vivo* using a transgenic mouse line with cardiomyocyte-specific overexpression of human sEH. However, there are surprising few studies that characterize the early maladaptive ventricular remodeling response following IR in mice. A more thorough understanding of the pathophysiology of myocardial remodeling following AMI in mice will facilitate the design of experimental studies that elucidate the role of therapeutic pathways in the disease. Consequently, we first characterized the impact of IR injury (30-minute of myocardial ischemia followed by 2 weeks of reperfusion) in mice *in vivo*. We observed that IR induced transient but marked myocardial cell death and inflammation acutely following IR and generated substantial fibrosis at an early chronic time point. New approaches are needed to

better discriminate between adaptive and maladaptive fibrosis. This is an important future area of investigation because novel therapies that attenuate adaptive fibrosis would be deleterious.

In contrast to induction of myocardial fibrosis, IR did not produce significant changes in myocardial structure, systolic function, or diastolic function in early chronic remodeling. This finding is in line with data suggesting that the fibrotic response following AMI precedes the impairment of cardiac function and structure (15). A future investigation evaluating the impact of 30-minute myocardial IR in mice on cardiac structure and function at a late chronic time point is warranted.

Altogether, we found that our *in vivo* mouse model was best suited for investigating the impact of intervention fibrotic responses in early chronic myocardial remodeling independent of cardiac structure or function. These findings set the foundation for the evaluation of the contribution of cardiomyocyte sEH to maladaptive ventricular remodeling in mice post-AMI. We discovered that cardiomyocyte-specific overexpression of human sEH exhibited enhanced IR-induced myocardial collagen deposition during early chronic ventricular remodeling following IR. Although, this suggests that myocardial sEH activity is a key mediator of collagen deposition, it is unknown whether the observed enhancement of cardiac fibrosis in the presence of cardiomyocyte sEH overexpression was independent of infarct size following IR. A few studies have shined light on this question, reporting evidence that this effect is independent of changes to infarct size (16-18). Administration of a sEH inhibitor to α-MHC-*EPHX2* mice following the acute phase of IR would provide insight on whether the enhanced fibrosis was independent of infarct size, and is an important future direction for this line of investigation. Furthermore, it is unknown if the observed changes in myocardial collagen deposition are a result of increased collagen synthesis, impaired collagen proteolytic degradation, or both. Our

findings suggest that the enhanced collagen deposition may be, at least in part, a consequence of reduced ECM degradation in α-MHC-*EPHX2* mouse hearts. Future studies which investigate the role of cardiomyocyte sEH on the time course of the aforementioned mediators in the infarcted heart following IR would elucidate the mechanism by which sEH overexpression caused increased collagen deposition.

In contrast, cardiomyocyte-specific overexpression did not alter systolic function, diastolic function, or cardiac structure in early ventricular remodeling. Based on the results of our studies characterizing the *in vivo* IR model in which IR did not produce functional impairment or structural damage, it was not surprising that the transgenic mice did not exhibit altered structure or function following IR. Fibrosis inevitably leads to some degree of systolic or diastolic dysfunction (15), so the relevance of an intervention that never impacts cardiac function is unknown. An investigation of the impact of cardiomyocyte sEH overexpression in an AMI model that produces greater levels of maladaptive remodeling such as a PO model or an IR model of late chronic remodeling would provide further insight into the role of cardiomyocyte sEH on cardiac function and structure following AMI.

Overall, this is the first study to investigate the impact of cardiomyocyte sEH on maladaptive ventricular remodeling following AMI. This work opens the door for future studies investigating the role of cardiomyocyte-derived sEH in the development of heart disease. The direct implication of EETs in this observation is needed to establish that lower cardiac EETs promote fibrosis post-AMI.

Thus, we demonstrated that the EET metabolic pathway may play a role in the pathophysiology of CAD and its associated complications including the development of coronary atherosclerosis (Aim 1; clinical), post-AMI mortality (Aim 2; clinical), and post-AMI

early ventricular remodeling (Aim 3; clinical). In Aim 1, we showed that obstructive CAD is strongly associated with lower plasma EETs, thereby identifying a potential subset of the CAD population that may be at greater risk of a more aggressive disease course. In Aim 2, we showed that a functionally relevant polymorphism associated with increased EET hydrolysis may be associated with increased mortality following AMI. In Aim 3, we showed in a mouse model of IR-induced maladaptive ventricular remodeling (a key consequence of CAD) that cardiomyocyte-specific overexpression of human sEH and putative reduction in cardiac EETs enhances collagen deposition. Collectively, these data provide evidence that lower EETs may promote deleterious consequences in CAD and post-AMI, and in turn suggest that promoting the effects of EETs may have therapeutic utility in CAD and AMI patients predisposed to low circulating EET levels. Furthermore, plasma EETs levels or *EPHX2* Lys55Arg genotype may be promising biomarkers that detect which CAD patients may derive the greatest benefit from EET-promoting agents.

Clinical Implications

Despite advances in evidence-based medical therapies, CAD remains a leading cause of mortality in the US (1) and novel therapeutic strategies are needed to further improve outcomes. A series of recent failures in CAD drug development suggest that innovative approaches are needed to reduce high attrition rates and more successfully translate novel therapies into clinical practice (2-4). Compared to the conventional 'one-size fits all' methodology to drug development, a precision medicine approach has the potential to facilitate the development of novel therapeutics candidates and increase the probability of success for these therapies (19). This approach prospectively identifies subsets of patients that exhibit dysfunction in a specific pathway (putative responders), thereby enabling novel or existing therapies that target the pathway to maximize their therapeutic effect and improve outcomes. This approach has shown great clinical success in cancer, and is promising in several areas of CVD (Appendix A). Importantly, the discovery of biomarkers involved in the pathogenesis of CAD is needed to identify subsets of high-risk patients who would derive the greatest benefit from therapies that modulate that pathway (20, 21).

Our study in CAD patients referred for angiography demonstrates that obstructive CAD is strongly associated with lower EETs and thereby identifies a subset of the CAD population that may be at greater risk. We also showed, in a mouse model of IR-induced maladaptive ventricular remodeling (a key consequence of CAD), that cardiomyocyte-specific overexpression of human sEH and putative reduction in cardiac EETs enhances collagen deposition. This further suggests that lower EETs may promote deleterious consequences post-AMI. Collectively, these data provide evidence that promoting the effects of EETs may have therapeutic utility in CAD

and AMI patients predisposed to low circulating EET levels. Furthermore, EET levels may be a promising biomarker that detects the CAD patients at highest risk of adverse outcomes that may derive the greatest benefit from EET-promoting agents.

Notably, numerous sEH inhibitors have been discovered by drug companies and an academic group. Many of these agents have properties favorable to further drug development (22). One agent that has shown promise in rodent studies (23) is being developed for chronic obstructive pulmonary disease (COPD) in clinical trials (NCT01762774, NCT02006537). In addition, EET mimics are being optimized in the early discovery stage into candidates which may also show promise in further preclinical studies (24). In parallel, tools for the high-throughput quantification of CYP-derived eicosanoids in humans are advancing, showing promise as a feasible biomarker that can be measured in the clinical setting (25). Thus, the technology is in place for the successful development of EET-promoting therapies.

The findings from this dissertation contribute to the science evaluating the therapeutic utility of EET-promoting agents, thereby complimenting the aforementioned advances which have improved the profile of drug candidates and the efficiency of the quantification of EET metabolic pathway biomarkers. Follow-up preclinical studies elucidating underlying mechanisms and follow-up clinical studies which validate our findings across the full spectrum of CAD are still needed before this work can truly advance the field; however, positive follow-up results will set the foundation for the rational design of prospective, biomarker-guided interventional studies in targeted subsets of the CAD population (low EET levels) with enriched potential to derive clinical benefit from emerging EET-promoting therapies.

Conclusions

In conclusion, we found that obstructive CAD is significantly and independently associated with lower circulating EET levels secondary to suppressed EET biosynthesis using a targeted metabolomics approach. In addition, using a candidate gene approach, we observed that *EPHX2* p.Lys55Arg may be associated with mortality in the AMI subset of an ACS population. This paves the way for a validation study in an independent population with full 5-year mortality available to substantiate these preliminary findings. Moreover, we characterized a mouse model of IR injury-induce maladaptive ventricular remodeling, showing its effect on myocardial cell death, inflammation, and collagen induction. This allowed us to ultimately demonstrate that mice with cardiomyocyte-specific overexpression of human sEH exhibited enhanced IR-induced myocardial collagen deposition. Overall, this dissertation used both pre-clinical and human studies to provide insight into the role of the EET metabolic pathway in the pathophysiology of CAD and its associated complications. We show that alterations in the EET metabolic pathway which are predicted to reduce EET levels may promote the development of coronary atherosclerosis, post-AMI early ventricular remodeling, and post-AMI mortality. Collectively, this work sets the stage for future studies that investigate the therapeutic utility of modulating EETs in CAD patients.

REFERENCES

(1) Mozaffarian, D. *et al.* Heart disease and stroke statistics--2015 update: a report from the American Heart Association. *Circulation* 131, e29-322 (2015).

(2) Yellon, D.M. & Hausenloy, D.J. Myocardial reperfusion injury. *N Engl J Med* 357, 1121-35 (2007).

(3) Mullard, A. GSK's darapladib failures dim hopes for anti-inflammatory heart drugs. *Nat Rev Drug Discov* 13, 481-2 (2014).

(4) Pammolli, F., Magazzini, L. & Riccaboni, M. The productivity crisis in pharmaceutical R&D. *Nat Rev Drug Discov* 10, 428-38 (2011).

(5) Libby, P. & Theroux, P. Pathophysiology of coronary artery disease. *Circulation* 111, 3481-8 (2005).

(6) Frangogiannis, N.G. Regulation of the inflammatory response in cardiac repair. *Circ Res* 110, 159-73 (2012).

(7) Oni-Orisan, A., Alsaleh, N., Lee, C.R. & Seubert, J.M. Epoxyeicosatrienoic acids and cardioprotection: the road to translation. *J Mol Cell Cardiol* 74, 199-208 (2014).

(8) Maddox, T.M. *et al.* Nonobstructive coronary artery disease and risk of myocardial infarction. *JAMA* 312, 1754-63 (2014).

(9) Gross, G.J., Falck, J.R., Gross, E.R., Isbell, M., Moore, J. & Nithipatikom, K. Cytochrome P450 and arachidonic acid metabolites: role in myocardial ischemia/reperfusion injury revisited. *Cardiovasc Res* 68, 18-25 (2005).

(10) Poeckel, D. & Funk, C.D. The 5-lipoxygenase/leukotriene pathway in preclinical models of cardiovascular disease. *Cardiovasc Res* 86, 243-53 (2010).

(11) Yuhki, K. *et al.* Roles of prostanoids in the pathogenesis of cardiovascular diseases: Novel insights from knockout mouse studies. *Pharmacol Ther* 129, 195-205 (2011).

(12) Morgan, E.T. Regulation of cytochrome p450 by inflammatory mediators: why and how? *Drug Metab Dispos* 29, 207-12 (2001).

(13) Hansson, G.K. Inflammation, atherosclerosis, and coronary artery disease. *N Engl J Med* 352, 1685-95 (2005).

(14) Burchfield, J.S., Xie, M. & Hill, J.A. Pathological ventricular remodeling: mechanisms: part 1 of 2. *Circulation* 128, 388-400 (2013).

(15) van den Borne, S.W., Diez, J., Blankesteijn, W.M., Verjans, J., Hofstra, L. & Narula, J. Myocardial remodeling after infarction: the role of myofibroblasts. *Nat Rev Cardiol* 7, 30-7 (2010).

(16) Sirish, P. *et al.* Unique mechanistic insights into the beneficial effects of soluble epoxide hydrolase inhibitors in the prevention of cardiac fibrosis. *Proc Natl Acad Sci U S A* 110, 5618-23 (2013).

(17) Kompa, A.R. *et al.* Soluble epoxide hydrolase inhibition exerts beneficial anti-remodeling actions post-myocardial infarction. *Int J Cardiol* 167, 210-9 (2013).

(18) Merabet, N. *et al.* Soluble epoxide hydrolase inhibition improves myocardial perfusion and function in experimental heart failure. *J Mol Cell Cardiol* 52, 660-6 (2012).

(19) Pacanowski, M.A., Leptak, C. & Zineh, I. Next-generation medicines: past regulatory experience and considerations for the future. *Clin Pharmacol Ther* 95, 247-9 (2014).

(20) Ganesh, S.K. *et al.* Genetics and genomics for the prevention and treatment of cardiovascular disease: update: a scientific statement from the American Heart Association. *Circulation* 128, 2813-51 (2013).

(21) Waldman, S.A. & Terzic, A. Molecular insights provide the critical path to disease mitigation. *Clin Pharmacol Ther* 95, 3-7 (2014).

(22) Shen, H.C. & Hammock, B.D. Discovery of inhibitors of soluble epoxide hydrolase: a target with multiple potential therapeutic indications. *J Med Chem* 55, 1789-808 (2012).

(23) Podolin, P.L. *et al.* In vitro and in vivo characterization of a novel soluble epoxide hydrolase inhibitor. *Prostaglandins Other Lipid Mediat* 104-105, 25-31 (2013).

(24) Falck, J.R. *et al.* 14,15-Epoxyeicosa-5,8,11-trienoic Acid (14,15-EET) surrogates: carboxylate modifications. *J Med Chem* 57, 6965-72 (2014).

(25) Zhu, P., Peck, B., Licea-Perez, H., Callahan, J.F. & Booth-Genthe, C. Development of a semi-automated LC/MS/MS method for the simultaneous quantitation of 14,15-epoxyeicosatrienoic acid, 14,15-dihydroxyeicosatrienoic acid, leukotoxin and leukotoxin diol in human plasma as biomarkers of soluble epoxide hydrolase activity in vivo. *J Chromatogr B Analyt Technol Biomed Life Sci* 879, 2487-93 (2011).

APPENDIX A - PHARMACOGENOMICS IN HEART FAILURE: WHERE ARE WE NOW AND HOW CAN WE REACH CLINICAL APPLICATION[1]

Introduction

Heart failure has reached epidemic proportions. Approximately 5 million adults have heart failure in the United States with recent projections suggesting that by 2030, the prevalence of this syndrome will increase another 25%. (1) Thus, heart failure has tremendous impact on the health care system and constitutes a major medical and societal burden. Heart failure is characterized by insufficient cardiac performance to meet metabolic requirements or accommodate systemic venous return. (2) The body's neurohormonal system including the renin-angiotensin-aldosterone system (RAAS) and the sympathetic nervous system (SNS) is activated in order to compensate for these deficiencies (2) but activation of these systems contribute to worsening heart failure, worsened quality of life, and poor outcomes such as the need for a heart transplant, or sudden cardiac death. (3) Evidence-based medical therapies that suppress these responses can substantially reduce the progression of this syndrome. (4-6) Accordingly, comprehensive heart failure management guidelines from both the American College of Cardiology (ACC)/American Heart Association (AHA) and the Heart Failure Society of America (HFSA) recommend specific pharmacological management, mostly focused on neurohormonal suppression, to improve outcomes in all patients with heart failure and reduced ejection fraction. (7, 8) β blockers and angiotensin converting enzyme (ACE)-inhibitors are considered the foundation, but evidence has shown important roles for other therapies which help delay progression of heart failure and reduce mortality including angiotensin receptor blockers

[1]Oni-Orisan, A. & Lanfear, D.E. Pharmacogenomics in heart failure: where are we now and how can we reach clinical application? *Cardiol Rev* 22, 193-8 (2014).

(ARB)s, aldosterone antagonists, hydralazine/isosorbide combination, and even device therapies such as implanted defibrillators and cardiac resynchronization therapy (CRT). (7, 8) In addition, while there is no evidence for mortality benefits with loop diuretics and digoxin, these agents are indispensable, improving symptoms and possibly reducing hospitalizations. (9, 10) It is thus evident that heart failure patients are currently subjected to a multiplicity of medications to achieve maximum benefit and optimized outcomes. This polypharmacy in health failure patients is associated with increased risk of toxicity, drug interactions, and poor compliance. (11) Current guidelines do offer some advice regarding tailoring of therapy on clinical grounds; for example, the HFSA guidelines recommend that factors such as age, ethnicity, heart failure severity, renal function, and serum potassium should be used to choose which of the many agents a heart failure patient should receive in his or her regimen. (7) However, even in patients who appear to have similar clinical factors, a great deal of variability exists in response to treatment. (12) Genetic variability in response to heart failure treatment exists (13) and genetic information may complement conventional clinical information in tailoring therapy to an individual patient, ultimately improving outcomes. The present review focuses on available data from pharmacogenomic studies in heart failure medications, particularly focusing on new developments over the past 2 years (earlier literature has been nicely described elsewhere (14, 15)), summarized by medication class. Proof-of-principle findings are presented that are important to be aware of, but actionable genetic testing to guide therapeutic choices in heart failure remains limited to date. Thus, the review also shows that further work in this area is needed before the clinical implementation of heart failure pharmacogenomics becomes a reality, and we provide a glimpse of the future needs and directions.

Beta adrenergic antagonists

The role of the adrenergic signaling pathway of the SNS in heart failure is characterized by a vicious cycle in which chronic stimulation of the adrenergic receptor (AR) by circulating catecholamines norepinephrine (NE) and epinephrine promotes cardiac dysfunction that results in the release of more adrenergic-stimulating catecholamines and further disease progression. (16) While the sub-cellular mechanism of action is not completely elucidated, it is clear that β blockers work by suppression of the adrenergic pathway and interruption of this vicious cycle. (17) Due to evidence of survival benefit, β blockers have been a mainstay of heart failure pharmacotherapy for almost 20 years. (18-20) However, there is great variation in response to β blocker therapy including certain subsets of the heart failure population that do not receive the same mortality and morbidity benefit. (21, 22) SNPs in the β1-AR (*ADRB1)*, β2-AR (*ADRB2)*, α2C AR (*ADRA2C),* and G-protein receptor kinase 5 (*GRK5)* genes of the adrenergic system may partially explain the variable effects received from β blockade. In fact, most of the published pharmacogenomic literature over the past 2 years concerning heart failure has focused on response to β blockers; thus we have given it first and most attention among the drug classes of interest.

β1-AR is the primary pharmacologic target of β blockers. One of the most widely-studied polymorphisms for heart failure in *ADRB1* is the Arg389Gly variant. Arg389 is associated with enhanced adrenergic response to agonist stimulation of β1-AR in vitro (23) and in vivo(24). Importantly, in a genetic substudy of the β Blocker Evaluation of Survival Trial (BEST), a relationship between β_1 genotype and mortality response to treatment with the β blocker bucindolol was found.(25) BEST was a large, randomized, clinical trial testing the efficacy of

bucindolol in heart failure patients. (26) The trial was terminated prematurely at 2 years due to a lack of mortality benefit, though bucindolol significantly improved mortality in the non-black subset (~75% of the patients).(26) As a result of clinical failure in the overall population, bucindolol was never approved by the FDA for the treatment of heart failure. Notably, bucindolol also acts as a potent sympatholytic in addition to its β blocking properties, reducing circulating NE levels to a much greater extent than the β blockers FDA-approved for heart failure (e.g. carvedilol and metoprolol succinate).(27) This distinct property of bucindolol may have reduced NE to deleteriously low levels thereby abrogating cardiac contractility and negating any beneficial effects realized through β blockade.(25) In the genetic substudy, Arg389 homozygotes were found to have a 34% mortality benefit from bucindolol. (25) A greater survival rate in patients with this genotype was found when NE levels did not decrease compared to baseline, suggesting that an enhanced β blockade affect rather than protection from exaggerated sympatholysis may be responsible for reduced mortality in this population. In contrast, no clinical benefit was observed in carriers of the Gly389 variant. (25) These results were backed up by *ex vivo* and cell data which also showed that enhanced bucindolol response was associated with Arg389. (25) In addition, the results may explain racial differences in bucindolol efficacy, as blacks were less likely to carry Arg389 compared to non-blacks. (25) However the relatively small difference in allele frequencies between racial groups (0.62 in blacks, 0.73 in non-blacks)(25) and contradictory clinical trial data that do not show variation in response to β blocker therapy across race(28), suggest that Arg389 does not sufficiently explain racial disparities in bucindolol response.

In addition to the Arg389Gly polymorphism, a variant at codon 49 also has been found to influence drug response and clinical adverse outcomes in heart failure patients. Specifically in a

population of patients with idiopathic dilated cardiomyopathy, Ser49 homozygotes had worsened prognosis (death or cardiac transplantation) compared to Gly49 carriers. (29) This association remained present among patients who received β blocker therapy (~39% of the population), though the specific β blocker drug patients were taking was not specified. (29) These data were supported by mechanistic follow-up studies where cells transfected with Gly49 had increased sensitivity to metoprolol as well as enhanced catecholamine-induced β1-AR desensitization, which is considered a protective response to heart failure progression. (30) An expanded clinical follow-up confirmed that Gly49 carriers had better survival compared to Ser49 homozygotes, suggesting that higher β blocker doses may be warranted in Ser49Ser patients to achieve optimal survival response. (31)

ADRB2 has a role in adrenergic signaling in parallel with *ADRB1*. Indeed, clinical trial data from the COMET trial and experimental evidence both suggest that antagonism of β_2 AR is at least partially responsible for beneficial effects of carvedilol in heart failure. (32, 33) *ADRB2* genotype may be important in heart failure pathophysiology and response to β blocker therapy. Kaye et al. were able to show that among heart failure patients receiving carvedilol, the proportion of patients with a favorable EF response to therapy (≥10% improvement in absolute LVEF or ≥5% improvement in absolute FS) was significantly higher in Glu27 carriers compared to Gln27 homozygous patients(34). These findings were validated in a larger population.(35) Moreover, this effect has been replicated in terms of survival in several subsequent studies. (36-38) For example, in a well-treated cohort of advanced heart failure patients (81% were receiving β blockers), individuals who carried 2 copies of the *ADRB2* Arg16-Gln27 haplotype were more likely to die or require a heart transplant.(38)

The *ADRA2C* gene is responsible for the expression of the α_{2C} AR, an autoreceptor located on presynaptic adrenergic neurons, which limits the release of NE through a negative feedback system. (39, 40) Genetic disruption of α_2 ARs in mice resulted in elevated NE levels and hearts with significant hypertrophy. (40) The multiple-nucleotide polymorphism α_{2C}322–325 deletion (Del) similarly increased risk of developing heart failure in black patients (41), who have a minor allele frequency of 0.4 compared with 0.04 in whites (42). In a BEST DNA substudy, *ADRA2C* variability surprisingly did not alter baseline levels of NE or the natural course of heart failure progression in placebo-treated patients. *ADRA2C* genotype, however, did affect response to bucindolol treatment. (42) Patients who were carriers of the Del allele had enhanced norepinephrine reduction from bucindolol compared to wild-type patients. Furthermore, bucindolol was found to improve survival only in α_{2C}322–325 wild-type homozygotes. (42) Though the precise mechanisms by which *ADRA2C* genotype impacts the ability of bucindolol to reduce NE levels remain unknown, these results are consistent with previous findings(25) that an exaggerated sympatholytic response to bucindolol is associated with reduced survival response to bucindolol.

GRK5 codes for G-protein receptor kinase 5 which desensitize β AR signaling. (43) Substitution of Gln at the 41st amino acid position with Leu has been found to be a gain-of-function allele resulting in enhanced desensitization, (43) analogous to an endogenous β blocking effect. In a prospective cohort of African American heart failure patients, who have 10-fold higher allele frequencies of this gain-of-function polymorphism than Caucasians, the presence of *GRK5* Leu41 was just as protective in preventing cardiac death or heart transplant as β blocker use. (43) These findings were recapitulated in an expanded population of African American heart failure patients: *GRK5* Leu41 improved survival. (44)

Inconsistencies that contradict the above associations between variants in genes of the adrenergic system and survival response to β blockers exist in the literature. For example, the significant relationship between *ADRB1* Arg389Gly genotype and mortality response to bucindolol is less clear with the β blocker therapies FDA-approved for heart failure(27, 45-48); however, the aforementioned differences in sympatholytic properties among β blockers may explain why the pharmacogenetic association with *ADRB1*Arg389Gly in heart failure patients is inconsistent across members of this drug class. Moreover, De Groote et al. did not find a significant genetic association between any of the five aforementioned adrenergic receptor polymorphisms and survival in β blocker-treated heart failure patients. (49) An investigation in a large registry of heart failure patients with left ventricular dysfunction receiving metoprolol or carvedilol showed that individual variants and haplotypes involving *ADRB1*, *ADRB2*, and *ADRA2C* were not found to have a significant effect on survival.(27) Altogether, these results imply that other factors such as race, disease severity, specific β blocker, and phenotype may interact with pharmacogenomic associations. In addition, SNPs may interact with each other and attenuate the elucidation of these associations.

Despite these challenges (or perhaps because of them), the pharmacogenetics of β blockers in heart failure continues to be an active area of investigation in recent years. Further work has attempted to sort out these inconsistencies, validate findings, and fully characterize the subset of optimal responders to β blocker therapy. An approach that continues to be used to address contradictions in the literature is the investigation of associations between genetic combinations and response to β blocker therapy, rather than individual polymorphisms. (50) This strategy has been adopted by multiple investigators in recent years. Petersen et al. observed that heart failure patients who were homozygous for *ADRB* Arg389 and carriers of *ADRB2* Gln27 in

combination received less survival benefit from carvedilol treatment. (51) In contrast, this genotype combination did not impact response to metoprolol, likely due to differences in pharmacological properties. (51) More recently, O'Connor et al. have further elucidated the interaction of multiple adrenergic polymorphisms on β blocker response with another genetic substudy in BEST.(52) In particular they reported an additive loss of bucindolol response in terms of morbidity and mortality in carriers of β_1 Gly389 and α_{2C}322–325 Del alleles, consistent with the effects of the individual SNPs on bucindolol response. (52) And an even more recent BEST substudy shows that genotype combinations determined from β_1 Gly389 and α_{2C}322–325 Del interact with response to bucindolol in terms of its efficacy in preventing ventricular arrhythmias in heart failure patients(53); this morbidity response to bucindolol is similar to the abovementioned mortality response when using the same SNP combinations. Another important issue that is often overlooked in heart failure pharmacogenomic studies involves the impact of other comorbidities. This issue has been recently explored as well. In a substudy of BEST, atrial fibrillation status did not affect response to bucindolol. β_1 Arg389 homozygote patients, but not β_1 Gly389 carriers, had reduced death and hospitalization from bucindolol; which confirms the pharmacogenomic association discovered in the full BEST genetic population. (54) On the contrary, atrial fibrillation history impacted genetic response to β blockers in a population of elderly patients (age > 65) with heart failure. (55) Patients who were β_1 Arg389 homozygotes and also suffered from atrial fibrillation had blunted heart rate reduction from carvedilol, but not bisoprolol; no attenuation in response to therapy was seen with patients in normal sinus rhythm regardless of β blocker or genotype (55) demonstrating that comorbidities may interact with pharmacogenetic associations. Indeed β blocker response to adrenergic polymorphisms in acute myocardial infarction patients conflict with those seen in heart failure patients.(56) In addition to

these studies which look at the impact of gene-gene interactions and comorbidities on pharmacogenomic associations, investigators continue to report data on individual polymorphisms. In a prospectively recruited population of heart failure patients, Talameh et al. showed that β_1 Ser49Ser homozygotes, but not Gly49 carriers, had enhanced survival response to β blocker therapy, using a larger population to corroborate previous findings that β blocker therapy has a greater influence on outcomes only in patients with Ser49Ser genotype. (31, 57) Another recent genetic substudy looked at the impact of genotype on dose response in heart failure patients receiving metoprolol or carvedilol. (58) β_1 Arg389 homozygote patients had increased mortality and worsened quality of life from lower β blocker doses, whereas dose did not affect outcomes in Gly389 carriers. (58) This contribution is significant, because few have assessed quality of life outcomes or gene-dose response in pharmacogenomic heart failure studies. (58) Collectively, these recent findings indicate that while progress in this field continues, more work is still needed before clinical utility of β blocker pharmacogenomics can be achieved. At the current rate, this goal does not seem achievable in the near future; a heightened effort is warranted.

Drugs targeting the renin-angiotensin-aldosterone system

The RAAS also plays a key role during the development and worsening of heart failure. (59) Several classes of agents for heart failure are available that work at different sites within the RAAS to suppress its effects. In particular, ACE inhibitors help to comprise the cornerstone of modern heart failure pharmacotherapy and have compelling evidence of survival benefit in multiple clinical trials. (60, 61) ACE inhibitors act by blocking ACE-mediated conversion of angiotensin I to angiotensin II, thereby reducing vasoconstriction, salt-retention, and hypertrophy that occur with this neurohormone. (62) Genetic modifiers of ACE inhibitor effectiveness have been long sought with some early success. An insertion (I)/deletion (D) polymorphism in *ACE* is responsible for half of the variance in systemic ACE levels; the D allele is associated with increased ACE. (63) The presence of this variant is also associated with heart failure incidence and severity. (64, 65) Additionally, past research has shown that this polymorphism alters response to ACE inhibitors. Cuoco et al. showed in a population of heart failure patients (90% receiving ACE inhibitors) that carriers of the D allele had significantly improved LVEF compared to wild-type patients after a mean follow-up of ~39 months. (66) In contrast, in a population of patients with left ventricular hypertrophy and hypertension receiving ACE inhibitors, patients with the D/D genotype had less improvement in hypertrophy. (67) In a third study, the presence of the D allele had no impact on mortality in diastolic heart failure patients who received ACE inhibitors. (68) This finding that does not concur with either of the above results, but does agree with an earlier study in systolic heart failure patients that also showed a diminished impact of the polymorphism on outcomes in patients receiving ACE inhibitor therapy, specifically at higher doses. (69)

Currently, the pharmacogenomic impact of *ACE* genetic variation in heart failure remains a controversial subject. In a recent genetic substudy of a randomized trial investigating the impact of pharmacist intervention on outcomes in heart failure patients (68% receiving ACE inhibitors and 13% receiving ARBs at baseline), the *ACE* I/D polymorphism was not found to be associated with the composite of ED visits and hospitalizations. (70) Further work, including the resolution of the aforementioned conflicting data, is necessary to elucidate the potential application of using of pharmacogenomic information to guide the therapeutic regimen of RAAS drugs in heart failure.

Other heart failure therapies

Guidelines recommend additional therapy as adjuncts to β blockers and ACE inhibitors for relieving symptoms, delaying the progression of cardiac dysfunction, and improving survival in heart failure patients. (7, 8) Among others, adjunct therapies with the most promising pharmacogenetic evidence are digoxin and loop diuretics.

It is fairly well established that digoxin reduces symptoms of heart failure and hospitalizations. (10) Digoxin has been used for centuries in heart failure and continues to be recommended in this population, but only at doses that correlate with relatively low serum levels due to increased mortality at higher levels. (7, 71) Given this narrow therapeutic range, factors which impact digoxin concentration may have important clinical implications. P-glycoprotein which is coded by *ABCB1* plays a role in digoxin elimination.(72) The TTT haplotype is a combination of three SNPs (the substitution of thymine at positions 1236, 2677, and 3435) in *ABCB1* that are highly linked and have been found to be associated with digoxin serum levels. (73) In particular, a 2008 study reported that the TTT haplotype was associated with increased digoxin levels in a population of elderly Caucasian patients receiving digoxin. (73) This contrasts an earlier study that evaluated this association in a small population of heart failure patients did not find a significant *ABCB1*effect on digoxin levels, (74) suggesting that further work investigating the pharmacogenetics of digoxin is needed. This area continues to be investigated; a recent study confirms that the *ABCB1* TTT haplotype may be predictive of elevated digoxin concentrations in patients receiving this medication, especially in females. (75) However, similar to the 2008 digoxin report mentioned, this 2012 study did not include a population of exclusively heart failure patients. The negative finding in heart failure patients hint that perhaps clinical or

other factors related to the disease state may override any genetic association altering digoxin response. Validation in a larger independent population is necessary to establish if there is a genetic link to digoxin levels and clinical response in heart failure patients receiving digoxin.

Loop diuretics, similar to digoxin, have not been found to have a mortality benefit but are the most common agents used for symptomatic relief due to sodium and water retention. They act by inhibiting sodium-potassium-chloride luminal transporters in the loop of Henle causing an attenuation of the reabsorption of sodium and water. (76) Recently a small study in healthy volunteers suggests that genetics may play a clinically-relevant role in response to loop diuretics. (77) Polymorphisms in *GNB2*, *ANP*, *ACE*, and *ADD1* impacted the excretion amounts of sodium chloride, potassium, and calcium. (77) Similar to the pharmacogenetics of digoxin, further work including confirmation in heart failure patients and a link to clinical efficacy is a necessary fundamental to understand if clinical application is possible.

Future prospects for pharmacogenomics

Over the past 15 years the field of pharmacogenetics has spread to include therapy for heart failure. Since the earliest periods of discovery, β blocker pharmacogenomics has been the most heavily explored, however response to other heart failure therapies also have shown the potential to be impacted by genotype. Taken together, the knowledge base summarized above demonstrates that genetic information does have the potential to guide therapeutic regimens for patients with heart failure and to improve outcomes. Despite this wealth of investigation, however, the pharmacogenomics of heart failure therapies still have not reached clinical utility. Additional steps are needed before this can be realized.

First, clarifying the current areas of inconsistency between gene-drug response associations should be a high priority. These inconsistencies suggest that complex genetic and environmental factors play a role. There needs to be a continued focus on the creation of 'polygenic profiles' which serve as novel biomarkers for the response to heart failure medications and allows for the identification of 'full', 'intermediate', and 'non-' responder subsets. Additionally the consideration of comorbidities and other clinical factors are beginning to show utility in predicting which subsets of the heart failure population would respond best to certain agents; these results require further exploration.

Secondly, much emphasis has been placed on genes related to the adrenergic system as expected considering its great promise in predicting response to β blockers in clinical practice. Nonetheless, more attention needs to be placed on emerging pharmacogenetic biomarkers. In addition to the aforementioned pharmacogenetic findings that have been investigated in the past couple years involving ACE inhibitors, digoxin, and loop diuretics, novel genetic biomarkers in

the early phases of discovery have potential to determine drug response in the heart failure population. For example, a recent study has shown that variation in genes coding for matrix metalloproteinases may interact with response to therapies altering the risk of heart failure development in hypertension patients. (78) Furthermore, novel genetic biomarkers have the potential to predict response to heart failure therapies beyond pharmacological agents. De Maria et al. recently found that among heart failure patients receiving CRT, those who did not achieve clinically significant reverse remodeling were more likely to have the *NR3C2* minor C allele (rs5522 C/T) compared to patients who achieved reverse remodeling. (79) These data, of course require validation, but overall, support the potential of emerging genetic predictors of response to both pharmacological and non-pharmacological treatment in the early development as well as the advanced progression of heart failure.

Another important step is the continued and expanded use of genetic analyses of heart failure randomized clinical trials (Table). These datasets serve as critical platforms to determine pharmacogenetic associations because they can supply large cohorts in which the impact of the therapy-gene interaction on outcomes can be most clearly demonstrated. Although genetic substudies are limited when the initial intervention has already become standard of care since this may preclude replication in an independent population, alternates for the validation of pharmacogenomic findings exist; these are beyond the scope of this review and are reviewed in great depth elsewhere. (80) Furthermore, these types of studies are ideal for emerging therapies where they may aid in identifying the best responders to a therapy and reduce the probability of drug development failure in clinical trials. As a result of genetic substudies of BEST that have provided a wealth of knowledge, bucindolol may be the most auspicious candidate to be approved as a heart failure therapy that incorporates a pharmacogenomic-guided strategy. While

genetic information is now routinely being collected in clinical trials worldwide (81, 82), it is not always being actively utilized or opened for exploration, squandering many great opportunities.

Ultimately randomized clinical studies of pharmacogenomic-guided therapy would be needed to conclusively establish the utility of a pharmacogenomic approach in a clinical setting. The authors feel that one pharmacogenetic clinical trial success in heart failure would invigorate interest and open the flood gates for future studies. On the other hand, while randomized clinical trials represent the definitive proof, it is not a practical endeavor for each genetic variant and drug of potential interest. Indeed efforts to incorporate pharmacogenomic-guided decision making at the bedside at progressive institutions are taking place without the evidence of randomized, prospective trials.(83-85) The medical and scientific community still needs to grapple with and decide on the level of evidence required for universal integration of heart failure pharmacogenomics in clinical practice.

In conclusion, progress in the field of heart failure pharmacogenetics continues, but further research is necessary. A collective and concerted effort between basic, clinical, and translational researchers is merited to achieve its incorporation into guidelines as a standard of clinical care.

Tables

Table B.1 Recent heart failure pharmacogenomic findings from clinical trials (2012-present).

Gene (genotype)	Parent trial	Drug	Primary endpoint	Association
ADRA2C (322–325), *ADRB1* (Arg389Gly)	BEST* (1)	Bucindolol	ACM, ACM or transplant	Carriers of Gly389 and Del in combination had complete loss of bucindolol response in HF patients
ADRA2C (322–325), *ADRB1* (Arg389Gly)	BEST* (2)	Bucindolol	Incidence of VT/VF	Carriers of Gly389 and Del in combination had complete loss of bucindolol response in HF patients
ADRB1 (Arg389Gly)	CIBIS-ELD† (3)	Bisoprolol, carvedilol	HR	Arg389 homozygotes had reduced carvedilol response in elderly (age > 65) HF patients with AF
ADRB1 (Arg389Gly)	BEST* (4)	Bucindolol	ACM or HFH, CVM or CVH, HR	Arg389 homozygotes had reduced bucindolol response in HF patients with AF (for all endpoints but HR)
ADRB1 (Arg389Gly)	HF-ACTION†† (5)	Any HF β blocker	ACM or ACH	Arg389 homozygotes had reduced β blocker response (low doses) in HF patients

*Efficacy of bucindolol versus placebo in patients with heart failure
†Efficacy and safety of carvedilol versus bisoprolol in elderly patients with heart failure
††Efficacy of exercise training versus usual care in patients with heart failure
ACM, all-cause mortality; ACH, all-cause hospitalization; AF, atrial fibrillation; CVH, cardiovascular hospitalization; CVM, cardiovascular mortality; HF, heart failure; HFH, heart failure hospitalization; HR, heart rate; VF, ventricular fibrillation; VT, ventricular tachycardia

REFERENCES

(1) Go, A.S. *et al.* Heart disease and stroke statistics--2013 update: a report from the American Heart Association. *Circulation* 127, e6-e245 (2013).

(2) Kemp, C.D. & Conte, J.V. The pathophysiology of heart failure. *Cardiovasc Pathol* 21, 365-71 (2012).

(3) Watson, R.D., Gibbs, C.R. & Lip, G.Y. ABC of heart failure. Clinical features and complications. *BMJ* 320, 236-9 (2000).

(4) Effects of enalapril on mortality in severe congestive heart failure. Results of the Cooperative North Scandinavian Enalapril Survival Study (CONSENSUS). The CONSENSUS Trial Study Group. *N Engl J Med* 316, 1429-35 (1987).

(5) Hjalmarson, A. *et al.* Effect of metoprolol CR/XL in chronic heart failure: Metoprolol CR/XL Randomised Intervention Trial in Congestive Heart Failure (MERIT-HF). *Lancet* 353, 2001-7 (1999).

(6) Zannad, F. *et al.* Eplerenone in patients with systolic heart failure and mild symptoms. *N Engl J Med* 364, 11-21 (2011).

(7) Heart Failure Society of America *et al.* Executive Summary: HFSA 2010 Comprehensive Heart Failure Practice Guideline. *J Card Fail* 16, 475-539 (2010).

(8) Yancy, C.W. *et al.* 2013 ACCF/AHA Guideline for the Management of Heart Failure: A Report of the American College of Cardiology Foundation/American Heart Association Task Force on Practice Guidelines. *J Am Coll Cardiol*, (2013).

(9) Chiong, J.R. & Cheung, R.J. Loop diuretic therapy in heart failure: the need for solid evidence on a fluid issue. *Clin Cardiol* 33, 345-52 (2010).

(10) Digitalis Investigation Group. The effect of digoxin on mortality and morbidity in patients with heart failure. *N Engl J Med* 336, 525-33 (1997).

(11) Flesch, M. & Erdmann, E. The problem of polypharmacy in heart failure. *Curr Cardiol Rep* 8, 217-25 (2006).

(12) van Campen, L.C., Visser, F.C. & Visser, C.A. Ejection fraction improvement by beta-blocker treatment in patients with heart failure: an analysis of studies published in the literature. *J Cardiovasc Pharmacol* 32 Suppl 1, S31-5 (1998).

(13) Talameh, J.A., McLeod, H.L., Adams Jr, K.F. & Patterson, J.H. Genetic tailoring of pharmacotherapy in heart failure: optimize the old, while we wait for something new. *J Card Fail* 18, 338-49 (2012).

(14) Talameh, J.A. & Lanfear, D.E. Pharmacogenetics in chronic heart failure: new developments and current challenges. *Curr Heart Fail Rep* 9, 23-32 (2012).

(15) Johnson, J.A. & Liggett, S.B. Cardiovascular pharmacogenomics of adrenergic receptor signaling: clinical implications and future directions. *Clin Pharmacol Ther* 89, 366-78 (2011).

(16) Dorn, G.W. Adrenergic signaling polymorphisms and their impact on cardiovascular disease. *Physiol Rev* 90, 1013-62 (2010).

(17) Satwani, S., Dec, G.W. & Narula, J. Beta-adrenergic blockers in heart failure: review of mechanisms of action and clinical outcomes. *J Cardiovasc Pharmacol Ther* 9, 243-55 (2004).

(18) Packer, M. *et al.* Effect of carvedilol on the morbidity of patients with severe chronic heart failure: results of the carvedilol prospective randomized cumulative survival (COPERNICUS) study. *Circulation* 106, 2194-9 (2002).

(19) Packer, M. *et al.* The effect of carvedilol on morbidity and mortality in patients with chronic heart failure. U.S. Carvedilol Heart Failure Study Group. *N Engl J Med* 334, 1349-55 (1996).

(20) The Cardiac Insufficiency Bisoprolol Study II (CIBIS-II): a randomised trial. *Lancet* 353, 9-13 (1999).

(21) Domanski, M.J. *et al.* A comparative analysis of the results from 4 trials of beta-blocker therapy for heart failure: BEST, CIBIS-II, MERIT-HF, and COPERNICUS. *J Card Fail* 9, 354-63 (2003).

(22) Lanfear, D.E. *et al.* Association of β-blocker exposure with outcomes in heart failure differs between African American and white patients. *Circ Heart Fail*, (2012).

(23) Mason, D.A., Moore, J.D., Green, S.A. & Liggett, S.B. A gain-of-function polymorphism in a G-protein coupling domain of the human beta1-adrenergic receptor. *J Biol Chem* 274, 12670-4 (1999).

(24) Bengtsson, K. *et al.* Polymorphism in the beta(1)-adrenergic receptor gene and hypertension. *Circulation* 104, 187-90 (2001).

(25) Liggett, S.B. *et al.* A polymorphism within a conserved beta(1)-adrenergic receptor motif alters cardiac function and beta-blocker response in human heart failure. *Proc Natl Acad Sci U S A* 103, 11288-93 (2006).

(26) Beta-Blocker Evaluation of Survival Trial Investigators. A trial of the beta-blocker bucindolol in patients with advanced chronic heart failure. *N Engl J Med* 344, 1659-67 (2001).

(27) Sehnert, A.J. *et al.* Lack of association between adrenergic receptor genotypes and survival in heart failure patients treated with carvedilol or metoprolol. *J Am Coll Cardiol* 52, 644-51 (2008).

(28) Yancy, C.W. *et al.* Race and the response to adrenergic blockade with carvedilol in patients with chronic heart failure. *N Engl J Med* 344, 1358-65 (2001).

(29) Borjesson, M., Magnusson, Y., Hjalmarson, A. & Andersson, B. A novel polymorphism in the gene coding for the beta(1)-adrenergic receptor associated with survival in patients with heart failure. *Eur Heart J* 21, 1853-8 (2000).

(30) Levin, M.C., Marullo, S., Muntaner, O., Andersson, B. & Magnusson, Y. The myocardium-protective Gly-49 variant of the beta 1-adrenergic receptor exhibits constitutive activity and increased desensitization and down-regulation. *J Biol Chem* 277, 30429-35 (2002).

(31) Magnusson, Y. *et al.* Ser49Gly of beta1-adrenergic receptor is associated with effective beta-blocker dose in dilated cardiomyopathy. *Clin Pharmacol Ther* 78, 221-31 (2005).

(32) Molenaar, P., Christ, T., Ravens, U. & Kaumann, A. Carvedilol blocks beta2- more than beta1-adrenoceptors in human heart. *Cardiovasc Res* 69, 128-39 (2006).

(33) Poole-Wilson, P.A. *et al.* Comparison of carvedilol and metoprolol on clinical outcomes in patients with chronic heart failure in the Carvedilol Or Metoprolol European Trial (COMET): randomised controlled trial. *Lancet* 362, 7-13 (2003).

(34) Kaye, D.M., Smirk, B., Williams, C., Jennings, G., Esler, M. & Holst, D. Beta-adrenoceptor genotype influences the response to carvedilol in patients with congestive heart failure. *Pharmacogenetics* 13, 379-82 (2003).

(35) Metra, M. *et al.* Role of beta-adrenergic receptor gene polymorphisms in the long-term effects of beta-blockade with carvedilol in patients with chronic heart failure. *Cardiovasc Drugs Ther* 24, 49-60 (2010).

(36) Lanfear, D.E., Jones, P.G., Marsh, S., Cresci, S., McLeod, H.L. & Spertus, J.A. Beta2-adrenergic receptor genotype and survival among patients receiving beta-blocker therapy after an acute coronary syndrome. *JAMA* 294, 1526-33 (2005).

(37) de Groote, P. *et al.* Association between beta-1 and beta-2 adrenergic receptor gene polymorphisms and the response to beta-blockade in patients with stable congestive heart failure. *Pharmacogenet Genomics* 15, 137-42 (2005).

(38) Shin, J. *et al.* Relation of beta(2)-adrenoceptor haplotype to risk of death and heart transplantation in patients with heart failure. *Am J Cardiol* 99, 250-5 (2007).

(39) Hoehe, M.R. *et al.* Genetic mapping of adrenergic receptor genes in humans. *J Mol Med (Berl)* 73, 299-306 (1995).

(40) Hein, L., Altman, J.D. & Kobilka, B.K. Two functionally distinct alpha2-adrenergic receptors regulate sympathetic neurotransmission. *Nature* 402, 181-4 (1999).

(41) Small, K.M., Wagoner, L.E., Levin, A.M., Kardia, S.L.R. & Liggett, S.B. Synergistic polymorphisms of beta1- and alpha2C-adrenergic receptors and the risk of congestive heart failure. *N Engl J Med* 347, 1135-42 (2002).

(42) Bristow, M.R. *et al.* An alpha2C-adrenergic receptor polymorphism alters the norepinephrine-lowering effects and therapeutic response of the beta-blocker bucindolol in chronic heart failure. *Circ Heart Fail* 3, 21-8 (2010).

(43) Liggett, S.B. *et al.* A GRK5 polymorphism that inhibits beta-adrenergic receptor signaling is protective in heart failure. *Nat Med* 14, 510-7 (2008).

(44) Cresci, S. *et al.* Clinical and genetic modifiers of long-term survival in heart failure. *J Am Coll Cardiol* 54, 432-44 (2009).

(45) Chen, L. *et al.* Arg389Gly-beta1-adrenergic receptors determine improvement in left ventricular systolic function in nonischemic cardiomyopathy patients with heart failure after chronic treatment with carvedilol. *Pharmacogenet Genomics* 17, (2007).

(46) Mialet-Perez, J. *et al.* Beta 1-adrenergic receptor polymorphisms confer differential function and predisposition to heart failure. *Nat Med* 9, 1300-5 (2003).

(47) Terra, S.G. *et al.* Beta1-adrenergic receptor polymorphisms and left ventricular remodeling changes in response to beta-blocker therapy. *Pharmacogenet Genomics* 15, (2005).

(48) White, H.L. *et al.* An evaluation of the beta-1 adrenergic receptor Arg389Gly polymorphism in individuals with heart failure: a MERIT-HF sub-study. *Eur J Heart Fail* 5, 463-8 (2003).

(49) de Groote, P. *et al.* The impact of beta-adrenoreceptor gene polymorphisms on survival in patients with congestive heart failure. *Eur J Heart Fail* 7, 966-73 (2005).

(50) Taylor, M.R.G. Pharmacogenetics of the human beta-adrenergic receptors. *Pharmacogenomics J* 7, 29-37 (2006).

(51) Petersen, M. *et al.* Association of beta-adrenergic receptor polymorphisms and mortality in carvedilol-treated chronic heart-failure patients. *Br J Clin Pharmacol* 71, 556-65 (2011).

(52) O'Connor, C.M. *et al.* Combinatorial pharmacogenetic interactions of bucindolol and β1, α2C adrenergic receptor polymorphisms. *PLoS One* 7, e44324 (2012).

(53) Aleong, R.G., Sauer, W.H., Robertson, A.D., Liggett, S.B. & Bristow, M.R. Adrenergic receptor polymorphisms and prevention of ventricular arrhythmias with bucindolol in patients with chronic heart failure. *Circ Arrhythm Electrophysiol* 6, 137-43 (2013).

(54) Kao, D.P. *et al.* Effect of bucindolol on heart failure outcomes and heart rate response in patients with reduced ejection fraction heart failure and atrial fibrillation. *Eur J Heart Fail* 15, 324-33 (2013).

(55) Rau, T. *et al.* Impact of the β1-adrenoceptor Arg389Gly polymorphism on heart-rate responses to bisoprolol and carvedilol in heart-failure patients. *Clin Pharmacol Ther* 92, 21-8 (2012).

(56) Cresci, S. *et al.* Adrenergic-pathway gene variants influence beta-blocker-related outcomes after acute coronary syndrome in a race-specific manner. *J Am Coll Cardiol* 60, 898-907 (2012).

(57) Talameh, J. *et al.* Beta-1 adrenergic receptor genotype Ser49Gly is associated with beta-blocker survival benefit in patients with heart failure [abstract]. *J Am Coll Cardiol* 59, E861-E (2012).

(58) Fiuzat, M. *et al.* Association between adrenergic receptor genotypes and beta-blocker dose in heart failure patients: analysis from the HF-ACTION DNA substudy. *Eur J Heart Fail* 15, 258-66 (2013).

(59) Francis, G.S. & Tang, W.H. Pathophysiology of congestive heart failure. *Rev Cardiovasc Med* 4 Suppl 2, S14-20 (2003).

(60) Effect of enalapril on survival in patients with reduced left ventricular ejection fractions and congestive heart failure. The SOLVD Investigators. *N Engl J Med* 325, 293-302 (1991).

(61) Effects of enalapril on mortality in severe congestive heart failure. Results of the Cooperative North Scandinavian Enalapril Survival Study (CONSENSUS). The CONSENSUS Trial Study Group. *N Engl J Med* 316, 1429-35 (1987).

(62) Brown, N.J. & Vaughan, D.E. Angiotensin-converting enzyme inhibitors. *Circulation* 97, 1411-20 (1998).

(63) Rigat, B., Hubert, C., Alhenc-Gelas, F., Cambien, F., Corvol, P. & Soubrier, F. An insertion/deletion polymorphism in the angiotensin I-converting enzyme gene accounting for half the variance of serum enzyme levels. *J Clin Invest* 86, 1343-6 (1990).

(64) Schut, A.F.C. *et al.* Angiotensin converting enzyme insertion/deletion polymorphism and the risk of heart failure in hypertensive subjects. *Eur Heart J* 25, 2143-8 (2004).

(65) Fatini, C. *et al.* ACE insertion/deletion, but not -240A>T polymorphism, modulates the severity in heart failure. *J Investig Med* 56, 1004-10 (2008).

(66) Cuoco, M.A., Pereira, A.C., Mota Gde, F., Krieger, J.E. & Mansur, A.J. Genetic polymorphism, medical therapy and sequential cardiac function in patients with heart failure. *Arq Bras Cardiol* 90, 252-6 (2008).

(67) Kohno, M. *et al.* Association between angiotensin-converting enzyme gene polymorphisms and regression of left ventricular hypertrophy in patients treated with angiotensin-converting enzyme inhibitors. *Am J Med* 106, 544-9 (1999).

(68) Wu, C.K. *et al.* Demonstrating the pharmacogenetic effects of angiotensin-converting enzyme inhibitors on long-term prognosis of diastolic heart failure. *Pharmacogenomics J* 10, 46-53 (2009).

(69) McNamara, D.M. *et al.* Pharmacogenetic interactions between angiotensin-converting enzyme inhibitor therapy and the angiotensin-converting enzyme deletion polymorphism in patients with congestive heart failure. *J Am Coll Cardiol* 44, 2019-26 (2004).

(70) Kim, K.M. *et al.* Pharmacogenetics and healthcare outcomes in patients with chronic heart failure. *Eur J Clin Pharmacol* 68, 1483-91 (2012).

(71) Rathore, S.S., Curtis, J.P., Wang, Y., Bristow, M.R. & Krumholz, H.M. Association of serum digoxin concentration and outcomes in patients with heart failure. *JAMA* 289, 871-8 (2003).

(72) Gozalpour, E., Wittgen, H.G., van den Heuvel, J.J., Greupink, R., Russel, F.G. & Koenderink, J.B. Interaction of digitalis-like compounds with p-glycoprotein. *Toxicol Sci* 131, 502-11 (2013).

(73) Aarnoudse, A.J. *et al.* Common ATP-binding cassette B1 variants are associated with increased digoxin serum concentration. *Pharmacogenet Genomics* 18, 299-305 (2008).

(74) Kurzawski, M., Bartnicka, L., Florczak, M., Gornik, W. & Drozdzik, M. Impact of ABCB1 (MDR1) gene polymorphism and P-glycoprotein inhibitors on digoxin serum concentration in congestive heart failure patients. *Pharmacol Rep* 59, 107-11 (2007).

(75) Neuvonen, A., Palo, J. & Sajantila, A. Post-mortem ABCB1 genotyping reveals an elevated toxicity for female digoxin users. *Int J Legal Med* 125, 265-9 (2011).

(76) Brater, D.C. Diuretic therapy. *N Engl J Med* 339, 387-95 (1998).

(77) Vormfelde, S.V. & Brockmoller, J. The genetics of loop diuretic effects. *Pharmacogenomics J* 12, 45-53 (2012).

(78) Tanner, R.M. *et al.* Pharmacogenetic associations of MMP9 and MMP12 variants with cardiovascular disease in patients with hypertension. *PLoS One* 6, e23609 (2011).

(79) De Maria, R. *et al.* Genetic variants of the renin-angiotensin-aldosterone system and reverse remodeling after cardiac resynchronization therapy. *J Card Fail* 18, 762-8 (2012).

(80) Aslibekyan, S., Claas, S.A. & Arnett, D.K. To replicate or not to replicate: the case of pharmacogenetic studies: Establishing validity of pharmacogenomic findings: from replication to triangulation. *Circ Cardiovasc Genet* 6, 409-12 (2013).

(81) Armstrong, P.W. & Rouleau, J.L. A Canadian context for the Acute Study of Clinical Effectiveness of Nesiritide and Decompensated Heart Failure (ASCEND-HF) trial. *Can J Cardiol* 24 Suppl B, 30B-2B (2008).

(82) Godard, B., Schmidtke, J., Cassiman, J.J. & Ayme, S. Data storage and DNA banking for biomedical research: informed consent, confidentiality, quality issues, ownership, return of benefits. A professional perspective. *Eur J Hum Genet* 11, S88-S122 (2003).

(83) Crews, K.R. *et al.* Development and implementation of a pharmacist-managed clinical pharmacogenetics service. *Am J Health Syst Pharm* 68, 143-50 (2011).

(84) Johnson, J.A., Burkley, B.M., Langaee, T.Y., Clare-Salzler, M.J., Klein, T.E. & Altman, R.B. Implementing personalized medicine: development of a cost-effective customized pharmacogenetics genotyping array. *Clin Pharmacol Ther* 92, 437-9 (2012).

(85) Peterson, J.F. *et al.* Electronic health record design and implementation for pharmacogenomics: a local perspective. *Genet Med* 15, 833-41 (2013).

APPENDIX B - EPOXYEICOSATRIENOIC ACIDS AND CARDIOPROTECTION: THE ROAD TO TRANSLATION[2]

Introduction

Despite major advances in evidence-based medical therapies, cardiovascular disease (CVD) remains the leading cause of morbidity and mortality worldwide. In the western world, CVD has been the leading cause of death for almost a century and its prevalence is expected to continue to rise tremendously (1, 2). Most notably, acute myocardial infarction (AMI) events, complications of CVD, are a primary source of the public health burden associated with this illness (1, 2). AMI is typically characterized by rupture of an atheromatous plaque resulting in an intracoronary thrombus and myocardial ischemia (3). The restoration of blood flow, termed ischemia-reperfusion (IR), is imperative to prevent further myocardial cell necrosis. Paradoxically, however, IR also triggers injury to the myocardium (4). Consequently, identification and characterization of the key pathways that regulate IR injury will facilitate the development of novel therapeutic strategies that mitigate IR injury and its pathological consequences, thereby reducing the risk of adverse outcomes following AMI.

It is now well-established that cytochrome P450 (CYP)-derived epoxyeicosatrienoic acids (EETs), endogenous lipid metabolites of arachidonic acid, elicit potent anti-inflammatory, vasodilatory, fibrinolytic, anti-apoptotic, pro-angiogenic, and smooth muscle cell anti-migratory effects in the cardiovascular system (5, 6). Furthermore, accumulating preclinical evidence from *in vitro, ex vivo,* and *in vivo* models of AMI demonstrate that EETs directly protect the myocardium following ischemia via a variety of mechanisms (7-9). Additionally, associations

[2]Oni-Orisan, A., Alsaleh, N., Lee, C.R. & Seubert, J.M. Epoxyeicosatrienoic acids and cardioprotection: the road to translation. *J Mol Cell Cardiol* 74, 199-208 (2014).

between genetic polymorphisms in the CYP epoxygenase pathway and the risk of developing CVD have been reported in humans (10). Therefore, therapeutic interventions that promote the cardioprotective effects of EETs offer considerable promise as a novel therapeutic strategy to reduce sequelae following AMI; however, key questions remain to be addressed prior to translation of EET-promoting strategies into successful proof-of-concept phase I and II clinical trials. The acute and chronic cardioprotective effects of EETs and underlying mechanisms have not been fully characterized. Furthermore, the association between genetic polymorphisms in the CYP epoxygenase-EET pathway and poor prognosis has not been studied in patients suffering from an AMI. These are currently active areas on investigation.

This review aims to 1) outline the known cardioprotective effects of EETs and underlying mechanisms with a particular focus on myocardial IR injury, 2) describe studies in human cohorts that demonstrate a relationship between EETs and associated pathways with the risk of coronary artery disease (CAD), and 3) discuss preclinical and clinical areas that require further investigation in order to increase the probability of successfully translating this rapidly emerging body of evidence into a clinically applicable therapeutic strategy for AMI.

The CYP epoxygenase pathway

Arachidonic acid is metabolized by CYP epoxygenase enzymes to form bioactive EETs (Fig. 1) (11). CYP2J and CYP2C epoxygenases are the primary source of all four EET regioisomers (5,6-, 8,9-, 11,12-, and 14,15- EETs) (12). Each regioisomer is composed of 2 different stereoisomers (R,S or S,R configuration) (12). CYP2J2, CYP2C8 and CYP2C9 are extensively and constitutively expressed in human heart tissue (13, 14). The predominant fate of EETs is through rapid metabolism by soluble epoxide hydrolase (sEH) into dihydroxyeicosatrienoic acids (DHETs), which generally have less biological activity (6, 7). *EPHX2* codes for human sEH (15) and is expressed in a multitude of cell types (16). Importantly, sEH is highly expressed in the myocardium (16).

In parallel, arachidonic acid is also metabolized by cyclooxygenase, lipoxygenase and CYP hydroxylase enzymes to produce biologically active metabolites that play a functional role in myocardial IR injury (17-19). In addition to arachidonic acid-derived products, other members of the n-6 polyunsaturated fatty acid (PUFA) family (most notably linoleic acid) and of the n-3 PUFA family such as docosahexaenoic acid (DHA) and eicosapentaenoic acid (EPA) play a role in cardiovascular disease (20). CYP-dependent epoxy-derivatives of these PUFAs are also potent biological mediators in the cardiovascular system and may be subsequently metabolized into vicinal diols by epoxide hydrolases (12, 21, 22). Although these emerging data are beyond the scope of this review, we summarize select examples from the literature throughout the review that will stimulate future research in this area.

A variety of pharmacologic and genetic strategies have been utilized to characterize the functional role of EETs in preclinical studies. Administration of exogenous EETs and synthetic

EET analogs has been utilized as agonists to characterize the direct cardioprotective effects of EETs (23). The synthetic analog 14,15-epoxyeicosa-5(Z)-enoic acid (14,15-EEZE) has the unique property of exhibiting putative EET receptor antagonist-like activity (24), and consequently has also been very useful to study EET action. An alternative approach is to target enzymes involved in the biosynthesis (CYP epoxygenases) and metabolism (sEH) of endogenous EETs. Notably, cardiomyocyte-specific CYP2J2 overexpression (α-MHC-CYP2J2-transgenic [Tr] mice), global disruption of *Ephx2* (*Ephx2*$^{-/-}$ mice), and pharmacologic inhibition of sEH have each been utilized to increase EETs *in vivo* and study the contribution of the CYP epoxygenase-EET pathway to cardioprotection (25-27).

Acute EET effects following IR

Accumulating evidence, across multiple laboratories and species, has demonstrated that EETs abrogate a variety of acute pathophysiological responses following myocardial IR, including the reduction of left ventricular infarct size and improved recovery of left ventricular function (Table 1) (8). Furthermore, as outlined in more detail below, EETs elicit these cardioprotective effects through multiple mechanisms, namely through activation of prosurvival signaling, attenuation of apoptosis, and promotion of mitochondrial protection acutely following IR (Table 1, Fig. 2B).

Promotion of prosurvival signaling

Numerous signal-transduction pathways are activated following IR, dictate the extent of cell survival following myocardial injury, and thus are pro-survival therapeutic targets for cardioprotection (28, 29). Our group has shown that α-MHC-CYP2J2-Tr mice exhibit increased myocardial DHET biosynthesis (the stable metabolite of EETs) and improved left ventricular developed pressure (LVDP) following 20 minutes of ischemia and 40 minutes of reperfusion compared to wild-type littermate controls (30). This cardioprotection was thought to be mediated by putative mitochondrial K_{ATP} (mitoK_{ATP}) channel-derived and p42/p44 mitogen-activated protein kinase (p42/p44 MAPK) prosurvival signaling (30). The exogenous administration of 11,12-EET produced a similar recovery of ventricular function (30). Further evidence of improved recovery of LVDP following IR was observed in *Ephx2*$^{-/-}$ mice, which was reversed by 14,15-EEZE implicating that the effect was promulgated directly by EETs. Infarct size was also reduced in these mice (31). These actions were mediated via activation of sarcolemma K_{ATP}

(sarcK_{ATP}) and mitoK_{ATP} channels as well as phosphatidylinositol-3 kinase (PI3K) signaling (31). Results in canine and rat models of AMI have confirmed the role of K_{ATP} channels in EET-mediated cardioprotection (32-34).

Further research has brought the role of prosurvival signaling in EET-mediated cardioprotection to a more detailed level of understanding. Evidence suggests the timing of EET administration relative to IR injury is important and that EET-mediated cardioprotection is regulated by the activation of sarcK_{ATP} channels only if EETs are administered during the ischemic period (35). Selective inhibition of PI3K was found to attenuate improved LVDP and infarct size from an agent that possesses both EET-mimetic and sEH inhibitory properties, implicating class-I isozymes of PI3K in EET-mediated cardioprotection (36). Moreover, phosphatidylinositol-3 kinase-alpha (PI3Kα) was reported to be the specific isoform within the class-I PI3K family that was implicated in EET-mediated protection (37). Interestingly, these effects occurred through a PI3Kα-dependent activation of sarcK_{ATP} channels (37). Results from another study conflict with this data by showing that EETs activate sarcK_{ATP} channels independent of PI3K-mediated pathways (38). Experimental factors such as species (rats versus mice), EET regioisomer (14,15-EETs versus 11,12 EETs), and inhibitor (wortmannin versus PI-103) may explain these discordant findings. Indeed, evidence from a study that improved LVDP following IR injury with 11,12-EET that was absent in 14,15-EET at the same dose suggests that the cardioprotective potency of EETs may vary by regioisomer (39). Studies have also implicated endothelial NO synthase (eNOS) (35), signal transducer and activator of transcription 3 (STAT3) (40), brain natriuretic peptide (BNP) (41), and opioid receptor (42) signaling in EET-mediated cardioprotection. Overall, work remains necessary to further delineate the relative

contribution of specific signaling pathways and regioisomers to the cardioprotective effects of EETs.

Attenuation of apoptosis

It is well-established that activation of apoptosis promotes infarct size and worsens recovery of cardiac function following IR injury (43). Importantly, EETs possess potent anti-apoptotic properties in cardiomyocytes. Cultured cells from neonatal rat hearts and a mouse atrial lineage (HL-1) that were pretreated with EETs had reduced expression of multiple markers of apoptosis and maintained rhythmic myocyte beating after 8 hours of hypoxia and 16 hours of reoxygenation (44). In a subsequent study, the anti-apoptotic properties of EETs were further demonstrated in isolated myocardium from patients with cardiovascular disease, highlighting the observation that cellular mechanisms of EET-mediated cardioprotection in rodents also occur in the human heart (38).

Preservation of mitochondrial function and structure

Mitochondria provide the primary source of energy that fuels the contractile apparatus and act as key regulators of cell survival and death (45). IR injury can cause significant mitochondrial damage resulting in cellular death and cardiac dysfunction (45). Specifically ischemia causes the mitochondrial permeability transition pore (mPTP), a non-specific pore in the inner membrane of mitochondria, to open allowing free passage of molecules <1.5 kDa (46). The accumulation of these molecules in the mitochondria due to prolonged pore opening results in mitochondrial dysfunction and integrity and eventually leads to irreversible cell death (46). Signal transduction pathways, including a large proportion of those mentioned previously that

are implicated in EET-mediated cardioprotection, converge onto the mPTP thereby promoting or suppressing its opening following cardiac injury (47). In addition, the mitochondrial membrane potential ($\Delta\Psi_m$), which reflects the electrochemical gradient important for ATP generation, influences mPTP opening: its depletion following cardiac injury enhances mPTP opening (46). Agents that prevent these processes have been found to reduce infarct size and improve recovery of cardiac function (43). Emerging evidence demonstrates that EETs possess potent protective effects directly limiting mitochondria damage. For example, hearts from α-MHC-CYP2J2-Tr mice had limited mitochondrial swelling and fragmentation following IR compared to hearts from wild-type littermate controls (48). Cell culture experiments demonstrated that exogenous administration of EETs slowed the loss of $\Delta\Psi_m$ and prevented opening of the mPTP following the induction of stress to cardiac cells; this was reversed by 14,15-EEZE (48, 49). And recent data show that EET-mediated protection of mitochondria involves regulating an autophagic response, which shifts the cell pathway in starved cardiac cells from death via apoptosis or necrosis toward survival, representing a novel prosurvival mechanism in cardiac cells (50). However, an important issue that remains unknown is how the EET protective signals reach the mitochondria and preserve its structure. One potential mechanism implicates caveolins (cardioprotective structural proteins) in the EET-mediated preservation of mitochondrial structural integrity following IR (51). In particular, compared to untreated wild-type mice, plasma membrane and mitochondria isolated from the hearts of *Ephx2*$^{-/-}$ and EET-treated wild-type mice exhibited an attenuated IR-induced loss of caveolin-1 (Cav-1), but not caveolin-3 (Cav-3) isoform expression (51). Altogether, these results underscore the important role of preserving mitochondrial function and architecture following IR injury.

Altogether, these preclinical findings in acute models of IR have made important contributions to the characterization of EET-mediated cardioprotection, confirming a direct protective effect of EETs on cardiomyocytes and offering mechanistic insight. It is worth reemphasizing that a structure-activity relationship exists with EETs based on the observations that 1) the endogenously formed EET regioisomers exert their biological effects at varying potencies, and 2) synthetic analogs of EETs agonize and antagonize their effects at varying degrees (52). This is the main reason why, although it remains to be discovered, at least one EET-specific receptor (whether at the cell surface or intracellularly) is widely believed to exist (9, 53). Thus, identification and characterization of an EET receptor would provide critical insight into the diverse biological effects of EETs, including cardioprotection, and drive future research and drug discovery.

Chronic EET effects following ischemia reperfusion

Following the acute recovery phases of an AMI, the infarcted and inflamed myocardium chronically promotes LV remodeling, which manifests as scar tissue formation (fibrosis), LV dysfunction, and ultimately heart failure (54, 55). Fibrosis following AMI leads to electrical conduction abnormalities, which predispose patients to ventricular arrhythmias and higher risk of sudden cardiac death (56). Thus, this chronic maladaptive remodeling process is associated with worsened prognosis following AMI (57).

Chronic preclinical models of ischemic cardiomyopathy have recently been utilized to determine the impact of increasing EETs on longer term endpoints following AMI. In a mouse model of post-AMI heart failure, where the left anterior descending (LAD) coronary artery was occluded for 45 minutes followed by 3 weeks of reperfusion, administration of a sEH inhibitor reduced collagen deposition (fibrosis), reduced arrhythmia, and improved LV fractional shortening (systolic function) (58). However, it is important to note that the sEH inhibitor was administered three days before the induction of AMI; thus it is unknown whether the observed attenuation of cardiac remodeling was derived independently of infarct size reduction and the other beneficial actions of EETs that occur acutely following IR. In a clinical situation, a pharmacological agent indicated to reduce IR injury would most likely be administered during or after, and not prior to, the ischemic phase. Three recent studies have provided insight into this important issue. In one study, a sEH inhibitor was administered immediately following permanent LAD occlusion in rats; pharmacologic suppression of sEH attenuated LV ejection fraction (systolic function) independent of collagen deposition reduction in the infarct zone following 5 weeks of occlusion (59). A second study by a separate group utilized a more chronic

model of heart failure in rats (permanent LAD ligation for 50 days), but administered a sEH inhibitor at distinct time points after the initial phase of infarct healing: 8 days (42-day sEH inhibitor treatment) or 47 days (3-day inhibitor treatment) following LAD occlusion (60). It was discovered that both regimens improved LV ejection fraction at 50 days; however, only long term treatment elicited an improvement in LV end-diastolic pressure (diastolic function) (60). A third study in mice utilizing a model of IR injury demonstrated that sEH inhibition administered a week following AMI was still able to attenuate chronic collagen deposition measured three weeks later (61). Collectively, these studies demonstrate that sEH inhibition improves maladaptive chronic ventricular remodeling independent of the aforementioned acute reductions in infarct size elicited by EETs. It is also important to note that these effects were not reported to be related to blood pressure reduction, suggesting that direct action on cardiomyocytes is a likely mechanism of cardioprotection. More rigorous investigation, including the use of other pharmacologic and genetic tools that promote or depress the effects of EETs, is warranted to further define the contribution of sEH and EETs to the pathogenesis and progression of ischemic cardiomyopathy.

Chronic EET effects in non-ischemic cardiomyopathy

Non-ischemic cardiomyopathy is caused by variety of factors unrelated to an AMI (i.e., longstanding hypertension) and is a source of devastating consequences including arrhythmia, left ventricular dysfunction, heart failure, and mortality (62). Importantly, EETs have been found to be cardioprotective in rodent models of non-ischemic cardiomyopathy. Furthermore, in the majority of models, these protective effects were not reported to be dependent on blood pressure lowering.

Inhibition of sEH was found to reverse transverse aortic constriction (TAC)-induced cardiac hypertrophy (63). Furthermore, angiotensin II, a potent driver of cardiac hypertrophy, upregulates sEH expression in cardiomyocytes and pharmacologic sEH inhibition attenuates angiotensin II-induced cardiac hypertrophy (64). CYP2J overexpression also reversed decline in cardiac function from tumor necrosis factor alpha (TNF-α) administration to rats (65) and prevented the development of TAC-induced arrhythmias in mice (66). These results are confirmed when sEH is modulated genetically, as *Ephx2*$^{-/-}$ mice were protected from cardiac dysfunction and arrhythmia following chronic high dose angiotensin II treatment or TAC banding (67). Spontaneously hypertensive heart failure rats were found to have increased transcript levels of *Ephx2* and lower 14,15-EET levels compared to spontaneously hypertensive rats that do not develop heart failure, further suggesting an important role for sEH-mediated EET hydrolysis in the development of heart failure unrelated to IR injury and AMI (67). In contrast to preclinical models of IR, EET-mediated cardioprotection in non-ischemic cardiomyopathy has not been demonstrated in non-rodent models and remains an important future direction for this line of investigation.

EET action in cardiac non-myocytes

In addition to cardiomyocytes, the heart is composed of fibroblasts, endothelial cells, and vascular smooth muscle cells (68). It is clear that these other cell types are important in the production and action of EETs in the heart (Fig. 2A); however, the contribution of EETs that act on or are produced by these other cell types to the cardioprotection phenotype observed in preclinical studies is less certain.

Action of EETs derived from cardiac endothelial cells on myocardial cells

CYP epoxygenases and sEH are highly expressed in endothelial cells (69, 70). Isolated hearts from transgenic mice with endothelial sEH or CYP2J2 overexpression (Tie2-sEH-Tr and Tie2-CYP2J2-Tr mice) did not alter the recovery of LVDP or infarct size following IR compared to wild-type mice, demonstrating that endothelial-derived EETs do not have a significant impact on acute myocardial recovery in this model of IR injury (71). Intriguingly, isolated hearts from transgenic mice with endothelial CYP2C8 overexpression (Tie2-CYP2C8-Tr mice) had worsened LVDP and infarct size compared to hearts from wild-type mice (71). This demonstrates that the specific CYP epoxygenase isoform catalyzing the formation of EETs in the endothelium appears to play an important role in cardiac function in mice (71). Increased parallel production of reactive oxygen species (ROS) and linoleic acid-derived metabolites were found to be the cause of the enhanced IR injury in Tie2-CYP2C8-Tr mice (71). Specifically, CYP2C8 overexpression catalyzed the formation of epoxyoctadecaenoic acids (EpOMEs, leukotoxin) from linoleic acid in endothelial cells, which are subsequently metabolized by sEH to dihydroxyoctadecaenoic acids (DHOMEs, leukotoxin diol) (71). Enhanced endothelial DHOME,

along with reactive oxygen species (ROS), formation mediated the cardiodepressive phenotype observed in Tie2-CYP2C8-Tr, but not Tie2-CYP2J2-Tr, mice (71). It remains unclear whether similar CYP isoform specific effects occur in cardiomyocytes.

Action of EETs derived from cardiac endothelial cells on cardiac smooth muscle cells

Endothelial-derived EETs exert their vasodilatory action in coronary vessels through calcium-activated potassium channel (Kca)-dependent hyperpolarization of smooth muscle cells independent of prostaglandin or NO synthesis (72, 73). Interestingly, this effect has been found to be greatest in smaller coronary arterioles, rather than larger epicardial coronary arteries (74). Despite these findings, EET-mediated vasodilation in the setting of IR injury and its putative beneficial effect of aiding in the perfusion of oxygenated blood to ischemic regions of the heart remain unclear. Altogether, further work is necessary to validate the role of endothelial EETs in cardioprotection, especially in *in vivo* and chronic models of AMI.

Action of EETs in cardiac endothelial cells

Endothelial-derived EETs have well-established pro-angiogenic properties through a multitude of signaling pathways that are reviewed in great detail elsewhere (75). Experimental studies demonstrate that angiogenesis is associated with cardioprotection in chronic phases following IR (76). Few studies have investigated the role of EET-derived angiogenesis in cardioprotection following IR and as a result this topic remains poorly understood. One report revealed that inhibition of sEH promotes capillary tube formation (angiogenesis) in the isolated endothelial progenitor cells (EPCs) of post-AMI patients (compared to control subjects) through the EET–PPARγ pathway (77). It is unknown if these effects occur with *in vivo* administration of

a sEH inhibitor. Moreover, the EPCs were derived from whole blood and the effect of sEH inhibitor specifically on coronary vasculature formation was not evaluated (77). Finally, it remains to be determined if these effects impact myocardial recovery following AMI. Consequently, further work is necessary to confirm and better understand these findings.

Action of EETs on inflammatory cells and cardiac fibroblasts

We mentioned earlier that inflammation promotes cardiac remodeling and fibrosis following myocardial IR injury. Although they are not a permanent cellular component of the myocardium, bone-marrow derived inflammatory cells such as monocytes and neutrophils drive this inflammatory process when they infiltrate the site of injury following IR (78). Substantial evidence indicates that EETs, through inhibition of nuclear factor-kappaB (NF-κB) activation, attenuate inflammation in endothelial cells and monocytes (6) and mitigate macrophage/neutrophil infiltration in the vasculature (79); these effects have not been extensively studied in the coronary vasculature following myocardial ischemic injury. Kompa et al. demonstrated that sEH inhibition impedes the infiltration of macrophages in the peri-infarct region of the myocardium in rats following permanent LAD ligation (59). Intriguingly, sEH inhibition did not reduce macrophage infiltration in the infarct region of the myocardium (59). Further investigation is warranted to fully characterize the contribution of inflammation reduction in EET-mediated cardioprotection. Inflammation precedes the development of chronic myocardial fibrosis during the following IR injury. Cardiac fibroblasts accelerate this maladaptive remodeling via secretion of growth factors and cytokines (68). Inhibition of sEH has been found to directly block the proliferation, differentiation, migration, and secretion capacity of fibroblasts (59, 61). More work is necessary to directly implicate EETs in sEH inhibition-

mediated fibroblast suppression and to provide further mechanistic insight into this effect. Overall, further studies are necessary to determine the functional role of these cell-types in EET-mediated cardioprotection relative to cardiomyocytes.

Clinical studies investigating the role of EETs in the progression of CVD

Since pharmacological tools that directly and specifically manipulate EETs are currently not available for clinical use, we and others have relied on genetic and biomarker-driven observational studies to understand the role of the CYP epoxygenase-EET pathway in human CVD. Associations between the risk of developing a cardiovascular event and polymorphisms in genes coding for CYP2J2 (80-82), CYP2C8/9 (82, 83), and sEH (*EPHX2)* (84-89) have been discovered. Studies evaluating genetic variation and risk of CVD development have been summarized in great detail elsewhere (10) and continue to be an active area of investigation (88, 89).

Inconsistencies in the strength of the associations between genetic variation in the CYP epoxygenase-EET pathway and CVD susceptibility have been reported across studies, suggesting that the relationship is likely complex and most profound in certain subsets of the population (10). For instance, associations between *EPHX2*, *CYP2J2* and *CYP2C8* variants and CAD risk have often been most pronounced in cigarette smokers (81, 82, 84, 87). Although the mechanism remains unclear, this suggests that the pathologic impact of genetic predisposition to alter CYP-derived EET levels may be greatest in the presence of underlying cardiovascular dysfunction. Indeed, modulation of CYP-derived EETs has minimal impact on basal cardiovascular function in preclinical models; whereas, the blood pressure lowering, anti-inflammatory, and cardioprotective effects are most substantial upon induction of a pathologic stimulus (6). The relationship between genetic and metabolic variation in CYP epoxygenase-EET pathway genes and prognosis in patients with established CAD, however, has not been investigated and requires rigorous study.

Recently, we measured circulating eicosanoid metabolite concentrations in a cohort of patients with established and stable CAD and a corresponding population of healthy volunteers at low risk for CAD (90). The 14,15-EET:DHET ratio in plasma (a biomarker of sEH metabolic function) was significantly greater in CAD patients relative to healthy volunteers suggesting that sEH metabolic function was suppressed in the presence of established CAD (90). In concordance, plasma EET levels were also higher in CAD patients (90). Given the aforementioned evidence demonstrating the cardioprotective effects of EETs in preclinical models of CVD, these findings allude to the possible presence of a compensatory increase in EET levels in the presence of established CAD. Interestingly, this observation is consistent with a prior study in which myocardial biopsies obtained patients who developed heart failure (defined as ejection fraction < 45%) secondary to CAD exhibited lower *EPHX2* mRNA expression compared to the biopsies obtained from control CAD patients without evidence of heart failure (67). However, these preliminary observations must be interpreted with caution until further studies validate the observed differences in additional populations.

Despite the observed presence of lower sEH metabolic function and higher EET levels in this population of patients with established CAD, compared to healthy volunteer controls, substantial inter-individual variation in the 14,15-EET:DHET ratio and EET levels existed within the CAD population and the presence of obesity, advanced age, and cigarette smoking were the strongest predictors of low 14,15 EET:DHET ratios (higher sEH metabolic function) and low EETs (90, 91). Consistent with the aforementioned preclinical evidence demonstrating the cardiovascular protective effects of EETs, lower 14,15-EET:DHET ratios (i.e., higher sEH metabolic function) and lower EET levels were significantly associated with pro-inflammatory phenotypes predictive of poor prognosis (higher circulating levels of the chemokine monocyte

chemoattractant protein-1 and cellular adhesion molecules) (91). Importantly, these associations were independent of clinical factors (91). Taken together, these initial findings suggest that the subset of CAD patients with enhanced sEH metabolic function and low EET levels may be predisposed to poorer prognosis and thus likely to derive therapeutic benefit from an intervention that promotes the biological effects of EETs. However, subsequent studies remain necessary to first determine the association between inter-individual variation in the CYP epoxygenase-EET pathway and prognosis (i.e., clinical outcomes rather than surrogate markers) in patients with existing CAD.

Importantly, evaluation of genetic and metabolic variation in the CYP epoxygenase-EET pathway, biomarkers of cardiovascular inflammation and cardiac remodeling, and prognosis in patients during and following the acute stage of an AMI has not been completed to date. Completion of such studies offers enormous potential to facilitate initial translation of the aforementioned growing body of preclinical evidence and guide the rational design of prospective, proof-of-concept clinical trials that aim to evaluate the cardioprotective effects of novel therapeutic strategies that promote the effects of EETs following an AMI.

Discussion: key considerations prior to initiation of proof-of-concept clinical trials

Despite major medical advances over the past four decades, there still exists a major need to develop cardioprotective therapies that reduce death and improve quality of life in AMI patients. Over the past decade, there have been numerous unsuccessful clinical trials involving novel AMI therapeutics that had shown initial promise in preclinical studies (4). These failures underscore the complex pathophysiology of AMI and suggest that full preclinical elucidation into the cardioprotective effects of candidate agents is necessary to increase the probability for success in clinical trials. Past clinical trial failures were likely a consequence of being rushed through development before obtaining rigorous mechanistic insight in preclinical studies, and were therefore wrought by limitations in their design (4). Specifically, important study design details such as timing and dose of intervention were determined based on theoretical evidence and not validated *a priori* in animal models of AMI (4). Investigating the effects of a cardioprotective strategy across multiple experimental systems *in vitro, ex vivo,* and *in vivo* and ensuring that preclinical findings can be replicated across these experimental systems before human testing would allow for full mechanistic elucidation, facilitate a more accurate prediction of which drug candidates should be carried forward to humans, and ultimately improve clinical trial design. Significant initiatives have already begun to alleviate these major preclinical challenges in AMI therapy translation. For example, an NIH consortium of investigators called CAESAR (Consortium for preclinicAl assESsment of cARardioprotective therapies) has been set up to examine therapies in preclinical studies using the same rigorous standards that are used in clinical trials to ensure reproducibility and screen for truly effective therapeutic candidates (92).

Considering the thousands of interventions that have been reported to be cardioprotective in preclinical studies over the past few decades (92), it is not feasible for every promising intervention to be evaluated through this mechanism. Thus, a collective and collaborative effort between basic, clinical, and translational scientists using the same rigorous standards is needed to develop therapeutic strategies that promote the cardioprotective effects of EETs. In addition to the aforementioned issues in the development of therapeutic strategies for AMI, further considerations must be kept in mind in order to facilitate specifically the translation of EET-promoting strategies into successful proof-of-concept phase I and II clinical trials.

Development of therapeutic strategies that promote EET action in humans

The successful development of this strategy for AMI is only as promising as the pharmacologic agents that modulate the CYP epoxygenase-EET pathway. The potential for clinical translation of exogenous EET administration is limited due to its short half-life and poor solubility. Synthetic EET analogs overcome this limitation. Historically, synthetic EET analogs conducive to *in vivo* dosing were not available (23); however, in recent years, a novel generation of EET analogs have been developed. These improved agents are orally bioavailable and reach therapeutic levels in live animals as illustrated by their protective effects in *in vivo* rodent models of renal injury (93, 94). Despite this steadfast improvement, lack of a known EET receptor continues to slow progress in this area. Discovery of the putative EET receptor(s) would further contribute to the field by elucidating structure-activity relationships and facilitating the design of agents with further improvements; efforts are ongoing.

Over the past decade, a variety of selective and potent sEH inhibitors have been optimized through structure-activity relationship techniques. The history of sEH inhibitor

development is akin to that of EET analog development: compared to earlier members of the class, newer sEH inhibitors possess pharmacokinetic properties in animals predicted to be more favorable for oral human administration. Thus these agents are being actively developed and evaluated in both academic and pharmaceutical industry laboratories for a variety of indications and offer considerable promise as a therapeutic strategy for ischemic CVD (21, 95). Thus, the sEH inhibitors and synthetic EET analogs are the most conducive therapeutic strategies poised for translation into humans in the near future. Investigators should prudently select new generation agents from these classes to evaluate their effects, especially in chronic and *in vivo* preclinical models of AMI where drugs ideal for chronic dosing are most important.

Potential unintended effects of increasing EET levels

EETs have a myriad of biological functions and therapeutically promoting these actions has the potential to cause unintended effects that should be considered. For instance, as mentioned earlier, EETs have potent vasodilatory effects. Although this could be beneficial in hypertensive patients, delayed restoration of blood pressure may have played a role in the increased mortality of *Ephx2*$^{-/-}$ mice observed in a model of cardiac arrest-induced hypotension followed by cardiopulmonary resuscitation (CPR) (96). The precise cause of death, including the direct role of EETs, remains unknown, but these data may have important clinical implications since cardiac arrest and hypotensive shock are complications of AMI. Future preclinical studies are warranted to replicate these findings and implicate EETs as the causative mediator of this effect.

Despite their vasodilatory effects in the peripheral and coronary vasculature, EETs have vasoconstrictive effects in the pulmonary vasculature and may be important mediators in

pulmonary hypertension (97, 98). *Ephx2*$^{-/-}$ mice develop pulmonary vascular remodeling, right ventricular hypertrophy, and reduced exercise capacity (pulmonary hypertension) (99). Interestingly, these phenotypes were not replicated in wild-type mice receiving chronic administration of a sEH inhibitor (99). This suggests that the role of EETs and sEH in pulmonary hypertension is complex and further work is necessary to determine if EET-mediated pulmonary vasoconstriction is deleterious in the setting of an AMI or chronic cardiac remodeling.

Similar to Kca-mediated hyperpolarization of smooth muscle cells to induce vasodilation, EETs activate Kca-mediated hyperpolarization in platelets (100). This leads to reduced platelet activation and prevents platelet adhesion to endothelial cells (100). Such findings have been recapitulated *in vivo* in the skin muscle of hamsters (101) and in the cerebral arterioles of mice (102). As agents that promote the EETs progress through development, we believe that the clinical relevance of this anti-platelet effect is enormous considering the well-established importance of long-term, anti-platelet therapies in patients suffering from an AMI (103, 104). Of note, epoxydocosapentaenoic acids (EDPs) and epoxydocosapentaenoic acid (EEQs), which are CYP-dependent epoxy-derivatives of DHA and EPA, respectively (Fig. 1), are potent inhibitors of platelet aggregation (105). Further preclinical studies are needed to grasp the potential additive/synergistic benefit of epoxyeicosanoid anti-platelet effects on top of their cardioprotective effects, specifically in the coronary arteries during IR injury.

EETs enhanced tumorigenesis and multiorgan metastasis in multiple mouse models of cancer (106, 107). Specifically, these enhanced effects were observed in *Ephx2*-/-, Tie2-CYP2J2-Tr, and Tie2-CYP2C8-Tr mice; observed after the direct administration of EETs and sEH inhibitors; and mediated via the pro-angiogenic (VEGF-secreting) properties of EETs in the endothelium (106). Though these effects have not been observed to occur in the absence of

spontaneous tumor models, these findings raise a serious concern about the potential cancer causing ability of therapies that increase endogenous EET levels. Importantly, the pro-angiogenic effects of EETs also promote wound healing and tissue regeneration (108, 109), which may be beneficial in myocardial recovery following IR injury. Furthermore, EDPs inhibit tumor growth and metastasis through anti-angiogenic effects (110); however, the impact of the synthetic EET analogs on these phenotypes has not been well characterized. More studies are clearly necessary to determine the role of CYP epoxygenase-EET and parallel metabolic pathways in the regulation of angiogenesis, especially in the setting of an AMI.

In addition to studying these biological effects of EETs for the purpose of understanding potential risks and benefits, this knowledge can also guide early drug design of EET-promoting agents. For example, a new series of sEH inhibitors have been modified to reduce their pro-angiogenic properties while maintaining potent and selective sEH inhibition (111). Similarly, modification of synthetic EET analogs can alter their biological properties (112), (analogous to the aforementioned varying potencies across EET regioisomers). In fact, data suggests that EET-mediated cancer cell proliferation is regioisomer-specific (113). Consequently, further research in this area is clearly needed to select the most promising compounds for further development and subsequent translation into clinical studies. Furthermore, considering the complex course of pathological events in response to IR injury in the myocardium, optimizing the timing, dose, duration, and route of administration of EET-modulating therapeutics will be essential to maximize the cardioprotective benefits while minimizing the potential harmful effects of these strategies.

The use of clinically relevant models of AMI including assessing the impact of comorbidities

An additional reason for drug development failure is the evaluation of candidate agents in animal models that are not clinically-relevant and therefore poorly mimic the AMI patient population (92). Indeed, the majority of preclinical AMI models in the literature involve young, healthy animals lacking the comorbid conditions that are typically associated with the AMI population in humans (4). Importantly, efforts have begun to determine the impact of these conditions on EET-mediated cardioprotection. For instance, it is well known that aging, a risk factor highly prevalent in the AMI population, exacerbates myocardial IR injury (28). Cardioprotection from cardiomyocyte-specific CYP2J2 overexpression in the isolated hearts of young α-MHC-CYP2J2-Tr mice were lost in aged α-MHC-CYP2J2-Tr hearts following global IR injury (114). However, this loss was regained when aged α-MHC-CYP2J2-Tr hearts were perfused with a sEH inhibitor, suggesting that pharmacological inhibition of sEH activity remains cardioprotective even in aged hearts (114). Future studies in clinically-relevant AMI models are needed in order to determine if the cardioprotective effects of EETs are influenced by conditions such as aging, diabetes, and obesity.

Subsets of the AMI population may derive greater benefit from agents that promote the cardioprotective effects of EETs

Even after addressing all of the aforementioned considerations in the translation of EET-promoting therapeutics, the innate heterogeneity of the AMI population is an important barrier to the successful translation of AMI therapeutics (4) as novel treatments may not work in broad

populations. As technology advances and we enter an era of personalized medicine, genetic and biochemical biomarkers offer considerable promise to identify which patients are defective in the specific pathway that the drug targets, are at increased risk of poor prognosis, and may derive the most benefit from that therapeutic intervention. Thus, selective administration of EET promoting therapy to a pre-identified population of 'responders' predisposed to low EET levels may increase the probability of clinical trial success. Notably, the *EPHX2* Lys55Arg polymorphism is a promising genetic biomarker that may help identify patients predisposed to low EET levels since variant carriers have enhanced sEH metabolic function and increased risk of incident CAD (84). Moreover, direct measurement of EET levels has the potential to identify these patients. Indeed, higher throughput methods to quantify eicosanoids in a clinical setting have been found to be precise, accurate, and feasible (115). Altogether, further work is necessary to determine 1) which biomarkers can best identify the subset of AMI patients with reduced EET levels and 2) if these patients have poorer prognosis before the initiation of clinical trials that test whether interventions are likely to be most effective in those subsets.

Summary/ Conclusion

After a 1997 paper reported that EETs were cardioprotective in *ex vivo* and *in vitro* models (39), it took about 10 years before the first *in vivo* reports began to recapitulate these findings. Since then, much attention has been focused on the role of the CYP epoxygenase-EET pathway in AMI and the potential for therapeutic modulation of this pathway to improve outcomes in humans. In parallel, the improvement of experimental strategies to manipulate the pathway through pharmacologic and genetic approaches has allowed for great advances in the knowledge surrounding EET-mediated cardioprotection. Evidence for the beneficial effects of EETs has been replicated using multiple species, experimental heart disease models, and phenotypes relevant to cardioprotection, which underscores the great promise of this therapeutic strategy. Most of the data in the literature highlight the acute role of EETs in prosurvival pathway-mediated mitochondrial preservation in cardiomyocytes following AMI, but EETs have also been found to attenuate chronic cardiac remodeling and elicit protective effects in other cell types following AMI. It remains unknown whether EETs cause deleterious effects that could outweigh these cardioprotective benefits. Moreover, it is poorly understood if modulation of parallel epoxide and diol metabolites derived from other PUFAs impacts this benefit-risk ratio. Consequently, further work will be critical to move this line of investigation closer to clinical trials.

Ultimately, randomized controlled trials will be necessary to determine the benefits and risks of therapeutic strategies that promote the effects of EETs in patients experiencing an AMI. Before advancing promising agents that promote the effects of EETs into clinical trials, additional preclinical and human investigations are needed in order to lay an essential foundation

for the rational design of these future prospective trials and select the agent, dosing strategy, and patient population most likely to circumvent clinical failure. A concerted effort to address these prerequisites will serve to improve the probability of translational success from a rapidly emerging body of evidence into a clinically applicable therapeutic strategy for patients with AMI.

Figures

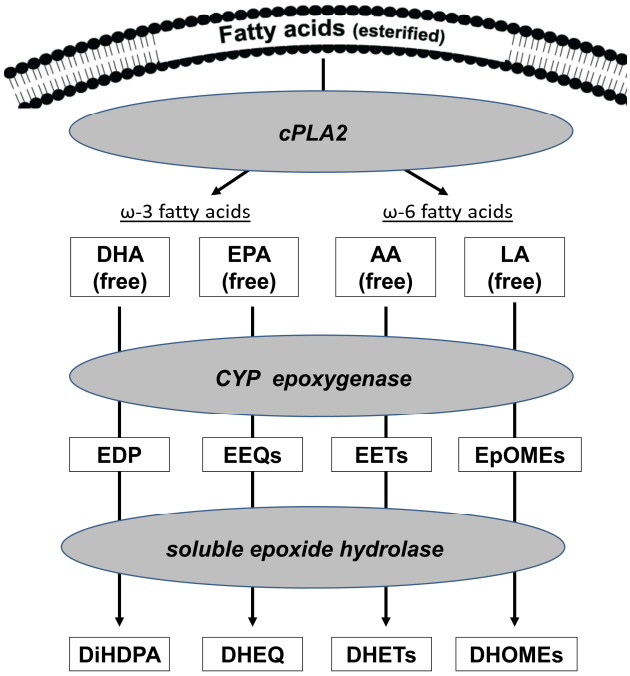

Figure B.1 Cytochrome P450 (CYP) epoxygenase–epoxyeicosatrienoic acid (EET) and parallel pathways. Through the activation of cytosolic phospholipase A2 (cPLA2) in cardiomyocytes followingAMI,membrane-bound fatty acids are released into the cytosol and subsequently metabolized by CYP epoxygenases to form biologically active eicosanoids. The CYP2J and CYP2C epoxygenases produce four regioisomers of EETs from arachidonic acid (AA) that elicit various biological effects. These bioactive epoxyeicosanoids are extensively hydrolyzed by soluble epoxide hydrolase into the less biologically active dihydroxyeicosatrienoic acid (DHET) metabolites. DHA, docosahexaenoic acid; DHEQ, dihydroxy-eicosatetraenoic acid; DHOME, dihydroxyoctadecaenoic acid; DiHDPA, dihydroxy-

docosapentaenoic acid; EDP, epoxydocosapentaenoic acid; EEQ, epoxyeicosatetraenoic acid; EPA, eicosapentaenoic acid; EpOME, epoxyoctadecaenoic acid; LA, linoleic acid.

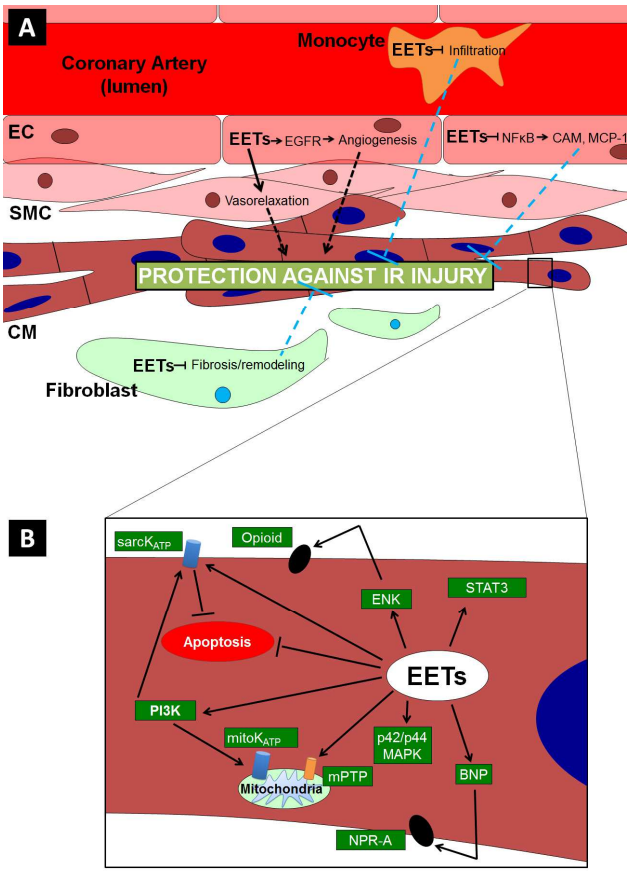

Figure B.2 Epoxyeicosatrienoic acid (EET) cardioprotection in the heart. A) EETs elicit action in cardiac endothelial cells (pro-angiogenic, anti-inflammatory), smooth muscle cells (vasodilatory), fibroblasts (anti-fibrotic), and inflammatory cells (anti-inflammatory). These effects may protect the myocardium following IR injury. B) EETs derived from cardiomyocytes (CMs) elicit direct cardioprotection of the myocardium during the acute phase following IR injury. They activate prosurvival signaling pathways, many of which converge ontomitochondria and promote its preservation. BNP, B-type natriuretic peptide; CAM, cell adhesion molecules; EC, endothelial cell; EGFR, epidermal growth factor receptor; ENK, enkephalin; IR, ischemia reperfusion; MCP-1, monocyte chemoattractant

protein-1; mitoKATP, mitochondrial ATP-activated K+ channel; mPTP, mitochondrial permeability transition pore; NF-κB, nuclear factor-κB; NPR-A, natriuretic peptide receptor type-A; p42/p44MAPK, p42/p44 mitogen-activated protein kinase; PI3K, phosphoinositide 3-kinase; sarcKATP, sarcolemmal ATP-activated K+ channel; SMC, smooth muscle cell; STAT3, signal transducer and activator of transcription.

Tables

Table B.1 Mechanisms underlying direct cardioprotective effects of epoxyeicosatrienoic acids (EETs) on cardiomyocytes

EET action	Model	Mechanisms
Reduced myocardial cell death and apoptosis	Hypoxia-reoxygenation *(in vitro);* OGD/RGR (*in vitro*)	PI3K/Akt signaling (36, 38, 44) K_{ATP} channel signaling (37, 38) STAT3 signaling (40)
Improved recovery of left ventricular developed pressure	Global ischemia and reperfusion *(ex vivo)*	K_{ATP} channel signaling (30, 31, 37, 48) p42/p44 MAPK signaling (30) PI3K/Akt signaling (30, 31, 36, 41, 116) BNP/NPR-A signaling (41) Opioid signaling (42) Protein phosphatase 2A signaling (114) Reduced leukotoxin diol levels (114) Reduced oxidative stress (114) Preservation of caveolin-1 (51)
Reduced left ventricular infarct size	Global ischemia and reperfusion *(ex vivo);* Ischemia-reperfusion *(in vivo)*	PI3K/Akt signaling (31, 36) K_{ATP} channel signaling (26, 31-35, 37) STAT3 signaling (40) Opioid signaling (42) eNOS activation (35) Initial ROS formation (34) Inhibition of mPTP opening (35)
Reduced chronic left ventricular remodeling[a]	Ischemia-reperfusion *(in vivo)*	Increased eNOS : iNOS ratio (60) Reduced myocardial collagen deposition (58-61) Reduced cardiac fibroblast activation (59) Reduced inflammatory cytokines (58, 61) Reduced macrophage infiltration (59) Reduced oxidative stress (60)

[a]Chronic ischemia-reperfusion involved reperfusion periods of at least 2 weeks following ischemia
Akt, protein kinase B; BNP, B-type natriuretic peptide; eNOS, endothelial nitric oxide synthase; iNOS, inducible nitric oxide synthase; KATP, ATP-activated K^+ channel; mPTP, mitochondrial permeability transition pore; NPR-A, natriuretic peptide receptor type-A; OGD, oxygen and glucose deprivation; p42/p44 MAPK, p42/p44 mitogen-activated protein kinase; PI3K, phosphoinositide 3-kinase; RGR, reoxygenation and glucose repletion; ROS, reactive oxygen species; STAT3, signal transducer and activator of transcription 3

REFERENCES

(1) Canada, P.H.A.o. 2009 tracking heart disease and stroke in canada. Vol. 29 (ed. Canada, P.H.A.o.) (Ottawa, ON, 2009).

(2) Go, A.S. et al. Heart disease and stroke statistics--2013 update: a report from the American Heart Association. Circulation 127, e6-e245 (2013).

(3) Davies, M.J. & Thomas, A.C. Plaque fissuring--the cause of acute myocardial infarction, sudden ischaemic death, and crescendo angina. Br Heart J 53, 363-73 (1985).

(4) Yellon, D.M. & Hausenloy, D.J. Myocardial reperfusion injury. N Engl J Med 357, 1121-35 (2007).

(5) Imig, J.D. & Hammock, B.D. Soluble epoxide hydrolase as a therapeutic target for cardiovascular diseases. Nat Rev Drug Discov 8, 794-805 (2009).

(6) Deng, Y., Theken, K.N. & Lee, C.R. Cytochrome p450 epoxygenases, soluble epoxide hydrolase, and the regulation of cardiovascular inflammation. J Mol Cell Cardiol 48, 331-41 (2010).

(7) Seubert, J.M., Zeldin, D.C., Nithipatikom, K. & Gross, G.J. Role of epoxyeicosatrienoic acids in protecting the myocardium following ischemia/reperfusion injury. Prostaglandins Other Lipid Mediat 82, 50-9 (2007).

(8) Nithipatikom, K. & Gross, G.J. Review article: epoxyeicosatrienoic acids: novel mediators of cardioprotection. J Cardiovasc Pharmacol Ther 15, 112-9 (2010).

(9) Imig, J.D. Epoxides and soluble epoxide hydrolase in cardiovascular physiology. Physiol Rev 92, 101-30 (2012).

(10) Theken, K.N. & Lee, C.R. Genetic variation in the cytochrome P450 epoxygenase pathway and cardiovascular disease risk. Pharmacogenomics 8, 1369-83 (2007).

(11) Capdevila, J.H., Falck, J.R. & Estabrook, R.W. Cytochrome P450 and the arachidonate cascade. FASEB J 6, 731-6 (1992).

(12) Spector, A.A., Fang, X., Snyder, G.D. & Weintraub, N.L. Epoxyeicosatrienoic acids (EETs): metabolism and biochemical function. Prog Lipid Res 43, 55-90 (2004).

(13) Wu, S., Moomaw, C.R., Tomer, K.B., Falck, J.R. & Zeldin, D.C. Molecular cloning and expression of CYP2J2, a human cytochrome P450 arachidonic acid epoxygenase highly expressed in heart. J Biol Chem 271, 3460-8 (1996).

(14) DeLozier, T.C. et al. Detection of human CYP2C8, CYP2C9, and CYP2J2 in cardiovascular tissues. Drug Metab Dispos 35, 682-8 (2007).

(15) Larsson, C., White, I., Johansson, C., Stark, A. & Meijer, J. Localization of the human soluble epoxide hydrolase gene (EPHX2) to chromosomal region 8p21-p12. Hum Genet 95, 356-8 (1995).

(16) Enayetallah, A.E., French, R.A., Thibodeau, M.S. & Grant, D.F. Distribution of soluble epoxide hydrolase and of cytochrome P450 2C8, 2C9, and 2J2 in human tissues. J Histochem Cytochem 52, 447-54 (2004).

(17) Gross, G.J., Falck, J.R., Gross, E.R., Isbell, M., Moore, J. & Nithipatikom, K. Cytochrome P450 and arachidonic acid metabolites: role in myocardial ischemia/reperfusion injury revisited. Cardiovasc Res 68, 18-25 (2005).

(18) Poeckel, D. & Funk, C.D. The 5-lipoxygenase/leukotriene pathway in preclinical models of cardiovascular disease. Cardiovasc Res 86, 243-53 (2010).

(19) Yuhki, K. et al. Roles of prostanoids in the pathogenesis of cardiovascular diseases: Novel insights from knockout mouse studies. Pharmacol Ther 129, 195-205 (2011).

(20) Baum, S.J. et al. Fatty acids in cardiovascular health and disease: a comprehensive update. J Clin Lipidol 6, 216-34 (2012).

(21) Shen, H.C. & Hammock, B.D. Discovery of inhibitors of soluble epoxide hydrolase: a target with multiple potential therapeutic indications. J Med Chem 55, 1789-808 (2011).

(22) Arnold, C. et al. Arachidonic acid-metabolizing cytochrome P450 enzymes are targets of {omega}-3 fatty acids. J Biol Chem 285, 32720-33 (2010).

(23) Imig, J.D. et al. Development of epoxyeicosatrienoic acid analogs with in vivo anti-hypertensive actions. Front Physiol 1, 157 (2010).

(24) Gauthier, K.M. et al. 14,15-Epoxyeicosa-5(Z)-enoic acid: a selective epoxyeicosatrienoic acid antagonist that inhibits endothelium-dependent hyperpolarization and relaxation in coronary arteries. Circ Res 90, 1028-36 (2002).

(25) Oni-Orisan, A. et al. Dual modulation of cyclooxygenase and CYP epoxygenase metabolism and acute vascular inflammation in mice. Prostaglandins Other Lipid Mediat 104-105, 67-73 (2013).

(26) Batchu, S.N., Law, E., Brocks, D.R., Falck, J.R. & Seubert, J.M. Epoxyeicosatrienoic acid prevents postischemic electrocardiogram abnormalities in an isolated heart model. J Mol Cell Cardiol 46, 67-74 (2009).

(27) Liu, Y., Dang, H.X., Li, D., Pang, W., Hammock, B.D. & Zhu, Y. Inhibition of Soluble Epoxide Hydrolase Attenuates High-Fat-Diet-Induced Hepatic Steatosis by Reduced Systemic Inflammatory Status in Mice. PLoS One 7, (2012).

(28) Ferdinandy, P., Schulz, R. & Baxter, G.F. Interaction of cardiovascular risk factors with myocardial ischemia/reperfusion injury, preconditioning, and postconditioning. Pharmacol Rev 59, 418-58 (2007).

(29) Hausenloy, D.J. & Yellon, D.M. New directions for protecting the heart against ischaemia-reperfusion injury: targeting the Reperfusion Injury Salvage Kinase (RISK)-pathway. Cardiovasc Res 61, 448-60 (2004).

(30) Seubert, J. et al. Enhanced postischemic functional recovery in CYP2J2 transgenic hearts involves mitochondrial ATP-sensitive K+ channels and p42/p44 MAPK pathway. Circ Res 95, 506-14 (2004).

(31) Seubert, J.M. et al. Role of soluble epoxide hydrolase in postischemic recovery of heart contractile function. Circ Res 99, 442-50 (2006).

(32) Nithipatikom, K., Moore, J.M., Isbell, M.A., Falck, J.R. & Gross, G.J. Epoxyeicosatrienoic acids in cardioprotection: ischemic versus reperfusion injury. Am J Physiol Heart Circ Physiol 291, H537-42 (2006).

(33) Gross, G.J. et al. Effects of the selective EET antagonist, 14,15-EEZE, on cardioprotection produced by exogenous or endogenous EETs in the canine heart. Am J Physiol Heart Circ Physiol 294, H2838-44 (2008).

(34) Gross, G.J., Hsu, A., Falck, J.R. & Nithipatikom, K. Mechanisms by which epoxyeicosatrienoic acids (EETs) elicit cardioprotection in rat hearts. J Mol Cell Cardiol 42, 687-91 (2007).

(35) Gross, G.J., Hsu, A., Pfeiffer, A.W. & Nithipatikom, K. Roles of endothelial nitric oxide synthase (eNOS) and mitochondrial permeability transition pore (mPTP) in epoxyeicosatrienoic acid (EET)-induced cardioprotection against infarction in intact rat hearts. J Mol Cell Cardiol 59, 20-9 (2013).

(36) Batchu, S.N. et al. Cardioprotective effect of a dual acting epoxyeicosatrienoic acid analogue towards ischaemia reperfusion injury. Br J Pharmacol 162, 897-907 (2011).

(37) Batchu, S.N. et al. Role of PI3Kα and sarcolemmal ATP-sensitive potassium channels in epoxyeicosatrienoic acid mediated cardioprotection. J Mol Cell Cardiol 53, 43-52 (2012).

(38) Bodiga, S. et al. Protective actions of epoxyeicosatrienoic acid: dual targeting of cardiovascular PI3K and KATP channels. J Mol Cell Cardiol 46, 978-88 (2009).

(39) Wu, S. et al. Molecular cloning, expression, and functional significance of a cytochrome P450 highly expressed in rat heart myocytes. J Biol Chem 272, 12551-9 (1997).

(40) Merkel, M.J. et al. Inhibition of soluble epoxide hydrolase preserves cardiomyocytes: role of STAT3 signaling. Am J Physiol Heart Circ Physiol 298, H679-H87 (2010).

(41) Chaudhary, K.R. et al. Role of B-type natriuretic peptide in epoxyeicosatrienoic acid-mediated improved post-ischaemic recovery of heart contractile function. Cardiovasc Res 83, 362-70 (2009).

(42) Gross, G.J., Baker, J.E., Hsu, A., Wu, H.-e., Falck, J.R. & Nithipatikom, K. Evidence for a role of opioids in epoxyeicosatrienoic acid-induced cardioprotection in rat hearts. Am J Physiol Heart Circ Physiol 298, H2201-H7 (2010).

(43) Machado, N.G., Alves, M.G., Carvalho, R.A. & Oliveira, P.J. Mitochondrial involvement in cardiac apoptosis during ischemia and reperfusion: can we close the box? Cardiovasc Toxicol 9, 211-27 (2009).

(44) Dhanasekaran, A. et al. Multiple antiapoptotic targets of the PI3K/Akt survival pathway are activated by epoxyeicosatrienoic acids to protect cardiomyocytes from hypoxia/anoxia. Am J Physiol Heart Circ Physiol 294, H724-H35 (2008).

(45) Solaini, G. & Harris, D.A. Biochemical dysfunction in heart mitochondria exposed to ischaemia and reperfusion. Biochem J 390, 377-94 (2005).

(46) Halestrap, A.P., Clarke, S.J. & Javadov, S.A. Mitochondrial permeability transition pore opening during myocardial reperfusion--a target for cardioprotection. Cardiovasc Res 61, 372-85 (2004).

(47) Miura, T. & Tanno, M. The mPTP and its regulatory proteins: final common targets of signalling pathways for protection against necrosis. Cardiovasc Res 94, 181-9 (2012).

(48) Katragadda, D., Batchu, S.N., Cho, W.J., Chaudhary, K.R., Falck, J.R. & Seubert, J.M. Epoxyeicosatrienoic acids limit damage to mitochondrial function following stress in cardiac cells. J Mol Cell Cardiol 46, 867-75 (2009).

(49) Batchu, S.N. et al. Novel soluble epoxide hydrolase inhibitor protects mitochondrial function following stress. Can J Physiol Pharmacol 90, 811-23 (2012).

(50) Samokhvalov, V. et al. Epoxyeicosatrienoic acids protect cardiac cells during starvation by modulating an autophagic response. Cell Death Dis 4, e885 (2013).

(51) Chaudhary, K.R. et al. Effect of ischemia reperfusion injury and epoxyeicosatrienoic acids on caveolin expression in mouse myocardium. J Cardiovasc Pharmacol 61, 258-63 (2013).

(52) Imig, J.D., Dimitropoulou, C., Reddy, D.S., White, R.E. & Falck, J.R. Afferent arteriolar dilation to 11,12-EET analogs involves PP2A activity and Ca2+-Activated K+ channels. Microcirculation 15, 137-50 (2008).

(53) Wang, D. & Dubois, R.N. Epoxyeicosatrienoic acids: a double-edged sword in cardiovascular diseases and cancer. J Clin Invest 122, 19-22 (2012).

(54) van Nieuwenhoven, F.A. & Turner, N.A. The role of cardiac fibroblasts in the transition from inflammation to fibrosis following myocardial infarction. Vascul Pharmacol 58, 182-8 (2013).

(55) Sutton, M.G. & Sharpe, N. Left ventricular remodeling after myocardial infarction: pathophysiology and therapy. Circulation 101, 2981-8 (2000).

(56) Mehta, D., Curwin, J., Gomes, J.A. & Fuster, V. Sudden death in coronary artery disease: acute ischemia versus myocardial substrate. Circulation 96, 3215-23 (1997).

(57) Carrabba, N., Parodi, G., Valenti, R., Migliorini, A., Bellandi, B. & Antoniucci, D. Prognostic value of reverse left ventricular remodeling after primary angioplasty for STEMI. Atherosclerosis 222, 123-8 (2012).

(58) Li, N. et al. Beneficial effects of soluble epoxide hydrolase inhibitors in myocardial infarction model: insight gained using metabolomic approaches. J Mol Cell Cardiol 47, 835-45 (2009).

(59) Kompa, A.R. et al. Soluble epoxide hydrolase inhibition exerts beneficial anti-remodeling actions post-myocardial infarction. Int J Cardiol 167, 210-9 (2013).

(60) Merabet, N. et al. Soluble epoxide hydrolase inhibition improves myocardial perfusion and function in experimental heart failure. J Mol Cell Cardiol 52, 660-6 (2012).

(61) Sirish, P. et al. Unique mechanistic insights into the beneficial effects of soluble epoxide hydrolase inhibitors in the prevention of cardiac fibrosis. Proc Natl Acad Sci U S A 110, 5618-23 (2013).

(62) Dec, G.W. & Fuster, V. Idiopathic dilated cardiomyopathy. N Engl J Med 331, 1564-75 (1994).

(63) Xu, D. et al. Prevention and reversal of cardiac hypertrophy by soluble epoxide hydrolase inhibitors. Proc Natl Acad Sci U S A 103, 18733-8 (2006).

(64) Ai, D. et al. Soluble epoxide hydrolase plays an essential role in angiotensin II-induced cardiac hypertrophy. Proc Natl Acad Sci U S A 106, 564-9 (2009).

(65) Zhao, G. et al. Epoxyeicosatrienoic acids protect rat hearts against tumor necrosis factor-alpha-induced injury. J Lipid Res 53, 456-66 (2012).

(66) Westphal, C. et al. CYP2J2 overexpression protects against arrhythmia susceptibility in cardiac hypertrophy. PLoS One 8, e73490 (2013).

(67) Monti, J. et al. Soluble epoxide hydrolase is a susceptibility factor for heart failure in a rat model of human disease. Nat Genet 40, 529-37 (2008).

(68) Souders, C.A., Bowers, S.L.K. & Baudino, T.A. Cardiac fibroblast: the renaissance cell. Circ Res 105, 1164-76 (2009).

(69) Fang, X. et al. Pathways of epoxyeicosatrienoic acid metabolism in endothelial cells. J Biol Chem 276, 14867-74 (2001).

(70) Ai, D. et al. Angiotensin II up-regulates soluble epoxide hydrolase in vascular endothelium in vitro and in vivo. Proc Natl Acad Sci U S A 104, 9018-23 (2007).

(71) Edin, M.L. et al. Endothelial expression of human cytochrome p450 epoxygenase CYP2C8 increases susceptibility to ischemia-reperfusion injury in isolated mouse heart. FASEB J 25, 3436-47 (2011).

(72) Quyyumi, A.A. & Ozkor, M. Vasodilation by hyperpolarization beyond NO. Hypertension 48, 1023-5 (2006).

(73) Li, P.L. & Campbell, W.B. Epoxyeicosatrienoic acids activate K+ channels in coronary smooth muscle through a guanine nucleotide binding protein. Circ Res 80, 877-84 (1997).

(74) Oltman, C.L., Weintraub, N.L., VanRollins, M. & Dellsperger, K.C. Epoxyeicosatrienoic acids and dihydroxyeicosatrienoic acids are potent vasodilators in the canine coronary microcirculation. Circ Res 83, 932-9 (1998).

(75) Pozzi, A. & Zent, R. Regulation of endothelial cell functions by basement membrane- and arachidonic acid-derived products. Wiley Interdiscip Rev Syst Biol Med 1, 254-72 (2009).

(76) Chung, N.A., Lydakis, C., Belgore, F., Blann, A.D. & Lip, G.Y. Angiogenesis in myocardial infarction. An acute or chronic process? Eur Heart J 23, 1604-8 (2002).

(77) Xu, D.-y. et al. A potent soluble epoxide hydrolase inhibitor, t-AUCB, acts through PPARγ to modulate the function of endothelial progenitor cells from patients with acute myocardial infarction. Int J Cardiol 167, 1298-304 (2013).

(78) Kania, G., Blyszczuk, P. & Eriksson, U. Mechanisms of cardiac fibrosis in inflammatory heart disease. Trends Cardiovasc Med 19, 247-52 (2009).

(79) Deng, Y. et al. Endothelial CYP epoxygenase overexpression and soluble epoxide hydrolase disruption attenuate acute vascular inflammatory responses in mice. FASEB J 25, 703-13 (2011).

(80) Spiecker, M. et al. Risk of coronary artery disease associated with polymorphism of the cytochrome P450 epoxygenase CYP2J2. Circulation 110, 2132-6 (2004).

(81) Liu, P.-Y. et al. Synergistic effect of cytochrome P450 epoxygenase CYP2J2*7 polymorphism with smoking on the onset of premature myocardial infarction. Atherosclerosis 195, 199-206 (2007).

(82) Lee, C.R., North, K.E., Bray, M.S., Couper, D.J., Heiss, G. & Zeldin, D.C. CYP2J2 and CYP2C8 polymorphisms and coronary heart disease risk: the atherosclerosis risk in communities (ARIC) study. Pharmacogenet Genomics 17, 349-58 (2007).

(83) Yasar, U. et al. Allelic variants of cytochromes P450 2C modify the risk for acute myocardial infarction. Pharmacogenetics 13, 715-20 (2003).

(84) Lee, C.R. et al. Genetic variation in soluble epoxide hydrolase (EPHX2) and risk of coronary heart disease: the atherosclerosis risk in communities (ARIC) study. Hum Mol Genet 15, 1640-9 (2006).

(85) Fornage, M. et al. The soluble epoxide hydrolase gene harbors sequence variation associated with susceptibility to and protection from incident ischemic stroke. Hum Mol Genet 14, 2829-37 (2005).

(86) Fornage, M., Boerwinkle, E., Doris, P.A., Jacobs, D., Liu, K. & Wong, N.D. Polymorphism of the soluble epoxide hydrolase is associated with coronary artery calcification in African-American subjects. Circulation 109, 335-9 (2004).

(87) Wei, Q. et al. Sequence variation in the soluble epoxide hydrolase gene and subclinical coronary atherosclerosis: interaction with cigarette smoking. Atherosclerosis 190, 26-34 (2007).

(88) Lee, C.R. et al. Genetic variation in soluble epoxide hydrolase (EPHX2) is associated with forearm vasodilator responses in humans. Hypertension 57, 116-22 (2011).

(89) Fava, C. et al. Homozygosity for the EPHX2 K55R polymorphism increases the long-term risk of ischemic stroke in men: a study in Swedes. Pharmacogenet Genomics 20, 94-103 (2010).

(90) Theken, K.N. et al. Evaluation of cytochrome P450-derived eicosanoids in humans with stable atherosclerotic cardiovascular disease. Atherosclerosis 222, 530-6 (2012).

(91) Schuck, R.N. et al. Cytochrome P450-derived eicosanoids and vascular dysfunction in coronary artery disease patients. Atherosclerosis 227, 442-8 (2013).

(92) Lefer, D.J. & Bolli, R. Development of an NIH consortium for preclinical assessment of cardioprotective therapies (CAESAR): a paradigm shift in studies of infarct size limitation. J Cardiovasc Pharmacol Ther 16, 332-9 (2011).

(93) Khan, M.A., Liu, J., Kumar, G., Skapek, S.X., Falck, J.R. & Imig, J.D. Novel orally active epoxyeicosatrienoic acid (EET) analogs attenuate cisplatin nephrotoxicity. FASEB J 27, 2946-56 (2013).

(94) Hye Khan, M.A. et al. Orally active epoxyeicosatrienoic Acid analog attenuates kidney injury in hypertensive dahl salt-sensitive rat. Hypertension 62, 905-13 (2013).

(95) Liu, J.Y. et al. Substituted phenyl groups improve the pharmacokinetic profile and anti-inflammatory effect of urea-based soluble epoxide hydrolase inhibitors in murine models. Eur J Pharm Sci 48, 619-27 (2013).

(96) Hutchens, M.P., Nakano, T., Dunlap, J., Traystman, R.J., Hurn, P.D. & Alkayed, N.J. Soluble epoxide hydrolase gene deletion reduces survival after cardiac arrest and cardiopulmonary resuscitation. Resuscitation 76, 89-94 (2008).

(97) Loot, A.E. & Fleming, I. Cytochrome P450-derived epoxyeicosatrienoic acids and pulmonary hypertension: central role of transient receptor potential C6 channels. J Cardiovasc Pharmacol 57, 140-7 (2011).

(98) Keseru, B. et al. Epoxyeicosatrienoic acids and the soluble epoxide hydrolase are determinants of pulmonary artery pressure and the acute hypoxic pulmonary vasoconstrictor response. FASEB J 22, 4306-15 (2008).

(99) Keseru, B. et al. Hypoxia-induced pulmonary hypertension: comparison of soluble epoxide hydrolase deletion vs. inhibition. Cardiovasc Res 85, 232-40 (2010).

(100) Krotz, F. et al. Membrane-potential-dependent inhibition of platelet adhesion to endothelial cells by epoxyeicosatrienoic acids. Arterioscler Thromb Vasc Biol 24, 595-600 (2004).

(101) Krotz, F. et al. A sulfaphenazole-sensitive EDHF opposes platelet-endothelium interactions in vitro and in the hamster microcirculation in vivo. Cardiovasc Res 85, 542-50 (2010).

(102) Heizer, M.L., McKinney, J.S. & Ellis, E.F. 14,15-epoxyeicosatrienoic acid inhibits platelet aggregation in mouse cerebral arterioles. Stroke 22, 1389-93 (1991).

(103) O'Gara, P.T. et al. 2013 ACCF/AHA guideline for the management of ST-elevation myocardial infarction: executive summary: a report of the American College of Cardiology Foundation/American Heart Association Task Force on Practice Guidelines. Circulation 127, 529-55 (2013).

(104) Writing Committee, M. et al. 2012 ACCF/AHA focused update of the guideline for the management of patients with unstable angina/Non-ST-elevation myocardial infarction (updating the 2007 guideline and replacing the 2011 focused update): a report of the American College of Cardiology Foundation/American Heart Association Task Force on practice guidelines. Circulation 126, 875-910 (2012).

(105) Jung, F. et al. Effect of cytochrome P450-dependent epoxyeicosanoids on Ristocetin-induced thrombocyte aggregation. Clin Hemorheol Microcirc 52, 403-16 (2012).

(106) Panigrahy, D. et al. Epoxyeicosanoids stimulate multiorgan metastasis and tumor dormancy escape in mice. J Clin Invest 122, 178-91 (2012).

(107) Panigrahy, D., Greene, E.R., Pozzi, A., Wang, D.W. & Zeldin, D.C. EET signaling in cancer. Cancer Metastasis Rev 30, 525-40 (2011).

(108) Panigrahy, D. et al. Epoxyeicosanoids promote organ and tissue regeneration. Proc Natl Acad Sci U S A 110, 13528-33 (2013).

(109) Kalish, B.T., Kieran, M.W., Puder, M. & Panigrahy, D. The growing role of eicosanoids in tissue regeneration, repair, and wound healing. Prostaglandins Other Lipid Mediat 104, 130-8 (2013).

(110) Zhang, G. et al. Epoxy metabolites of docosahexaenoic acid (DHA) inhibit angiogenesis, tumor growth, and metastasis. Proc Natl Acad Sci U S A 110, 6530-5 (2013).

(111) Hwang, S.H. et al. Synthesis and biological evaluation of sorafenib- and regorafenib-like sEH inhibitors. Bioorg Med Chem Lett 23, 3732-7 (2013).

(112) Falck, J.R. et al. 14,15-Epoxyeicosa-5,8,11-trienoic acid (14,15-EET) surrogates containing epoxide bioisosteres: influence upon vascular relaxation and soluble epoxide hydrolase inhibition. J Med Chem 52, 5069-75 (2009).

(113) Mitra, R. et al. CYP3A4 mediates growth of estrogen receptor-positive breast cancer cells in part by inducing nuclear translocation of phospho-Stat3 through biosynthesis of (+/-)-14,15-epoxyeicosatrienoic acid (EET). J Biol Chem 286, 17543-59 (2011).

(114) Chaudhary, K.R. et al. Differential effects of soluble epoxide hydrolase inhibition and CYP2J2 overexpression on postischemic cardiac function in aged mice. Prostaglandins Other Lipid Mediat 104–105, 8-17 (2013).

(115) Zhu, P., Peck, B., Licea-Perez, H., Callahan, J.F. & Booth-Genthe, C. Development of a semi-automated LC/MS/MS method for the simultaneous quantitation of 14,15-epoxyeicosatrienoic acid, 14,15-dihydroxyeicosatrienoic acid, leukotoxin and leukotoxin diol in human plasma as biomarkers of soluble epoxide hydrolase activity in vivo. J Chromatogr B Analyt Technol Biomed Life Sci 879, 2487-93 (2011).